Coinage Metal Catalyzed Alkylations of Alkynes and Allenes

Mitchell Thomas Lee

A dissertation

submitted in partial fulfillment of the

requirements for the degree of

Doctor of Philosophy

University of Washington

2021

Reading Committee:

Gojko Lalic, Chair

Forrest E. Michael

Alshakim Nelson

Program Authorized to Offer Degree:

Chemistry

University of Washington

Abstract

Coinage Metal Catalyzed Alkylations of Alkynes and Allenes

Mitchell Thomas Lee

Chair of the Supervisory Committee:

Professor Gojko Lalic

Department of Chemistry

The formation of new C–C σ bonds is a fundamental aspect of organic synthesis. These bond forming reactions are valued, in part, for their ability to bring together fragments and rapidly develop molecular complexity in convergent syntheses. Herein is described three new coinage metal catalyzed C–C σ bond forming reactions. The first is a copper-catalyzed hydroalkylation of allenes. This reaction makes use of an allyl copper intermediate that undergoes an S_E2'alkylation with an alkyl triflate. An investigation of the reaction mechanism revealed the viability of both mononuclear copper and dinuclear copper intermediates, including a unique dinuclear copper allyl species.

Following this, the development of a photoinduced copper-catalyzed alkylation of terminal alkynes with primary, secondary, or tertiary bridgehead alkyl iodides as electrophiles is discussed. The reaction provides access to challenging dialkyl internal alkynes as well as an alternative to the traditional bimetallic Sonogashira reaction. Like the Sonogashira reaction, it proceeds though a copper acetylide intermediate, but this intermediate is now directly activated by blue light rather than transmetallated to a second transition metal catalyst. Key to the success of the reaction was

the suppression of light promoted polymerization of the starting material by using a terpyridine ligand on copper.

Finally, an in-depth investigation of a *Z*-selective hydroalkylation of terminal alkynes is reported. Highly diastereoselective synthesis of these, thermodynamically less stable, *Z*-alkene diastereomers has been difficult. To address this challenge, a silver catalyzed hydroalkylation of terminal alkynes with alkylboranes as the coupling partner was developed. The new approach employs the stereoelectronic requirements of a 1,2-metallate shift in the intermediary boronate complex to achieve >300:1 *Z:E* selectivity. The exceptional selectivity and novelty of the approach led to a full investigation of the mechanism. The proposed mechanism proceeds through an isolable silver coordinated boronate complex that then undergoes a diastereodeterming and rate limiting 1,2-metallate shift. The proposed mechanism relies on the results of stoichiometric analysis of many of the elementary steps, kinetic measurements, KIE and competition experiments, X-ray crystallography, and DFT calculations.

TABLE OF CONTENTS

LIST OF FIGURES

LIST OF TABLES

LIST OF SCHEMES

LIST OF ABBREVIATIONS

9-BBN	9-borabicyclo[3.3.1]nonane
Ac	acetyl
Ar	aryl
B	Base
Bn	benzyl
Boc	tert-butyloxycarbonyl
C	Celsius
cat	catalyst
CPCM	conductor-like polarizable continuum model
Cy	cyclohexyl
DCE	1,2-dichloroethane
DCM	dichloromethane
DFT	density functional theory
DIAD	Diisopropyl azodicarboxylate
DMEDA	1,2-Dimethylethylenediamine
DMF	dimethylformamide
dtbpy	4,4’-Di-tert-butyl-2,2’-dipyridine
E^+	electrophile
EI	electron ionization
equiv	equivalents
ESI	electrospray ionization
Et	ethyl

FID	flame ionization detector
FTIR	Fourier transform infrared

FTIR band abbreviations

s	strong
m	medium
w	weak
br	broad

GC	gas chromatography
GPC	gel permeation chromatography
h	hour
Hex	hexanes
Hz	hertz
ICP	inductively coupled plasma
IPr	1,3-Bis-(2,6-diisopropylphenyl)imidazolium
i-Pr	isopropyl
IR	infrared
KIE	kinetic isotope effect
L	ligand
LED	light emitting diode
M	metal
Me	methyl
min	minutes
mol	mole

MS	mass spectrometry
n-Bu	butyl
NHC	N-heterocyclic carbene
NMR	nuclear magnetic resonance

NMR splitting pattern abbreviations

s	singlet
d	doublet
t	triplet
q	quartet
p	pentet
h	heptet
m	multiplet
br	broad

ORTEP	Oak Ridge Thermal Ellipsoid Plot
OTf	trifluoromethanesulfonate
Ph	phenyl
pin	pinacol
PMHS	polymethylhydrosiloxane
POV-Ray	The Persistence of Vision Ray Tracer
ppb	parts per billion
ppm	parts per million
PyBox	pyridine bisoxazoline
Rf	retention factor

SCE	saturated calomel electrode
S_E2	substitution electrophilic bimolecular
SET	single electron transfer
SIPr	1,3-Bis-(2,6-diisopropylphenyl)imidazolinium
S_N2	substitution nucleophilic bimolecular
TBAF	tetrabutylammoium fluoride
TBS	tert-butyldimethylsilyl
t-Bu	tert-butyl
TEMPO	2,2,6,6-Tetramethylpiperidine 1-oxy
THF	tetrahydrofuran
TIPS	triisopropylsilyl
TLC	thin layer chromatography
TMB	1,3,5-trimethoxybenzne
TMDSO	tetramethyldisiloxane
TMPDA	N,N,N',N'-Tetramethyl-p-phenylenediamine
TMS	Tetramethylsilane
TMS	trimethylsilyl
Tri	2,4-bis[2,6-bis(1-methylethyl)phenyl]-2,4-dihydro-5-phenyl-3H-1, 2,4-Triazol-3-ylidene
Ts	p-poluenesulfonyl

ACKNOWLEDGEMENTS

First and foremost, I would like to thank my graduate advisor, Gojko Lalic, for spending the time to discuss the details of reactions and the process of discovery daily at the outset of my graduate career and for letting me to think and discover on my own as the years progressed. Thank you for the dedication, guidance, and genuine desire to help me succeed in my graduate career and beyond. As happy as I am to be moving on, I am grateful for time I was able to spend in your lab learning about chemistry and myself.

I would also like to thank Forrest Michael for serving on all my exam committees during graduate school. Your insights and probing questions during both exams and joint group meetings were invaluable to developing and understanding the reactions I worked on and pushed me to re-examine my results to continue learning about how they were gathered and what they allow me to conclude.

Next, I would like to thank my lab members: Hester Dang, Melrose Mailig, Julia Nguyen, Mary Nguyen, Avijit Hazra, Megan Armstrong, Madison Goodstein, Andrea Chong, Jason Chen, James Baumann, Austin Shaff, Evan Long, and Anton Taraskin. To those that started ahead of me, thank you for the training and guidance as I started my graduate career. To everyone, thank you for all the support, for making the time in lab more enjoyable, and for joining me on the long journey of graduate school. Additionally, a special thank you to Avijit for the endless discussions about troubleshooting reactions, new experiments, mechanistic details, and life in general. Lastly, I would like to thank Wei Pin Teh, while a member of the Michael lab rather than the Lalic Lab, he has been a great friend throughout graduate school, both in and outside of chemistry.

Finally, I would like to thank my Family for their love, encouragement, and support throughout my life.

DEDICATION

To my Mom, Dad, and Brother.

Chapter 1. CATALYTIC HYDROALKYLATION OF ALLENES

Portions of this chapter as well as figures, schemes, and tables were adapted or reproduced from the following manuscript, with permission from Lee, M.; Nguyen, M.; Brandt, C.; Kaminsky, W.; Lalic, G. Catalytic Hydroalkylation of Allenes. *Angew. Chem. Int. Ed.* **2017**, *56* (49), 15703–15707. Copyright 2017 Wiley-VCH Verlag GmbH & Co. KGaA, Weinheim

1.1 **INTRODUCTION**

Reductive cross-coupling reactions of unsaturated compounds have been extensively studied over the last decade and have been developed into a powerful tool for the formation of carbon–carbon bonds. These reactions obviate the need for the stoichiometric preparation of reactive organometallic intermediates and allow the direct use of unsaturated compounds as coupling partners.[1,2] As a result, reductive cross-coupling reactions often provide a more efficient alternative to the traditional cross coupling of organometallic reagents and organic electrophiles.

Most reductive cross-coupling reactions involve π-electrophiles, such as aldehydes,[3–12] ketones,[13] imines,[14–21] and activated alkenes.[22–24] π-Electrophiles can be generated in situ from suitable precursors, as demonstrated by Krische et al. For example, primary[25–37] and secondary[38–40] alcohols can be used as coupling partners in reactions with a range of unsaturated compounds. Reactions with σ-electrophiles are generally significantly more challenging and less common. Notable early examples of such reactions are the reductive cross-coupling of alkynes with epoxides developed by Jamison et al.,[41,42] and the reductive cross-coupling of functionalized alkenes with alkyl zinc reagents developed by Sigman et al.[43–45] More recently, several intermolecular hydroalkylation reactions have been developed using alkyl halides or sulfonate esters as coupling

partners.[46] In 2015, Kambe et al. reported copper-catalyzed hydroalkylation of 1,3-dienes.[47] The same year, our group reported E-selective hydroalkylation of terminal alkynes,[48,49] while the Z-selective hydroalkylation of aryl alkynes was reported by Hu et al.[50] In 2016, Fu et al. reported Markovnikov hydroalkylation of terminal alkynes using a nickel catalyst.[51] Despite these developments in the hydroalkylation of alkynes and certain alkenes, hydroalkylations of allenes are still relatively rare.

The most general method for the reductive cross-coupling of allenes is a recently reported hydroallylation with allylic chlorides as coupling partners.[52] However, hydroalkylation reactions with simple σ-electrophiles remain limited to intramolecular reactions of specific classes of functionalized allenes,[53,54] with no general methods for the intermolecular hydroalkylation of simple allenes.

Herein, we report a copper-catalyzed hydroalkylation of allenes with alkyl triflates as electrophiles. We describe the reaction development and the exploration of the substrate scope. We propose a reaction mechanism and describe the isolation, structure, and reactivity of a new catalytic intermediate.

1.2 RESULTS AND DISCUSSION

1.2.1 *Reaction Development*

Using our previous work on the hydroalkylation of alkynes as a starting point,[48,49] we developed a method for the hydroalkylation of allenes shown in **Scheme 1.1**. The best results in the reaction were obtained using alkyl triflates as electrophiles, SIPrCuF as a catalyst, $(Me_2HSi)_2O$

as a hydride source, and CsF as a turnover reagent. The hydroalkylation product was formed as a single regioisomer.

Scheme 1.1 Copper-Catalyzed Hydroalkylation of Allenes

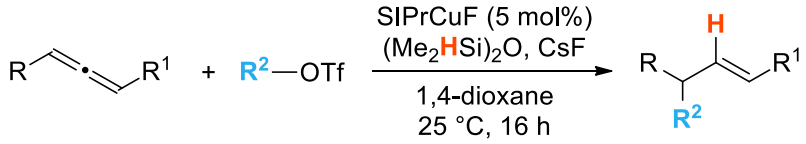

In the process of the reaction development, we made several observations, as summarized in **Table 1.1**. Changes in the stoichiometry of the substrates are well-tolerated, and a high yield (91 %) of the desired product can be obtained even when neither coupling partner is used in excess. IPrCuF can also be used as a catalyst with a relatively small decrease in yield.

The use of $(Me_2HSi)_2O$ is essential for the success of the reaction, and even closely related silanes provide lower yields of the hydroalkylation product. High yields are obtained when fewer equivalents of silane or CsF are used in the reaction, while less than 5 % of the product is obtained with KF as a turnover reagent. The reaction can be performed at a high concentration of alkyl triflate without a decrease in yield. Finally, in addition to 1,4-dioxane, the reaction can also be performed in Et_2O, while the use of other common organic solvents leads to lower yields.

Table 1.1 Reaction Development

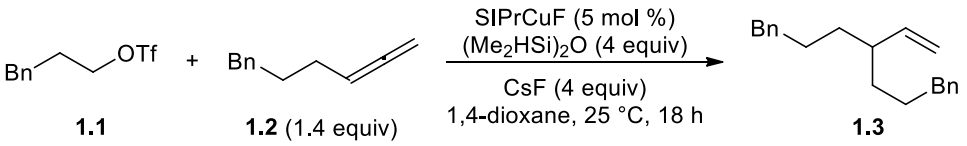

1.1 **1.2** (1.4 equiv) **1.3**

Entry	Change from best conditions	Yield[a]
1	none	99%
2	1.0 equiv of allene and 1.4 equiv of ROTf	99%
3	1.0 equiv of allene	91%
4	IPrCuF instead of SIPrCuF	81%
5	$(EtO)_3SiH$ instead of $(Me_2HSi)_2O$	91%
6	PMHS instead of $(Me_2HSi)_2O$	66%
7	2.0 equiv of $(Me_2HSi)_2O$	91%
8	2.0 equiv of CsF	98%
9	KF instead of CsF	1%
10	0.5 M ROTf vs 0.1 M ROTf	99%
11	Et_2O	96%
12	THF	46%
13	CH_2Cl_2	77%
14	toluene	66%

[a] GC yields are reported. All reactions performed on 0.1 mmol scale.

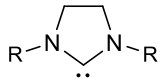

SIPr *R = (2,6-i-Pr)$_2$C$_6$H$_3$*

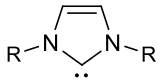

IPr *R = (2,6-i-Pr)$_2$C$_6$H$_3$*

1.2.2 *Substrate Scope*

Hydroalkylation can be accomplished with a range of allenes and alkyl triflates. In all cases, only one regioisomer of the product is obtained. The reaction can be performed in the presence of a variety of functional groups, alkyl bromides (**1.4**), including silyl ethers (**1.5**), aryl iodides (**1.6**), aryl boronic esters (**1.8**), esters (**1.9**), sulfonamides (**1.10**, **1.12**), tosylates (**1.11**), and aryl bromides (**1.13**). 1,1-Disubstituted allenes provide compounds containing a quaternary carbon center (**1.16**). With silyl-substituted allenes, the alkenyl silane product is obtained in high yield, as a single diastereoisomer (**1.17**). Four 1,3-disubstituted allenes were tested, but were either too low yielding for isolation, or were obtained as a mixture of isomers (see section 1.4.10). Finally, we found that

the hydroalkylation product can be obtained in good yield on a large preparative scale (4 mmol; see 3, **Table 1.2**).

Table 1.2 Substrate Scope[a]

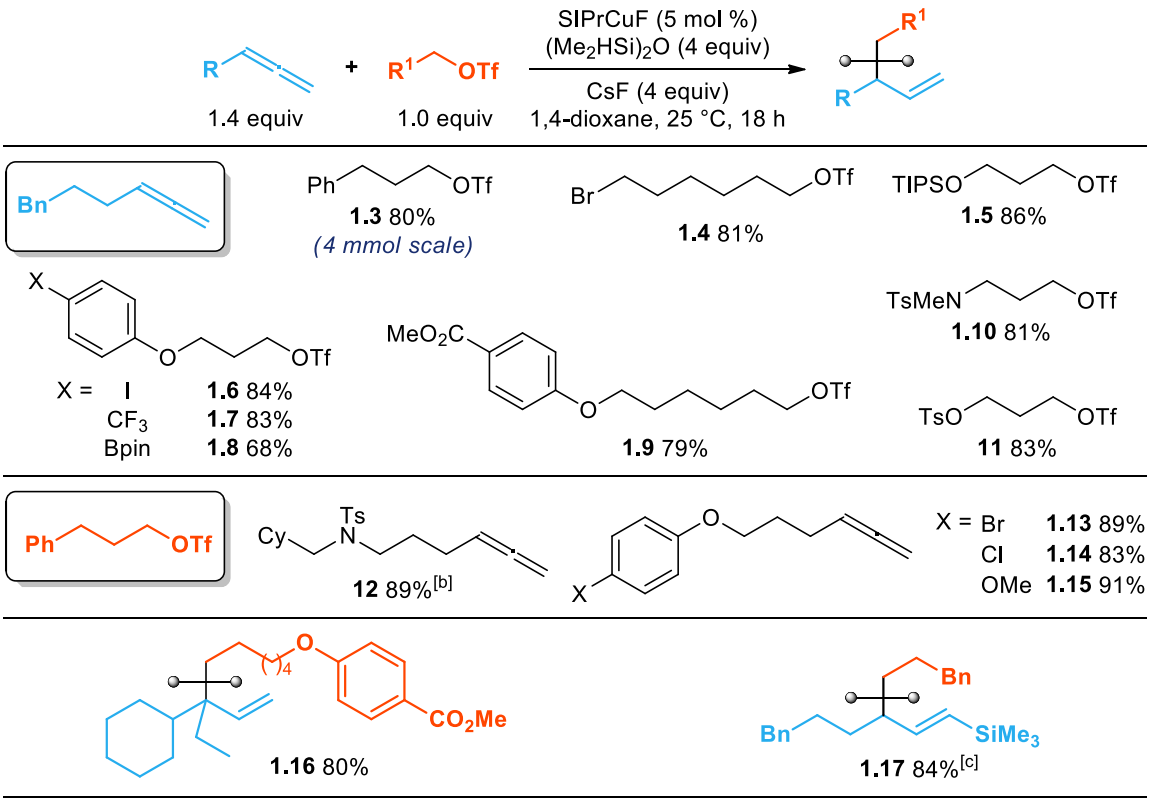

[a] Reactions performed on a 0.5 mmol scale unless otherwise specified. Yields of pure isolated products are reported. [b] NMR yield. [c] IPrCuF used as a catalyst. Reaction performed at 45 °C.

Overall, the exploration of the substrate scope demonstrates that the new hydroalkylation reaction provides access to a wide range of substituted terminal alkenes and vinyl silanes and is compatible with a variety of functional groups. The hydroalkylation is complementary to S_N2' allylic substitution reactions,[55,56] which require alkyl organometallic reagents as coupling partners. The reversed polarity of the hydroalkylation reaction allows alkylation with substrates that carry highly electrophilic functional groups, such as alkyl bromides (**1.4**) and sulfonate esters (**1.11**). To provide a better understanding of the underlying chemistry and enable further development of the hydroalkylation reaction, we explored the mechanism of the reaction.

1.2.3 *Mechanism*

There are two plausible mechanisms for the hydroalkylation reaction (**Scheme 1.2**). The mechanism shown in **Scheme 1.2a** is based on the generally accepted mechanism for most copper-catalyzed hydrofunctionalization reactions reported so far.[57] According to this proposal, copper hydride formation is followed by hydrocupration of the allene and alkylation of the allyl copper intermediate. An alternative mechanism featuring dinuclear cationic complexes $[(NHCCu)_2(\mu\text{-}X)]OTf$ (X=F, H, allyl; **1.22**, **1.23**, **1.24**) is based on the mechanism of a related hydroalkylation of alkynes recently reported by our group.[49,58,59] The two plausible mechanisms shown in **Scheme 1.2** are closely related, and the major difference is that all mononuclear copper complexes that are intermediates in the first proposal are replaced by cationic dinuclear intermediates in the second proposal.

Scheme 1.2 Plausible Mechanisms for the Hydroalkylation of Allenes

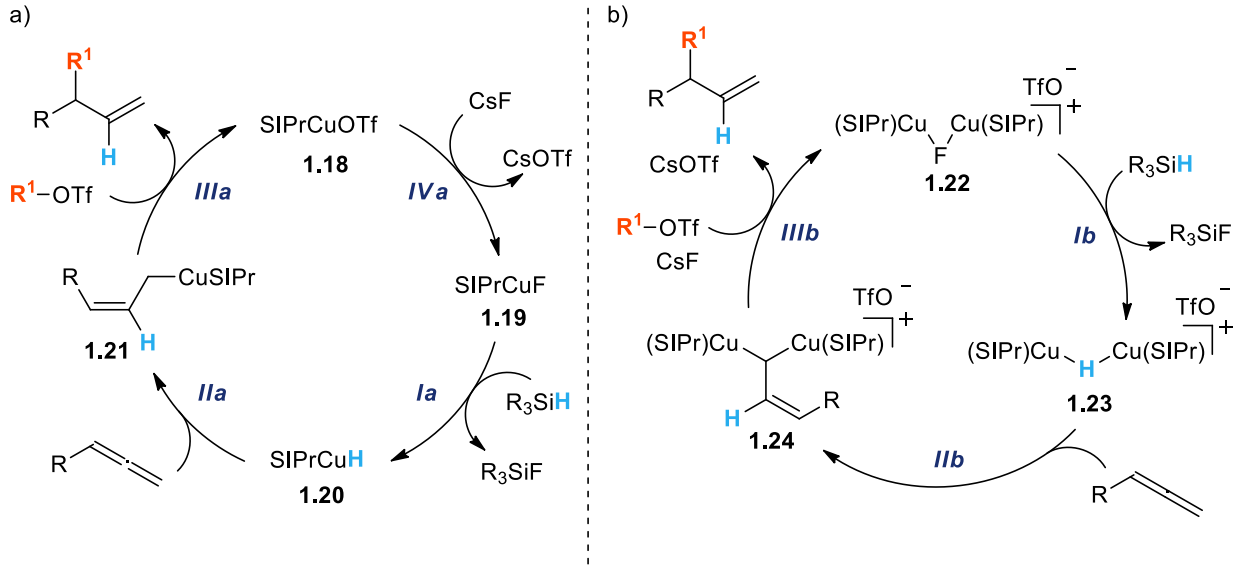

One of the key differences between the two mechanisms is the difference in the reactivity of the copper hydride responsible for the hydrocupration of the allene. We have previously established that dinuclear $[(NHCCu)_2(\mu\text{-}H)]OTf$ (**1.23**) does not react with alkyl triflates, while

the NHCCuH reacts quickly to give alkanes.[49] As a result, an important implication of the first proposal is that the hydrocupration of allenes needs to be faster than the reduction of alkyl triflates by SIPrCuH (**1.20**). We performed a stoichiometric competition experiment shown in **Scheme 1.3a** and observed formation of the hydroalkylation product (**1.3**) in 84 % yield and reduction of the alkyl triflate in just 6 % yield. This result confirms that the hydroalkylation of allenes is faster than the reduction of alkyl triflates and confirms the plausibility of the mechanism shown in **Scheme 1.2a**.

Scheme 1.3 Stoichiometric Experiments (Mechanism a)

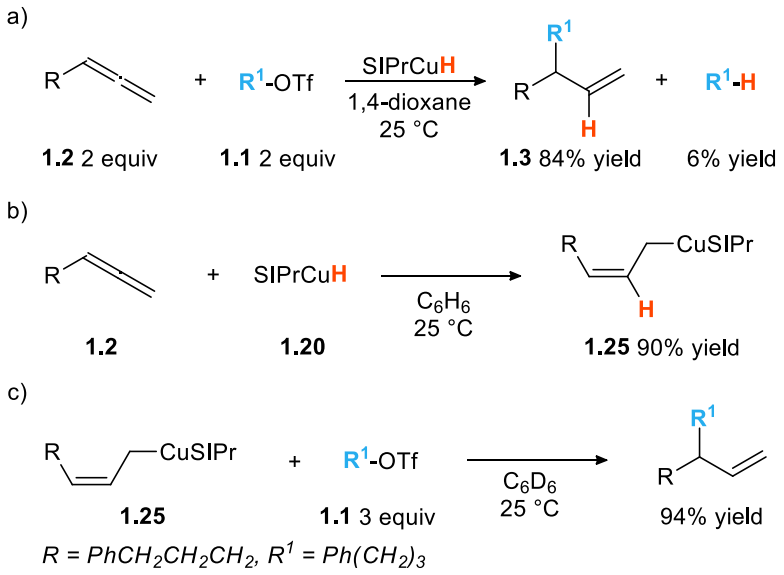

Next, we explored the formation of the allyl copper intermediate and its reaction with alkyl triflates. We isolated the SIPrCu(allyl) complex **1.25** from a stoichiometric hydrocupration reaction (**Scheme 1.3b**). It is interesting to note the *Z* configuration of the alkene in the X-ray crystal structure of the copper allyl complex shown in **Figure 1.1**. In a stoichiometric reaction, SIPrCu(allyl) complex **1.25** reacts with alkyl triflate to produce the desired product in 94 % yield (**Scheme 1.3c**). The S_E2' regioselectivity of the alkylation is surprising in light of the S_E2 reactivity of allylcopper complexes with allylic chlorides previously reported.[52]

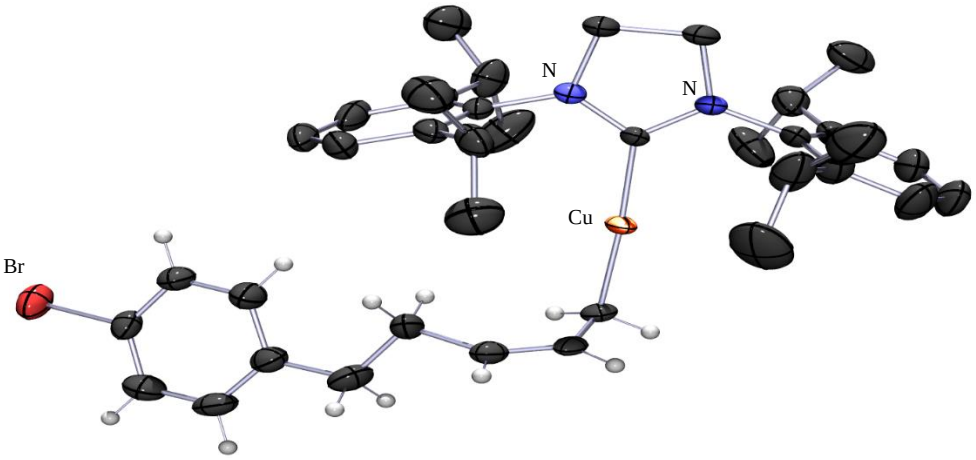

Figure 1.1 POV-Ray rendered ORTEP of SIPrCu(allyl) complex **1.25** with thermal ellipsoids at the 50% probability level

In the stoichiometric alkylation of **1.25**, we noticed that while the first 50 % of the product is formed within the first 6 minutes, it takes 4 hours to reach 87 % yield. The significant decrease in the rate of the reaction is consistent with the idea that the SIPrCu(allyl) complex is sequestered by SIPrCuOTf formed as a byproduct of the alkylation reaction. Such formation of the dinuclear [(SIPrCu)$_2$(μ-allyl)]OTf (**1.26**) complex from SIPrCuOTf with SIPrCu(allyl) (**1.25**) can be replicated in a stoichiometric reaction (**Scheme 1.4a**). The same complex can also be prepared through a reaction of dinuclear [(SIPrCu)$_2$(μ-H)]OTf with allene **1.2** (**Scheme 1.4b**). Access to the dinuclear allyl complex allowed us to explore its reactivity toward alkyl triflates. The stoichiometric reaction of **1.26** with alkyl triflate **1.1** yields the expected alkylation product at a significantly lower rate than the reaction of the mononuclear complex under the same reaction conditions. The successful alkylation of the dinuclear [(SIPrCu)2(μ-allyl)]OTf complex is surprising considering that the analogous [(NHCCu)2(μ-alkenyl)]OTf complex does not react with alkyl triflates under a variety of conditions.[49]

Scheme 1.4 Stoichiometric Experiments (Mechanism b)

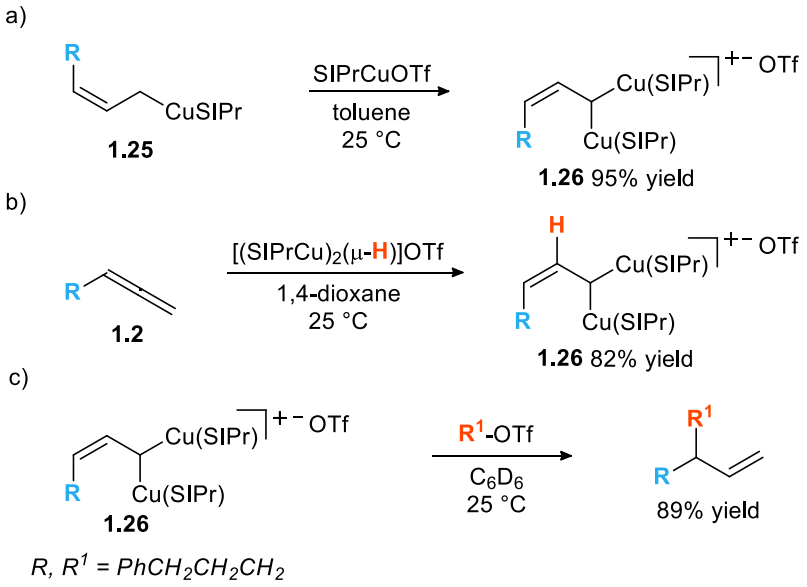

The results of experiments shown in **Scheme 1.3** and **Scheme 1.4** demonstrate the feasibility of key elementary steps of both catalytic cycles shown in **Scheme 1.2**. However, we favor mechanism (b) shown in **Scheme 1.2b**. In previous work, we have shown that in a related reduction of alkyl triflates and hydroalkylation of alkynes, the catalyst turnover (step **IVa** in **Scheme 1.2a**) is rate limiting, most likely because of the slow phase transfer of the fluoride. One consequence of the slow entry of fluoride into the catalytic cycle is a relatively high concentration of NHCCuOTf, which forces the formation of the dinuclear intermediates. Considering that the elementary steps involved in mechanism (a), that is, hydrocupration and alkylation of the organocopper intermediate, are faster with allenes than with alkynes, the formation of SIPrCuF is most likely still rate limiting and would force the shift towards mechanism (b).

The mechanism shown in **Scheme 1.2b** features dinuclear copper allyl complexes (**1.24**) as key intermediates. These complexes are related to the cationic dinuclear alkenyl complexes previously described by Sadighi and later by us. However, they have never been reported or characterized before. Attempts to obtain crystals of **1.26** were not successful, and we focused on

crystallization of a closely related complex that contains a para-bromobenzene moiety (**1.27**, **Figure 1.2a**). After considerable effort, we obtained an X-ray crystal structure of **1.27**, which shows surprising structural features distinct from those found in dinuclear alkenyl copper complexes.

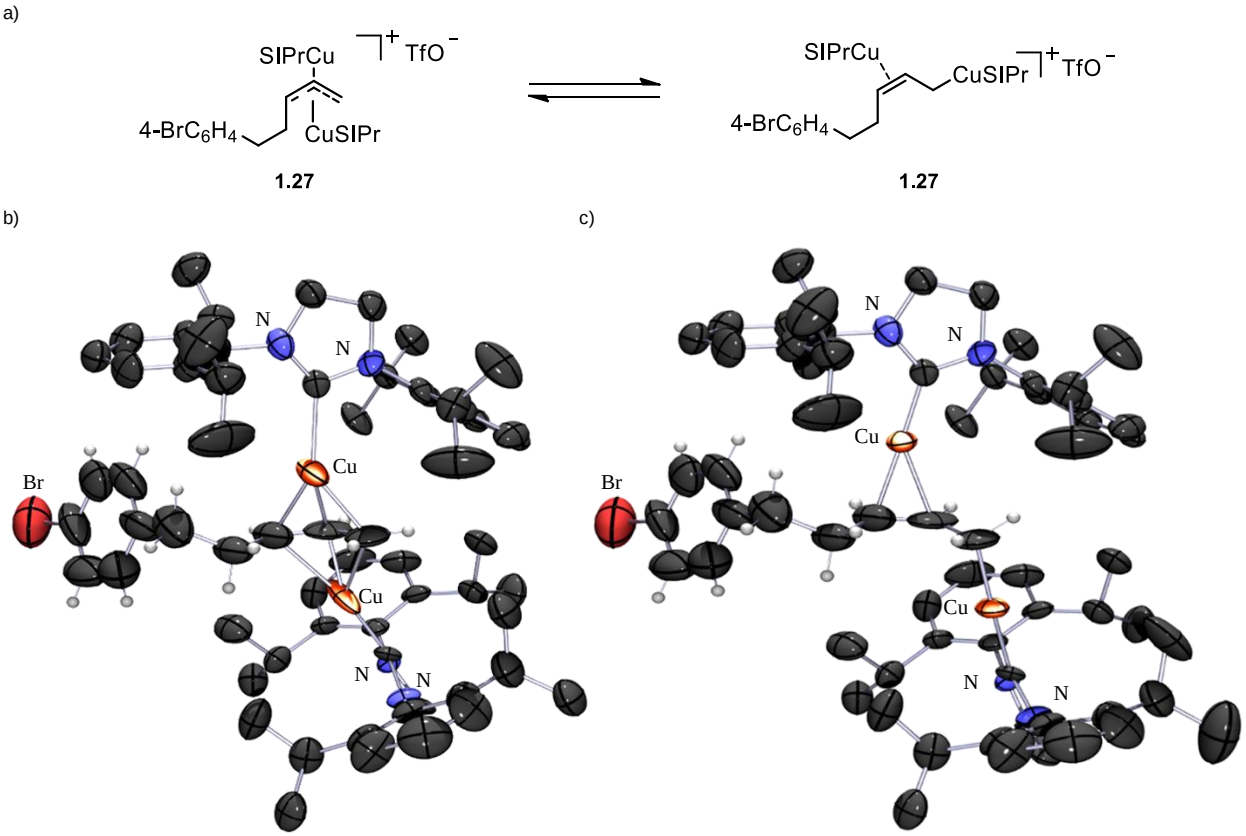

Figure 1.2 POV-Ray rendered ORTEP of the crystal structure of complex **1.27**. The counterion and most hydrogen atoms were removed for clarity a) schematics of complex **1.27**. b) POV-Ray rendered ORTEP of the minor configuration with thermal ellipsoids at 40% probability level. c) POV-Ray rendered ORTEP of the major configuration with thermal ellipsoids at 40% probability level.

The crystal structure of **1.27** contains two configurations (**Figure 1.2**), with the Z double bond preserved in both. It is interesting to note that the 1H NMR spectrum of **1.26** and **1.27** features broad signals consistent with a dynamic structure. The minor configuration in the X-ray structure contains symmetrically arranged metal centers bonded to a π-allyl fragment from the opposite faces (**Figure 1.2b**). This structural arrangement is very unusual for late transition-metal

complexes, with no other examples of ally fragments sandwiched between two metal centers available in the Cambridge Crystallographic Data Centre.

In the major configuration (**Figure 1.2c**), the two metal centers distort from the symmetrical arrangement towards the opposite ends of the allyl fragment. In the resulting arrangement of copper atoms, one is σ-bonded to the allyl fragment, while the other is π-bonded to the alkene. This bonding arrangement contrasts with dinuclear alkenyl copper complexes, in which metal centers do not interact with the alkene and instead form a three-center-two-electron bond with the alkenyl carbon. This structural difference is consistent with the difference in reactivity of two types of dinuclear complexes. The nonsymmetrical configuration of the dinuclear allyl copper complex with the σ-bonded allyl copper fragment offers a plausible explanation for the much higher reactivity of these complexes towards alkyl triflates relative to the reactivity of analogous alkenyl complexes.

1.3 CONCLUSION

In summary, the results of our studies on the hydroalkylation of allenes and alkynes point to several important differences in the reactivity of these classes of compounds. First, while the hydrocupration of allenes by SIPrCuH is faster than the reduction of alkyl triflates, the opposite is true for the reaction of alkynes. This is in line with the generally higher reactivity of allenes. The second difference is the much higher reactivity of dinuclear [$(SIPrCu)_2$(μ-allyl)]OTf complexes, which react with alkyl triflates. The analogous [$(NHCCu)_2$(μ-alkenyl)]OTf complexes do not react with alkyl triflates under a wide range of reaction conditions. These differences in the reactivity of allenes and alkynes point to opportunities for taking different approaches to the development of reactions for their hydrofunctionalization.

1.4 EXPERIMENTAL

1.4.1 *General Procedures*

All reactions were performed under an atmosphere of nitrogen with flame-dried or oven-dried (120 °C) glassware, using standard Schlenk techniques, or in a nitrogen-filled glovebox (NexusII from Vacuum Atmospheres). Column chromatography was performed using a Biotage Iso-1SV flash purification system with silica gel from Agela Technologies Inc. (60Å, 40-60 μm, 230-400 mesh). ^{1}H- and ^{13}C-NMR spectra were recorded on a Bruker AV-300 or AV-500 spectrometer. ^{1}H NMR chemical shifts (δ) are reported in parts per million (ppm) downfield of TMS and are referenced relative to the residual solvent peak ($CDCl_3$ (7.26 ppm), C_6D_6 (7.16 ppm), or CD_2Cl_2 (5.32 ppm)). ^{13}C chemical shifts are reported in parts per million downfield of TMS and are referenced to the carbon resonance of the solvent ($CDCl_3$: δ 77.2 ppm, C_6D_6: δ 128.1 ppm, CD_2Cl_2: δ 54.0 ppm). Data are represented as follows: chemical shift, multiplicity (s = singlet, bs = broad singlet, d = doublet, t = triplet, q = quartet, p = pentet, h = heptet m = multiplet, br = broad), integration, and coupling constants in Hertz (Hz). GC analysis was performed on a Shimadzu GC-2010 instrument with a flame ionization detector and a SHRXI-5MS column (15 m, 0.25 mm inner diameter, 0.25 μm film thickness). The following temperature program was used: 2 min @ 60 °C, 13 °C/min to 160 °C, 30 °C/min to 250 °C, 5.5 min @ 250 °C. Infrared (IR) spectra were recorded on a Perkin Elmer Spectrum RX I spectrometer. IR peak absorbencies are represented as follows: s = strong, m = medium, w = weak, br = broad.

1.4.2 *Materials*

Toluene, benzene, ether, DCM, and THF were dried by passing through columns of neutral alumina. 1,4-dioxane was distilled over calcium hydride, degassed, and stored over

activated molecular sieves. All other solvents were used as received. Deuterated solvents were purchased from Cambridge Isotope Laboratories, Inc. Common commercial reagents were purchased from Sigma-Aldrich Co., VWR International, LLC., TCI America, or STREM Chemicals, Inc. $(Me_2SiH)_2O$ (TMDSO) was purchased from Oakwood Chemical and vacuum transferred over calcium hydride before use. Cesium fluoride was purchased from Matrix Scientific or Sigma Aldrich. The material was dried rigorously by flame-drying under vacuum followed by grinding with a mortar and pestle in a glove box. This process was repeated three times. 2,6-Lutidine was purchased from TCI America and distilled over calcium hydride, then vacuum transferred from aluminum trichloride. Triflic anhydride was purchased from Oakwood Chemical and vacuum transferred over P_2O_5.

1.4.3 *General Method for the Catalytic Hydroalkylation of Allenes*

In a nitrogen-filled glovebox a dram vial was charged with SIPrCuF (5 mol %, 2.4 mg, 0.005 mmol) and a stir bar. To this was added CsF (4 equiv, 60.8 mg, 0.40 mmol) and 1,4-dioxane (1.0 mL). The reaction mixture was stirred and $(Me_2HSi)_2O$ (TMDSO) (4 equiv, 53.2 mg, 0.40 mmol) was added. Within 15 seconds of stirring the solution at 25 °C, a bright yellow color was observed. Allene (1.4 equiv, 0.14 mmol) was added and the reaction was stirred for 5 min at 25 °C. During this time, the yellow color slowly dissipated to a light gray. Alkyl triflate (1.0 equiv, 0.10 mmol) was then added and the reaction was capped and stirred for 18 h at 25 °C. After 18h the reaction was removed from the glove box and quenched with ethanolamine (5 equiv, 30 µL, 0.50 mmol) and diluted with ether (2 mL). Trimethoxybenzene (TMB) was then added as an internal standard (0.5 equiv, 8.40 mg, 0.05 mmol), and the reaction mixture was further diluted with ether (10 mL) and washed with 1 M HCl (3 mL). It was then washed with saturated sodium bicarbonate and brine. The combined organic layers were dried over magnesium sulfate and

concentrated under reduced pressure. The resulting oil was either filtered through a plug of silica with EtOAc as the eluent to obtain a sample for GC analysis, or was purified by silica gel chromatography.

1.4.4 *Large Scale Reaction in **Table 1.2***

In a nitrogen-filled glovebox a 75 mL round bottom with a Teflon screw top was charged with SIPrCuF (5 mol %, 94.6 mg, 0.20 mmol) and a stir bar. To this was added CsF (4 equiv, 2.43 g, 16.0 mmol) and 1,4-dioxane (40.0 mL). The reaction mixture was stirred and TMDSO (4 equiv, 2.15 g, 16.0 mmol) was added. Within 15 seconds of stirring the solution at 25 °C, a bright yellow color was observed. Allene **1.2** (1.4 equiv, 886.1 mg, 5.6 mmol) was added and the reaction was stirred for 15 min at 25 °C. During this time, the yellow color slowly dissipated to a light gray. Alkyl triflate **1.1** (1.0 equiv, 1.07 g 4.0 mmol) was then added and the reaction was capped and stirred for 18 h at 25 °C. After 18h the reaction was removed from the glove box and quenched with ethanolamine (5 equiv, 1.20 mL, 20.0 mmol), diluted with ether (500 mL) and washed with 1 M HCl (30 mL). It was then washed with saturated sodium bicarbonate and brine. The combined organic layers were dried over magnesium sulfate and concentrated under reduced pressure. The resulting oil was purified by silica gel chromatography to give **3** (895.4 mg, 80%).

1.4.5 *Characterization of Hydroalkylation Products*

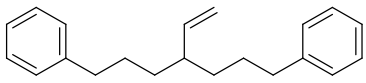

(4-vinylheptane-1,7-diyl)dibenzene (1.3): Compound was isolated as a colorless oil (116.5 mg, 84% yield). ^{1}H NMR (500 MHz, CD_2Cl_2) δ 7.32 – 7.26 (m, 4H), 7.24 – 7.14 (m, 6H), 5.62 – 5.46 (m, 1H), 5.09 – 4.93 (m, 2H), 2.76 – 2.47 (m, 4H), 2.12 – 1.96 (m, 1H), 1.74 – 1.51 (m, 4H), 1.50 – 1.38 (m, 2H), 1.38 – 1.24 (m, 2H). ^{13}C NMR (126 MHz, CD_2Cl_2) δ 143.8, 143.5, 128.9, 128.7,

126.1, 114.7, 44.5, 36.5, 35.1, 29.8 GC/MS (EI) calculated for $[M]^+$ 278.20, found 278.20. FTIR (neat, cm^{-1}): 3062 (m), 3024 (m), 3000 (m), 2930 (s), 2855 (s), 1941 (w), 1868 (w), 1803 (w), 1745 (w), 1639 (m), 1603 (m) 1495 (s), 1452 (s), 995 (m), 909 (m), 747 (s), 698 (s)

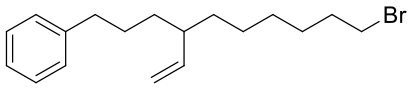

(10-bromo-4-vinyldecyl)benzene (1.4): Compound was isolated as a colorless oil (131.0 mg, 81% yield). ^{1}H NMR (300 MHz, CD_2Cl_2) δ 7.32 – 7.20 (m, 2H), 7.20 – 7.06 (m, 3H), 5.63 – 5.43 (m, 1H), 5.07 – 4.83 (m, 2H), 3.40 (t, *J* = 6.8 Hz, 2H), 2.69 – 2.46 (m, 2H), 2.06 – 1.90 (m, 1H), 1.89 – 1.75 (m, 2H), 1.69 – 1.52 (m, 2H), 1.47 – 1.14 (m, 10H). ^{13}C NMR (75 MHz, CD_2Cl_2) δ 144.0, 143.5, 128.9, 128.7, 126.1, 114.5, 44.5, 36.5, 35.4, 35.2, 34.8, 33.4, 29.8, 29.4, 28.7, 27.5. GC/MS (EI) calculated for $[M]^+$ 322.13, found 322.15. FTIR (neat, cm^{-1}): 3062 (m), 3025 (m), 2927 (s), 2854 (s), 1639 (m), 1603 (m), 996 (m), 911 (s), 740 (s), 698 (s)

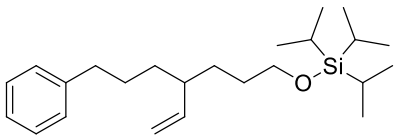

triisopropyl((7-phenyl-4-vinylheptyl)oxy)silane (1.5): Compound was isolated as a colorless oil (161.2 mg, 86% yield). ^{1}H NMR (300 MHz, CD_2Cl_2) δ 7.32 – 7.22 (m, 2H), 7.22 – 7.12 (m, 3H), 5.65 – 5.46 (m, 1H), 5.04 – 4.90 (m, 2H), 3.68 (t, *J* = 6.3 Hz, 2H), 2.72 – 2.49 (m, 2H), 2.12 – 1.91 (m, 1H), 1.77 – 1.18 (m, 8H), 1.18 – 0.99 (m, 21H). ^{13}C NMR (75 MHz, CD_2Cl_2) δ 143.95, 143.55, 128.96, 128.77, 126.12, 114.64, 64.08, 44.40, 36.56, 35.25, 31.68, 31.23, 29.80, 18.44, 12.64. GC/MS (EI) calculated for $[M]^+$ 374.30, found 374.30. FTIR (neat, cm^{-1}): 3063 (m), 3026 (m), 2939 (s), 2865 (s), 16239 (w), 1604 (w), 1495 (m), 1463 (m), 1105 (s), 995 (m), 910 (m)

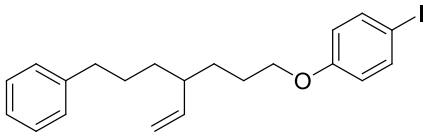

1-iodo-4-((7-phenyl-4-vinylheptyl)oxy)benzene (1.6): Compound was isolated as a white solid (175.5 mg, 84% yield). ^{1}H NMR (500 MHz, CD_2Cl_2) δ 7.57 (d, *J* = 7.7 Hz, 2H), 7.36 – 7.26 (m, 2H), 7.26 – 7.16 (m, 3H), 6.70 (d, *J* = 7.7 Hz, 2H), 5.64 – 5.52 (m, 1H), 5.10 – 4.99 (m, 2H), 3.91 (t, *J* = 6.3 Hz, 2H), 2.70 – 2.55 (m, 2H), 2.13 – 2.01 (m, 1H), 1.88 – 1.76 (m, 1H), 1.76 – 1.52 (m, 4H), 1.52 – 1.43 (m, 1H), 1.43 – 1.27 (m, 2H). ^{13}C NMR (126 MHz, CD_2Cl_2) δ 159.6, 143.4, 138.7, 128.9, 128.7, 126.1, 117.4, 115.2, 82.7, 68.7, 44.4, 36.5, 35.2, 31.7, 29.7, 27.4. GC/MS (EI) calculated for $[M]^+$ 420.10, found 420.20. FTIR (neat, cm^{-1}): 3063 (m), 3025 (m), 2931 (s), 1586 (m), 1571 (w), 1242 (s), 819 (w)

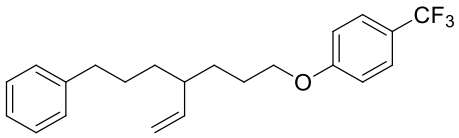

1-((7-phenyl-4-vinylheptyl)oxy)-4-(trifluoromethyl)benzene (1.7): Compound was isolated as a colorless oil (150.2 mg, 83% yield). ^{1}H NMR (300 MHz, CD_2Cl_2) δ 7.57 (d, *J* = 8.6 Hz, 2H), 7.34 – 7.25 (m, 2H), 7.25 – 7.13 (m, 3H), 6.98 (d, *J* = 8.6 Hz, 2H), 5.74 – 5.47 (m, 1H), 5.17 – 4.90 (m, 2H), 3.99 (t, *J* = 6.5 Hz, 2H), 2.75 – 2.50 (m, 2H), 2.20 – 1.96 (m, 1H), 1.96 – 1.22 (m, 8H).^{13}C NMR (126 MHz, CD_2Cl_2) δ 162.4, 143.5, 143.4, 129.0, 128.8, 127.4 (dd, *J* = 7.0, 3.4 Hz), 126.2, 125.3 (q, *J* = 270.8 Hz), 122.8 (q, *J* = 32.5 Hz), 115.3, 115.0, 68.9, 44.5, 36.5, 35.3, 31.7, 29.8, 27.4. GC/MS (EI) calculated for $[M]^+$ 362.19, found 362.25. FTIR (neat, cm^{-1}): 3063 (m), 3026 (m), 2933 (s), 2857 (m), 1616 (s), 1518 (s), 1329 (s), 1257 (s), 1160 (s), 1111 (s), 913 (m), 748 (m)

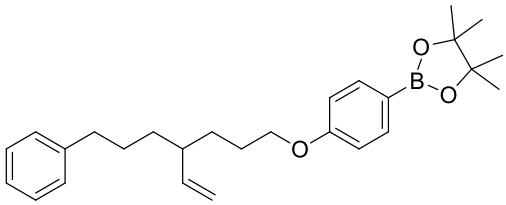

4,4,5,5-tetramethyl-2-(4-((7-phenyl-4-vinylheptyl)oxy)phenyl)-1,3,2-dioxaborolane (1.8): Compound was isolated as a colorless oil (143.6 mg, 68% yield). ^{1}H NMR (500 MHz, CD_2Cl_2) δ 7.70 (d, *J* = 8.3 Hz, 2H), 7.33 – 7.24 (m, 2H), 7.23 – 7.15 (m, 3H), 6.89 (d, *J* = 8.4 Hz, 2H), 5.63 – 5.51 (m, 1H), 5.07 – 4.97 (m, 2H), 3.96 (t, *J* = 6.5 Hz, 2H), 2.68 – 2.53 (m, 2H), 2.12 – 2.01 (m, 1H), 1.88 – 1.76 (m, 1H), 1.76 – 1.51 (m, 4H), 1.51 – 1.43 (m, 1H), 1.42 – 1.25 (m, 15H). ^{13}C NMR (126 MHz, CD_2Cl_2) δ 162.3, 143.5, 143.4, 136.9, 128.9, 128.7, 126.1, 115.1, 114.3, 84.0, 68.4, 44.4, 36.5, 35.2, 31.7, 30.3, 29.8, 27.5, 25.2. GC/MS (EI) calculated for $[M]^+$ 420.28, found 420.25. FTIR (neat, cm^{-1}): 3062 (m), 3026 (m), 2976 (s), 2930 (s), 2858 (m), 1604 (s), 1568 (m), 1361 (s), 1245 (s), 1090 (s), 699 (m)

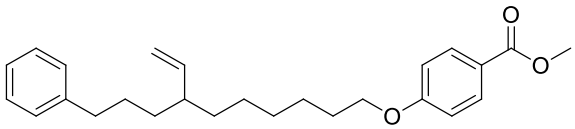

methyl 4-((10-phenyl-7-vinyldecyl)oxy)benzoate (1.9): Compound was isolated as a colorless oil (156.8 mg, 79% yield). ^{1}H NMR (300 MHz, CD_2Cl_2) δ 7.97 (d, *J* = 8.7 Hz, 2H), 7.35 – 7.10 (m, 5H), 6.91 (d, *J* = 8.7 Hz, 2H), 5.64 – 5.46 (m, 1H), 5.06 – 4.87 (m, 2H), 4.00 (t, *J* = 6.5 Hz, 2H), 3.85 (s, 3H), 2.69 – 2.49 (m, 2H), 2.08 – 1.91 (m, 1H), 1.87 – 1.71 (m, 2H), 1.71 – 1.16 (m, 12H). ^{13}C NMR (75 MHz, CD_2Cl_2) δ 167.2, 163.6, 144.0, 143.5, 132, 128.9, 128.8, 126.1, 123.0, 114.6, 114.5, 68.8, 52.2, 44.6, 36.5, 35.5, 35.2, 30.0, 29.8, 29.7, 27.6, 26.5. GC/MS (EI) calculated for $[M]^+$ 394.25, found 394.30. FTIR (neat, cm^{-1}): 3057 (m), 3024 (m), 2928 (s), 2855 (m), 1717 (s), 1605 (s), 1278 (s), 1254 (s), 1103 (s), 846 (m), 697 (m)

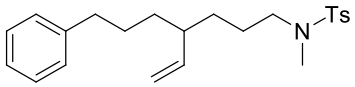

N, 4-dimethyl-N-(7-phenyl-4-vinylheptyl)benzenesulfonamide (1.10): Compound was isolated as a colorless oil (156.5 mg, 81% yield^{1}H NMR (300 MHz, CD_2Cl_2) δ 7.64 (d, *J* = 8.1 Hz, 2H), 7.33 (d, *J* = 8.1 Hz, 2H), 7.30 – 7.22 (m, 2H), 7.22 – 7.12 (m, 3H), 5.59 – 5.44 (m, 1H), 5.04 – 4.91 (m, 2H), 3.03 – 2.80 (m, 2H), 2.71 – 2.48 (m, 5H), 2.42 (s, 3H), 2.08 – 1.91 (m, 1H), 1.73 – 1.14 (m, 8H). ^{13}C NMR (75 MHz, CD_2Cl_2) δ 143.9, 143.4, 143.4, 135.3, 130.2, 128.9, 128.8, 127.9, 126.1, 115.1, 50.7, 44.3, 36.5, 35.2, 35.0, 32.2, 29.7, 25.7, 21.8. GC/MS (EI) calculated for $[M]^+$ 385.21, found 385.25. FTIR (neat, cm^{-1}): 3063 (m), 3026 (m), 2930 (s), 2857 (m), 1639 (w), 1598 (m) 1453 (m), 1342 (s), 1161 (s), 815 (m)

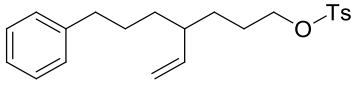

7-phenyl-4-vinylheptyl 4-methylbenzenesulfonate (1.11): Compound was isolated as a colorless oil (154.4 mg, 83% yield). ^{1}H NMR (500 MHz, CD_2Cl_2) δ 7.77 (d, *J* = 7.6 Hz, 2H), 7.37 (d, *J* = 7.7 Hz, 2H), 7.30 – 7.24 (m, 2H), 7.21 – 7.13 (m, 3H), 5.49 – 5.39 (m, 1H), 4.96 (d, *J* = 10.1 Hz, 1H), 4.90 (d, *J* = 17.1 Hz, 1H), 3.98 (t, *J* = 6.2 Hz, 2H), 2.64 – 2.49 (m, 2H), 2.44 (s, 3H), 1.95 – 1.84 (m, 1H), 1.71 – 1.43 (m, 4H), 1.43 – 1.30 (m, 2H), 1.30 – 1.12 (m, 2H). ^{13}C NMR (75 MHz, CD_2Cl_2) δ 145.5, 143.4, 142.9, 133.8, 130.4, 128.9, 128.8, 128.4, 126.2, 115.4, 71.5, 44.1, 36.4, 35.1, 31.0, 29.6, 27.2, 21.9. GC/MS (EI) calculated for $[M]^+$ 372.18, found 372.25. FTIR (neat, cm^{-1}): 3064 (m), 3026 (m), 2929 (s), 2856 (m), 1598 (m), 1452 (m), 1360 (s), 1176 (s), 922 (m), 663 (m)

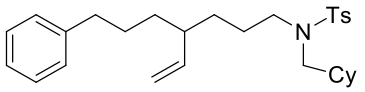

N-(cyclohexylmethyl)-4-methyl-N-(7-phenyl-4-vinylheptyl)benzenesulfonamide (1.12): Compound was isolated as a colorless oil after HPLC. (NMR yield of the reaction was determined to be 89%). ^{1}H NMR (300 MHz, CD_2Cl_2) δ 7.64 (d, *J* = 8.2 Hz, 2H), 7.35 – 7.21 (m, 4H), 7.20 – 7.11 (m, 3H), 5.54 – 5.39 (m, 1H), 5.01 – 4.87 (m, 2H), 3.01 (t, *J* = 7.6 Hz, 2H), 2.88 (d, *J* = 7.4 Hz, 2H), 2.70 – 2.46 (m, 2H), 2.41 (s, 3H), 2.01 – 1.82 (m, 1H), 1.79 – 1.01 (m, 19H), 0.93 – 0.81 (m, 2H). ^{13}C NMR (75 MHz, CD_2Cl_2) δ 143.6, 143.4, 143.3, 137.8, 130.1, 128.9, 128.8, 127.7, 126.1, 115.0, 55.4, 49.5, 44.3, 37.0, 36.5, 35.2, 32.6, 31.4, 29.7, 27.1, 26.7, 26.5, 21.8. GC/MS (EI) calculated for $[M]^+$ 467.29, found 467.35. FTIR (neat, cm^{-1}): 3061 (w), 3025 (w), 2924 (s), 2851 (m), 1639 (w), 1598 (m), 1450 (m), 1156 (s), 813 (m)

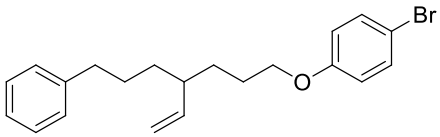

1-bromo-4-((7-phenyl-4-vinylheptyl)oxy)benzene (1.13): Compound was isolated as a white solid (155.2 mg, 83% yield). ^{1}H NMR (500 MHz, CD_2Cl_2) δ 7.40 (d, *J* = 7.8 Hz, 2H), 7.34 – 7.25 (m, 2H), 7.25 – 7.16 (m, 3H), 6.81 (d, *J* = 7.8 Hz, 2H), 5.67 – 5.48 (m, 1H), 5.10 – 4.99 (m, 2H), 3.91 (t, *J* = 6.3 Hz, 2H), 2.71 – 2.54 (m, 2H), 2.15 – 2.00 (m, 1H), 1.88 – 1.77 (m, 1H), 1.77 – 1.64 (m, 2H), 1.64 – 1.53 (m, 2H), 1.53 – 1.44 (m, 1H), 1.44 – 1.28 (m, 2H). ^{13}C NMR (126 MHz, CD_2Cl_2) δ 158.9, 143.4, 132.7, 128.9, 128.8, 126.1, 116.8, 115.2, 112.9, 68.8, 44.4, 36.5, 35.2, 31.7, 29.8, 27.5. GC/MS (EI) calculated for $[M]^+$ 372.11, found 372.15. FTIR (neat, cm^{-1}): 3063 (m), 3025 (m), 2932 (s), 2855 (m), 1590 (m), 1488 (s), 1243 (s), 821 (s)

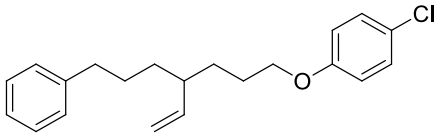

1-chloro-4-((7-phenyl-4-vinylheptyl)oxy)benzene (1.14): Compound was isolated as a white solid (144.9 mg, 88% yield). ^{1}H NMR (300 MHz, CD_2Cl_2) δ 7.39 – 7.10 (m, 7H), 6.86 (d, *J* = 8.9 Hz, 2H), 5.70 – 5.48 (m, 1H), 5.13 – 4.96 (m, 2H), 3.92 (t, *J* = 6.5 Hz, 2H), 2.78 – 2.47 (m, 2H), 2.17 – 1.95 (m, 1H), 1.95 – 1.23 (m, 8H). ^{13}C NMR (75 MHz, CD_2Cl_2) δ 158.5, 143.5, 129.8, 129.0, 128.8, 126.2, 125.7, 116.4, 115.2, 69.0, 44.5, 36.6, 35.3, 31.8, 29.8, 27.6. GC/MS (EI) calculated for $[M]^+$ 328.16, found 328.20. FTIR (neat, cm^{-1}): 3063 (m), 2929 (s), 2855 (m), 1597(m), 1494 (S), 1092 (m), 748 (m)

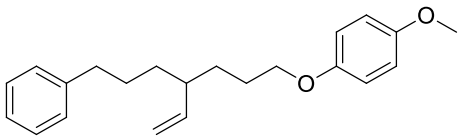

1-methoxy-4-((7-phenyl-4-vinylheptyl)oxy)benzene (1.15): Compound was isolated as a colorless oil (147.6 mg, 91% yield). ^{1}H NMR (300 MHz, C_6D_6) δ 7.24 – 7.18 (m, 2H), 7.14 – 7.04 (m, 3H), 6.89 – 6.74 (m, 4H), 5.50 – 5.32 (m, 1H), 5.07 – 4.82 (m, 2H), 3.66 (t, *J* = 6.4 Hz, 2H), 3.35 (s, 3H), 2.62 – 2.32 (m, 2H), 1.97 – 1.78 (m, 1H), 1.78 – 1.07 (m, 8H). ^{13}C NMR (126 MHz, $CDCl_3$) δ 153.9, 153.9, 142.9, 142.8, 128.5, 128.4, 125.8, 115.6, 114.9, 114.8, 68.9, 55.9, 44.0, 36.2, 34.8, 31.4, 29.2, 27.3. GC/MS (EI) calculated for $[M]^+$ 324.21, found 324.30. FTIR (neat, cm^{-1}): 3063 (m), 3025 (m), 2935 (s), 2857 (s), 1639 (m), 1602 (m), 1504 (s), 1441 (s), 1230 (s), 1041 (s), 910 (s), 730 (s), 699 (s)

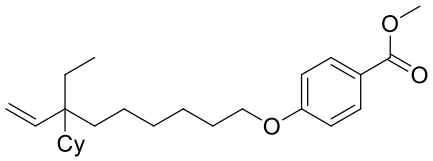

methyl 4-((7-cyclohexyl-7-ethylnon-8-en-1-yl)oxy)benzoate (1.16): Compound was isolated as a colorless oil (154.0 mg, 80% yield). ^{1}H NMR (500 MHz, $CDCl_3$) δ 7.97 (d, *J* = 8.7 Hz, 2H), 6.90 (d, *J* = 8.8 Hz, 2H), 5.65 (dd, *J* = 17.8, 11.1 Hz, 1H), 5.05 (d, *J* = 11.1 Hz, 1H), 4.83 (d, *J* = 17.8 Hz, 1H), 4.00 (t, *J* = 6.5 Hz, 2H), 3.87 (s, 3H), 1.85 – 1.57 (m, 8H), 1.51 – 1.29 (m, 8H), 1.27 – 1.01 (m, 7H), 0.98 – 0.87 (m, 2H), 0.74 (t, *J* = 7.4 Hz, 3H). ^{13}C NMR (126 MHz, $CDCl_3$) δ 167.0, 163.1, 144.5, 131.7, 122.5, 114.2, 113.0, 68.3, 51.9, 44.1, 43.7, 32.6, 30.5, 29.3, 27.4, 27.4, 27.3, 27.2, 26.9, 26.2, 25.3, 23.3, 8.0. GC/MS (EI) calculated for $[M]^+$ 386.57, found 386.50 FTIR (neat, cm^{-1}): 3060 (m), 2960 (s), 2924 (s), 2850 (s), 1720 (s), 1604 (s), 1510 (s), 1434 (s), 1279 (s), 1255 (s), 1103 (s), 770 (s),

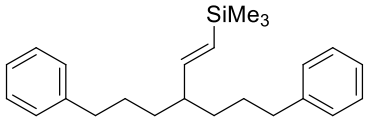

(E)-trimethyl(6-phenyl-3-(3-phenylpropyl)hex-1-en-1-yl)silane (1.17): Compound was isolated as a colorless oil (147.8 mg, 84% yield). ^{1}H NMR (500 MHz, CD_2Cl_2) δ 7.32 – 7.24 (m 4H), 7.22 – 7.13 (m, 6H), 5.74 (dd, *J* = 18.5, 8.1 Hz, 1H), 5.62 (d, *J* = 18.6 Hz, 1H), 2.68 – 2.50 (m, 4H), 2.12 – 2.01 (m, 1H), 1.68 – 1.48 (m, 4H), 1.48 – 1.36 (m, 2H), 1.35 – 1.23 (m, 2H), 0.08 (s, 9H). ^{13}C NMR (75 MHz, CD_2Cl_2) δ 151.9, 143.6, 130.4, 129.0, 128.8, 126.1, 47.1, 36.5, 35.0, 29.7, -0.8. GC/MS (EI) calculated for $[M]^+$ 350.24, found 350.30. FTIR (neat, cm^{-1}): 3085 (m), 3062 (m), 3026 (m), 2929 (s), 2855 (m), 1939 (w), 1869 (w), 1799 (w), 1734 (w), 1614 (m), 1495 (m), 1453 (m), 1246 (m), 866 (m), 837 (m)

1.4.6 *Synthesis and Characterization of Allenes*

General method for the synthesis of allene substrates 1.2, 1.28-1.31 and 1.34

A reaction flask charged with a stir bar was flame-dried under vacuum and allowed to cool under nitrogen. Paraformaldehyde (2.5 equiv), dioxane (volume to make the reaction 0.1 M with respect to the alkyne), alkyne (1.0 equiv), dicyclohexylamine (1.8 equiv), and CuI (0.5 equiv) were added sequentially to the reaction flask. The reaction flask was then equipped with a reflux condenser and protected from light with aluminum foil. The reaction mixture was stirred under reflux overnight. Then the reaction was cooled to room temperature, diluted with water and 2 mL ammonium hydroxide and extracted with ether (3 x 50 mL). The combined organic layers were washed with brine, dried over magnesium sulfate and concentrated under reduced pressure. The resulting oil was purified by flash chromatography.

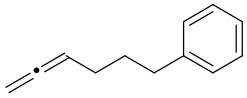

hexa-4,5-dien-1-ylbenzene (1.2): Compound was isolated as a colorless oil (2300 mg, 73% yield). It is a known compound and spectral data match the reported literature values.[60]

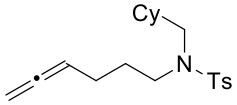

N-(cyclohexylmethyl)-N-(hexa-4,5-dien-1-yl)-4-methylbenzenesulfonamide (1.28): Compound was isolated as a colorless oil. ^{1}H NMR (300 MHz, $CDCl_3$) δ 7.67 (d, *J* = 8.2 Hz, 2H), 7.28 (d, *J* = 8.1 Hz, 2H), 5.06 (p, *J* = 6.6 Hz, 1H), 4.67 (dt, *J* = 6.6, 3.3 Hz, 2H), 3.16 – 3.03 (m, 2H), 2.91 (d, *J* = 7.4 Hz, 2H), 2.41 (s, 3H), 2.02 – 1.89 (m, 2H), 1.80 – 1.48 (m, 8H), 1.31 – 1.07 (m, 3H), 0.95 – 0.78 (m, 2H). ^{13}C NMR (75 MHz, $CDCl_3$) δ 208.8, 143.0, 137.4, 129.6, 127.4,

89.2, 75.4, 55.3, 48.8, 36.8, 31.1, 28.0, 26.7, 26.0, 25.6, 21.6. GC/MS (EI) calculated for $[M]^+$ 347.19, found 347.20. FTIR (neat, cm-1): FTIR (neat, cm^{-1}): 3066 (w), 3028 (w), 2922 (s), 2850 (s), 1955 (m), 1598 (m), 1449 (m), 1339 (s), 1156 (s), 1091 (m), 841 (m), 814 (m), 737 (m), 655 (s)

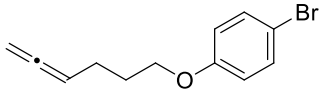

1-bromo-4-(hexa-4,5-dien-1-yloxy)benzene (1.29): Compound was isolated as a colorless oil. ^1H NMR (300 MHz, $CDCl_3$) δ 7.36 (d, *J* = 8.9 Hz, 2H), 6.78 (d, *J* = 8.9 Hz, 2H), 5.15 (p, *J* = 6.6 Hz, 1H), 4.70 (dt, *J* = 6.6, 3.3 Hz, 2H), 3.96 (t, *J* = 6.4 Hz, 2H), 2.24 – 2.12 (m, 2H), 1.96 – 1.85 (m, 2H). ^{13}C NMR (75 MHz, $CDCl_3$) δ 208.9, 158.4, 132.4, 116.6, 112.9, 89.3 75.4, 67.6, 28.6, 24.7. GC/MS (EI) calculated for $[M]^+$ 252.01, found 252.05. FTIR (neat, cm^{-1}): 3094 (w), 3037 (w), 2943 (m), 2871 (m), 1955 (m), 1591 (m), 1577 (m), 1489 (s), 1469 (m), 1244 (s), 844 (m), 820 (m)

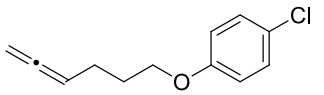

1-chloro-4-(hexa-4,5-dien-1-yloxy)benzene (1.30): Compound was isolated as a colorless oil. ^1H NMR (300 MHz, $CDCl_3$) δ 7.22 (d, *J* = 8.9 Hz, 2H), 6.82 (d, *J* = 8.9 Hz, 2H), 5.16 (p, *J* = 6.6 Hz, 1H), 4.70 (dt, *J* = 6.6, 3.3 Hz, 2H), 3.97 (t, *J* = 6.3 Hz, 2H), 2.29 – 2.08 (m, 2H), 2.00 – 1.80 (m, 2H). ^{13}C NMR (75 MHz, $CDCl_3$) δ 208.7, 157.8, 129.4, 125.5, 115.9, 89.3, 75.5, 67.6, 28.6, 24.7. GC/MS (EI) calculated for $[M]^+$ 208.07, found 208.10. FTIR (neat, cm^{-1}): 3103 (w), 3040 (w), 2945 (m), 2871 (m), 1955 (m), 1596 (m), 1580 (m), 1492 (s), 1471 (m), 1244 (s), 846 (m), 823 (m)

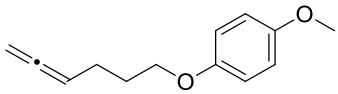

1-(hexa-4,5-dien-1-yloxy)-4-methoxybenzene (1.31): Compound was isolated as a colorless oil. ^{1}H NMR (300 MHz, C_6D_6) δ 6.86 – 6.67 (m, 4H), 5.03 (p, *J* = 6.7 Hz, 1H), 4.60 (dt, *J* = 6.7, 3.3 Hz, 2H), 3.65 (t, *J* = 6.3 Hz, 2H), 3.35 (s, 3H), 2.17 – 1.94 (m, 2H), 1.84 – 1.61 (m, 2H). ^{13}C NMR (126 MHz, $CDCl_3$) δ 208.7, 153.9, 153.4, 115.6, 114.7, 89.4, 75.3, 67.9, 55.8, 28.8, 24.7. GC/MS (EI) calculated for $[M]^+$ 204.12, found 204.20. FTIR (neat, cm^{-1}): 3046 (w), 2992 (m), 2947 (s), 2869 (s), 2833 (s), 1955 (s), 1511 (s), 1467 (s), 1441 (s), 1241 (s), 1041 (s), 825 (s), 741 (m), 728 (m)

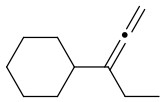

penta-1,2-dien-3-ylcyclohexane (1.32): Under air, to a solution of 2-pentyn-1-ol (1.68 g, 20.0 mmol, 1 equiv) in Et_2O (40 mL) at 0 °C, were added p-toluenesulfonyl chloride (4.58 g, 24.0 mmol, 1.2 equiv) and crushed KOH (7.87 g, 140.0 mmol, 7 equiv) in this order. The resulting mixture was stirred for 45 min in the ice-bath before being poured into ice water. The mixture was extracted with Et_2O (40 mL × 3), and then the combined organic layers were dried over $MgSO_4$, filtered and evaporated to give the propargyl tosylate as a slightly yellow oil. This was then added to a dried 300-mL 2-neck flask along with CuBr (286.9 mg, 2.0 mmol, 0.10 equiv) and THF (40 mL). The mixture was cooled to –40 °C, and 2.0 M CyMgCl in Et_2O (11 mL, 22.0 mmol, 1.10 equiv) was added dropwise over 1 h. The resulting mixture was stirred for 3.5 h before being quenched by NH_4Cl aq. (150 mL). The aqueous layer was extracted with Et_2O (50 mL × 3). The combined organic layers were dried over $MgSO_4$, filtered and concentrated under reduced pressure. The residue was purified by flash chromatography to give **S5** as a colorless liquid. ^{1}H NMR (300 MHz,

$CDCl_3$) δ 4.69 (dd, *J* = 5.7, 3.3 Hz, 2H), 2.02 – 1.89 (m, 2H), 1.81 – 1.64 (m, 5H), 1.37 – 1.06 (m, 6H), 1.00 (t, *J* = 7.4 Hz, 3H). ^{13}C NMR (75 MHz, $CDCl_3$) δ 205.4, 110.7, 76.8, 40.4, 32.4, 26.8, 26.6, 23.4, 12.5. GC/MS (EI) calculated for $[M]^+$ 150.14, found 150.10. FTIR (neat, cm^{-1}): 2965 (s), 2925 (s), 2851 (s), 1952 (m), 1714 (m), 1448 (s), 842 (s)

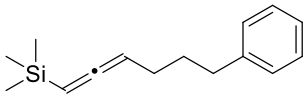

trimethyl(6-phenylhexa-1,2-dien-1-yl)silane (1.33): was synthesized by adapting a known procedure and isolated as a colorless oil.[61] ^{1}H NMR (300 MHz, $CDCl_3$) δ 7.34 – 7.25 (m, 2H), 7.24 – 7.13 (m, 3H), 4.94 (dt, *J* = 7.1, 3.7 Hz, 1H), 4.81 (q, *J* = 6.8 Hz, 1H), 2.72 – 2.61 (m, 2H), 2.03 (qd, *J* = 7.1, 3.7 Hz, 2H), 1.81 – 1.66 (m, 3H), 0.11 (s, 9H). ^{13}C NMR (75 MHz, $CDCl_3$) δ 210.2, 142.7, 128.6, 128.4, 125.8, 83.2, 82.9, 35.5, 31.5, 27.5, -0.7. GC/MS (EI) calculated for $[M]^+$ 230.15, found 230.20. FTIR (neat, cm^{-1}): 3084 (w), 3062 (m), 3026 (m), 2956 (s), 2860 (m), 2170 (w), 1937 (s), 1718 (m), 1675 (s), 1496 (m), 1453 (m), 1248 (s), 842 (s), 759 (m), 698 (m)

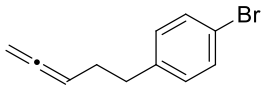

1-bromo-4-(penta-3,4-dien-1-yl)benzene (**1.34)**: Compound was isolated as a colorless oil. ^{1}H NMR (300 MHz, $CDCl_3$) δ 7.40 (d, *J* = 8.2 Hz, 2H), 7.07 (d, *J* = 8.2 Hz, 2H), 5.12 (p, *J* = 6.6 Hz, 1H), 4.68 (dt, *J* = 6.6, 3.1 Hz, 2H), 2.69 (t, *J* = 7.7 Hz, 2H), 2.36 – 2.23 (m, 2H). ^{13}C NMR (75 MHz, $CDCl_3$) δ 208.8, 140.8, 131.5, 130.4, 119.8, 89.2, 75.4, 34.9, 29.8. GC/MS (EI) calculated for $[M]^+$ 222.00, found 222.00. FTIR (neat, cm^{-1}): 3023 (w), 2981 (w), 2923 (m), 2857 (m), 1954 (s), 1488 (s), 1440 (m), 1072 (s), 1011 (s), 845 (s), 801 (s)

1.4.7 *Synthesis and Characterization of Alkyne Starting Materials*

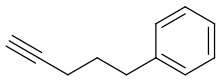

pent-4-yn-1-ylbenzene (1.35): was purchased from GSF Chemicals and used directly.

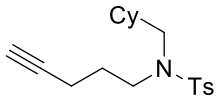

N-(cyclohexylmethyl)-4-methyl-N-(pent-4-yn-1-yl)benzenesulfonamide (1.36): A reaction flask charged with a stir bar was flame-dried under vacuum and allowed to cool under nitrogen. To the reaction flask were added cyclohexanecarboxaldehyde (1.12 g, 10.0 mmol, 1 equiv), 4-pentyn-1-amine (997.6 mg, 12 mmol, 1.2 equiv), sodium triacetoxyborohydride (3.39 g, 16.0 mmol, 1.6 equiv), acetic acid (571.9 µL, 10 mmol, 1.0 equiv) and DCE (50 mL). The reaction was monitored by TLC and after completion, the mixture was filtered through sequential plugs of celite and alumina. The filtrate was concentrated under reduced pressure and used in the next step without further purification. The crude oil along with tosyl chloride (5.34 g, 28.0 mmol, 2.5 equiv), TMPDA (4.67 g, 28.0 mmol, 2.5 equiv) and DCM (45 mL) were added to a flame-dried reaction flask and stirred at room temperature and the reaction was monitored by TLC. After completion, the reaction was quenched with DMEDA (1.83 µL, 16.8 mmol, 1.5 equiv) and filtered through celite. The solution was then washed with water, dried over $MgSO_4$ and concentrated under reduced pressure. The resulting oil was used to make the allene without further purification.

Compounds **1.37-1.39** were prepared using the following procedure. A reaction flask charged with a stir bar was flame-dried under vacuum and allowed to cool under nitrogen. The flask was then charged with triphenylphosphine (1.2 equiv), phenol (1.1 equiv), THF (final concentration of

alkyne was 0.1 M) and terminal alkyne (1.0 equiv). The reaction mixture was cooled to 0 °C with an ice bath. To the cooled reaction mixture was added DIAD (1.2 equiv) dropwise. The reaction mixture was allowed to warm to room temperature and stirred overnight. The THF was removed under reduced pressure and the mixture was suspended in hexane and stirred vigorously for 30 min. The solid triphenylphosphine oxide was removed by filtration through a plug of celite. The solvent was removed under reduced pressure and the crude product was purified by flash chromatography or carried on directly to the allene.

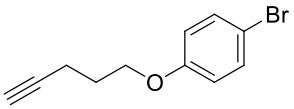

1-bromo-4-(pent-4-yn-1-yloxy)benzene (1.37): is a known compound and spectral data match the reported literature values.[62]

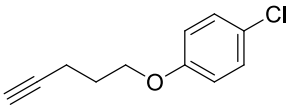

1-Chloro-4-(pent-4-yn-1-yloxy)benzene (1.38): was isolated as a colorless oil. ^{1}H NMR (300 MHz, C_6D_6) δ 7.04 (d, *J*= 9.0 Hz, 2H), 6.45 (d, *J*= 9.0 Hz, 2H), 3.45 (t, *J*= 6.2 Hz, 2H), 2.04 (td, *J*= 7.0, 2.7 Hz, 2H), 1.72 (t, *J*= 2.7 Hz, 1H), 1.65 – 1.49 (m, 2H). ^{13}C NMR (126 MHz, $CDCl_3$) δ 157.7, 129.4, 125.7, 116.0, 83.4, 69.1, 66.6, 28.2, 15.3. GC/MS (EI) calculated for $[M]^+$ 194.05, found 194.10. FTIR (neat, cm^{-1}): 3292 (s), 3066 (w), 3037 (w), 2118 (w), 1774 (m), 1596 (m), 1581 (m), 1497 (s), 1470 (s), 1243 (s), 824 (m)

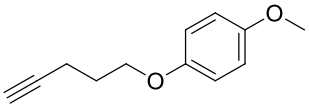

1-methoxy-4-(pent-4-yn-1-yloxy)benzene (1.39): is a known compound and spectral data match the reported literature values.[63]

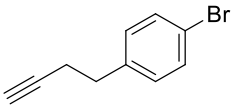

1-bromo-4-(but-3-yn-1-yl)benzene (1.40): was synthesized using an adapted procedure.[64] **1.40** is a known compound and spectral data match the reported literature values.[65]

1.4.8 *Synthesis and Characterization of Alkyl Triflates*

A reaction flask charged with a stir bar was flame-dried under vacuum and allowed to cool under nitrogen. To the flask was then added alcohol (1.0 equiv), DCM (volume to make the reaction 1.0 M with respect to the alcohol), and 2,6-lutidine (1.6 equiv). The mixture was cooled to -78 °C with a dry ice acetone bath. Triflic anhydride (1.2 equiv) was added dropwise to the cooled mixture while stirring. The reaction progress was monitored by TLC and when full conversion of the alcohol had occurred, the cold mixture was poured into hexanes (3x the reaction volume) in an Erlenmeyer flask. The mixture was immediately poured onto a silica plug and the plug was washed with a mixture of hexanes and ethyl acetate that moved the product to Rf 0.5. The clean fractions from the silica gel plug were concentrated under reduced pressure and used without further purification.

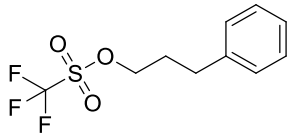

3-phenylpropyl trifluoromethanesulfonate (1.1): Compound was isolated as a colorless oil. ^{1}H NMR (300 MHz, C_6D_6) δ 7.14 – 6.98 (m, 3H), 6.80 (d, *J* = 7.1 Hz, 2H), 3.76 (t, *J* = 6.2 Hz, 2H), 2.16 (t, *J* = 7.5 Hz, 2H), 1.46 – 1.23 (m, 2H).

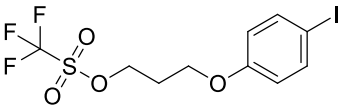

3-(4-iodophenoxy)propyl trifluoromethanesulfonate (1.41): Compound was isolated as a white solid. ^{1}H NMR (300 MHz, C_6D_6) δ 7.36 (d, *J* = 8.5 Hz, 2H), 6.20 (d, *J* = 8.5 Hz, 2H), 3.94 (t, *J* = 6.1 Hz, 2H), 3.09 (t, *J* = 5.8 Hz, 2H), 1.40 – 1.19 (m, 2H).

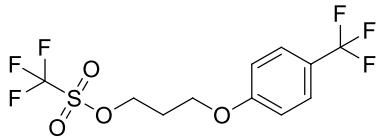

3-(4-(trifluoromethyl)phenoxy)propyl trifluoromethanesulfonate (1.42): Compound was isolated as a white solid. ^{1}H NMR (300 MHz, C_6D_6) δ 7.30 (d, *J* = 8.6 Hz, 2H), 6.40 (d, *J* = 8.6 Hz, 2H), 3.93 (t, *J* = 6.0 Hz, 2H), 3.12 (t, *J* = 5.8 Hz, 2H), 1.40 – 1.21 (m, 2H).

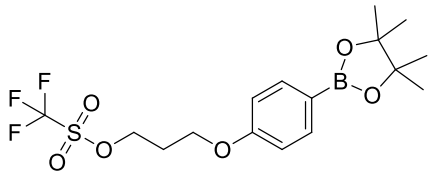

3-(4-(4,4,5,5-tetramethyl-1,3,2-dioxaborolan-2-yl)phenoxy)propyl trifluoromethanesulfonate (1.43): Compound was isolated as a white solid. ^{1}H NMR (300 MHz, C_6D_6) δ 8.16 (d, *J* = 8.6 Hz, 2H), 6.71 (d, *J* = 8.6 Hz, 2H), 3.96 (t, *J* = 6.4 Hz, 2H), 3.21 (t, *J* = 5.8 Hz, 2H), 1.40 – 1.27 (m, 2H), 1.15 (s, 12H).

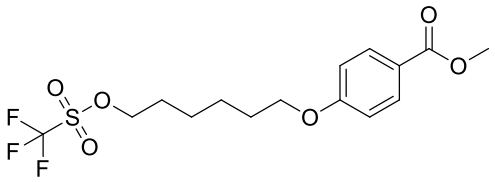

methyl 4-((6-(((trifluoromethyl)sulfonyl)oxy)hexyl)oxy)benzoate (1.44): is a known compound and spectral data match the reported literature values. [66]

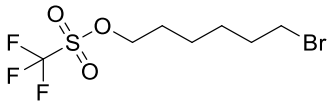

6-bromohexyl trifluoromethanesulfonate (1.45): is a known compound and spectral data match the reported literature values.[48]

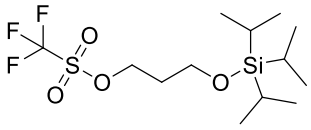

3-((triisopropylsilyl)oxy)propyl trifluoromethanesulfonate (1.46): is a known compound and spectral data match the reported literature values.[64]

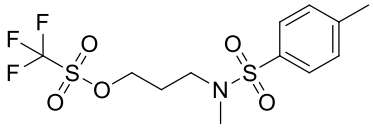

3-(N,4-dimethylphenylsulfonamido)propyl trifluoromethanesulfonate (1.47): Compound was isolated as a colorless oil. ^{1}H NMR (300 MHz, $CDCl_3$) δ 7.67 (d, *J* = 8.0 Hz, 2H), 7.34 (d, *J* = 8.0 Hz, 2H), 4.67 (t, *J* = 6.2 Hz, 2H), 3.11 (t, *J* = 6.6 Hz, 2H), 2.76 (s, 3H), 2.44 (s, 3H), 2.24 – 1.97 (m, 2H).

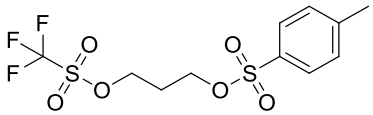

3-(((trifluoromethyl)sulfonyl)oxy)propyl 4-methylbenzenesulfonate (1.48): Compound was isolated as a colorless oil. ^{1}H NMR (300 MHz, C_6D_6) δ 7.74 (d, *J* = 7.8 Hz, 2H), 6.75 (d, *J* = 7.8 Hz, 2H), 3.97 (t, *J* = 6.1 Hz, 2H), 3.28 (t, *J* = 5.8 Hz, 2H), 1.86 (s, 3H), 1.52 – 1.40 (m, 2H).

1.4.9 *Synthesis and Characterization of Alcohol Starting Materials*

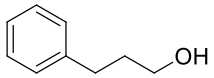

3-phenylpropan-1-ol (1.49): was purchased from Alpha Aeser and used directly.

Compounds **1.50-1.53** were made using the same procedure as **1.37-1.39** using **1.55** or mono TBS protected hexane diol as the starting material instead of the alkyne and was followed immediately by 1M TBAF in THF (2 equiv) deprotection to yield the compounds.

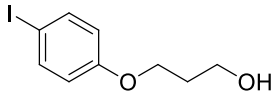

3-(4-iodophenoxy)propan-1-ol (1.50): is a known compound and spectral data match the reported literature values.[67]

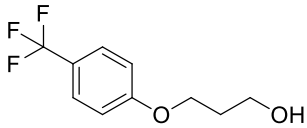

3-(4-(trifluoromethyl)phenoxy)propan-1-ol (1.51): Compound was isolated as a pale yellow oil ^{1}H NMR (300 MHz, $CDCl_3$) δ 7.54 (d, *J* = 8.7 Hz, 2H), 6.96 (d, *J* = 8.7 Hz, 2H), 4.15 (t, *J* = 6.0 Hz, 2H), 3.86 (t, *J* = 6.0 Hz, 2H), 2.06 (p, *J* = 6.0 Hz, 2H), 1.81 (s, 1H). ^{13}C NMR (126 MHz,

$CDCl_3$) δ 161.5, 128.5, 127.0 (q, *J* = 3.8 Hz), 124.6 (dd, *J* = 541.0, 271.9 Hz), 123.1 (dd, *J* = 64.3, 31.6 Hz), 114.6, 65.7, 60.0, 32.0. GC/MS (EI) calculated for $[M]^+$ 220.07, found 220.10. FTIR (neat, cm^{-1}): 3349 (b), 3084 (w), 3056 (w), 2955 (s), 2884 (s), 1615 (s), 1519 (s), 1330 (s), 1258 (s), 1160 (s), 1109 (s), 1068 (s), 835 (s)

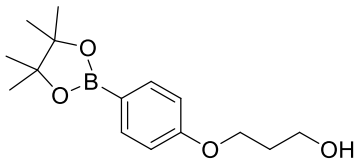

3-(4-(4,4,5,5-tetramethyl-1,3,2-dioxaborolan-2-yl)phenoxy)propan-1-ol (1.52): Compound was isolated as a colorless oil. ^1H NMR (500 MHz, $CDCl_3$) δ 7.74 (d, *J* = 8.2 Hz, 2H), 6.90 (d, *J* = 8.2 Hz, 2H), 4.15 (t, *J* = 6.0 Hz, 2H), 3.87 (t, *J* = 6.0 Hz, 2H), 2.05 (p, *J* = 6.0 Hz, 2H), 1.62 (s, 1H), 1.33 (s, 12H). ^{13}C NMR (126 MHz, $CDCl_3$) δ 161.4, 136.5, 113.9, 83.6, 65.5, 60.5, 32.0, 24.9, 21.9. GC/MS (EI) calculated for $[M]^+$ 278.17, found 278.20. FTIR (neat, cm^{-1}): 3399 (b), 3037 (w), 2977 (s), 2932 (s), 2881 (m), 1716 (m), 1605 (s), 1361 (s), 1090 (m), 1059 (m), 860 (m), 833 (m)

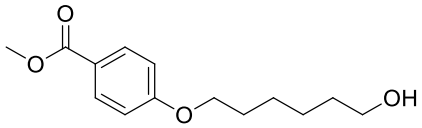

methyl 4-((6-hydroxyhexyl)oxy)benzoate (1.53): is a known compound and spectral data match the reported literature values. [66]

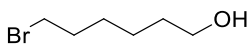

6-bromohexan-1-ol (1.54): was purchased from TCI America and was used directly.

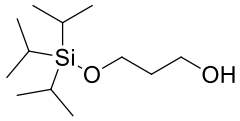

3-((triisopropylsilyl)oxy)propan-1-ol (1.55): is a known compound and spectral data match the reported literature values.[68]

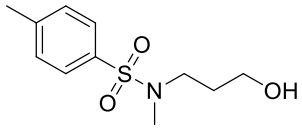

N-(3-hydroxypropyl)-N,4-dimethylbenzenesulfonamide (1.56): is a known compound and spectral data match the reported literature values.[69] **1.56** was prepared using the same procedure as **1.50-1.53** using N,4-dimethylbenzenesulfonamide instead of the phenol and **1.55** instead of the alkyne and was followed immediately by 1 M TBAF in THF (2 equiv) deprotection to yield the clean compound after flash chromatography.

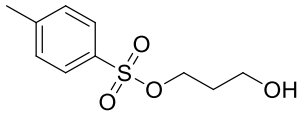

3-hydroxypropyl 4-methylbenzenesulfonate (1.57): is a known compound and spectral data match the reported literature values.[70]

1.4.10 *Catalytic Hydroalkylation of 1,3 Disubstituted Allenes*

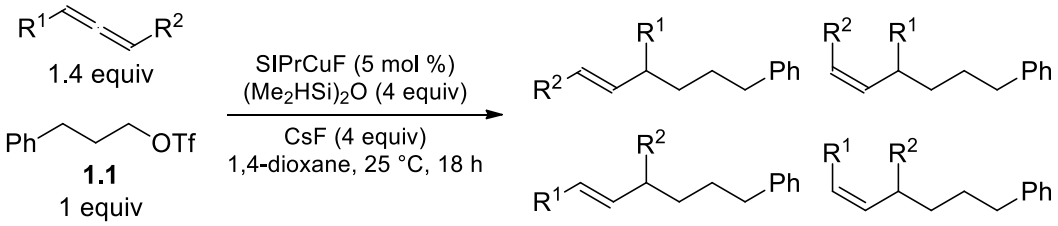

Four different allenes, seen below, were subjected to the standard reaction conditions following the general method for the catalytic hydroalkylation of allenes using **1.1** as the alkyl triflate. The reaction mixtures were analyzed by GC/MS at 18h and then products were isolated when applicable.

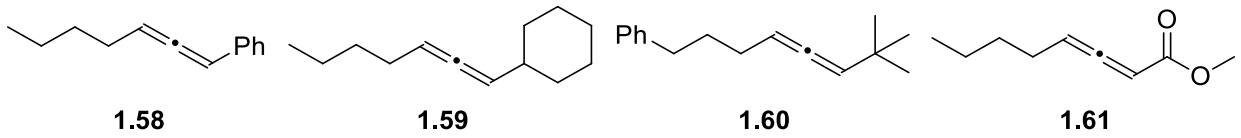

1.58 **1.59** **1.60** **1.61**

R^1 =*n*-butyl, R^2 = phenyl (**1.58**): Compound was found to be a 4:2:3 mixture of 3 of the four possible isomers by GC/MS. Isolation was not attempted. GC/MS (EI) calculated for $[M]^+$ 292.22, found 292.25

R^1 =n butyl, R^2 = cyclohexyl:

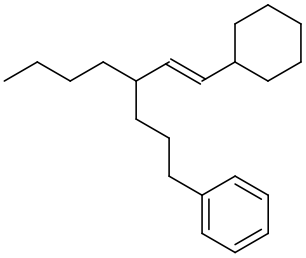

(E)-(4-(2-cyclohexylvinyl)octyl)benzene (**1.59**): Compound was isolated as a colorless oil (40.2 mg, 26% yield, 11:1:1:1 mixture of isomers by GC/MS). Major Isomer: ^{1}H NMR (300 MHz, $CDCl_3$) δ 7.32 – 7.27 (m, 1H), 7.25 – 7.12 (m, 4H), 5.29 (dd, *J* = 15.4, 6.7 Hz, 1H), 5.03 (dd, *J* = 15.4, 8.7 Hz, 1H), 2.68 – 2.45 (m, 2H), 1.99 – 1.80 (m, 2H), 1.80 – 1.55 (m, 8H), 1.45 – 0.98 (m, 15H), 0.86 (t, *J* = 6.8 Hz, 3H). ^{13}C NMR (126 MHz, $CDCl_3$) δ 143.2, 136.5, 132.2, 128.5, 128.3, 125.7, 42.8, 40.9, 36.2, 35.5, 35.4, 33.6, 29.6, 29.3, 26.4, 26.3, 22.9, 14.3. GC/MS (EI) calculated for $[M]^+$ 298.27, found 298.30. FTIR (neat, cm^{-1}): 3084 (w), 3062 (w), 2923 (s), 2851 (s), 1604 (m), 1495 (m), 1448 (s), 968 (m), 746 (m)

R^1 =*t*-butyl, R^2 = $PhCH_2CH_2CH_2$ (**1.60**): One of the four isomers was visible by GC/MS, but too small for isolation. A large amount of the starting allene was still present. GC/MS (EI) calculated for $[M]^+$ 334.27, found 334.30

R^1 =n butyl, R^2 = C(O)OMe:

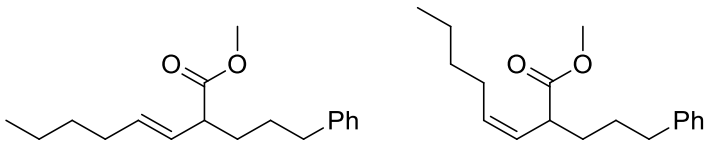

(E)-methyl 2-(3-phenylpropyl)oct-3-enoate (1.61) and **(Z)-methyl 2-(3-phenylpropyl)oct-3-enoate (1.62):** Compounds were isolated as a colorless oil (118.4 mg, 86% yield, 2:1 mixture of isomers by GC/MS). Major isomer: ^{1}H NMR (300 MHz, $CDCl_3$) δ 7.34 – 7.27 (m, 2H), 7.25 (s,

1H), 7.22 – 7.11 (m, 4H), 5.62 – 5.45 (m, 1H), 5.44 – 5.28 (m, 1H), 3.66 (s, 4H), 3.05 – 2.90 (m, 1H), 2.72 – 2.51 (m, 3H), 2.14 – 1.94 (m, 3H), 1.85 – 1.70 (m, 1H), 1.69 – 1.49 (m, 5H), 1.43 – 1.22 (m, 6H), 0.88 (t, J = 7.0 Hz, 4H). ^{13}C NMR (126 MHz, $CDCl_3$) δ 175.2, 142.3, 133.8, 128.5, 128.4, 127.5, 125.9, 51.8, 49.2, 35.7, 32.3, 32.2, 31.5, 29.1, 22.3, 14.0. Minor Isomer: ^{1}H NMR (300 MHz, $CDCl_3$) δ 3.44 – 3.27 (m, 1H) All other peaks are overlapping with the major isomer. ^{13}C NMR (126 MHz, $CDCl_3$) δ 175.1, 142.2, 133.1, 127.3, 43.9, 32.5, 31.8, 29.0, 27.4, 22.4. All other peaks are overlapping with the major isomer. GC/MS (EI) calculated for $[M]^+$ 274.19, found 274.25. FTIR (neat, cm^{-1}) 3084 (w), 3062 (w), 2953 (s), 2928 (s), 2858 (s), 1737 (s), 1603 (m), 1496 (m), 1453 (s), 1434 (s), 1258 (m), 1193 (m), 1157 (m), 748 (m), 698 (m)

1.4.11 *Catalytic Intermediates and Stoichiometric Experiments*

SIPrCu complexes **1.18, 1.19, 1.20, 1.22** and **1.23** have been previously characterized.[49]

1.4.11.1 Competition experiment between **1.1** and **1.2** with SIPrCuH

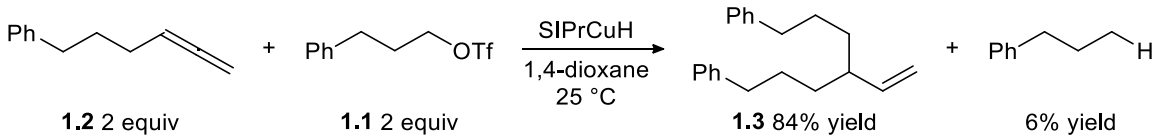

In a nitrogen-filled glovebox SIPrCuF (1 equiv, 11.8 mg, 0.025 mmol) was weighed into a shell vial; to this was added TMB (1 equiv, 4.2 mg 0.025 mmol). A dram vial was charged with **1.1** (2 equiv, 13.4 mg, 0.050 mmol) a stir bar and 50 µL 1,4-dioxane. A 0.10 g/mL solution of **1.2** was prepared and **1.2** (2 equiv, 80 µL, 7.9 mg, 0.050 mmol) was added to the solution of **1.1**. A 0.08 g/mL solution of TMDSO was prepared and TMDSO (2 equiv, 80 µL, 6.7 mg, 0.050 mmol) was added to the solution of **1.1** and **1.2**. SIPrCuF and TMB were suspended in 180µL dioxane.

While stirring the solution of **1.1**, **1.2** and TMDSO at 25 °C, the suspension of SIPrCuF and TMB was added. The shell vial was then rinsed with 3 x 80 µL 1,4-dioxane. After 17 h, 100 µL of the reaction was removed from the glove box and quenched with ethanolamine (5 equiv, 1.5 µL, 0.50 mmol) and diluted with EtOAc (0.5 mL). The resulting mixture was filtered through a plug of silica with excess EtOAc for GC analysis.

1.4.11.2 Isolation of the SIPrCu(allyl) complex (**1.25**)

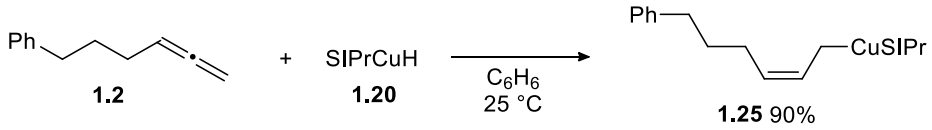

In a nitrogen-filled glovebox, a 20 mL scintillation vial was charged with SIPrCuO*t*-Bu (1.0 equiv, 160 mg, 0.303 mmol) and a stir bar. To this was added benzene (0.30 mL). With the mixture stirring, TMDSO (1 equiv, 40.8 mg,.0303 mmol) was added and the mixture turned into a bright orange solution. **1.2** (2 equiv, 96.0 mg, 0.607 mmol) was added dropwise to the stirring solution. The reaction was stirred for 1 h during which time, the solution gradually became light yellow in color. Pentane (15 mL) was then added to the stirring solution and a white solid precipitated out. The solids were then filtered through a fritted funnel, washed with minimal pentane, collected and dried under vacuum. The white solid (110.3 mg, 90%) was stored at -35 °C under an inert atmosphere. ^{1}H NMR (300 MHz, C_6D_6) δ 7.24 – 7.18 (m, 6H), 7.13 – 7.02 (m, 5H), 6.11 – 5.90 (m, 1H), 4.89 – 4.67 (m, 1H), 3.14 (s, 4H), 3.09 – 2.89 (m, 4H), 2.73 – 2.54 (m, 2H), 2.10 – 1.91 (m, 2H), 1.82 – 1.64 (m, 2H), 1.50 (d, *J* = 6.8 Hz, 12H), 1.36 (d, *J* = 9.0 Hz, 2H), 1.21 (d, *J* = 7.0 Hz, 12H).

Bromo substituted analogue of **1.25** was prepared in the same manner as **1.25** (see reaction below) and the complex (**1.63**) was isolated as a white solid. ^{1}H NMR (300 MHz, C_6D_6) δ 7.31 (d, *J* = 8.3 Hz, 2H), 7.12 (s, 2H), 7.04 (d, *J* = 7.8 Hz, 4H), 6.83 (d, *J* = 8.3 Hz, 2H), 6.15-5.91 (m, 1H), 4.83 – 4.60 (m, 1H), 3.15 (s, 4H), 3.07 – 2.89 (m, 4H), 2.56 – 2.35 (m, 2H), 2.24 – 2.03 (m, 2H), 1.47 (d, *J* = 6.8 Hz, 12H), 1.34 (d, *J* = 9.4 Hz, 2H), 1.20 (d, *J* = 6.9 Hz, 12H).

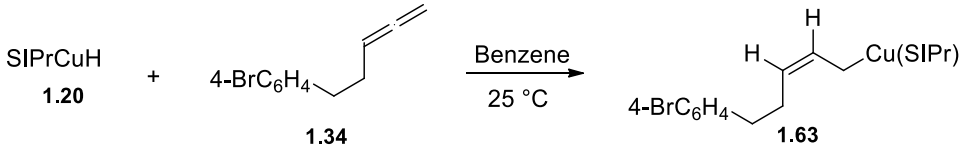

Additionally, a crystal for X-Ray crystallography was obtained by slow diffusion of pentane into a saturated solution of **1.63** in benzene at 25 ºC.

1.4.11.3 Stoichiometric reaction of **1.25** with **1.1**

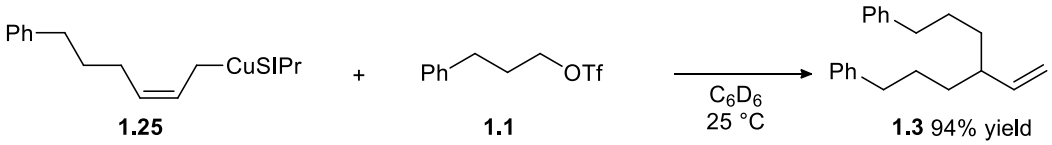

In a nitrogen-filled glovebox, **1.25** (1 equiv, 9.2 mg, 0.015 mmol) was weighed into a dram vial. To this was added TMB (1.51 equiv, 3.8 mg, 0.023 mmol). The solids were dissolved in 150 µL C_6D_6 and transferred to a J. Young NMR tube. The vial was rinsed with 2 x 150 µL C_6D_6. The J. Young NMR tube was capped and removed from the glove box at which time an NMR spectrum was obtained. The J. Young NMR tube was the returned to the glove box. A 0.08 mg/L solution of **1.1** was made in C_6D_6 and **1.1** (2 equiv, 98.1 µL, 8.0 mg, 0.030 mmol) was added to the J. Young NMR tube. The J. Young NMR tube was shaken, removed from the glove box and a time course was taken.

NMR time course of the reaction between **1.25** and **1.1**

min	% Yield of **1.3**
0	0
6	47
14	53
46	68
72	69
82	71
240	87
1020	94

1.4.11.4 Stoichiometric reaction of **1.25** with SIPrCuOTf

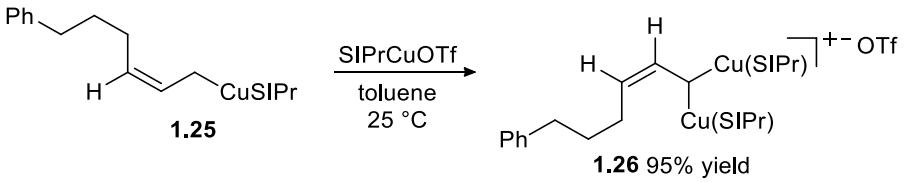

In a nitrogen-filled glovebox, a 20 mL scintillation vial was charged with **1.25** (1.0 equiv, 75.9 mg, 0.124 mmol) and a stir bar. To this was added SIPrCuOTf (1.0 equiv, 74.6 mg 0.124 mmol). Toluene (0.30 mL) was then added and the reaction was stirred at 25 °C for 1 h. After 1 h, toluene was removed under vacuum and the resulting thick oil was triturated with pentane and toluene to give a white solid. The solid was filtered through a fritted funnel, washed with several portions of pentane, collected and dried under vacuum. The white solid (**1.26**) was stored at -35 °C under an inert atmosphere. ^{1}H NMR (500 MHz, C_6D_6) δ 7.29 – 7.21 (m, 2H), 7.13 – 7.07 (m, 4H), 7.07 – 6.92 (m, 10H), 5.77 (bs, 1H), 4.07 – 3.49 (bm, 8H), 3.06 (bs, 8H), 2.27 (bs, 2H), 1.56 – 0.82 (m, 58H).

1.4.11.5 Stoichiometric reaction of **1.2** with dinuclear [(SIPrCu)$_2$(μ-H)]OTf (**1.23**):

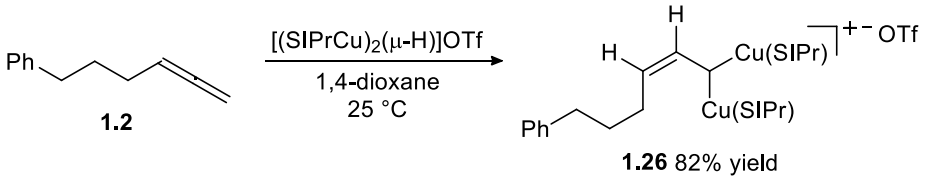

In a nitrogen-filled glovebox, **1.23** (1 equiv, 105.7 mg, 0.100 mmol) was weighed into a dram vial and charged with a stir bar. In a separate dram vial a stock solution of **1.2** (3.75 equiv, 59.3 mg, 0.375 mmol) and TMB (1.25 equiv, 21.0 mg, 0.125 mmol) was made in 500 µL of 1, 4-dioxane to give a 0.12 g/mL and 0.04 g/mL solution of **1.2** and TMB respectively. **1.23** was suspended in 600 µL 1, 4-dioxane. To the stirring solution of **1.23**, was added 400 µL of the stock solution of **1.2** (3.0 equiv, 47.5 mg, 0.300 mmol) and TMB (1 equiv, 16.8 mg, 0.100 mmol). 20 µL aliquots of the reaction were taken at 4, 8 and 19 hours. The aliquots were quenched with 100 µL deoxygenated 1.0M HCl, the resulting solution was diluted with EtOAc, filtered through a silica plug, and analyzed by GC-FID. The yield of **1.26** was determined using the combined yield of the reduced forms of the allene as a proxy. This gave yields of 30%, 76% and 82% after 4, 8, and 19 hours respectively.

1.4.11.6 Stoichiometric reaction between the dinuclear allyl complex (**1.26**) and **1.1** and the related NMR time course:

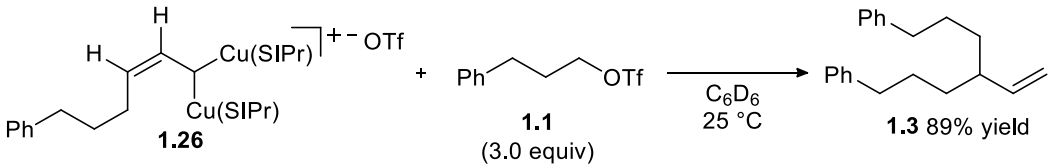

In a nitrogen-filled glovebox, **1.26** (1 equiv, 18.2 mg, 0.015 mmol) was weighed into a dram vial and transferred to a J. Young NMR tube using 3 x 300 µL C_6D_6. To this was added TMB (0.5 equiv, 100µL, 1.3 mg, 0.008 mmol) from a 0.013 g/mL solution of TMB in C_6D_6. The J.

Young NMR tube was capped and removed from the glove box at which time an NMR spectrum was obtained. The J. Young NMR tube was the returned to the glove box. A 0.08 g/mL solution of **1** was made in C_6D_6 and **1** (3 equiv, 100 µL, 8.0 mg, 0.030 mmol) was added to the J. Young NMR tube. The J. Young NMR tube was shaken, removed from the glove box and a time course was taken.

min	% Yield of **1.3**
0	0
7	14
15	11
20	11
30	15
45	21
75	28
150	42
240	53
1160	81
1320	84
1440	84
1680	85
3060	89

1.4.11.7 Crystallization of Dinuclear Complexes

Complex **1.27** and several closely related complexes were prepared according to the following schemes. SIPrCu(allyl) complex (**1.63**) was prepared from **1.34** and SIPrCuH. Two dinuclear complexes, [(SIPrCu)$_2$(µ-allyl)]OTf (**1.27**) and [(SIPrCu)(IPrCu)(µ-allyl)]OTf (**1.64**), were then prepared in a reaction of SIPrCu(allyl) complex (**1.63**) with either IPrCuOTf or SIPrCuOTf. IPrCuOTf (**1.65**) has been previously synthesized and characterized.[48]

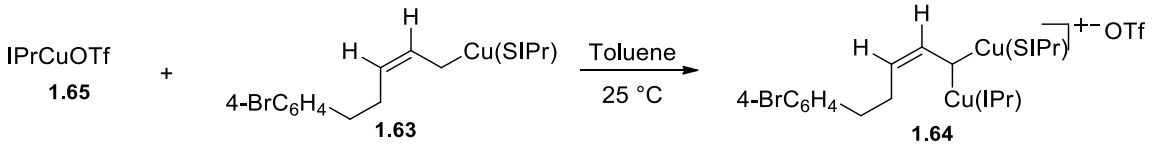

[(SIPrCu)(IPrCu)(μ-allyl)]OTf complex (**1.64):** Compound was isolated as a white solid. ^{1}H NMR (300 MHz, C_6D_6) δ 7.36 (d, *J* = 8.0 Hz, 2H), 7.24 - 7.17 (m, 2H), 7.14 – 7.07 (m, 2H), 7.05 – 6.87 (m, 9H), 6.61 (d, *J* = 8.0 Hz, 2H), 6.03 – 5.65 (m, 1H), 3.96 (s, 4H), 3.39 (bs, 1H), 3.19 – 2.96 (m, 4H), 2.61 – 2.29 (m, 4H), 1.90 (bs, 2H), 1.47 (bs, 2H), 1.35 – 0.98 (m, 50H).

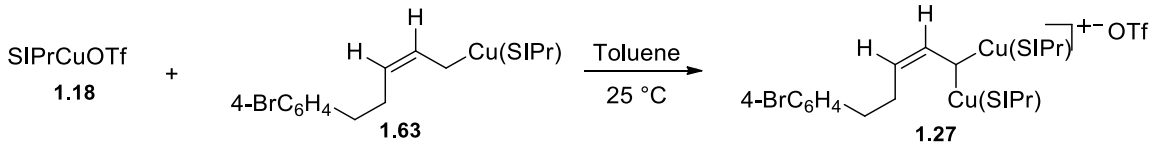

[(SIPrCu)$_2$(μ-allyl)]OTf complex **(27**): Compound was isolated as a white solid.^{1}H NMR (300 MHz, C_6D_6) δ 7.34 (d, *J* = 8.1 Hz, 2H), 7.14 – 6.91 (m, 12H), 6.59 (d, *J* = 8.1 Hz, 2H), 5.90 – 5.69 (m, 1H), 4.03 – 3.66 (m, 8H), 3.36 (bs, 1H), 3.21 - 2.86 (m, 8H), 2.00 – 1.65 (bs, 2H), 1.60 – 1.39 (bs, 2H), 1.39 – 1.13 (m, 51H), 1.05 (d, *J* = 6.7 Hz, 2H).

We attempted crystallization of both complexes **1.27** and **1.64** under a wide range of conditions. However, we were able to obtain crystals suitable for X-ray crystallography only by using samples of complex **1.64**. The crystals for X-ray crystallography were obtained using the following procedure: In the nitrogen-filled glove box, the freshly made **1.64** (13 mg, 0.01 mmol) was put into a dram vial. Minimal volume of benzene (~0.3 mL) was used to fully dissolve the complex and rinse the walls of the vial. The dram vial was then placed into a 20 mL scintillation vial containing ether (5 mL). The scintillation vial was capped placed on a shelf and left alone for

4 days. Leaving crystals for several days post crystal formation resulted in decomposition of **1.64**. According to the results of X-ray analysis described below, the crystal obtained from a sample of **1.64** contained two components. The major component was not the mixed [(SIPrCu)(IPrCu)(μ-allyl)]OTf complex that was expected, but was instead $[(SIPrCu)_2(\mu\text{-allyl})]OTf$. The minor component is either **1.27** or **1. 1.64**. The crystallographic data did not permit the unambiguous assignment of that aspect of the structure and the carbons were left saturated in the ORTEP[80] structure. More details about the X-ray structure of **1.27** are provided in the following section.

1.4.12 *X-Ray Crystallography*

1.4.12.1 SIPrCu(allyl) complex (**1.63**)

A colorless prism, measuring 0.49 x 0.43 x 0.26 mm^3 was mounted on a loop with oil. Data was collected at -173°C on a Bruker APEX II single crystal X-ray diffractometer, Mo-radiation.

Crystal-to-detector distance was 40 mm and exposure time was 45 seconds per frame for all sets. The scan width was 0.5°. Data collection was 100% complete to 25° in ϑ. A total of 61092 reflections were collected covering the indices, -55<=h<=55, -11<=k<=11, -21<=l<=21. 7294 reflections were symmetry independent and the elevated R_{int} = 0.0624 indicating the crystal was of good quality. Indexing and unit cell refinement indicated a primitive monoclinic lattice. The space group was found to be C 2/c (No. 15).

The data was integrated and scaled using SAINT,[71] SADABS[72] within the APEX2[73] software package by Bruker.

Solution by direct methods (SHELXS, SIR97[74,75]) produced a complete heavy atom phasing model consistent with the proposed structure. The structure was completed by difference

Fourier synthesis with SHELXL97.[76–78] Scattering factors are from Waasmair and Kirfel.[79] Hydrogen atoms were placed in geometrically idealized positions and constrained to ride on their parent atoms with C---H distances in the range 0.95-1.00 Angstrom. Isotropic thermal parameters U_{eq} were fixed such that they were $1.2U_{eq}$ of their parent atom Ueq for CH's and $1.5U_{eq}$ of their parent atom U_{eq} in case of methyl groups. All non-hydrogen atoms were refined anisotropically by full-matrix least-squares.

The substrate bound to the metal complex was disordered in two positions.

Table 1.3 summarizes the data collection details. **Figure 1.3** shows an ORTEP[80] of the asymmetric unit.

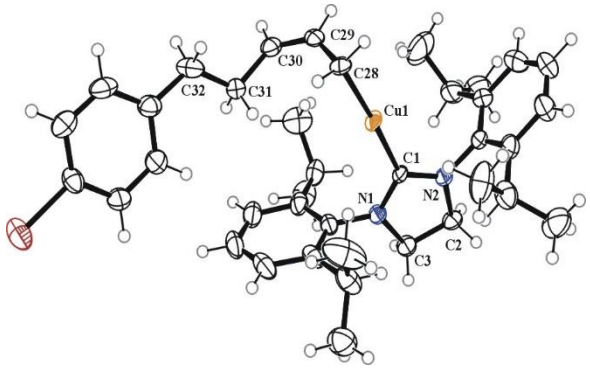

Figure 1.3. ORTEP[80] of the structure of SIPr(allyl)Cu complex **1.63** with thermal ellipsoids at the 50% probability level. Disorder omitted for clarity

Table 1.3: Crystallographic Data: SIPr(allyl)Cu Complex **1.63**.

Empirical formula	C38 H50 Br1 Cu1 N2
Formula weight	678.25
Temperature	100(2) K
Wavelength	0.71073 Å

Crystal system	Monoclinic	
Space group	C 2/c	
Unit cell dimensions	a = 44.365(16)Å	□= 90°.
	b = 9.568(4) Å	□= 99.305(19)°.
	c = 17.076(6) Å	□ = 90°.
Volume	7153(5) $Å^3$	
Z	8	
Density (calculated)	1.260 Mg/m^3	
Absorption coefficient	1.755 mm^{-1}	
F(000)	2848	
Crystal size	0.49 x 0.43 x 0.0.260 mm^3	
Theta range for data collection	1.861 to 26.381°.	
Index ranges	-55<=h<=55, -11<=k<=11, -21<=l<=21	
Reflections collected	61092	
Independent reflections	7294 [R(int) = 0.0624]	
Completeness to theta = 25.00°	100.0 %	
Max. and min. transmission	0.7454 and 0.6577	
Refinement method	Full-matrix least-squares on F^2	

Data / restraints / parameters	7294 / 0 / 410
Goodness-of-fit on F^2	0.995
Final R indices [I>2sigma(I)]	R1 = 0.0477, wR2 = 0.1229
R indices (all data)	R1 = 0.0600, wR2 = 0.1298
Largest diff. peak and hole	1.217 and -0.954 e.$Å^{-3}$

1.4.12.2 [(SIPrCu)$_2$(μ-allyl)]OTf (**1.27**)

A quite small colorless prism, measuring 0.16 x 0.09 x 0.05 mm^3 was mounted on a loop with oil. Data was collected at -173°C on a Bruker APEX II single crystal X-ray diffractometer, Mo-radiation.

Crystal-to-detector distance was 40 mm and exposure time was 240 seconds per frame for all sets. The scan width was 1°. Data collection was 99.2% complete to 25° in ϑ. A total of 107550 reflections were collected covering the indices, -16<=h<=16, -30<=k<=30, -24<=l<=23. 12760 reflections were symmetry independent and the elevated R_{int} = 0.1544 reflected the small sample size. Indexing and unit cell refinement indicated a primitive monoclinic lattice. The space group was found to be P 2_1/c (No.14).

The data was integrated and scaled using SAINT,[71] SADABS[72] within the APEX2[73] software package by Bruker.

Solution by direct methods (SHELXS, SIR97[74,75]) produced a complete heavy atom phasing model consistent with the proposed structure. The structure was completed by difference

Fourier synthesis with SHELXL97.[76–78] Scattering factors are from Waasmair and Kirfel.[79] Hydrogen atoms were placed in geometrically idealized positions and constrained to ride on their parent atoms with C---H distances in the range 0.95-1.00 Angstrom. Isotropic thermal parameters U_{eq} were fixed such that they were $1.2U_{eq}$ of their parent atom Ueq for CH's and $1.5U_{eq}$ of their parent atom U_{eq} in case of methyl groups. All non-hydrogen atoms were refined anisotropically by full-matrix least-squares.

The structure appeared disordered, with a major configuration (83.1(4)%) of asymmetrically bonded Cu, whereas the remainder shows a symmetric configuration. Because of disorder, restraints were needed to stabilize the refinement. Hydrogen atoms were mostly visible in the electron density map. Notable, C63 and C64 appeared as aromatic atoms, C2 and C3 as well as C29 and C30 appeared as methylene with equal electron density on the hydrogen positions similar to all other hydrogen atoms. The minor configuration was tested for a shorter C-C bond between C29B and C30B, but the result was inconclusive and hydrogens were assigned as methylene as well. The OTf appears disordered, mostly in response to disordered ethyl ether, of which the contribution to the diffraction pattern was removed from the structure via SQUEEZE.[81,82]

Table 1.4 summarizes the data collection details. **Figure 1.4** and **Figure 1.5** show ORTEPs[80] of the asymmetric unit of the major and minor configuration, disordered solvent not shown.

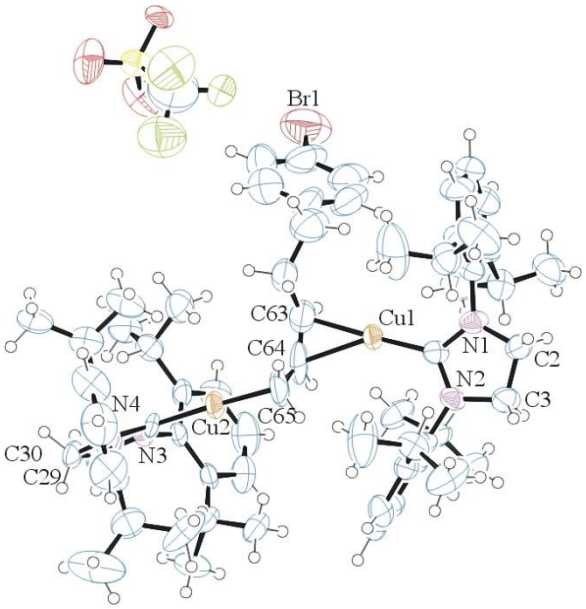

Figure 1.4. ORTEP[80] of the major configuration of [(SIPrCu)$_2$(μ-allyl)]OTf (**1.27**) with thermal ellipsoids at the 50% probability level.

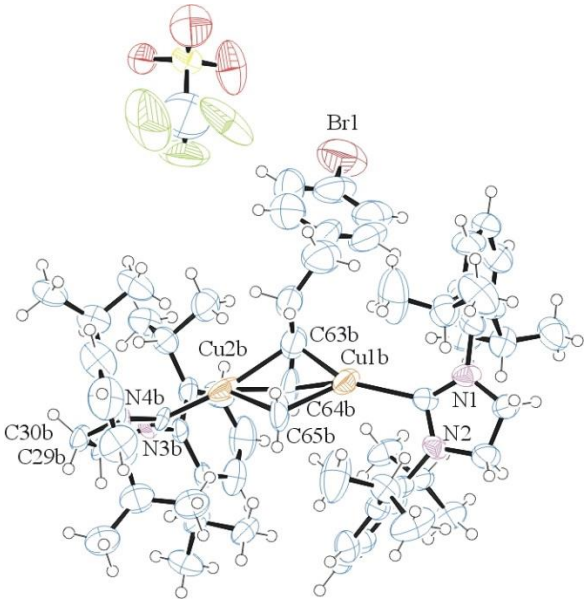

Figure 1.5. ORTEP[80] of the minor configuration of [(SIPrCu)$_2$(μ-allyl)]OTf (**1.27**) with thermal ellipsoids at the 50% probability level.

Table 1.4: Crystallographic Data: $[(SIPrCu)_2(\mu\text{-allyl})]OTf$

Empirical formula	C66 H88 Br Cu2 F3 N4 O3 S	
Formula weight	1281.45	
Temperature	100(2) K	
Wavelength	0.71073 Å	
Crystal system	Monoclinic	
Space group	P 2_1/c	
Unit cell dimensions	a = 14.095(5) Å	□= 90.000(5)°.
	b = 25.360(5) Å	□= 102.528(5)°.
	c = 20.126(5) Å	□ = 90.000(5)°.
Volume	7023(3) $Å^3$	
Z	4	
Density (calculated)	1.212 Mg/m^3	
Absorption coefficient	1.255 mm^{-1}	
F(000)	2688	
Crystal size	0.16 x 0.09 x 0.05 mm^3	
Theta range for data collection	1.31 to 25.35°.	
Index ranges	-16<=h<=16, -30<=k<=30, -24<=l<=23	

Reflections collected	107550
Independent reflections	12760 [R(int) = 0.1544]
Completeness to theta = 25.00°	99.2 %
Max. and min. transmission	0.9399 and 0.8244
Refinement method	Full-matrix least-squares on F^2
Data / restraints / parameters	12760 / 167 / 907
Goodness-of-fit on F^2	0.980
Final R indices [I>2sigma(I)]	R1 = 0.0974, wR2 = 0.2090
R indices (all data)	R1 = 0.2232, wR2 = 0.2579
Largest diff. peak and hole	0.477 and -0.871 e.$Å^{-3}$

1.5 REFERENCES FOR CHAPTER 1

(1) Han, S. B.; Kim, I. S.; Krische, M. J. Enantioselective Iridium-Catalyzed Carbonyl Allylation from the Alcohol Oxidation Level via Transfer Hydrogenation: Minimizing Pre-Activation for Synthetic Efficiency. *Chem. Commun.* **2009**, No. 47, 7278–7287.

(2) Feng, J.; Kasun, Z. A.; Krische, M. J. Enantioselective Alcohol C–H Functionalization for Polyketide Construction: Unlocking Redox-Economy and Site-Selectivity for Ideal Chemical Synthesis. *J. Am. Chem. Soc.* **2016**, *138* (17), 5467–5478.

(3) Oblinger, E.; Montgomery, J. A New Stereoselective Method for the Preparation of Allylic Alcohols. *J. Am. Chem. Soc.* **1997**, *119* (38), 9065–9066.

(4) Miller, K. M.; Huang, W.-S.; Jamison, T. F. Catalytic Asymmetric Reductive Coupling of Alkynes and Aldehydes: Enantioselective Synthesis of Allylic Alcohols and α-Hydroxy Ketones. *J. Am. Chem. Soc.* **2003**, *125* (12), 3442–3443.

(5) Mahandru, G. M.; Liu, G.; Montgomery, J. Ligand-Dependent Scope and Divergent Mechanistic Behavior in Nickel-Catalyzed Reductive Couplings of Aldehydes and Alkynes. *J. Am. Chem. Soc.* **2004**, *126* (12), 3698–3699.

(6) *Metal Catalyzed Reductive C-C Bond Formation: A Departure from Preformed Organometallic Reagents*; Krische, M. J., Ed.; Topics in Current Chemistry; Springer-Verlag: Berlin Heidelberg, 2007; Vol. 279.

(7) Malik, H. A.; Sormunen, G. J.; Montgomery, J. A General Strategy for Regiocontrol in Nickel-Catalyzed Reductive Couplings of Aldehydes and Alkynes. *J. Am. Chem. Soc.* **2010**, *132* (18), 6304–6305.

(8) Patman, R. L.; Chaulagain, M. R.; Williams, V. M.; Krische, M. J. Direct Vinylation of Alcohols or Aldehydes Employing Alkynes as Vinyl Donors: A Ruthenium Catalyzed C−C Bond-Forming Transfer Hydrogenation. *J. Am. Chem. Soc.* **2009**, *131* (6), 2066–2067.

(9) Leung, J. C.; Patman, R. L.; Sam, B.; Krische, M. J. Alkyne–Aldehyde Reductive C□C Coupling through Ruthenium-Catalyzed Transfer Hydrogenation: Direct Regio- and Stereoselective Carbonyl Vinylation to Form Trisubstituted Allylic Alcohols in the Absence of Premetallated Reagents. *Chem. – Eur. J.* **2011**, *17* (44), 12437–12443.

(10) Takai, K.; Sakamoto, S.; Isshiki, T. Regioselective Reductive Coupling of Alkynes and Aldehydes Leading to Allylic Alcohols. *Org. Lett.* **2003**, *5* (5), 653–655.

(11) Ogata, K.; Toh, A.; Shimada, D.; Fukuzawa, S. Nickel-Catalyzed Diastereoselective Reductive Coupling Reaction of Norbornene with Aldehydes in the Presence of Triethylborane. *Chem. Lett.* **2012**, *41* (2), 157–158.

(12) Wang, H.; Lu, G.; Sormunen, G. J.; Malik, H. A.; Liu, P.; Montgomery, J. NHC Ligands Tailored for Simultaneous Regio- and Enantiocontrol in Nickel-Catalyzed Reductive Couplings. *J. Am. Chem. Soc.* **2017**, *139* (27), 9317–9324.

(13) Ngai, M.-Y.; Barchuk, A.; Krische, M. J. Iridium-Catalyzed C−C Bond Forming Hydrogenation: Direct Regioselective Reductive Coupling of Alkyl-Substituted Alkynes to Activated Ketones. *J. Am. Chem. Soc.* **2007**, *129* (2), 280–281.

(14) Zhou, C.-Y.; Zhu, S.-F.; Wang, L.-X.; Zhou, Q.-L. Enantioselective Nickel-Catalyzed Reductive Coupling of Alkynes and Imines. *J. Am. Chem. Soc.* **2010**, *132* (32), 10955–10957.

(15) Yang, Y.; Perry, I. B.; Buchwald, S. L. Copper-Catalyzed Enantioselective Addition of Styrene-Derived Nucleophiles to Imines Enabled by Ligand-Controlled Chemoselective Hydrocupration. *J. Am. Chem. Soc.* **2016**, *138* (31), 9787–9790.

(16) Barchuk, A.; Ngai, M.-Y.; Krische, M. J. Allylic Amines via Iridium-Catalyzed C−C Bond Forming Hydrogenation: Imine Vinylation in the Absence of Stoichiometric Byproducts or Metallic Reagents. *J. Am. Chem. Soc.* **2007**, *129* (27), 8432–8433.

(17) Skucas, E.; Kong, J. R.; Krische, M. J. Enantioselective Reductive Coupling of Acetylene to N-Arylsulfonyl Imines via Rhodium Catalyzed C−C Bond-Forming Hydrogenation: (Z)-Dienyl Allylic Amines. *J. Am. Chem. Soc.* **2007**, *129* (23), 7242–7243.

(18) Kong, J.-R.; Cho, C.-W.; Krische, M. J. Hydrogen-Mediated Reductive Coupling of Conjugated Alkynes with Ethyl (N-Sulfinyl)Iminoacetates: Synthesis of Unnatural α-

Amino Acids via Rhodium-Catalyzed C−C Bond Forming Hydrogenation. *J. Am. Chem. Soc.* **2005**, *127* (32), 11269–11276.

(19) Patel, S. J.; Jamison, T. F. Catalytic Three-Component Coupling of Alkynes, Imines, and Organoboron Reagents. *Angew. Chem. Int. Ed.* **2003**, *42* (12), 1364–1367.

(20) Zhu, S.; Lu, X.; Luo, Y.; Zhang, W.; Jiang, H.; Yan, M.; Zeng, W. Ruthenium(II)-Catalyzed Regioselective Reductive Coupling of α-Imino Esters with Dienes. *Org. Lett.* **2013**, *15* (7), 1440–1443.

(21) Ngai, M.-Y.; Barchuk, A.; Krische, M. J. Enantioselective Iridium-Catalyzed Imine Vinylation: Optically Enriched Allylic Amines via Alkyne−Imine Reductive Coupling Mediated by Hydrogen. *J. Am. Chem. Soc.* **2007**, *129* (42), 12644–12645.

(22) Wang, C.-C.; Lin, P.-S.; Cheng, C.-H. Cobalt-Catalyzed Highly Regio- and Stereoselective Intermolecular Reductive Coupling of Alkynes with Conjugated Alkenes. *J. Am. Chem. Soc.* **2002**, *124* (33), 9696–9697.

(23) Li, W.; Herath, A.; Montgomery, J. Evolution of Efficient Strategies for Enone−Alkyne and Enal−Alkyne Reductive Couplings. *J. Am. Chem. Soc.* **2009**, *131* (46), 17024–17029.

(24) Wei, C.-H.; Mannathan, S.; Cheng, C.-H. Enantioselective Synthesis of β-Substituted Cyclic Ketones via Cobalt-Catalyzed Asymmetric Reductive Coupling of Alkynes with Alkenes. *J. Am. Chem. Soc.* **2011**, *133* (18), 6942–6944.

(25) Shibahara, F.; Bower, J. F.; Krische, M. J. Ruthenium-Catalyzed C−C Bond Forming Transfer Hydrogenation: Carbonyl Allylation from the Alcohol or Aldehyde Oxidation Level Employing Acyclic 1,3-Dienes as Surrogates to Preformed Allyl Metal Reagents. *J. Am. Chem. Soc.* **2008**, *130* (20), 6338–6339.

(26) Patman, R. L.; Williams, V. M.; Bower, J. F.; Krische, M. J. Carbonyl Propargylation from the Alcohol or Aldehyde Oxidation Level Employing 1,3-Enynes as Surrogates to Preformed Allenylmetal Reagents: A Ruthenium-Catalyzed C−C Bond-Forming Transfer Hydrogenation. *Angew. Chem. Int. Ed.* **2008**, *47* (28), 5220–5223.

(27) Shibahara, F.; Bower, J. F.; Krische, M. J. Diene Hydroacylation from the Alcohol or Aldehyde Oxidation Level via Ruthenium-Catalyzed C−C Bond-Forming Transfer Hydrogenation: Synthesis of β,γ-Unsaturated Ketones. *J. Am. Chem. Soc.* **2008**, *130* (43), 14120–14122.

(28) Zbieg, J. R.; McInturff, E. L.; Krische, M. J. Allenamide Hydro−Hydroxyalkylation: 1,2-Amino Alcohols via Ruthenium-Catalyzed Carbonyl Anti-Aminoallylation. *Org. Lett.* **2010**, *12* (11), 2514–2516.

(29) Zbieg, J. R.; McInturff, E. L.; Leung, J. C.; Krische, M. J. Amplification of Anti-Diastereoselectivity via Curtin−Hammett Effects in Ruthenium-Catalyzed Hydrohydroxyalkylation of 1,1-Disubstituted Allenes: Diastereoselective Formation of All-Carbon Quaternary Centers. *J. Am. Chem. Soc.* **2011**, *133* (4), 1141–1144.

(30) Zbieg, J. R.; Yamaguchi, E.; McInturff, E. L.; Krische, M. J. Enantioselective C-H Crotylation of Primary Alcohols via Hydrohydroxyalkylation of Butadiene. *Science* **2012**, *336* (6079), 324–327.

(31) McInturff, E. L.; Yamaguchi, E.; Krische, M. J. Chiral-Anion-Dependent Inversion of Diastereo- and Enantioselectivity in Carbonyl Crotylation via Ruthenium-Catalyzed Butadiene Hydrohydroxyalkylation. *J. Am. Chem. Soc.* **2012**, *134* (51), 20628–20631.

(32) Bower, J. F.; Skucas, E.; Patman, R. L.; Krische, M. J. Catalytic C−C Coupling via Transfer Hydrogenation: Reverse Prenylation, Crotylation, and Allylation from the Alcohol or Aldehyde Oxidation Level. *J. Am. Chem. Soc.* **2007**, *129* (49), 15134–15135.

(33) Bower, J. F.; Patman, R. L.; Krische, M. J. Iridium-Catalyzed C−C Coupling via Transfer Hydrogenation: Carbonyl Addition from the Alcohol or Aldehyde Oxidation Level Employing 1,3-Cyclohexadiene. *Org. Lett.* **2008**, *10* (5), 1033–1035.

(34) Han, S. B.; Kim, I. S.; Han, H.; Krische, M. J. Enantioselective Carbonyl Reverse Prenylation from the Alcohol or Aldehyde Oxidation Level Employing 1,1-Dimethylallene as the Prenyl Donor. *J. Am. Chem. Soc.* **2009**, *131* (20), 6916–6917.

(35) Moran, J.; Preetz, A.; Mesch, R. A.; Krische, M. J. Iridium-Catalysed Direct C–C Coupling of Methanol and Allenes. *Nat. Chem.* **2011**, *3* (4), 287–290.

(36) Geary, L. M.; Woo, S. K.; Leung, J. C.; Krische, M. J. Diastereo- and Enantioselective Iridium-Catalyzed Carbonyl Propargylation from the Alcohol or Aldehyde Oxidation Level: 1,3-Enynes as Allenylmetal Equivalents. *Angew. Chem. Int. Ed.* **2012**, *51* (12), 2972–2976.

(37) Nakai, K.; Yoshida, Y.; Kurahashi, T.; Matsubara, S. Nickel-Catalyzed Redox-Economical Coupling of Alcohols and Alkynes to Form Allylic Alcohols. *J. Am. Chem. Soc.* **2014**, *136* (22), 7797–7800.

(38) Leung, J. C.; Geary, L. M.; Chen, T.-Y.; Zbieg, J. R.; Krische, M. J. Direct, Redox-Neutral Prenylation and Geranylation of Secondary Carbinol C–H Bonds: C4-Regioselectivity in Ruthenium-Catalyzed C–C Couplings of Dienes to α-Hydroxy Esters. *J. Am. Chem. Soc.* **2012**, *134* (38), 15700–15703.

(39) Chen, T.-Y.; Krische, M. J. Regioselective Ruthenium Catalyzed Hydrohydroxyalkylation of Dienes with 3-Hydroxy-2-Oxindoles: Prenylation, Geranylation, and Beyond. *Org. Lett.* **2013**, *15* (12), 2994–2997.

(40) Geary, L. M.; Glasspoole, B. W.; Kim, M. M.; Krische, M. J. Successive C–C Coupling of Dienes to Vicinally Dioxygenated Hydrocarbons: Ruthenium Catalyzed [4 + 2] Cycloaddition across the Diol, Hydroxycarbonyl, or Dione Oxidation Levels. *J. Am. Chem. Soc.* **2013**, *135* (10), 3796–3799.

(41) Molinaro, C.; Jamison, T. F. Nickel-Catalyzed Reductive Coupling of Alkynes and Epoxides. *J. Am. Chem. Soc.* **2003**, *125* (27), 8076–8077.

(42) Beaver, M. G.; Jamison, T. F. Ni(II) Salts and 2-Propanol Effect Catalytic Reductive Coupling of Epoxides and Alkynes. *Org. Lett.* **2011**, *13* (15), 4140–4143.

(43) Urkalan, K. B.; Sigman, M. S. Palladium-Catalyzed Hydroalkylation of Styrenes with Organozinc Reagents To Form Carbon−Carbon Sp3−sp3 Bonds under Oxidative Conditions. *J. Am. Chem. Soc.* **2009**, *131* (50), 18042–18043.

(44) DeLuca, R. J.; Sigman, M. S. Anti-Markovnikov Hydroalkylation of Allylic Amine Derivatives via a Palladium-Catalyzed Reductive Cross-Coupling Reaction. *J. Am. Chem. Soc.* **2011**, *133* (30), 11454–11457.

(45) DeLuca, R. J.; Sigman, M. S. The Palladium-Catalyzed Anti-Markovnikov Hydroalkylation of Allylic Alcohol Derivatives. *Org. Lett.* **2013**, *15* (1), 92–95.

(46) Wang, Y.-M.; Bruno, N. C.; Placeres, Á. L.; Zhu, S.; Buchwald, S. L. Enantioselective Synthesis of Carbo- and Heterocycles through a CuH-Catalyzed Hydroalkylation Approach. *J. Am. Chem. Soc.* **2015**, *137* (33), 10524–10527.

(47) Iwasaki, T.; Shimizu, R.; Imanishi, R.; Kuniyasu, H.; Kambe, N. Copper-Catalyzed Regioselective Hydroalkylation of 1,3-Dienes with Alkyl Fluorides and Grignard Reagents. *Angew. Chem. Int. Ed.* **2015**, *54* (32), 9347–9350.

(48) Uehling, M. R.; Suess, A. M.; Lalic, G. Copper-Catalyzed Hydroalkylation of Terminal Alkynes. *J. Am. Chem. Soc.* **2015**, *137* (4), 1424–1427.

(49) Suess, A. M.; Uehling, M. R.; Kaminsky, W.; Lalic, G. Mechanism of Copper-Catalyzed Hydroalkylation of Alkynes: An Unexpected Role of Dinuclear Copper Complexes. *J. Am. Chem. Soc.* **2015**, *137* (24), 7747–7753.

(50) Cheung, C. W.; Zhurkin, F. E.; Hu, X. Z-Selective Olefin Synthesis via Iron-Catalyzed Reductive Coupling of Alkyl Halides with Terminal Arylalkynes. *J. Am. Chem. Soc.* **2015**, *137* (15), 4932–4935.

(51) Lu, X.-Y.; Liu, J.-H.; Lu, X.; Zhang, Z.-Q.; Gong, T.-J.; Xiao, B.; Fu, Y. 1,1-Disubstituted Olefin Synthesis via Ni-Catalyzed Markovnikov Hydroalkylation of Alkynes with Alkyl Halides. *Chem. Commun.* **2016**, *52* (30), 5324–5327.

(52) Fujihara, T.; Yokota, K.; Terao, J.; Tsuji, Y. Copper-Catalyzed Hydroallylation of Allenes Employing Hydrosilanes and Allyl Chlorides. *Chem. Commun.* **2017**, *53* (56), 7898–7900.

(53) Boutier, A.; Kammerer-Pentier, C.; Krause, N.; Prestat, G.; Poli, G. Pd-Catalyzed Asymmetric Synthesis of N-Allenyl Amides and Their Au-Catalyzed Cycloisomerizative Hydroalkylation: A New Route Toward Enantioenriched Pyrrolidones. *Chem. – Eur. J.* **2012**, *18* (13), 3840–3844.

(54) Bolte, B.; Gagosz, F. Gold and Brønsted Acid Catalyzed Hydride Shift onto Allenes: Divergence in Product Selectivity. *J. Am. Chem. Soc.* **2011**, *133* (20), 7696–7699.

(55) Baslé, O.; Denicourt-Nowicki, A.; Crévisy, C.; Mauduit, M. Asymmetric Allylic Alkylation. In *Copper-Catalyzed Asymmetric Synthesis*; John Wiley & Sons, Ltd, 2014; pp 85–126.

(56) Alexakis, A.; Bäckvall, J. E.; Krause, N.; Pàmies, O.; Diéguez, M. Enantioselective Copper-Catalyzed Conjugate Addition and Allylic Substitution Reactions. *Chem. Rev.* **2008**, *108* (8), 2796–2823.

(57) Jordan, A. J.; Lalic, G.; Sadighi, J. P. Coinage Metal Hydrides: Synthesis, Characterization, and Reactivity. *Chem. Rev.* **2016**, *116* (15), 8318–8372.

(58) Wyss, C. M.; Tate, B. K.; Bacsa, J.; Gray, T. G.; Sadighi, J. P. Bonding and Reactivity of a μ-Hydrido Dicopper Cation. *Angew. Chem. Int. Ed.* **2013**, *52* (49), 12920–12923.

(59) Wyss, C. M.; Tate, B. K.; Bacsa, J.; Wieliczko, M.; Sadighi, J. P. Dinuclear μ-Fluoro Cations of Copper, Silver and Gold. *Polyhedron* **2014**, *84*, 87–95.

(60) Xu, K.; Thieme, N.; Breit, B. Atom-Economic, Regiodivergent, and Stereoselective Coupling of Imidazole Derivatives with Terminal Allenes. *Angew. Chem. Int. Ed.* **2014**, *53* (8), 2162–2165.

(61) Jean Claude Clinet; Gerard Linstrumelle. Allenyllithium Reagents; V. An Efficient Route to Functionalized Allenes. *Synthesis* **1981**, No. 11, 875–878.

(62) Cornelissen, L.; Vercruysse, S.; Sanhadji, A.; Riant, O. Copper-Catalyzed Vinylsilane Allylation. *Eur. J. Org. Chem.* **2014**, *2014* (1), 35–38.

(63) Xu, B.; Lu, M.; Kang, J.; Wang, D.; Brown, J.; Peng, Z. Synthesis and Optical Properties of Conjugated Polymers Containing Polyoxometalate Clusters as Side-Chain Pendants. *Chem. Mater.* **2005**, *17* (11), 2841–2851.

(64) Nguyen, J.; Duncan, N.; Lalic, G. Direct β-Selective Cross-Coupling of Alkenyl Gold Complexes with Alkyl Electrophiles. *Eur. J. Org. Chem.* **2016**, *2016* (35), 5803–5806.

(65) Zhang, L.; Kozmin, S. A. Brønsted Acid-Promoted Cyclizations of Siloxyalkynes with Arenes and Alkenes. *J. Am. Chem. Soc.* **2004**, *126* (33), 10204–10205.

(66) Dang, H.; Mailig, M.; Lalic, G. Mild Copper-Catalyzed Fluorination of Alkyl Triflates with Potassium Fluoride. *Angew. Chem. Int. Ed.* **2014**, *53* (25), 6473–6476.

(67) Qu, W.; Kung, M.-P.; Hou, C.; Oya, S.; Kung, H. F. Quick Assembly of 1,4-Diphenyltriazoles as Probes Targeting β-Amyloid Aggregates in Alzheimer's Disease. *J. Med. Chem.* **2007**, *50* (14), 3380–3387.

(68) Villadsen, J. S.; Stephansen, H. M.; Maolanon, A. R.; Harris, P.; Olsen, C. A. Total Synthesis and Full Histone Deacetylase Inhibitory Profiling of Azumamides A–E as Well as B2- Epi-Azumamide E and B3-Epi-Azumamide E. *J. Med. Chem.* **2013**, *56* (16), 6512–6520.

(69) Cadot, C.; Dalko, P. I.; Cossy, J.; Ollivier, C.; Chuard, R.; Renaud, P. Free-Radical Hydroxylation Reactions of Alkylboronates. *J. Org. Chem.* **2002**, *67* (21), 7193–7202.

(70) Moussa, I. A.; Banister, S. D.; Beinat, C.; Giboureau, N.; Reynolds, A. J.; Kassiou, M. Design, Synthesis, and Structure−Affinity Relationships of Regioisomeric N-Benzyl Alkyl Ether Piperazine Derivatives as σ-1 Receptor Ligands. *J. Med. Chem.* **2010**, *53* (16), 6228–6239.

(71) Bruker. *SAINT*; BrukerAXS Inc: Madison, Wisconsin, USA, 2007.

(72) Bruker. *SADABS*; BrukerAXS Inc: Madison, Wisconsin, USA, 2007.

(73) Bruker. *APEX2*; BrukerAXS Inc: Madison, Wisconsin, USA, 2007.

(74) Altomare, A.; Burla, M. C.; Camalli, M.; Cascarano, G. L.; Giacovazzo, C.; Guagliardi, A.; Moliterni, A. G. G.; Polidori, G.; Spagna, R. SIR97: A New Tool for Crystal Structure Determination and Refinement. *J. Appl. Crystallogr.* **1999**, *32* (1), 115–119.

(75) Altomare, A.; Cascarano, G.; Giacovazzo, C.; Guagliardi, A. Completion and Refinement of Crystal Structures with SIR92. *J. Appl. Crystallogr.* **1993**, *26* (3), 343–350.

(76) G. M. Sheldrick. *SHELXL-97, Program for the Refinement of Crystal Structures*; University of Göttingen: Germany, 1997.

(77) Sheldrick, G. M. Crystal Structure Refinement with SHELXL. *Acta Crystallogr. Sect. C Struct. Chem.* **2015**, *71* (1), 3–8.

(78) S. Mackay; C. Edwards; A. Henderson; C. Gilmore; K. Shankland. *MaXus: A Computer Program for the Solution and Refinement of Crystal Structures from Diffraction Data*; University of Glasgow: Scotland, 1997.

(79) Waasmaier, D.; Kirfel, A. New Analytical Scattering-Factor Functions for Free Atoms and Ions. *Acta Crystallogr. A* **1995**, *51* (3), 416–431.

(80) Farrugia, L. J. ORTEP-3 for Windows - a Version of ORTEP-III with a Graphical User Interface (GUI). *J. Appl. Crystallogr.* **1997**, *30* (5), 565–565.

(81) Spek, A. L. Single-Crystal Structure Validation with the Program PLATON. *J. Appl. Crystallogr.* **2003**, *36* (1), 7–13.

(82) van der Sluis, P.; Spek, A. L. BYPASS: An Effective Method for the Refinement of Crystal Structures Containing Disordered Solvent Regions. *Acta Crystallogr. A* **1990**, *46* (3), 194–201.

Chapter 2. PHOTOINDUCED COPPER-CATALYZED COUPLING OF TERMINAL ALKYNES AND ALKYL IODIDES

Portions of this chapter as well as figures, schemes, and tables were adapted or reproduced from the following manuscript, with permission from Hazra, A.; Lee, M. T.; Chiu, J. F.; Lalic, G. Photoinduced Copper-Catalyzed Coupling of Terminal Alkynes and Alkyl Iodides. *Angew. Chem. Int. Ed.* **2018**, *57* (19), 5492–5496.

2.1 **INTRODUCTION**

The alkylation of terminal alkynes and their derivatives is an important approach to the synthesis of internal alkynes. Numerous methods are available for the alkylation of prefunctionalized alkyne substrates, such as haloalkynes,[1–5] metal acetylides,[6–11] alkynyl benziodoxolones,[12–15] and alkynyl sulfones.[16] In comparison, there are significantly fewer methods for the alkylation of terminal alkynes.

Most catalytic methods[17] for the alkylation of terminal alkynes rely on the in situ formation of copper acetylides, which serve as key catalytic intermediates (Scheme 1). They are easily formed from terminal alkynes in the presence of a weak base and a copper salt.[18] However, the low nucleophilicity of copper acetylides makes their alkylation challenging.[18] Direct alkylation can only be achieved by using strong electrophiles, such as primary alkyl triflates,[19] activated α- and β-haloamides,[20,21] oxocarbenium ions,[22–24] and iminium ions (**Scheme 2.1a**).[25–27]

Alternatively, the alkylation of copper acetylides can be accomplished under Sonogashira conditions,[28,29] which require an additional transition-metal catalyst (**Scheme 2.1b**). Although examples of Sonogashira alkylation reactions are relatively rare, the reaction can be accomplished by using primary alkyl halides and a palladium[30] or nickel catalyst.[31,32] More recently, two reports described the extension to reactions of secondary alkyl halides.[33,34] Overall, the Sonogashira reaction still provides the most general method for the alkylation of terminal alkynes.

Scheme 2.1 Copper-Catalyzed Alkylation of Terminal Alkynes

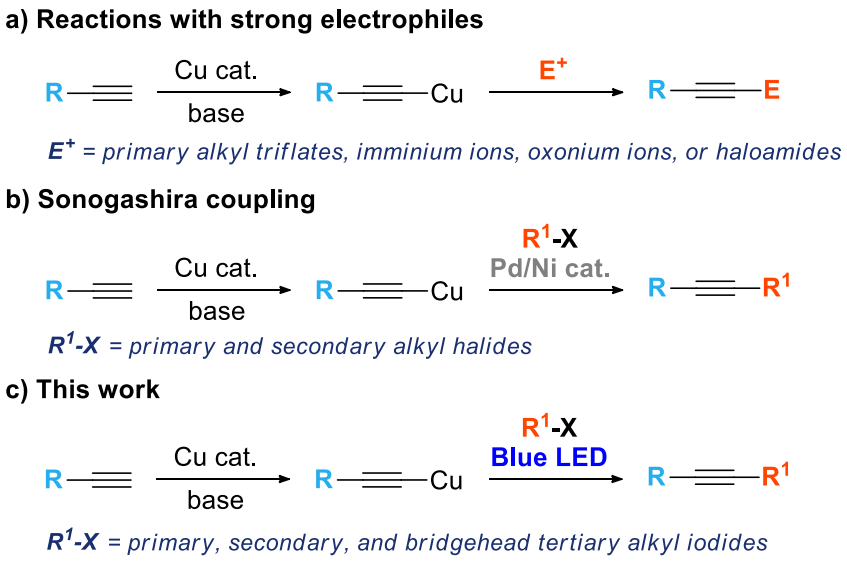

We were interested in developing a light-promoted copper-catalyzed coupling of terminal alkynes and alkyl halides that would obviate the need for palladium or nickel catalysts (**Scheme 2.1c**). Both metals are significantly more toxic than copper and are often difficult to remove from the alkylation product.

Our approach to the alkylation of terminal alkynes was inspired by photoinduced copper-catalyzed reactions developed independently by the groups of Fu and Peters[35–37] and by Hwang and co-workers.[38–40] The key sequence in the transformations reported by Fu and Peters is the photoexcitation of the copper–nucleophile complex followed by electron transfer to an alkyl

halide. This approach has been applied to alkylations of a range of nitrogen-based nucleophiles.[41–45] Applications to carbon-based nucleophiles have thus far been limited to the alkylation of cyanide[46] and specific types of heteroarenes.[47,48] Numerous investigations of the photophysical properties of copper acetylides suggest that the same approach can be used to accomplish the photoinduced copper-catalyzed alkylation of terminal alkynes according to the mechanism outlined in **Scheme 2.2**.

Scheme 2.2 Plausible Mechanism of Photoinduced Alkylation

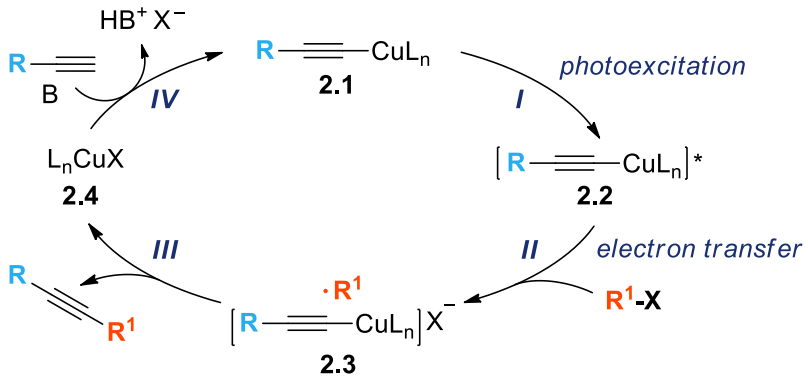

In 2012, simultaneously with the initial report by Fu and Peters,[35] Hwang et al. reported a method for the photoinduced copper-catalyzed arylation of terminal alkynes that involves photoexcitation of the copper acetylide intermediate.[38,49] Prior to Hwang's seminal work, it was known that the photoexcitation of copper acetylide complexes (acetylide→Cu transition) can be achieved with photons of relatively low energy (λ >350 nm).[50–52] The resulting excited states are long-lived (on the order of microseconds), and highly reducing (E1/2=−1.77 V vs. SCE).23c The redox potentials of alkyl iodides (EtI: E1/2=−0.92 V vs. SCE) suggest that they can be reduced by electron transfer from excited complex **2.2**.[53] Finally, organocopper complexes with similar photophysical properties to copper acetylides have been shown to undergo fast quenching of their excited states by electron transfer to a range of organohalides.[51]

2.2 RESULTS AND DISCUSSION

2.2.1 *Reaction Development*

Using the conditions established by Fu[35–37,41,42] and Hwang[38] as a starting point for our experiments, we explored the photochemical reaction of phenylacetylene with *n*-BuI using CuCl as the catalyst and an acetonitrile/methanol mixture as the solvent. The reaction resulted in the formation of only 12 % of the desired product and 16 % of the alkyne dimer. Together, these products accounted for only 28 % of the consumed alkyne. The rest of the starting alkyne was incorporated into low-molecular-weight polymers, identified by gel permeation chromatography (GPC) of the crude reaction mixture (**Scheme 2.3**). Similar results were obtained with alkyl- and aryl-substituted alkynes (**Scheme 2.5**).

Scheme 2.3 Initial Conditions and Mass Balance Analysis

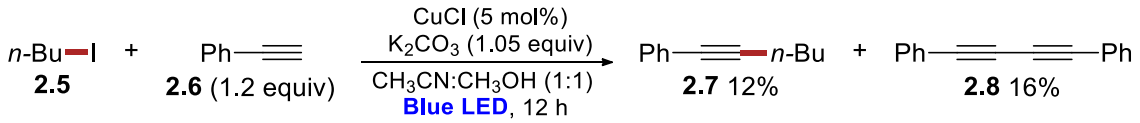

100% Conversion, low molecular weight polymers detected

Control experiments confirmed that polymerization occurs only in the presence of both light and the copper catalyst and suggested that the polymerization involves the photoactivated copper acetylide as a key intermediate. We surmised that with the proper choice of ligand for the copper catalyst, we could modulate the reactivity of the excited copper acetylide complex, suppress the polymer formation, and enable the desired alkylation. This approach was particularly attractive considering that ligand effects on reactivity in related photoexcited copper complexes have been rarely documented.

Exploration of a wide range of ligands and other reaction parameters led to the development of the alkylation reaction conditions shown in **Table 2.1**. The best results were

obtained using 4,4',4''-tri-tert-butyl-2,2':6',2''-terpyridine (**L1**) as the ligand, K_2CO_3 as the base, and acetonitrile/methanol (3:1) as the solvent system (entry 1). Throughout the optimization of this reaction, several observations were made, which have been summarized in **Table 2.1**.

Table 2.1 Reaction Development

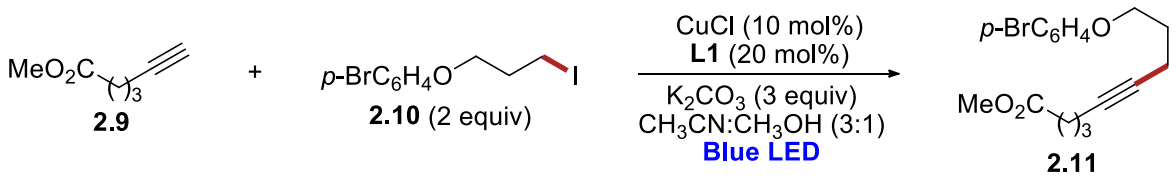

Entry	*Change from standard conditions*	*Yield*[a]
1	none	90%
2	No Blue LED	0%
3	No CuCl	0%
4	No ligand	20%
5	**L2** instead of **L1**	51%
6	**L3** instead of **L1**	14%
7	**L4** instead of **L1**	14%
8	CH_3CN	26%
9	CH_3OH	36%
10	CH_3CN:CH_3OH (1:1)	74%
11	Cs_2CO_3 as base	0%
12	12 mol% **L1**	84%

[a] GC yields are reported. All reactions performed on 0.25 mmol scale at 25 °C over 24 h.

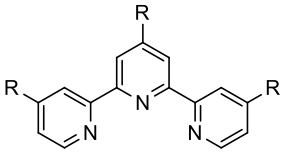

R = *t*-Bu **L1**
R = H **L2**

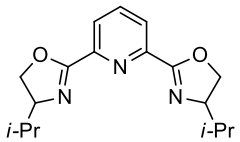

L3

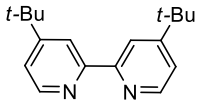

L4

Blue light and the copper catalyst were both necessary for the alkylation (entries 2 and 3). **L1** was determined to be essential for the success of the reaction (entry 4). In the absence of the ligand, we obtained only 20 % of the desired product, with the major product being polymerized starting material. Replacing **L1** with unsubstituted terpyridine (**L2**) or closely related PyBox (**L3**) compromised the yield (entries 5 and 6). Additionally, structurally similar bidentate ligands, such

as dtbpy (**L4**), were found to be ineffective (entry 7). The solvent was also important, with pure acetonitrile or pure methanol both giving significantly lower yields of the alkylation product (entries 8–10). Potassium carbonate was uniquely effective as the base, and even closely related cesium carbonate provided no alkylation product (entry 11). Decreasing the amount of ligand to 12 mol % did not lead to a considerable loss in yield (entry 12). Finally, we found that alkyl bromides and chlorides were not viable substrates.

2.2.2 *Substrate Scope*

The standard reaction conditions were effective for a diverse set of electrophiles (**Table 2.2**). Primary iodides as well as cyclic and acyclic secondary alkyl iodides were viable substrates and provided the desired alkylation products in high yields. The reaction was compatible with a wide range of functional groups and was successfully accomplished in the presence of aryl bromides (**2.11**), aryl chlorides (**2.12**), alcohols (**2.17**), silyl ethers (**2.18**), nitriles (**2.14**), esters, sulfonamides (**2.26**), and ethers (**2.22**).

Reactions with tertiary iodides proved to be more difficult. Under the standard reaction conditions, simple *tert*-butyl iodide underwent solvolysis faster than the coupling reaction. Changing to *tert*-butyl bromide slowed down the solvolysis, but no coupling product was obtained. We reasoned that destabilizing the tertiary carbocation intermediate would prevent solvolysis and allow the coupling to proceed. This strategy proved effective, and bridgehead tertiary iodides were found to be viable coupling partners. 1-Adamantyl (**2.29**), bicyclopentyl (**2.28**), and bicyclooctyl (**2.30**) iodide all provided the expected alkylation product in useful yields. These results are worth noting in light of the difficulties commonly encountered in alkynylations[54] and other cross-coupling reactions of tertiary bridgehead iodides.[55]

Table 2.2 Scope of Alkyl Iodides[a]

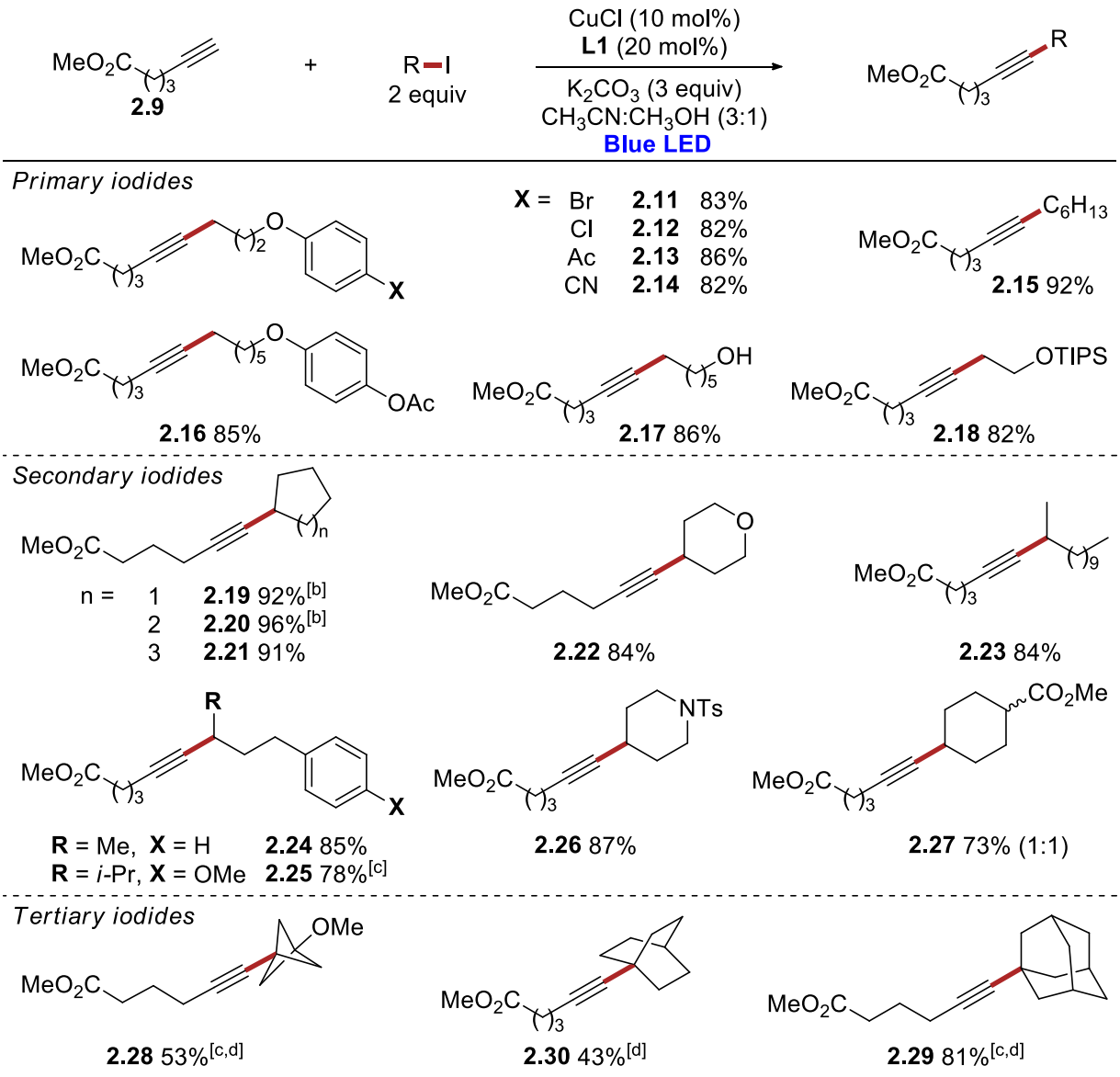

[a] All reactions were performed on a 0.5 mmol scale at 25 °C over 24 h unless otherwise specified. Yields are of the isolated product. The ratio of isomers reported in parenthesis was obtained by GC anlysis of the pure products. [b] 12 mol% ligand was used. [c] Reaction performed on a 0.25 mmol scale. [d] 48 hour reaction time.

We also explored the reaction with a range of terminal alkynes. A broad variety of alkyne coupling partners underwent the photoinduced coupling to furnish the corresponding products in very good yields (**Table 2.3**). Esters (**2.34**), nitriles (**2.37**), epoxides (**2.41**), ketones (**2.35**), aryl fluorides (**2.36**), and alkenes (**2.32**) were all compatible with the alkylation reaction. Similarly, the desired product was obtained in excellent yield in the presence of a primary amide (**2.40**), which

is known to undergo N alkylation under similar reaction conditions.[42] Finally, aryl (**2.42** and **2.43**) and heteroaryl (**2.38**) alkynes also furnished the desired product in good yields.

Table 2.3 Scope of Alkynes[a]

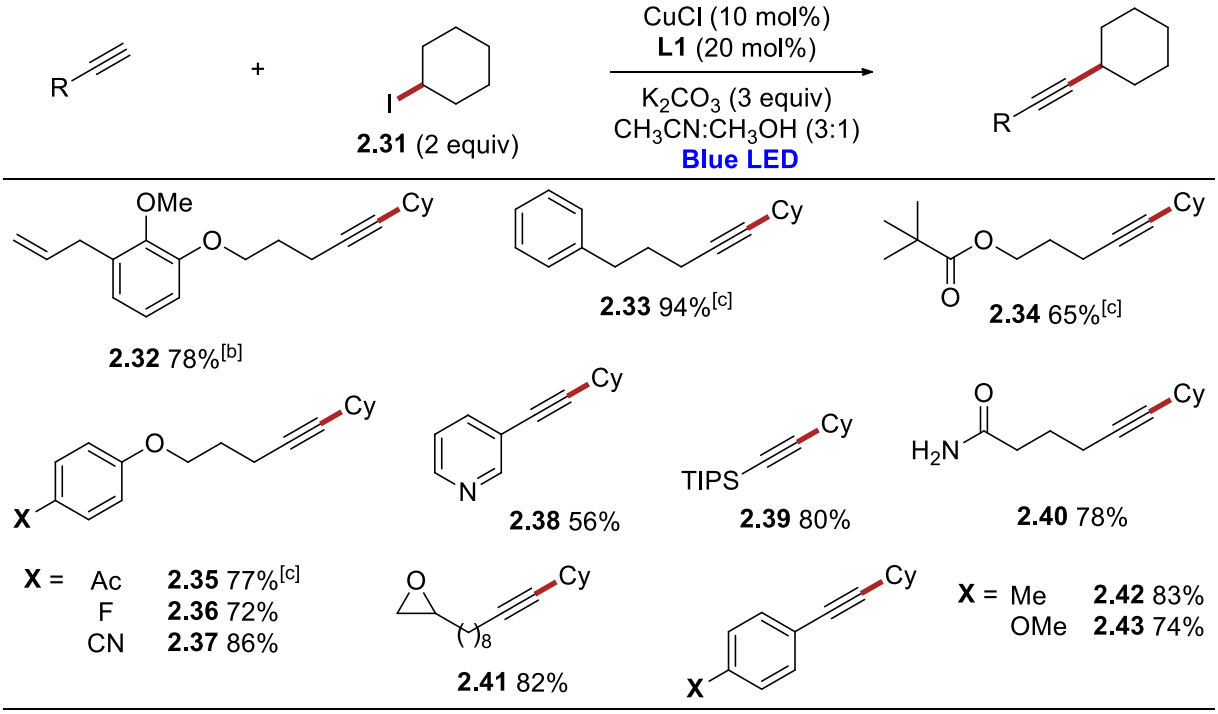

[a] Reactions were performed on a 0.5 mmol scale at 25 °C over 24 h. Yields are of the isolated product. Cy = cyclohexyl. [b] 48 hour reaction time. [c]12 mol% ligand was used.

2.2.3 *Mechanism*

Based on the mechanism of the related photoinduced copper-catalyzed alkylation, we propose that the alkylation of terminal alkynes proceeds according to the mechanism shown in Scheme 2. In an effort to probe the mechanism of the reaction, we performed the experiments shown in Scheme 3. The presence of one or more equivalents of TEMPO completely shut down the reaction, whereas 20 mol % of TEMPO partially hampered it. Additionally, a cyclohexyl–TEMPO adduct was isolated from the reaction mixture, indicating the presence of alkyl radical intermediates. The results of these experiments suggest the involvement of free-radical intermediates. A competition experiment with a primary and a secondary alkyl iodide resulted in

the formation of the two products in similar quantities (**Scheme 2.3b**). Considering the relatively small difference in the redox potentials of primary and secondary alkyl halides,[53] this result is consistent with electron transfer as the product- and rate-determining step of the reaction.

Scheme 2.4 Mechanistic Experiments

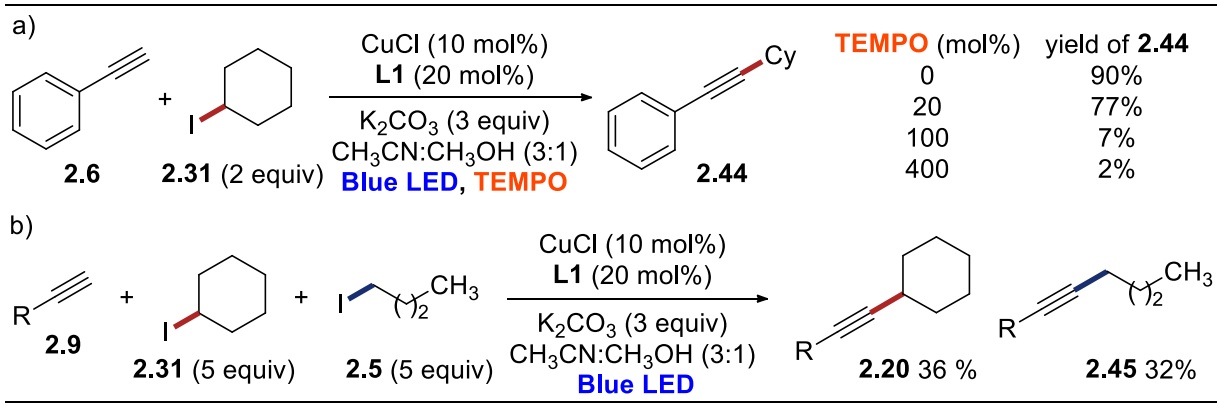

R= $MeO_2C(CH_2)_3$. Reactions performed on a 0.25 mmol scale at 25 °C over 24 h.

2.3 CONCLUSION

Overall, we have developed a photoinduced copper-catalyzed coupling of terminal alkynes with unactivated primary, secondary, and tertiary alkyl iodides. The reaction has a broad substrate scope and is compatible with esters, nitriles, alcohols, amides, epoxides, aryl halides, and ethers. The key for the success of the reaction is the tri-tert-butyl-terpyridine ligand, which favors the productive alkylation at the expense of the photoinduced copper-catalyzed polymerization of the starting materials. The alkylation reaction proceeds through a direct coupling between a copper acetylide and an unactivated alkyl iodide, most likely with the involvement of free-radical intermediates.

2.4 EXPERIMENTAL

2.4.1 *General Information*

All reactions were performed under a nitrogen atmosphere with flame-dried or oven-dried (120 °C) glassware, using standard Schlenk techniques, or in a glovebox (Nexus II from Vacuum Atmospheres). Column chromatography was performed using a Biotage Iso-1SV flash purification system with silica gel from Agela Technologies Inc. (60Å, 40-60 μm, 230-400 mesh. Infrared (IR) spectra were recorded on a Perkin Elmer Spectrum RX I spectrometer. IR peak absorbencies are represented as follows: s = strong, m = medium, w = weak, br = broad. ^{1}H- and ^{13}C-NMR spectra were recorded on a Bruker AV-300 or AV-500 spectrometer. ^{1}H NMR chemical shifts (δ) are reported in parts per million (ppm) downfield of TMS and are referenced relative to residual solvent peak ($CDCl_3$ (7.26 ppm), or C_6D_6 (7.16 ppm)). ^{13}C chemical shifts are reported in parts per million downfield of TMS and are referenced to the carbon resonance of the solvent ($CDCl_3$: δ 77.2 ppm, C_6D_6: δ 128.1 ppm). Data are represented as follows: chemical shift, multiplicity (s = singlet, d = doublet, t = triplet, q = quartet, p = pentet, hept = heptet, m = multiplet), integration, and coupling constants in Hertz (Hz). Mass spectra were collected on a JEOL HX-110 mass spectrometer. GC analysis was performed on a Shimadzu GC-2010 instrument with a flame ionization detector and a SHRXI-5MS column (15 m, 0.25 mm inner diameter, 0.25 μm film thickness). The following temperature program was used: 2 min @ 60 °C, 13 °C/min to 160 °C, 30 °C/min to 250 °C, 5.5 min @ 250 °C. Gel permeation chromatography was performed using a Waters chromatograph equipped with two 10 μm Malvern columns (300 mm × 7.8 mm) connected in series with increasing pore size (1000, 10 000 Å). ICP-MS experiments were performed using Perkin Elmer Optima 8300 inductively coupled plasma-optical emission spectrometer.

2.4.2 *Materials*

Acetonitrile was degassed and dried by passing through columns of neutral alumina. Methanol was degassed and stored over 4Å molecular sieves. Deuterated solvents were purchased from Cambridge Isotope Laboratories, Inc. and used as received. Commercial reagents were purchased from Sigma-Aldrich, TCI America, GFS-Chemicals, and AK-Scientific. K_2CO_3 was purchased from Alfa Aesar. Ligands were purchased from Sigma Aldrich. NHC ligand was synthesizes from known procedure. Blue LED lamps (34W, Kessil A160WE tuna blue) were used to irradiate the reaction. Fig. S1 shows the emission spectra of the light source the reaction chamber. The reaction chamber was composed of a 15.5 cm long dewar with a 7.5 cm internal diameter and 8.5 cm external dimeter and a hose connected to compressed air. The strength of the air flow was adjusted so that the temperature of the chamber never exceeded 25 °C. The reaction mixture was placed 6 cm from the light source.

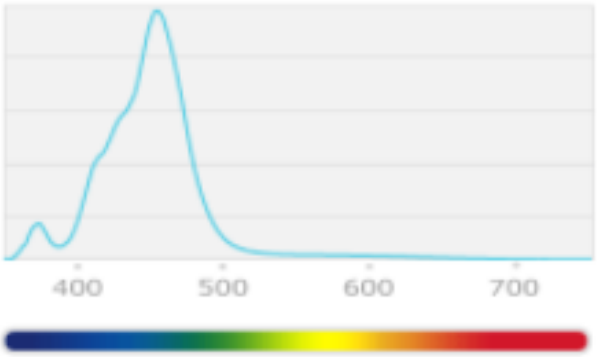

Figure 2.1 Emission spectrum of the Kessil lamp[56]

Figure 2.2 Reaction chamber

2.4.3 *Alkylation in the Absence of the Ligand*

The results of different combinations of alkynes and alkyl iodides that were tested using conditions similar to those reported by Hwang and Fu are shown in **Scheme 2.5**. All reactions were set up in a nitrogen-filled glovebox according to the following procedure. A dram vial was charged with a Teflon coated stir bar, CuCl, base, solvent and alkyne. The internal standard, 1,3,5-trimethoxy benzene (TMB), and the alkyl iodide were then added. The vial was placed in the reaction chamber (**Figure 2.2**) and held in place with a double-sided tape. To maintain a constant temperature over the course of the reaction, a continuous flow of air was passed through the reaction chamber. The reaction was stirred vigorously for the indicated time and yields were determined by GC.

Scheme 2.5 Supplementary Screening of Initial Substrates

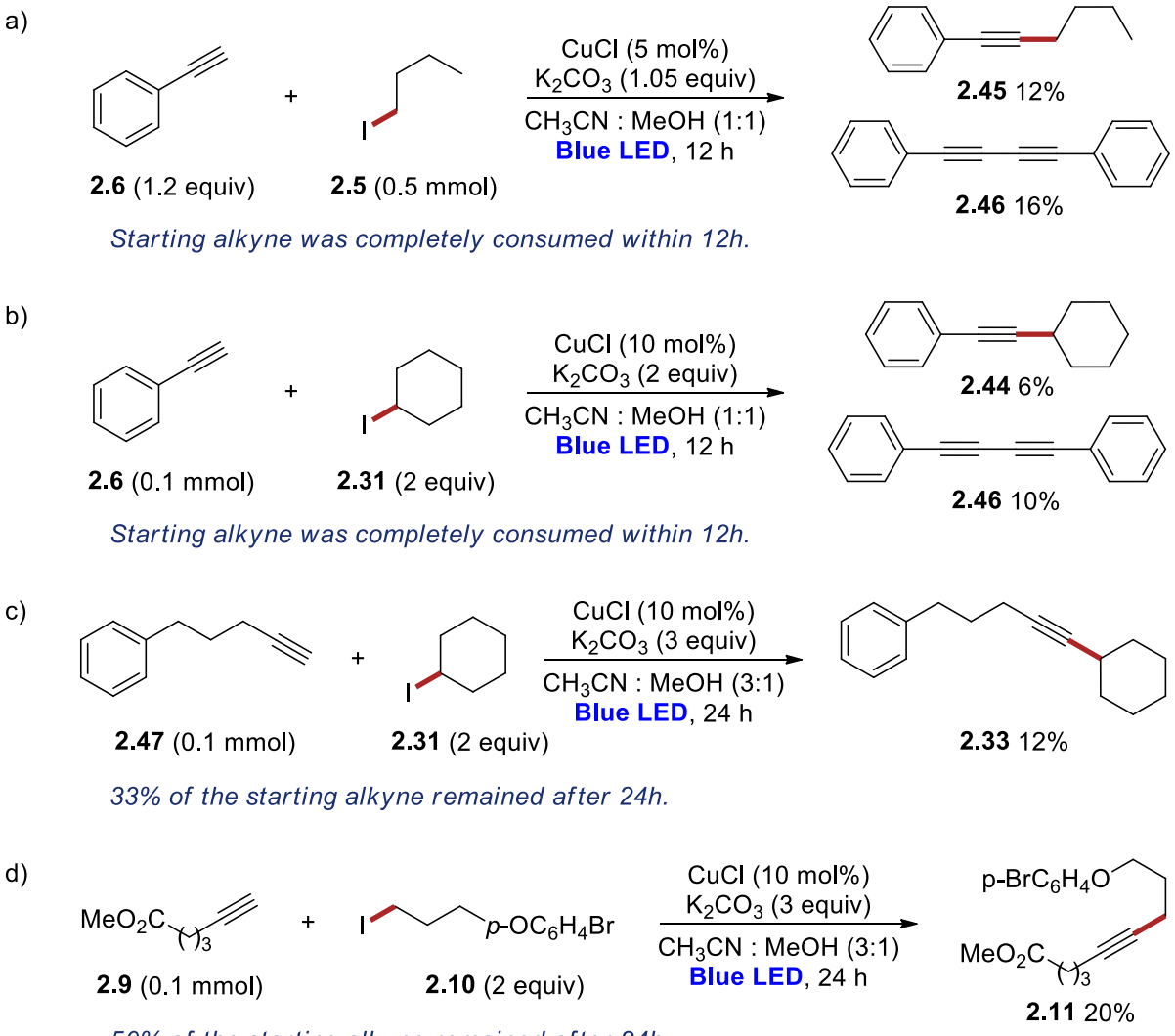

2.4.4 *Analysis of Literature Results*

Hwang et. al. reported[38] a photoinduced arylation of terminal alkynes, and in the same report described a single example of photoinduced alkylation (Table 2, entry 24 of the paper). In this example, phenylacetylene was reacted with 1-iodobutane to give the alkylated product in an isolated yield of 84%. However, in our hands, using the reported conditions, we obtained only 12% of the desired product and 16% of alkyne homocoupling product at the full conversion of the

starting materials (yields determined by GC analysis of the crude reaction mixture using an internal standard) (**Scheme 2.3**, and **Scheme 2.5a**) The light sources used in our and Hwang's experiments were different. However, it is important to note that we were able to reproduce the arylation of terminal alkynes reported by Hwang in the same paper.

The broad features in the NMR spectrum of isolated product provided by Hwang were consistent with the NMR spectrum of our crude reaction mixture. These features, together with the low mass balance in our reaction, suggested a presence of polymeric species and prompted further analysis of the reaction. Preparative GPC analysis allowed the isolation of the polymeric species with M_w 2.091×10^4 (± 2.688%) and polydispersity of 4.515. Using quantitative GPC analysis, we determined that the polymers accounted for 68% of the starting material. Similar results were obtained with cyclohexyl iodide as the coupling partner. Overall, we believe that our findings are consistent with the experimental evidence provided by Hwang. Similar problems with false isolated yields because of polymeric byproducts have been recently described by Rajanbabu et al.[57]

In other experiments described in **Scheme 2.5**, we observed similar results including the formation of low molecular weight polymers. However, we did observe some minor differences in products formed and in product distribution. For example, in the experiment using cyclohexyl iodide and phenylacetylene (**Scheme 2.5b**), the homocoupled alkyne further reacted with cyclohexyl iodide to form the ene-yne adduct in trace quantity.

2.4.5 *Reaction Development*

In a nitrogen-filled glovebox, a dram vial was charged with a Teflon coated stir bar, CuCl, ligand, base, solvent, and alkyne. Internal standard, 1,3,5-trimethoxy benzene (TMB), and alkyl iodide were then added. The vial was put in the reaction chamber (**Figure 2.2**) and held in place with

double-sided tape. A constant flow of air was passed though the chamber to maintain a constant temperature. The reaction was then stirred vigorously for 12 hours and yields were determined by GC.

Table 2.4 Supplementary Ligand Screen

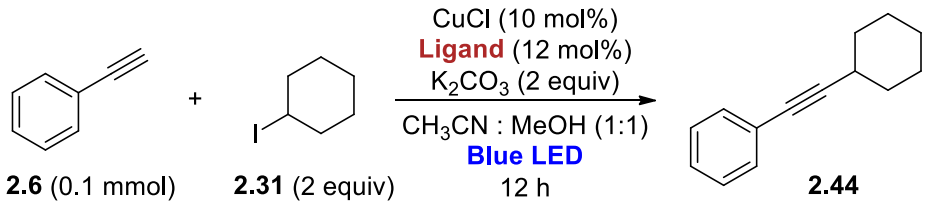

2.6 (0.1 mmol) + **2.31** (2 equiv) → **2.44**

No ligand 6%	**L1** 38%	**L3** 12%	**L4** 0%
L5 7%	**L6** 3%	**L7** 2%	**L8** 7%
L9 5%	**L10** 3%	**L11** 4%	**L12** 9%

GC yields are reported

Table 2.5 Supplementary Solvent Screen: CH_3CN:CH_3OH

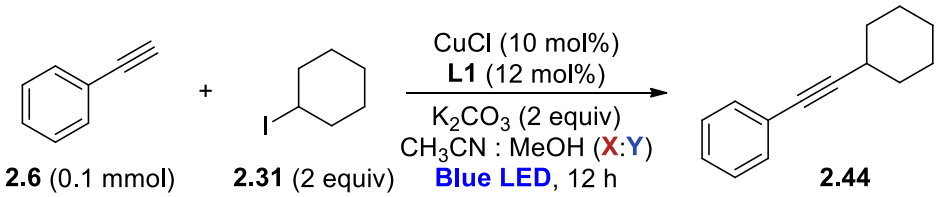

Entry	Acetonitrile: Methanol	Yield (%)
1	1:1	38
2	2:1	51
3	3:1	65
4	4:1	54
5	1:2	35
6	1:3	41
7	1:4	48

Table 2.6 Supplementary Base Screen

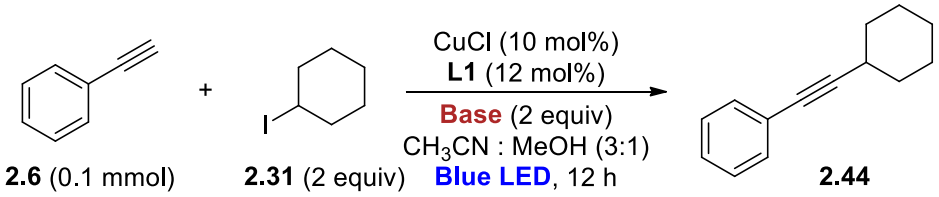

Entry	Base	Yield (%)
1	K_2CO_3	65
2	Na_2CO_3	12
3	Cs_2CO_3	0
4	Li_2CO_3	7
5	$KHCO_3$	8
6	K_3PO_4	16
7	K_2HPO_4	13
8	KH_2PO_4	8
9	Et_3N	11
10	K_2CO_3 (3 equiv, 24h)	90

Table 2.7 Supplementary Copper Salt Screen

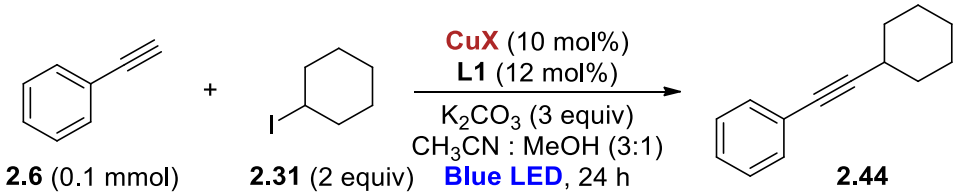

Entry	CuX	Yield (%)
1	CuCl	90
2	CuCl (5 mol%) & L1 (6%)	85
3	$(CuOTf)_2.C_6H_6$	86
4	$(CuOTf)_2.C_6H_6$ (no ligand)	12
5	CuI	80

2.4.6 *General Procedure for the Photoinduced Alkylation of Terminal Alkynes*

In a nitrogen-filled glovebox, a 1.5-dram vial was charged with a Teflon coated stir bar, CuCl (5.0 mg, 0.05 mmol, 0.10 equiv.), 4,4',4"-tri-tert-butyl-2,2':6',2"-terpyridine (40.0 mg, 0.10 mmol, 0.20 equiv.) and K_2CO_3 (207.3 mg, 1.50 mmol, 3.0 equiv.). A mixture of 1:3 methanol in acetonitrile (5 mL, 0.1 M) and alkyne (0.50 mmol, 1.0 equiv.) were then added. Alkyl iodide (1.00 mmol, 2 equiv.) was added to the reaction vessel, which was then capped and the reaction mixture wass stirred vigorously under the irradiation of blue light in the reaction chamber (Fig. S1). After the indicated time, the reaction was stopped. The reaction mixture was filtered through a pad of silica gel and washed with EtOAc and DCM. The filtrate was concentrated under reduced pressure and purified by silica gel chromatography.

2.4.7 *Characterization of the Internal Alkynes*

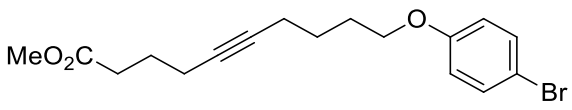

Methyl 9-(4-bromophenoxy)non-5-ynoate (2.11): compound was isolated as a colorless oil (141.3 mg, 83% yield). ^{1}H NMR (300 MHz, $CDCl_3$) δ 7.36 (d, *J* = 8.9 Hz, 2H), 6.78 (d, *J* = 8.9

Hz, 2H), 4.01 (t, *J* = 6.2 Hz, 2H), 3.67 (s, 3H), 2.41 (t, *J* = 7.5 Hz, 2H), 2.34 (tt, *J* = 6.8, 2.3 Hz, 2H), 2.21 (tt, *J* = 6.8, 2.3 Hz, 2H), 1.93 (p, *J* = 6.6 Hz, 2H), 1.79 (p, *J* = 7.1 Hz, 2H). ^{13}C NMR (126 MHz, $CDCl_3$) δ 173.8, 158.2, 132.4, 116.5, 112.9, 80.0, 79.8, 66.8, 51.7, 33.0, 28.7, 24.3, 18.4, 15.5. GC/MS (EI) calculated for $[M]^+$ 338.05, found 338.10. FTIR (neat, cm^{-1}): 3094 (w), 3066 (w), 2949 (m), 2847 (w), 1737 (s), 1591 (w), 1576 (w), 1489 (s), 1468 (m), 1436 (m), 1285 (m), 1244 (s), 1171 (m), 1051 (w), 1001 (w), 822 (m).

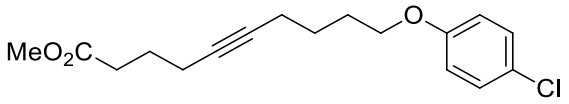

Methyl 9-(4-clorophenoxy)non-5-ynoate (2.12): compound was isolated as a colorless oil (121.0 mg, 82% yield). ^{1}H NMR (300 MHz, $CDCl_3$) δ 7.21 (d, *J* = 8.9 Hz, 2H), 6.82 (d, *J* = 8.9 Hz, 2H), 4.01 (t, *J* = 6.2 Hz, 2H), 3.66 (s, 3H), 2.41 (t, *J* = 7.5 Hz, 2H), 2.34 (tt, *J* = 6.8, 2.3 Hz, 2H), 2.21 (tt, *J* = 6.8, 2.3 Hz, 2H), 1.93 (p, *J* = 6.5 Hz, 2H), 1.79 (p, *J* = 7.2 Hz, 2H). ^{13}C NMR (126 MHz, $CDCl_3$) δ 173.8, 157.7, 129.4, 125.6, 115.9, 80.0, 79.8, 66.8, 51.7, 33.0, 28.7, 24.3, 18.3, 15.5. GC/MS (EI) calculated for $[M]^+$ 294.10, found 294.10. FTIR (neat, cm^{-1}): 3094 (w), 3070 (w), 2950 (m), 2872 (w), 2848 (w), 1736 (s) 1596 (w), 1581 (w), 1492 (s), 1283 (m), 1244 (s), 1169 (m), 1092 (m), 1051 (m), 1005 (m), 947 (w), 825 (m).

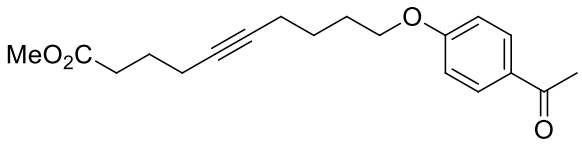

Methyl 9-(4-acetylphenoxy)non-5-ynoate (2.13): compound was isolated as a white solid (130.6 mg, 86% yield). ^{1}H NMR (300 MHz, $CDCl_3$) δ 7.91 (d, *J* = 8.9 Hz, 2H), 6.92 (d, *J* = 8.9 Hz, 2H), 4.11 (t, *J* = 6.2 Hz, 2H), 3.65 (s, 3H), 2.54 (s, 3H), 2.45 – 2.30 (m, 4H), 2.20 (tt, *J* = 6.9, 2.3 Hz,

2H), 1.96 (p, J = 6.5 Hz, 2H), 1.78 (p, J = 7.1 Hz, 2H). ^{13}C NMR (126 MHz, $CDCl_3$) δ 196.9, 173.8, 163.0, 130.7, 130.4, 114.27, 79.9, 79.8, 66.7, 51.7, 33.0, 28.6, 26.4, 24.3, 18.3, 15.5. GC/MS (EI) calculated for $[M]^+$ 302.15, found 302.20. FTIR (neat, cm^{-1}): 3076 (w), 3042 (w), 2950 (m), 2877 (w), 2846 (w), 1737 (s), 1677 (s), 1601 (s), 1576 (m), 1508 (m), 1434 (m), 1419 (m), 1254 (s) 1170 (m), 1049 (m), 947 (m), 830 (m).

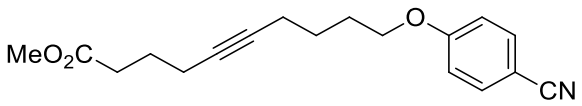

Methyl 9-(4-cyanophenoxy)non-5-ynoate (2.14): compound was isolated as a white solid (117.6 mg, 82% yield). ^{1}H NMR (300 MHz, $CDCl_3$) δ 7.55 (d, J = 8.7 Hz, 2H), 6.93 (d, J = 8.7 Hz, 2H), 4.08 (t, J = 6.2 Hz, 2H), 3.64 (s, 3H), 2.44 – 2.27 (m, 4H), 2.24 – 2.12 (m, 2H), 1.94 (p, J = 6.5 Hz, 2H), 1.77 (p, J = 7.2 Hz, 2H). ^{13}C NMR (75 MHz, $CDCl_3$) δ 173.6, 162.3, 134.0, 119.3, 115.3, 103.9, 80.0, 79.6, 66.9, 51.6, 32.9, 28.4, 24.2, 18.3, 15.4. GC/MS (EI) calculated for $[M]^+$ 285.14, found 385.10. FTIR (neat, cm^{-1}): 3101 (w), 3073 (w), 3047 (w), 2950 (m), 2877 (m), 2845 (m), 2224 (s), 1736 (s), 1606 (s), 1509 (s), 1468 (m), 1436 (m), 1302 (m) 1258 (s), 1172 (s), 1027 (m), 945 (w), 836 (m).

Methyl dodec-5-ynoate (2.15): compound was isolated as a colorless oil (97.0 mg, 92% yield). ^{1}H NMR (300 MHz, $CDCl_3$) δ 3.67 (s, 3H), 2.44 (t, J = 7.5 Hz, 2H), 2.28 – 2.18 (m, 2H), 2.18 – 2.06 (m, 2H), 1.80 (p, J = 7.1 Hz, 2H), 1.53 – 1.22 (m, 8H), 0.89 (t, J = 6.8 Hz, 3H). ^{13}C NMR (75 MHz, $CDCl_3$) δ 173.7, 81.3, 78.7, 51.5, 32.9, 31.4, 29.1, 28.6, 24.4, 22.6, 18.8, 18.3, 14.1. GC/MS

(EI) calculated for $[M]^+$ 210.16, found 210.15. FTIR (neat, cm^{-1}): 2932 (s), 2857 (s), 1737 (s), 1455 (s), 1435 (s), 1368 (m), 1221 (s) 1161 (s), 1058 (w), 999 (w), 862 (w), 727 (w).

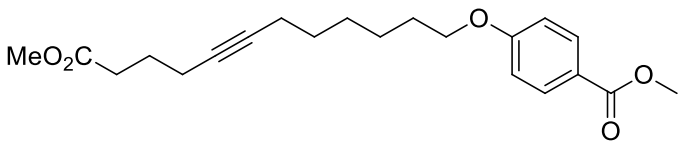

Methyl 4-((12-methoxy-12-oxododec-7-yn-1-yl)oxy)benzoate (2.16): compound was isolated as a colorless oil (152.8 mg, 85% yield). ^{1}H NMR (300 MHz, $CDCl_3$) δ 7.97 (d, *J* = 8.8 Hz, 2H), 6.89 (d, *J* = 8.8 Hz, 2H), 4.00 (t, *J* = 6.5 Hz, 2H), 3.87 (s, 3H), 3.66 (s, 3H), 2.42 (t, *J* = 7.5 Hz, 2H), 2.27 – 2.07 (m, 4H), 1.87 – 1.72 (m, 4H), 1.61 – 1.35 (m, 6H). ^{13}C NMR (126 MHz, $CDCl_3$) δ 173.9, 167.9 163.0, 131.7, 122.5, 114.2, 81.1, 79.1, 68.2, 51.9, 51.6, 33.0, 29.1, 29.0, 28.6, 25.7, 24.4, 18.8, 18.4. GC/MS (EI) calculated for $[M]^+$ 360.19, found 360.20. FTIR (neat, cm^{-1}): 3066 (w), 3000 (w), 2940 (s), 2858 (w), 1737 (s), 1716 (s), 1606 (s), 1511 (s), 1436 (s), 1280 (s), 1254 (s), 1168 (s), 1104 (m), 1010 (w), 847 (w), 771 (m), 696 (w).

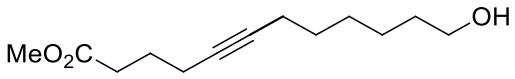

Methyl 12-hydroxydodec-5-ynoate (2.17): compound was isolated as a light yellow oil (96.7 mg, 86% yield). ^{1}H NMR (300 MHz, $CDCl_3$) δ 3.74 – 3.55 (m, 5H), 2.43 (t, *J* = 7.5 Hz, 2H), 2.30 – 2.06 (m, 4H), 1.80 (p, *J* = 7.0 Hz, 2H), 1.62 – 1.30 (m, 9H). ^{13}C NMR (75 MHz, $CDCl_3$) δ 173.9, 81.2, 78.9, 62.9, 51.62, 33.0, 32.7, 29.0, 28.6, 25.3, 24.3, 18.7, 18.3. GC/MS (EI) calculated for $[M]^+$ 226.16, found 226.10. FTIR (neat, cm^{-1}): 3366 (b), 2933 (s), 2858 (m), 1739 (s), 1436 (m), 1368 (w), 1225 (m), 1161 (m), 1055 (m).

Methyl 8-((triisopropylsilyl)oxy)oct-5-ynoate (2.18): compound was isolated as a colorless oil (133.3 mg, 82% yield). ^{1}H NMR (300 MHz, $CDCl_3$) δ 3.74 (t, *J* = 7.3 Hz, 2H), 3.66 (s, 3H), 2.48 – 2.31 (m, 4H), 2.19 (tt, *J* = 6.9, 2.2 Hz, 2H), 1.78 (p, *J* = 7.2 Hz, 2H), 1.26 – 0.84 (m, 21H). ^{13}C NMR (75 MHz, $CDCl_3$) δ 173.8, 80.1, 78.2, 62.7, 51.6, 33.0, 24.2, 23.4, 18.4, 18.1, 12.1. GC/MS (EI) calculated for $[M]^+$ 326.23, found 326.30. FTIR (neat, cm^{-1}): 2943 (s), 2866 (s), 1740 (s), 1464 (m), 1436 (m), 1381 (w), 1367 (w), 1246 (m), 1109 (s), 882 (m), 681 (m).

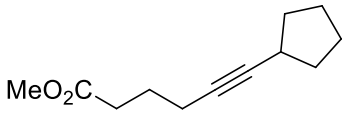

Methyl 6-cyclopentylhex-5-ynoate (2.19): compound was isolated as a clear colorless liquid (89.2 mg, 92% yield). ^{1}H NMR (500 MHz, $CDCl_3$) δ 3.67 (s, 3H), 2.60 – 2.51 (m, 1H), 2.43 (t, *J* = 7.4 Hz, 2H), 2.22 (t, *J* = 6.8 Hz, 2H), 1.87 (s, 2H), 1.83 – 1.75 (m, 2H), 1.74 – 1.63 (m, 2H), 1.56 – 1.47 (m, 4H). ^{13}C NMR (126 MHz, $CDCl_3$) δ 173.8, 85.6, 78.3, 51.5, 34.1, 32.9, 30.3, 24.9, 24.4, 18.4. GC/MS (EI) calculated for $[M]^+$ 194.13, found 194.00. FTIR (neat, cm^{-1}): 2927 (s), 2854 (s), 2358 (w), 2238 (w), 1738 (s), 1451 (s), 1366 (s), 1318 (s), 1235 (s), 1163 (s), 1058 (m), 863 (m), 755 (s).

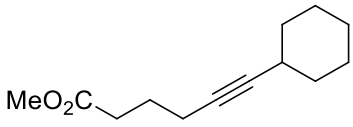

Methyl 6-cyclohexylhex-5-ynoate (2.20): compound was isolated as a clear colorless liquid (99.8 mg, 96% yield). ^{1}H NMR (500 MHz, $CDCl_3$) δ 3.67 (s, 3H), 2.43 (t, *J* = 7.4 Hz, 2H), 2.36 – 2.26 (m, 1H), 2.22 (t, *J* = 6.8 Hz, 2H), 1.86 – 1.71 (m, 4H), 1.70 – 1.64 (m, 2H), 1.54 – 1.45 (m, 1H),

1.43 – 1.32 (m, 2H), 1.30 – 1.20 (m, 3H). ^{13}C NMR (126 MHz, $CDCl_3$) δ 173.7, 85.6, 78.6, 51.4, 33.1, 32.9, 29.2, 26.0, 24.9, 24.4, 18.3. GC/MS (EI) calculated for $[M]^+$ 208.15, found 208.10. FTIR (neat, cm^{-1}): 2929 (s), 2852 (s), 2359 (w), 1740 (s), 1449 (s), 1365 (s), 1315 (s), 1222 (s), 1162 (s), 1055 (m).

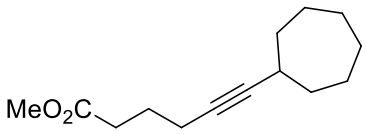

Methyl 6-cycloheptylhex-5-ynoate (2.21): compound was isolated as a clear colorless liquid (101.1 mg, 91% yield). ^{1}H NMR (500 MHz, $CDCl_3$) δ 3.62 (s, 3H), 2.51 – 2.43 (m, 1H), 2.38 (t, *J* = 7.5 Hz, 2H), 2.17 (td, *J* = 6.9, 2.1 Hz, 2H), 1.80 – 1.69 (m, 4H), 1.67 – 1.51 (m, 4H), 1.51 – 1.45 (m, 4H), 1.44 – 1.36 (m, 2H). ^{13}C NMR (126 MHz, $CDCl_3$) δ 173.7, 86.3, 78.8, 51.5, 35.1, 32.9, 31.2, 27.9, 25.6, 24.4, 18.3. GC/MS (EI) calculated for $[M]^+$ 222.16, found 222.10. FTIR (neat, cm^{-1}): 2929 (s), 2856 (s), 2339 (w), 2242 (w), 1737 (s), 1459 (s), 1438 (s), 1366 (s), 1321 (s), 1228 (s), 1159 (s), 1059 (m), 1008 (m), 863 (m).

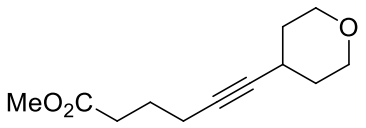

Methyl 6-(tetrahydro-2H-pyran-4-yl)hex-5-ynoate (2.22): compound was isolated as a clear colorless liquid (88.2 mg, 84% yield). ^{1}H NMR (500 MHz, $CDCl_3$) δ 3.97 – 3.76 (m, 2H), 3.64 (s, 3H), 3.43 (t, *J* = 10.0 Hz, 2H), 2.58 – 2.49 (m, 1H), 2.39 (t, *J* = 7.3 Hz, 2H), 2.20 (t, *J* = 6.7 Hz, 2H), 1.84 – 1.69 (m, 4H), 1.63 – 1.49 (m, 2H). ^{13}C NMR (126 MHz, $CDCl_3$) δ 173.6, 83.6, 79.8, 66.3, 51.5, 32.8, 32.6, 26.2, 24.2, 18.1. GC/MS (EI) calculated for $[M]^+$ 210.13, found 210.10.

FTIR (neat, cm^{-1}): 2956 (s), 2848 (s), 2359 (w), 2247 (w), 1738 (s), 1460 (s), 1438 (s), 1371 (m), 1314 (m), 1238 (s), 1162 (s), 1129 (s), 1085 (s), 1064 (s), 980 (m).

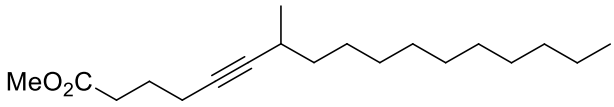

Methyl 7-methylheptadec-5-ynoate (2.23): compound was isolated as a clear colorless liquid (123.6 mg, 84% yield). ^{1}H NMR (500 MHz, $CDCl_3$) δ 3.64 (s, 3H), 2.40 (t, *J* = 7.5 Hz, 2H), 2.35 – 2.27 (m, 1H), 2.19 (dt, *J* = 7.5, 3.4 Hz, 2H), 1.77 (p, *J* = 7.5 Hz, 2H), 1.43 – 1.18 (m, 18H), 1.08 (d, *J* = 6.8 Hz, 3H), 0.85 (t, *J* = 6.7 Hz, 3H). ^{13}C NMR (126 MHz, $CDCl_3$) δ 173.8, 86.1, 78.8, 51.5, 37.4, 32.9, 32.0, 29.8, 29.7, 29.7, 29.6, 29.5, 27.5, 26.0, 24.4, 22.8, 21.5, 18.3, 14.2. GC/MS (EI) calculated for $[M]^+$ 294.26, found 294.30. FTIR (neat, cm^{-1}): 2925 (s), 2852 (s), 2233 (w), 1743 (s), 1453 (s), 1437 (s), 1374 (s), 1334 (s), 1314 (s), 1222 (s), 1161 (s), 1059 (m), 998 (m) 734 (s).

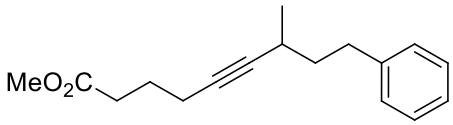

Methyl 7-methyl-9-phenylnon-5-ynoate (2.24): compound was isolated as a clear colorless liquid (109.7 mg, 85% yield). ^{1}H NMR (500 MHz, $CDCl_3$) δ 7.34 – 7.27 (m, 2H), 7.25 – 7.16 (m, 3H), 3.69 (s, 3H), 2.88 – 2.77 (m, 1H), 2.77 – 2.64 (m,1H), 2.49 (t, *J* = 7.4 Hz, 2H), 2.45 – 2.40 (m, 1H), 2.29 (t, *J* = 6.8 Hz, 2H), 1.86 (p, *J* = 7.1 Hz, 2H), 1.72 (dd, *J* = 15.0, 7.5 Hz, 2H), 1.18 (d, *J* = 6.8 Hz, 3H). ^{13}C NMR (126 MHz, $CDCl_3$) δ 173.7, 142.2, 128.5, 128.3, 125.8, 85.4, 79.6, 51.5, 39.1, 33.8, 32.9, 25.5, 24.4, 21.5, 18.3. GC/MS (EI) calculated for $[M]^+$ 258.16, found

258.20. FTIR (neat, cm^{-1}): 3025 (m), 2920 (s), 2868 (m), 1738 (s), 1603 (m), 1495 (s), 1453 (s), 1437 (s), 1372 (s), 1334 (s), 1247 (m), 1225 (s), 1162 (s), 1059 (m), 1030 (m), 749 (s), 700 (s).

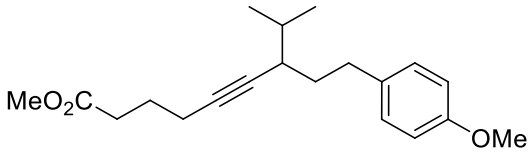

Methyl 7-isopropyl-9-(4-methoxyphenyl)non-5-ynoate (2.25): compound was isolated as a clear colorless liquid (62.4 mg, 78% yield). ^{1}H NMR (300 MHz, $CDCl_3$) δ 7.12 (d, *J* = 8.4 Hz, 2H), 6.83 (d, *J* = 8.4 Hz, 2H), 3.79 (s, 3H), 3.68 (s, 3H), 2.89 – 2.68 (m, 1H), 2.66 – 2.52 (m, 2H), 2.48 (t, *J* = 7.5 Hz, 2H), 2.28 (dt, *J* = 15.8, 9.7 Hz, 2H), 2.23 – 2.12 (m, 1H), 1.85 (p, 2H), 1.72 – 1.57 (m, 2H), 0.94 (dd, *J* = 6.3, 4.9 Hz, 6H). ^{13}C NMR (126 MHz, $CDCl_3$) δ 173.9, 157.9, 134.6, 129.5, 113.9, 82.7, 81.5, 55.4, 51.6, 38.5, 35.3, 33.3, 33.1, 31.8, 24.7, 21.2, 18.6, 18.5. GC/MS (EI) calculated for $[M]^+$ 316.20, found 316.20. FTIR (neat, cm^{-1}): 2956 (s), 2869 (s), 1738 (s), 1611 (s), 1583 (w), 1512 (s), 1462 (s), 1438 (s), 1367 (m), 1300 (m), 1246 (s), 1176 (s), 1037 (s).

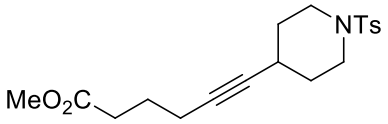

Methyl 6-(1-tosylpiperidin-4-yl)hex-5-ynoate (2.26): compound was isolated as a clear colorless liquid (157.9 mg, 87% yield). ^{1}H NMR (300 MHz, $CDCl_3$) δ 7.64 (d, *J* = 8.1 Hz, 2H), 7.32 (d, *J* = 8.1 Hz, 2H), 3.67 (s, 3H), 3.46 – 3.13 (m, 2H), 2.87 – 2.63 (m, 2H), 2.43 (s, 3H), 2.40 – 2.25 (m, 3H), 2.21 – 2.03 (m, 2H), 1.90 – 1.60 (m, 6H). ^{13}C NMR (126 MHz, $CDCl_3$) δ 173.6, 143.5, 133.4, 129.7, 127.8, 82.34, 81.0, 51.6, 44.6, 32.8, 31.3, 26.3, 24.2, 21.6, 18.1. GC/MS (EI) calculated for $[M]^+$ 363.15, found 363.10. FTIR (neat, cm^{-1}): 2929 (s), 2854 (s), 2304 (w), 1735 (s), 1715 (s), 1438 (s), 1343 (s), 1265 (s), 1165 (s), 1093 (s), 1050 (m), 930 (m).

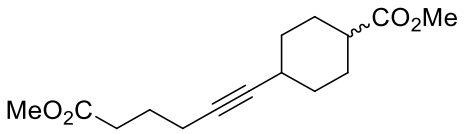

Methyl 4-(6-methoxy-6-oxohex-1-yn-1-yl)cyclohexanecarboxylate (2.27): compound was isolated as a clear colorless liquid (97.1 mg, 73% yield). ^{1}H NMR (500 MHz, $CDCl_3$) δ 3.79 – 3.36 (m, 6H), 2.59 (s, 1H), 2.38 (dt, 2H), 2.30 – 2.12 (m, 3H), 2.01 – 1.62 (m, 7H), 1.52 – 1.18 (m, 3H). ^{13}C NMR (126 MHz, $CDCl_3$) δ 176.1, 175.9, 173.7, 173.7, 84.9, 83.8, 80.3, 78.9, 51.6, 51.5, 42.4, 42.3, 33.0, 32.9, 32.4, 30.4, 29.0, 28.2, 27.0, 25.1, 24.4, 24.3, 18.3, 18.3 $[M]^+$ 266.15, found 266.20. FTIR (neat, cm^{-1}): 2925 (s), 2862 (s), 2235 (w), 1838 (m), 1738 (s), 1730 (s), 1711 (s), 1477 (s), 1460 (s), 1438 (s), 1376 (m), 1199 (s), 1167 (s), 1039 (m).

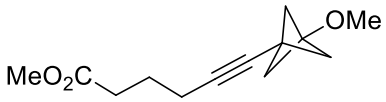

Methyl 6-(3-methoxybicyclo[1.1.1]pentan-1-yl)hex-5-ynoate (2.28): compound was isolated as a clear colorless liquid (29.4 mg, 53% yield). ^{1}H NMR (500 MHz, $CDCl_3$) δ 3.63 (s, 3H), 3.22 (s, 3H), 2.37 (t, J = 7.4 Hz, 2H), 2.21 (t, J = 7.0 Hz, 2H), 2.06 (s, 6H), 1.81 – 1.66 (m, 2H). ^{13}C NMR (126 MHz, $CDCl_3$) δ 173.7, 81.2, 78.2, 67.8, 55.4, 54.1, 51.6, 32.9, 24.0, 21.2, 18.5. GC/MS (EI) calculated for $[M]^+$ 222.13, found 222.20. FTIR (neat, cm-1): 2986 (s), 2914 (s), 2833 (s), 2359 (w), 2220 (w), 1738 (s), 1514 (s), 1460 (s), 1435 (s), 1370 (s), 1317 (s), 1257 (s), 1156 (s), 1121 (s), 1032 (s).

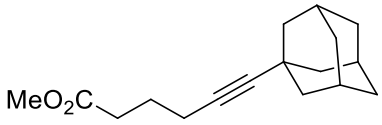

Methyl 6-((3r,5r,7r)-adamantan-1-yl)hex-5-ynoate (2.29): compound was isolated as a clear colorless liquid (52.6 mg, 81% yield). ^{1}H NMR (500 MHz, $CDCl_3$) δ 3.67 (s, 3H), 2.42 (t, *J* = 7.5 Hz, 2H), 2.22 (t, *J* = 6.9 Hz, 2H), 1.93 (s, 3H), 1.84 – 1.75 (m, 8H), 1.66 (s, 6H). ^{13}C NMR (126 MHz, $CDCl_3$) δ 174.1, 90.3, 77.6, 51.7, 43.5, 36.6, 33.0, 29.7, 28.3, 24.5, 18.4. GC/MS (EI) calculated for $[M]^+$ 260.18, found 260.20. FTIR (neat, cm^{-1}): 3053 (m), 2910 (s), 2851 (s), 2305 (w), 1731 (s), 1677 (w), 1452 (s), 1265 (s), 1225 (m), 1160 (w), 740 (s), 704 (s).

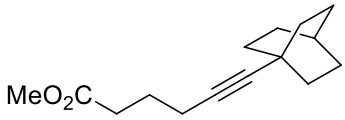

Methyl 6-(bicyclo[2.2.2]octan-1-yl)hex-5-ynoate (2.30): compound was isolated as a colorless oil (50.2 mg, 43% yield). ^{1}H NMR (300 MHz, $CDCl_3$) δ 3.67 (s, 3H), 2.41 (t, *J* = 7.5 Hz, 2H), 2.20 (t, *J* = 6.9 Hz, 2H), 1.83 – 1.71 (m, 2H), 1.71 – 1.47 (m, 12H), 1.30 – 1.16 (m, 1H). ^{13}C NMR (126 MHz, $CDCl_3$) δ 173.9, 89.3, 78.2, 51.2, 32.9, 32.5, 26.5, 25.9, 24.5, 23.4, 18.4. GC/MS (EI) calculated for $[M]^+$ 234.16, found 234.20. FTIR (neat, cm^{-1}): 2941 (s), 2905 (m), 2863 (m), 1738 (s), 1452 (m), 1434 (m), 1367 (w), 1320 (w), 1221 (m), 1160 (m), 1066 (w).

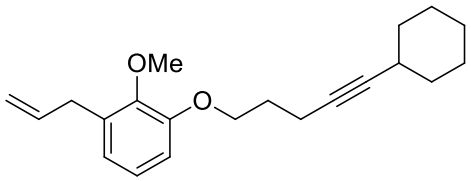

1-Allyl-3-((5-cyclohexylpent-4-yn-1-yl)oxy)-2-methoxybenzene (2.32): compound was isolated as a clear colorless liquid (112.4 mg, 72% yield). ^{1}H NMR (300 MHz, $CDCl_3$) δ 6.85 (d, *J* = 8.6

Hz, 1H), 6.80 – 6.61 (m, 2H), 5.96 (ddt, *J* = 16.7, 9.7, 6.7 Hz, 1H), 5.18 – 4.97 (m, 2H), 4.10 (t, *J* = 6.5 Hz, 2H), 3.85 (s, 3H), 3.33 (d, *J* = 6.7 Hz, 2H), 2.47 – 2.20 (m, 3H), 2.08 – 1.92 (m, 2H), 1.83 – 1.60 (m, 4H), 1.48 – 1.22 (m, 6H). ^{13}C NMR (126 MHz, $CDCl_3$) δ 149.6, 147.0, 137.8, 133.0, 120.6, 115.6, 113.7, 112.6, 85.4, 79.0, 68.0, 56.0, 39.9, 33.2, 29.2, 28.9, 26.0, 25.0, 15.6. GC/MS (EI) calculated for $[M]^+$ 312.21, found 312.20. FTIR (neat, cm^{-1}): 2998 (s), 2929 (s), 2851 (s), 2224 (m), 1638 (s), 1605 (s), 1598 (s), 1513 (s), 1466 (s), 1448 (s), 1420 (s), 1329 (m), 1260 (s), 1233 (s), 1156 (s), 1139 (s), 1037 (s), 993 (m), 913 (m), 849 (m), 802 (s), 747 (s).

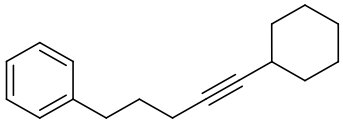

(5-Cyclohexylpent-4-yn-1-yl)benzene (2.33): compound was isolated as a clear colorless liquid (106.3 mg, 94% yield). ^{1}H NMR (300 MHz, $CDCl_3$) δ 7.35 – 7.27 (m, 2H), 7.23 – 7.13 (m, 3H), 2.76 – 2.69 (m, 2H), 2.45 – 2.27 (m, 1H), 2.19 (td, *J* = 7.0, 2.1 Hz, 2H), 1.87 – 1.63 (m, 6H), 1.52 – 1.22 (m, 6H). ^{13}C NMR (126 MHz, $CDCl_3$) δ 142.1, 128.7, 128.4, 125.9, 85.4, 79.7, 34.9, 33.3, 31.0, 29.3, 26.1, 25.1, 18.4. GC/MS (EI) calculated for $[M]^+$ 226.17, found 226.20. FTIR (neat, cm^{-1}): 3025 (m), 2930 (s), 2853 (s), 2236 (w), 1602 (m), 1492 (s), 1449 (s), 1346 (m), 1297 (m), 1216 (m), 1179 (m), 1079 (w).

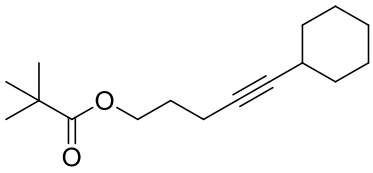

5-Cyclohexylpent-4-yn-1-yl pivalate (2.34): compound was isolated as a clear colorless liquid (81.3 mg, 65% yield). ^{1}H NMR (300 MHz, $CDCl_3$) δ 4.14 (t, *J* = 6.3 Hz, 2H), 2.47 – 2.09 (m, 3H),

1.91 – 1.63 (m, 6H), 1.47 – 1.24 (m, 6H), 1.20 (s, 9H). ^{13}C NMR (126 MHz, $CDCl_3$) δ 178.5, 85.5, 78.5, 63.2, 38.8, 33.2, 29.2, 28.4, 27.3, 26.0, 25.0, 15.6. GC/MS (EI) calculated for $[M]^+$ 250.19, found 250.20. FTIR (neat, cm^{-1}): 2931 (s), 2854 (s), 2358 (w), 2255 (w), 1727 (s), 1480 (s), 1449 (s), 1398 (m), 1364 (m), 1285 (s), 1160 (s), 1037 (m), 914 (m).

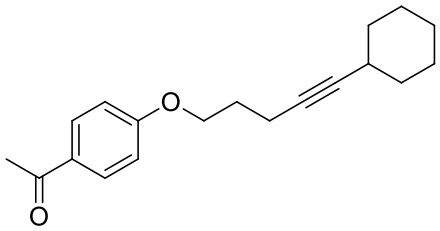

1-(4-((5-Cyclohexylpent-4-yn-1-yl)oxy)phenyl)ethanone (2.35): compound was isolated as a clear colorless liquid (109.4 mg, 77% yield). ^{1}H NMR (300 MHz, $CDCl_3$) δ 7.93 (d, *J* = 8.9 Hz, 2H), 6.93 (d, *J* = 8.9 Hz, 2H), 4.14 (t, *J* = 6.3 Hz, 2H), 2.55 (s, 3H), 2.47 – 2.21 (m, 3H), 1.97 (p, *J* = 6.5 Hz, 2H), 1.83 – 1.61 (m, 4H), 1.52 – 1.21 (m, 6H). ^{13}C NMR (126 MHz, $CDCl_3$) δ 196.7, 163.1, 130.6, 130.3, 114.2, 85.7, 78.5, 66.8, 33.1, 29.2, 28.7, 26.3, 26.0, 25.0, 15.5. GC/MS (EI) calculated for $[M]^+$ 284.18, found 284.10. FTIR (neat, cm^{-1}): 2929 (s), 2853 (s), 2240 (w), 1676 (s), 1601 (s), 1509 (s), 1448 (s), 1420 (s), 1358 (s), 1306 (s), 1256 (s), 1172 (s), 1116 (m).

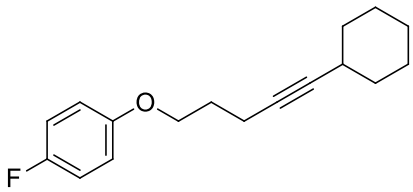

1-((5-Cyclohexylpent-4-yn-1-yl)oxy)-4-fluorobenzene (2.36): compound was isolated as a clear colorless liquid (93.7 mg, 72% yield). ^{1}H NMR (500 MHz, $CDCl_3$) δ 7.08 – 6.88 (m, 2H), 6.88 – 6.79 (m, 2H), 4.02 (t, *J* = 6.0 Hz, 2H), 2.47 – 2.19 (m, 3H), 2.05 – 1.88 (m, 2H), 1.82 – 1.60 (m, 4H), 1.50 (s, 1H), 1.40 – 1.23 (m, 5H). ^{13}C NMR (126 MHz, $CDCl_3$) δ 157.2 (d, *J* = 237.9 Hz),

155.2 (d, *J* = 1.4 Hz), 115.7 (d, *J* = 23.1 Hz), 115.5 (d, *J* = 7.9 Hz), 85.5, 78.7, 67.2, 33.1, 29.1, 28.9, 25.9, 24.9, 15.5. ^{19}F NMR (471 MHz, $CDCl_3$) δ -127.1. GC/MS (EI) calculated for $[M]^+$ 260.16, found 260.20. FTIR (neat, cm^{-1}): 3053 (w), 2932 (s), 2854 (m), 2304 (w), 1507 (s), 1469 (m), 1449 (m), 1256 (s), 1248 (s), 1210 (s), 1097 (m), 1054 (m), 948 (w), 895 (w), 830 (s), 739 (s), 705 (s).

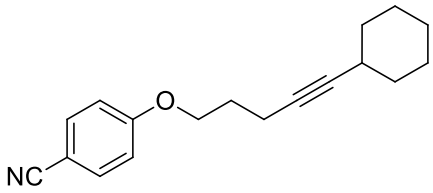

4-((5-Cyclohexylpent-4-yn-1-yl)oxy)benzonitrile (2.37): compound was isolated as a clear colorless liquid (114.9 mg, 86% yield). ^{1}H NMR (500 MHz, $CDCl_3$) δ 7.54 (d, *J* = 8.7 Hz, 2H), 6.93 (d, *J* = 8.7 Hz, 2H), 4.09 (t, *J* = 6.2 Hz, 2H), 2.35 (td, *J* = 6.2, 1.9 Hz, 2H), 2.32 – 2.24 (m, 1H), 1.94 (p, *J* = 6.2 Hz, 2H), 1.77 – 1.69 (m, 2H), 1.68 – 1.59 (m, 2H), 1.51 – 1.42 (m, 1H), 1.39 – 1.29 (m, 2H), 1.28 – 1.18 (m, 3H). ^{13}C NMR (126 MHz, $CDCl_3$) δ 162.4, 133.9, 119.2, 115.2, 103.8, 85.7, 78.3, 66.9, 33.1, 29.1, 28.5, 25.9, 24.9, 15.4. GC/MS (EI) calculated for $[M]^+$ 267.16, found 267.20. FTIR (neat, cm^{-1}): 2929 (s), 2852 (s), 2224 (s), 1598 (s), 1566 (w), 1506 (s), 1467 (m), 1443 (m), 1302 (s), 1258 (s), 1174 (s), 1045 (m), 912 (s), 834 (s), 733 (s).
1045(s).

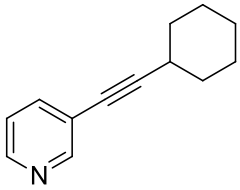

3-(Cyclohexylethynyl)pyridine (2.38): compound was isolated as a colorless oil (52.3 mg, 56% yield). ^{1}H NMR (300 MHz, $CDCl_3$) δ 8.62 (d, *J* = 1.5 Hz, 1H), 8.47 (dd, *J* = 4.9, 1.5 Hz, 1H), 7.66 (dt, *J* = 7.9, 1.9 Hz, 1H), 7.20 (dd, *J* = 7.9, 4.9 Hz, 1H), 2.68 – 2.51 (m, 1H), 1.96 – 1.82 (m, 2H), 1.82 – 1.69 (m, 2H), 1.61 – 1.47 (m, 3H), 1.42 – 1.29 (m, 3H). ^{13}C NMR (126 MHz, $CDCl_3$) δ 152.5, 147.9, 138.5, 122.9, 121.3, 98.1, 77.4, 32.6, 29.8, 25.9, 25.0. GC/MS (EI) calculated for $[M]^+$ 185.12, found 185.10. FTIR (neat, cm^{-1}): 3084 (w), 3027 (w), 2930 (s), 2853 (s), 2230 (w), 1585 (w), 1558 (w), 1476 (m), 1448 (m), 1405 (s), 1184 (w), 1022 (w), 952 (w), 803 (m).

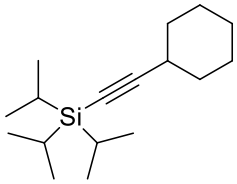

(Cyclohexylethynyl)triisopropylsilane (2.39): compound was isolated as a colorless oil (105.7mg, 80% yield). ^{1}H NMR (500 MHz, $CDCl_3$) δ 2.57 – 2.27 (m, 1H), 1.87 – 1.65 (m, 4H), 1.60 – 1.42 (m, 3H), 1.37 – 1.30 (m, 3H), 1.22 – 0.95 (m, 21H).1.25 – 0.98 (m, 21H). ^{13}C NMR (126 MHz, $CDCl_3$) δ 113.8, 79.7, 32.9, 30.0, 26.2, 24.6, 18.8, 11.5. GC/MS (EI) calculated for $[M]^+$ 264.23, found 264.20. FTIR (neat, cm^{-1}): 2924 (s), 2858 (s), 2358 (m), 2169 (m), 1462 (m). 1452 (m), 1377 (w), 1353 (w), 1311 (w), 1075 (m).

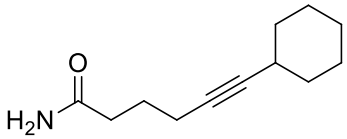

6-Cyclohexylhex-5-ynamide (2.40): compound was isolated as a white solid (75.5 mg, 78% yield). ^{1}H NMR (500 MHz, $CDCl_3$) δ 5.56 – 5.21 (m, 2H), 2.42 – 2.29 (m, 3H), 2.28 – 2.19 (m, 2H), 1.88 – 1.73 (m, 4H), 1.73 – 1.63 (m, 2H), 1.56 – 1.47 (m, 1H), 1.44 – 1.33 (m, 2H), 1.33 – 1.22 (m, 3H). ^{13}C NMR (75 MHz, $CDCl_3$) δ 175.9, 85.7, 78.7, 34.6, 33.1, 29.1, 25.9, 24.9, 24.8, 18.2. GC/MS (EI) calculated for $[M]^+$ 193.15, found 193.20. FTIR (neat, cm^{-1}): 3358 (s), 3193 (s), 2925 (s), 2851 (s), 2244 (w) 1654 (s), 1428 (m), 1347 (m), 1274 (m), 1130 (w), 911 (m), 735 (m).

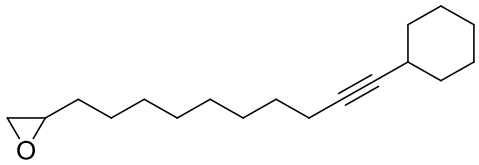

2-(10-Cyclohexyldec-9-yn-1-yl)oxirane (2.41): compound was isolated as a clear colorless liquid (107.5 mg, 82% yield). ^{1}H NMR (500 MHz, $CDCl_3$) δ 2.90 – 2.80 (m, 1H), 2.70 (t, J = 4.5 Hz, 1H), 2.42 (dd, J = 5.0, 2.7 Hz, 1H), 2.35 – 2.19 (m, 1H), 2.11 (td, J = 7.0, 2.0 Hz, 2H), 1.79 – 1.58 (m, 4H), 1.52 – 1.17 (m, 20H). ^{13}C NMR (126 MHz, $CDCl_3$) δ 84.7, 80.1, 52.4, 47.1, 33.3, 32.6, 29.5, 29.4, 29.3, 29.2, 29.1, 28.8, 26.1, 26.0, 25.0, 18.8. GC/MS (EI) calculated for $[M]^+$ 262.23, found 262.30. FTIR (neat, cm^{-1}): 2927 (s), 2854 (s), 2660 (w), 2249 (m), 1481 (m), 1448 (s), 1409 (s), 1328 (s), 1257 (s), 1233 (s), 1129 (m), 1012 (m).

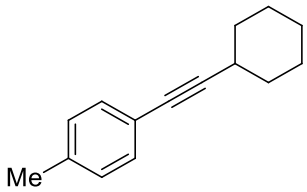

1-(Cyclohexylethynyl)-4-methylbenzene (2.42): compound was isolated as a clear colorless liquid (82.3 mg, 83% yield). ^{1}H NMR (300 MHz, $CDCl_3$) δ 7.29 (d, *J* = 8.0 Hz, 2H), 7.08 (d, *J* = 8.0 Hz, 2H), 2.70 – 2.48 (m, 1H), 2.33 (s, 3H), 1.97 – 1.70 (m, 4H), 1.64 – 1.46 (m, 3H), 1.43 – 1.25 (m, 3H). ^{13}C NMR (126 MHz, $CDCl_3$) δ 137.4, 131.6, 129.0, 121.2, 93.7, 80.7, 32.9, 29.8, 26.1, 25.1, 21.5. GC/MS (EI) calculated for $[M]^+$ 198.14, found 198.20. FTIR (neat, cm^{-1}): 3027 (w), 2930 (s), 2853 (s), 2228 (w), 1902 (w), 1510 (s), 1448 (m), 1349 (s), 1301 (w), 1258 (w), 1178 (m), 1105 (m), 1020 (m), 815 (m).

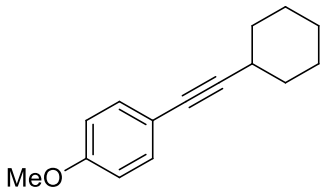

1-(Cyclohexylethynyl)-4-methoxybenzene (2.43): compound was isolated as a clear colorless liquid (79.2 mg, 74% yield. ^{1}H NMR (300 MHz, $CDCl_3$) δ 7.33 (d, *J* = 8.9 Hz, 2H), 6.81 (d, *J* = 8.9 Hz, 2H), 3.79 (s, 3H), 2.78 – 2.35 (m, 1H), 2.12 – 1.66 (m, 4H), 1.62 – 1.46 (m, 3H), 1.44 – 1.25 (m, 3H). ^{13}C NMR (126 MHz, $CDCl_3$) δ 159.1, 133.0, 116.5, 113.9, 92.9, 80.4, 55.3, 33.0, 29.8, 26.1, 25.1. GC/MS (EI) calculated for $[M]^+$ 214.14, found 214.20. FTIR (neat, cm^{-1}): 3028 (w), 2929 (s), 2852 (s), 2230 (w), 1606 (s), 1503 (s), 1448 (s), 1287 (s), 1247 (s), 1171 (m), 1105 (s), 1032 (s), 830 (s).

2.4.8 *Alkyne Starting Materials*

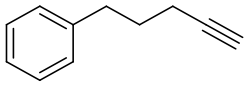

Pent-4-yn-1-ylbenzene (2.47): compound was purchased from GSF Chemicals and distilled over calcium hydride under vacuum before use.

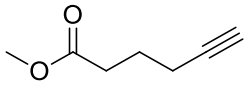

Methyl hex-5-ynoate (2.9): compound was purchased from Alfa Aesar and distilled over calcium hydride under vacuum before use.

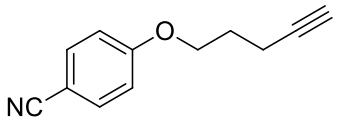

4-(Pent-4-yn-1-yloxy)benzonitrile (2.48): compound was prepared according to a known procedure and has been previously characterized.[58]

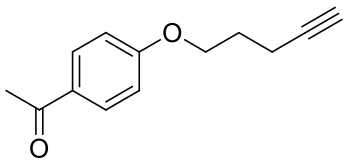

1-(4-(Pent-4-yn-1-yloxy)phenyl)ethenone (2.49): compound was prepared according to a known procedure and has been previously characterized.[59]

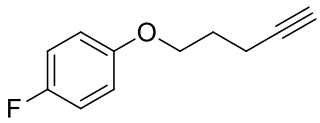

1-Fluoro-4-(pent-4-yn-1-yloxy)benzene (2.50): compound was prepared according to a known procedure and has been previously characterized.[59]

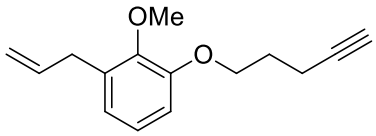

1-Allyl-2-methoxy-3-(pent-4-yn-1-yloxy)benzene (2.51): compound was prepared according to the following procedure. A reaction flask charged with stir bar was flame-dried under vacuum and allowed to cool under nitrogen. The flask was then charged with triphenylphosphine (2.2 g, 24.0 mmol, 1.2 equiv), eugenol (1.0 g, 7.7 mmol, 1.1 equiv), THF (14.0 mL, 0.5 M) and 4-pentyn-1-ol (654.0 µL, 7.0 mmol, 1.0 equiv). The reaction mixture was cooled to 0 °C with an ice bath. To the cooled reaction mixture was added DIAD (1.6 mL, 8.4 mmol, 1.2 equiv) dropwise. The reaction mixture was allowed to warm to 23 °C and stirred overnight. THF was removed under reduced pressure and the mixture was suspended in hexanes and stirred vigorously for 30 min. The solid triphenylphosphine oxide was removed by passing the mixture through a plug of celite. The solvent was removed under reduced pressure and the crude product was purified by silica gel chromatography. ^{1}H NMR (500 MHz, Chloroform-*d*) δ 6.88 (d, *J* = 7.8 Hz, 1H), 6.75 (d, *J* = 7.8 Hz, 2H), 6.01 (ddt, *J* = 16.8, 10.0, 6.7 Hz, 1H), 5.38 – 4.94 (m, 2H), 4.12 (t, *J* = 6.2 Hz, 2H), 3.88 (s, 3H), 3.48 – 3.14 (m, 2H), 2.46 (td, *J* = 7.0, 2.7 Hz, 2H), 2.19 – 1.81 (m, 3H).^{13}C NMR (126 MHz, $CDCl_3$) δ 149.4, 146.7, 137.6, 132.9, 120.4, 115.5, 114.0, 112.4, 83.5, 68.8, 67.5, 55.8, 39.7, 28.1, 15.1. FTIR (neat, cm^{-1}): 3258 (s), 2996 (s), 2927 (s), 2858 (s), 2340 (m), 2122 (m), 1634 (s),

1605 (s), 1512 (s), 1460 (s), 1447 (s), 1421 (s), 1330 (m), 1260 (s), 1234 (s), 1138 (s), 1037 (s), 994 (m), 913 (m), 847 (m), 802 (s), 746 (s).

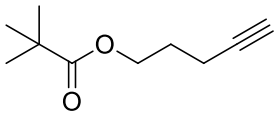

Pent-4-yn-1-yl pivalate (2.52): compound was prepared according to a known procedure and has been previously characterized.[60]

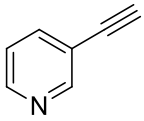

3-Ethynylpyridine (2.53): compound was purchased from Sigma-Aldrich and used directly.

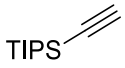

Ethynyltriisopropylsilane (2.54): compound was purchased from Alfa Aesar and used directly.

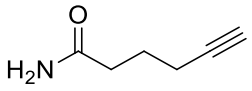

Hex-5-ynamide (2.55): compound was prepared according to a known procedure and has been previously characterized.[61]

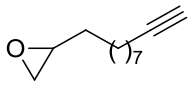

2-(10-Dec-9-yn-1-yl)oxirane (2.56): compound was prepared according to a known procedure and has been previously characterized.[60]

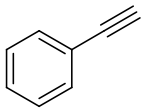

Ethynylbenzene (2.6): compound was purchased from Sigma-Aldrich and distilled over calcium hydride under vacuum before use.

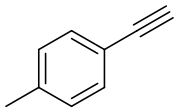

1-Ethynyl-4-methylbenzene (2.57): compound was purchased from Sigma-Aldrich and distilled over calcium hydride under vacuum before use.

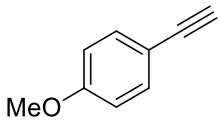

1-Ethynyl-4-methoxybenzene (2.58): compound was purchased from Sigma-Aldrich and distilled over calcium hydride under vacuum before use.

2.4.9 *Iodide Starting Materials*

All the iodides were prepared from the corresponding alcohol using the following procedure. A reaction flask charged with a Teflon coated stir bar was flame-dried under vacuum and allowed to cool under nitrogen. The flask was then charged with triphenylphosphine (2.2 g,

24.0 mmol, 1.2 equiv), imidazole (1.77 g, 26.0 mmol, 1.3 equiv). Anhydrous DCM was added to obtain a concentration of 0.3 M with respect to the alcohol. The flask was placed in an ice-bath and after 5 minutes of stirring, Iodine (6.9 g, 24.0 mmol, 1.2 equiv) was added and stirred for 15 minutes. Alcohol (20.0 mmol, 1.0 equiv) was added dropwise. The reaction was stirred overnight at room temperature.

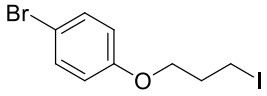

1-Bromo-4-(3-iodopropoxy)benzene (2.10): compound was isolated as a colorless oil. ^{1}H NMR (300 MHz, $CDCl_3$) δ 7.40 (d, *J* = 9.0 Hz, 2H), 6.81 (d, *J* = 9.0 Hz, 2H), 4.02 (t, *J* = 5.9 Hz, 2H), 3.38 (t, *J* = 6.7 Hz, 2H), 2.28 (p, *J* = 6.3 Hz, 2H). ^{13}C NMR (75 MHz, $CDCl_3$) δ 157.9, 132.4, 116.4, 113.2, 67.6, 32.9, 2.4. GC/MS (EI) calculated for $[M]^+$ 339.90, found 339.90. FTIR (neat, cm^{-1}): 3068 (w), 2923 (m), 2875 (m), 1589 (m), 1578 (m), 1488 (s), 1465 (s), 1286 (s), 1245 (s), 1171 (s), 1071 (m), 1001 (w), 820 (s), 639 (m).

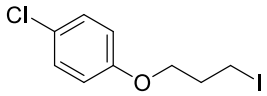

1-Chloro-4-(3-iodopropoxy)benzene (2.59): compound was isolated as a colorless. ^{1}H NMR (300 MHz, $CDCl_3$) δ 7.25 (d, *J* = 9.0 Hz, 2H), 6.85 (d, *J* = 9.0 Hz, 2H), 4.02 (t, *J* = 5.8 Hz, 2H), 3.37 (t, *J* = 6.7 Hz, 2H), 2.39 – 2.15 (m, 2H). ^{13}C NMR (75 MHz, $CDCl_3$) δ 157.4, 129.4, 125.9, 115.9, 67.7, 32.9, 2.4. GC/MS (EI) calculated for $[M]^+$ 295.95, found 295.95. FTIR (neat, cm^{-1}): 3052 (w), 2926 (m), 2870 (m), 1595 (m), 1580 (m), 1491 (s), 1466 (m), 1437 (m), 1245 (s), 1090 (m), 1020 (m), 1005 (m), 824 (s).

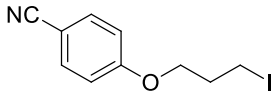

4-(3-Iodopropoxy)benzonitrile (2.60): compound was isolated as a colorless oil. ^{1}H NMR (300 MHz, $CDCl_3$) δ 7.57 (d, *J* = 8.8 Hz, 2H), 6.94 (d, *J* = 8.8 Hz, 2H), 4.08 (t, *J* = 5.8 Hz, 2H), 3.34 (t, *J* = 6.6 Hz, 2H), 2.28 (p, *J* = 6.2 Hz, 2H). ^{13}C NMR (75 MHz, $CDCl_3$) δ 162.0, 134.0, 119.2, 115.3, 104.2, 67.7, 32.5, 2.0. GC/MS (EI) calculated for $[M]^+$ 286.98, found 287.00. FTIR (neat, cm^{-1}): 3098 (w), 3074 (w), 2958 (m), 2935 (m), 2882 (w), 2222 (s), 1604 (s), 1574 (s), 1504 (s), 1567 (s), 1504 (s), 1420 (m), 1402 (m), 1299 (s), 1256 (s), 1172 (s), 1016 (s), 839 (s), 719 (m).

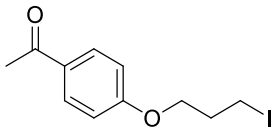

1-(4-(3-Iodopropoxy)phenyl)ethanone (2.61): compound was isolated as a colorless. ^{1}H NMR (300 MHz, $CDCl_3$) δ 7.94 (d, *J* = 8.9 Hz, 2H), 6.94 (d, *J* = 8.9 Hz, 2H), 4.11 (t, *J* = 5.8 Hz, 2H), 3.37 (t, *J* = 6.8 Hz, 2H), 2.56 (s, 3H), 2.30 (p, *J* = 6.3 Hz, 2H). ^{13}C NMR (75 MHz, $CDCl_3$) δ 196.7, 162.6, 130.7, 130.6, 114.2, 67.6, 32.8, 26.4, 2.2. GC/MS (EI) calculated for $[M]^+$ 304.00, found 304.00. FTIR (neat, cm^{-1}): 3098 (w), 3075 (w), 2948 (m), 2927 (s), 2870 (s), 1939 (w), 1914 (w), 1887 (w), 1663 (s), 1607 (m), 1433 (m), 1420 (m), 1357 (s), 1113 (m), 1050 (m), 836 (s).

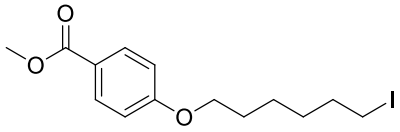

Methyl 4-((6-iodohexyl)oxy)benzoate (2.62): compound has been previously characterized and spectral data match the reported literature values.[62]

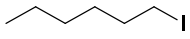

1-Iodohexane (2.63): compound has been previously characterized and spectral data match the reported literature values.[63]

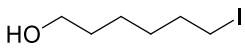

6-Iodohexan-1-ol (2.64): compound has been previously characterized and spectral data match the reported literature values.[64]

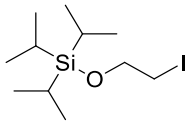

(2-Iodoethoxy)triisopropylsilane (2.65): compound has been previously characterized and spectral data match the reported literature values.[65]

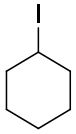

Iodocyclohexane (2.31): compound was purchased from Sigma-Aldrich and distilled over calcium hydride under vacuum before use.

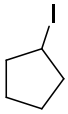

Iodocyclopentane (2.66): compound was purchased from Oakwood Chemicals and distilled over calcium hydride under vacuum before use.

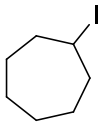

Iodocycloheptane (2.67): compound has been previously characterized and spectral data match the reported literature values. [66]

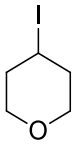

4-Iodotetrahydro-2H-pyran (2.68): compound has been previously characterized and spectral data match the reported literature values. [67]

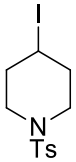

4-Iodo-1-tosylpiperidine (2.69): compound has been previously characterized and spectral data match the reported literature values.[68]

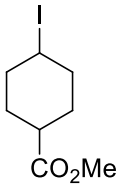

Methyl 4-iodocyclohexanecarboxylate (2.70): compound was prepared using the general method described above. ^{1}H NMR (300 MHz, Chloroform-*d*) δ 4.67 (s, 1H), 3.72 (s, 3H), 2.52 – 2.39 (m, 1H), 2.23 – 1.92 (m, 4H), 1.91 – 1.67 (m, 4H). GC/MS (EI) calculated for $[M]^{+}$ 268.00, found 268.10.

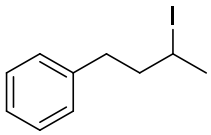

(3-iodobutyl)benzene (2.71): compound has been previously characterized and spectral data match the reported literature values.[69]

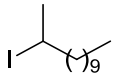

2-iodododecane (2.72): compound has been previously characterized and spectral data match the reported literature values.[69]

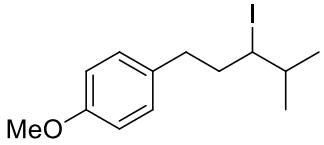

1-(3-Iodo-4-methylpentyl)-4-methoxybenzene (2.73): compound was prepared using the general method described above. ^{1}H NMR (500 MHz, $CDCl_3$) δ 7.14 (d, *J* = 8.5 Hz, 2H), 6.85 (d, *J* = 8.5 Hz, 2H), 4.21 – 3.89 (m, 1H), 3.80 (s, 3H), 2.89 (ddd, *J* = 13.7, 9.4, 4.9 Hz, 1H), 2.77 – 2.50 (m, 1H), 2.29 – 2.15 (m, 1H), 1.88 (dddd, *J* = 14.8, 8.9, 7.4, 3.7 Hz, 1H), 2.00 – 1.79 (m, 1H), 1.35 – 1.19 (m, 1H), 0.97 (dd, *J* = 21.4, 6.5 Hz, 6H).^{3}C NMR (126 MHz, $CDCl_3$) δ 158.1, 133.1, 129.6, 114.0, 55.4, 51.4, 48.0, 40.4, 39.4, 352., 33.5, 23.1, 20.1, 16.5. GC/MS (EI) calculated for $[M]^+$ 318.05, found 318.10. FTIR (neat, cm^{-1}): 2959 (s), 2870 (w), 1611 (s), 1583 (m), 1511 (s), 1462 (s), 1453 (s), 1385 (m), 1367 (m), 1314 (m), 1300 (s), 1246 (s), 1176 (s), 1037(s), 857 (w), 823 (s).

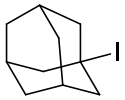

1-iodoadamantane (2.74): compound was purchased from Sigma-Aldrich and used directly.

1-iodo-3-methoxybicyclo[1.1.1]pentane (2.75): compound has been previously characterized and spectral data match the reported literature values.[70]

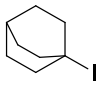

1-iodobicyclo[2.2.2]octane (2.76): compound has been previously characterized and spectral data match the reported literature values[71]

2.4.10 *Analysis of Palladium Impurities and Effects of Palladium(II) on the Reaction*

Trace amounts of palladium are known to perform cross coupling reactions[72] and it has been shown that as low as 100 ppb palladium is adequate for performing Sonogashira coupling[73]. Very often, trace impurities in bases (mostly Na_2CO_3), solvent, ligand or even glassware can be sources of this palladium. In order to assess the concentration of palladium present in our reaction we performed Inductively coupled plasma mass spectrometry (ICP-MS) on our base, ligand and reaction mixture. It was found that both K_2CO_3 and the ligand contain undetectable amounts of palladium (the detection limit for our instrument is 2 ppb). However, the reaction mixture was found to contain 91.2 ppb of palladium. To test the efficacy of palladium in our reaction medium,

we deliberately added 100 ppm palladium(II) from two different sources into separate reactions and performed them without the presence of light. The results have been summarized below. This result is consistent with the fact that photoactivation of copper acetylide is necessary and presence of trace amounts of palladium is *not responsible* for this reaction.

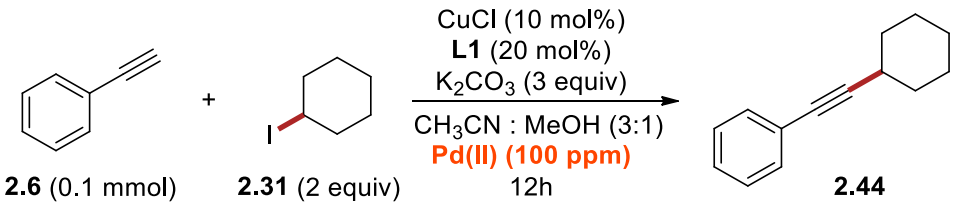

Pd(II) Source	$PdCl_2$	$Pd(OAc)_2$
Yield of **2.44**	0%	0%

2.4.11 *Radical Trap Experiment*

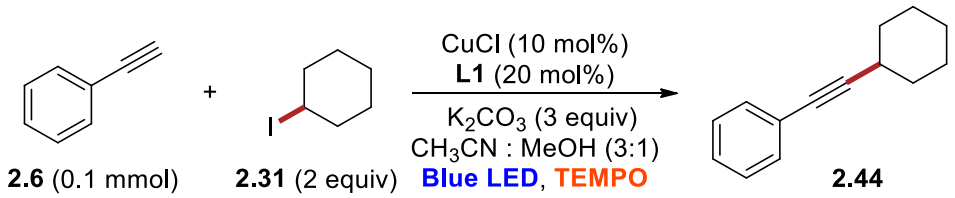

TEMPO (mol%)	0	20	100	400
Yield of **2.44**	90%	77%	7%	2%

In a nitrogen-filled glovebox, a dram vial was charged with a Teflon coated stir bar, CuCl (2.5 mg, 0.025 mmol, 0.10 equiv), 4,4',4"-tri-tert-butyl-2,2':6',2"-terpyridine (20.0 mg, 0.050 mmol, 0.20 equiv) and K_2CO_3 (103.8 mg, 0.75 mmol, 3.0 equiv). A mixture of 1:3 methanol in acetonitrile (2.5 mL, 0.1 M) and phenylacetylene (25.5 mg, 0.25 mmol, 1 equiv.) were then added. Internal standard, 1,3,5-trimethoxy benzene (TMB), cyclohexyl iodide (0.5 mmol, 2 equiv) and TEMPO were added to the reaction mixture, which was then capped and stirred vigorously under the irradiation of blue light in the reaction chamber (Fig. S1). After 24h, the reaction was stopped, and yields were determined by GC. The cyclohexyl-TEMPO adduct was isolated and characterized by NMR and GC/MS. The spectral data match the previously reported values.[74]

2.4.12 *1° vs 2° Alkyl Iodide Competition Experiment*

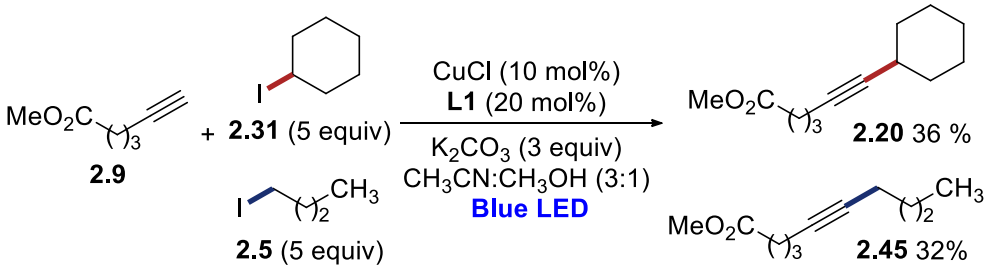

In a nitrogen-filled glovebox, a dram vial was charged with a Teflon coated stir bar, CuCl (2.5 mg, 0.025 mmol, 0.10 equiv), 4,4',4"-tri-tert-butyl-2,2':6',2"-terpyridine (20.0 mg, 0.050 mmol, 0.20 equiv) and K_2CO_3 (103.8 mg, 0.750 mmol, 3.0 equiv). A mixture of 1:3 methanol in acetonitrile (2.5 mL, 0.1 M) and methyl hex-5-ynoate (31.5 mg, 0.250 mmol, 1 equiv) were then added. Internal standard, 1,3,5-trimethoxy benzene (TMB), and cyclohexyl iodide (0.500 mmol, 2 equiv) were added to the reaction mixture, which was then capped and stirred vigorously under the irradiation of blue light in the reaction chamber (**Figure 2.2**). After the indicated time, the reaction was stopped, and yields were determined by GC.

2.5 REFERENCES FOR CHAPTER 2

(1) Cahiez, G.; Gager, O.; Buendia, J. Copper-Catalyzed Cross-Coupling of Alkyl and Aryl Grignard Reagents with Alkynyl Halides. *Angew. Chem. Int. Ed.* **2010**, *49* (7), 1278–1281.

(2) Shen, Y.; Huang, B.; Zheng, J.; Lin, C.; Liu, Y.; Cui, S. Csp–Csp3 Bond Formation via Iron(III)-Promoted Hydroalkynylation of Unactivated Alkenes. *Org. Lett.* **2017**, *19* (7), 1744–1747.

(3) Thaler, T.; Guo, L.-N.; Mayer, P.; Knochel, P. Highly Diastereoselective C(Sp3)–C(Sp) Cross-Coupling Reactions between 1,3- and 1,4-Substituted Cyclohexylzinc Reagents and

Bromoalkynes through Remote Stereocontrol. *Angew. Chem. Int. Ed.* **2011**, *50* (9), 2174–2177.

(4) He, J.; Wasa, M.; Chan, K. S. L.; Yu, J.-Q. Palladium(0)-Catalyzed Alkynylation of C(Sp3)–H Bonds. *J. Am. Chem. Soc.* **2013**, *135* (9), 3387–3390.

(5) Huang, L.; Olivares, A. M.; Weix, D. J. Reductive Decarboxylative Alkynylation of N-Hydroxyphthalimide Esters with Bromoalkynes. *Angew. Chem. Int. Ed.* **2017**, *56* (39), 11901–11905..

(6) Hatakeyama, T.; Okada, Y.; Yoshimoto, Y.; Nakamura, M. Tuning Chemoselectivity in Iron-Catalyzed Sonogashira-Type Reactions Using a Bisphosphine Ligand with Peripheral Steric Bulk: Selective Alkynylation of Nonactivated Alkyl Halides. *Angew. Chem. Int. Ed.* **2011**, *50* (46), 10973–10976.

(7) Ohmiya, H.; Yorimitsu, H.; Oshima, K. Cobalt-Mediated Cross-Coupling Reactions of Primary and Secondary Alkyl Halides with 1-(Trimethylsilyl)Ethenyl- and 2-Trimethylsilylethynylmagnesium Reagents. *Org. Lett.* **2006**, *8* (14), 3093–3096.

(8) Vechorkin, O.; Godinat, A.; Scopelliti, R.; Hu, X. Cross-Coupling of Nonactivated Alkyl Halides with Alkynyl Grignard Reagents: A Nickel Pincer Complex as the Catalyst. *Angew. Chem. Int. Ed.* **2011**, *50* (49), 11777–11781.

(9) Cheung, C. W.; Ren, P.; Hu, X. Mild and Phosphine-Free Iron-Catalyzed Cross-Coupling of Nonactivated Secondary Alkyl Halides with Alkynyl Grignard Reagents. *Org. Lett.* **2014**, *16* (9), 2566–2569.

(10) Caeiro, J.; Pérez Sestelo, J.; Sarandeses, L. A. Enantioselective Nickel-Catalyzed Cross-Coupling Reactions of Trialkynylindium Reagents with Racemic Secondary Benzyl Bromides. *Chem. – Eur. J.* **2008**, *14* (2), 741–746..

(11) Smith, J. M.; Qin, T.; Merchant, R. R.; Edwards, J. T.; Malins, L. R.; Liu, Z.; Che, G.; Shen, Z.; Shaw, S. A.; Eastgate, M. D.; Baran, P. S. Decarboxylative Alkynylation. *Angew. Chem. Int. Ed.* **2017**, *56* (39), 11906–11910.

(12) Le Vaillant, F.; Courant, T.; Waser, J. Room-Temperature Decarboxylative Alkynylation of Carboxylic Acids Using Photoredox Catalysis and EBX Reagents. *Angew. Chem. Int. Ed.* **2015**, *54* (38), 11200–11204.

(13) Liu, X.; Wang, Z.; Cheng, X.; Li, C. Silver-Catalyzed Decarboxylative Alkynylation of Aliphatic Carboxylic Acids in Aqueous Solution. *J. Am. Chem. Soc.* **2012**, *134* (35), 14330–14333.

(14) Huang, H.; Zhang, G.; Gong, L.; Zhang, S.; Chen, Y. Visible-Light-Induced Chemoselective Deboronative Alkynylation under Biomolecule-Compatible Conditions. *J. Am. Chem. Soc.* **2014**, *136* (6), 2280–2283.

(15) Yang, C.; Yang, J.-D.; Li, Y.-H.; Li, X.; Cheng, J.-P. 9,10-Dicyanoanthracene Catalyzed Decarboxylative Alkynylation of Carboxylic Acids under Visible-Light Irradiation. *J. Org. Chem.* **2016**, *81* (24), 12357–12363.

(16) Yang, J.; Zhang, J.; Qi, L.; Hu, C.; Chen, Y. Visible-Light-Induced Chemoselective Reductive Decarboxylative Alkynylation under Biomolecule-Compatible Conditions. *Chem. Commun.* **2015**, *51* (25), 5275–5278.

(17) Liu, W.; Li, L.; Li, C.-J. Empowering a Transition-Metal-Free Coupling between Alkyne and Alkyl Iodide with Light in Water. *Nat. Commun.* **2015**, *6*, ncomms7526.

(18) Evano, G.; Jouvin, K.; Theunissen, C.; Guissart, C.; Laouiti, A.; Tresse, C.; Heimburger, J.; Bouhoute, Y.; Veillard, R.; Lecomte, M.; Nitelet, A.; Schweizer, S.; Blanchard, N.; Alayrac, C.; Gaumont, A.-C. Turning Unreactive Copper Acetylides into Remarkably Powerful and

Mild Alkyne Transfer Reagents by Oxidative Umpolung. *Chem. Commun.* **2014**, *50* (70), 10008–10018.

(19) Jin, L.; Hao, W.; Xu, J.; Sun, N.; Hu, B.; Shen, Z.; Mo, W.; Hu, X. N-Heterocyclic Carbene Copper-Catalyzed Direct Alkylation of Terminal Alkynes with Non-Activated Alkyl Triflates. *Chem. Commun.* **2017**, *53* (29), 4124–4127.

(20) Luo, F.-X.; Xu, X.; Wang, D.; Cao, Z.-C.; Zhang, Y.-F.; Shi, Z.-J. Cu-Catalyzed Alkynylation of Unactivated C(Sp3)–X Bonds with Terminal Alkynes through Directing Strategy. *Org. Lett.* **2016**, *18* (9), 2040–2043.

(21) Yamane, Y.; Miwa, N.; Nishikata, T. Copper-Catalyzed Functionalized Tertiary-Alkylative Sonogashira Type Couplings via Copper Acetylide at Room Temperature. *ACS Catal.* **2017**, *7* (10), 6872–6876.

(22) Maity, P.; Srinivas, H. D.; Watson, M. P. Copper-Catalyzed Enantioselective Additions to Oxocarbenium Ions: Alkynylation of Isochroman Acetals. *J. Am. Chem. Soc.* **2011**, *133* (43), 17142–17145.

(23) Srinivas, H. D.; Maity, P.; Yap, G. P. A.; Watson, M. P. Enantioselective Copper-Catalyzed Alkynylation of Benzopyranyl Oxocarbenium Ions. *J. Org. Chem.* **2015**, *80* (8), 4003–4016.

(24) Dasgupta, S.; Rivas, T.; Watson, M. P. Enantioselective Copper(I)-Catalyzed Alkynylation of Oxocarbenium Ions to Set Diaryl Tetrasubstituted Stereocenters. *Angew. Chem. Int. Ed.* **2015**, *54* (47), 14154–14158.

(25) Bi, H.-P.; Zhao, L.; Liang, Y.-M.; Li, C.-J. The Copper-Catalyzed Decarboxylative Coupling of the Sp3-Hybridized Carbon Atoms of α-Amino Acids. *Angew. Chem. Int. Ed.* **2009**, *48* (4), 792–795.

(26) Zhang, C.; Seidel, D. Nontraditional Reactions of Azomethine Ylides: Decarboxylative Three-Component Couplings of α-Amino Acids. *J. Am. Chem. Soc.* **2010**, *132* (6), 1798–1799.

(27) Zhang, H.; Zhang, P.; Jiang, M.; Yang, H.; Fu, H. Merging Photoredox with Copper Catalysis: Decarboxylative Alkynylation of α-Amino Acid Derivatives. *Org. Lett.* **2017**, *19* (5), 1016–1019.

(28) Chinchilla, R.; Nájera, C. The Sonogashira Reaction: A Booming Methodology in Synthetic Organic Chemistry. *Chem. Rev.* **2007**, *107* (3), 874–922.

(29) Chinchilla, R.; Nájera, C. Recent Advances in Sonogashira Reactions. *Chem. Soc. Rev.* **2011**, *40* (10), 5084–5121.

(30) Eckhardt, M.; Fu, G. C. The First Applications of Carbene Ligands in Cross-Couplings of Alkyl Electrophiles: Sonogashira Reactions of Unactivated Alkyl Bromides and Iodides. *J. Am. Chem. Soc.* **2003**, *125* (45), 13642–13643.

(31) Pérez García, P. M.; Ren, P.; Scopelliti, R.; Hu, X. Nickel-Catalyzed Direct Alkylation of Terminal Alkynes at Room Temperature: A Hemilabile Pincer Ligand Enhances Catalytic Activity. *ACS Catal.* **2015**, *5* (2), 1164–1171.

(32) Vechorkin, O.; Barmaz, D.; Proust, V.; Hu, X. Ni-Catalyzed Sonogashira Coupling of Nonactivated Alkyl Halides: Orthogonal Functionalization of Alkyl Iodides, Bromides, and Chlorides. *J. Am. Chem. Soc.* **2009**, *131* (34), 12078–12079.

(33) Altenhoff, G.; Würtz, S.; Glorius, F. The First Palladium-Catalyzed Sonogashira Coupling of Unactivated Secondary Alkyl Bromides. *Tetrahedron Lett.* **2006**, *47* (17), 2925–2928.

(34) Yi, J.; Lu, X.; Sun, Y.-Y.; Xiao, B.; Liu, L. Nickel-Catalyzed Sonogashira Reactions of Non-Activated Secondary Alkyl Bromides and Iodides. *Angew. Chem. Int. Ed.* **2013**, *52* (47), 12409–12413.

(35) Creutz, S. E.; Lotito, K. J.; Fu, G. C.; Peters, J. C. Photoinduced Ullmann C–N Coupling: Demonstrating the Viability of a Radical Pathway. *Science* **2012**, *338* (6107), 647–651.

(36) Uyeda, C.; Tan, Y.; Fu, G. C.; Peters, J. C. A New Family of Nucleophiles for Photoinduced, Copper-Catalyzed Cross-Couplings via Single-Electron Transfer: Reactions of Thiols with Aryl Halides Under Mild Conditions (O °C). *J. Am. Chem. Soc.* **2013**, *135* (25), 9548–9552.

(37) Tan, Y.; Muñoz-Molina, J. M.; Fu, G. C.; Peters, J. C. Oxygen Nucleophiles as Reaction Partners in Photoinduced, Copper-Catalyzed Cross-Couplings: O-Arylations of Phenols at Room Temperature. *Chem. Sci.* **2014**, *5* (7), 2831–2835.

(38) Sagadevan, A.; Hwang, K. C. Photo-Induced Sonogashira C□C Coupling Reaction Catalyzed by Simple Copper(I) Chloride Salt at Room Temperature. *Adv. Synth. Amp Catal.* **2012**, *354* (18), 3421–3427.

(39) Reiser, O. Shining Light on Copper: Unique Opportunities for Visible-Light-Catalyzed Atom Transfer Radical Addition Reactions and Related Processes. *Acc. Chem. Res.* **2016**, *49* (9), 1990–1996.

(40) Paria, S.; Reiser, O. Copper in Photocatalysis. *ChemCatChem* **2014**, *6* (9), 2477–2483.

(41) Kainz, Q. M.; Matier, C. D.; Bartoszewicz, A.; Zultanski, S. L.; Peters, J. C.; Fu, G. C. Asymmetric Copper-Catalyzed C-N Cross-Couplings Induced by Visible Light. *Science* **2016**, *351* (6274), 681–684.

(42) Do, H.-Q.; Bachman, S.; Bissember, A. C.; Peters, J. C.; Fu, G. C. Photoinduced, Copper-Catalyzed Alkylation of Amides with Unactivated Secondary Alkyl Halides at Room Temperature. *J. Am. Chem. Soc.* **2014**, *136* (5), 2162–2167.

(43) Matier, C. D.; Schwaben, J.; Peters, J. C.; Fu, G. C. Copper-Catalyzed Alkylation of Aliphatic Amines Induced by Visible Light. *J. Am. Chem. Soc.* **2017**, *139* (49), 17707–17710.

(44) Bissember, A. C.; Lundgren, R. J.; Creutz, S. E.; Peters, J. C.; Fu, G. C. Transition-Metal-Catalyzed Alkylations of Amines with Alkyl Halides: Photoinduced, Copper-Catalyzed Couplings of Carbazoles. *Angew. Chem. Int. Ed.* **2013**, *52* (19), 5129–5133.

(45) Ahn, J. M.; Ratani, T. S.; Hannoun, K. I.; Fu, G. C.; Peters, J. C. Photoinduced, Copper-Catalyzed Alkylation of Amines: A Mechanistic Study of the Cross-Coupling of Carbazole with Alkyl Bromides. *J. Am. Chem. Soc.* **2017**, *139* (36), 12716–12723.

(46) Ratani, T. S.; Bachman, S.; Fu, G. C.; Peters, J. C. Photoinduced, Copper-Catalyzed Carbon–Carbon Bond Formation with Alkyl Electrophiles: Cyanation of Unactivated Secondary Alkyl Chlorides at Room Temperature. *J. Am. Chem. Soc.* **2015**, *137* (43), 13902–13907.

(47) Yang, F.; Koeller, J.; Ackermann, L. Photoinduced Copper-Catalyzed C−H Arylation at Room Temperature. *Angew. Chem. Int. Ed.* **2016**, *55* (15), 4759–4762.

(48) Gandeepan, P.; Mo, J.; Ackermann, L. Photo-Induced Copper-Catalyzed C–H Chalcogenation of Azoles at Room Temperature. *Chem. Commun.* **2017**, *53* (43), 5906–5909.

(49) Tlahuext-Aca, A.; Hopkinson, M. N.; Sahoo, B.; Glorius, F. Dual Gold/Photoredox-Catalyzed C(Sp)–H Arylation of Terminal Alkynes with Diazonium Salts. *Chem. Sci.* **2015**, *7* (1), 89–93.

(50) Yam, V. W. W.; Lee, W. K.; Lai, T. F. Synthesis, Spectroscopy, and Electrochemistry of Trinuclear Copper(I) Acetylides. X-Ray Crystal Structure of [Cu3(.Mu.-Ph2PCH2PPh2)3(.Mu.3-.Eta.1-C.Tplbond.CBu-Tert)(.Mu.3-Cl)]PF6. *Organometallics* **1993**, *12* (6), 2383–2387.

(51) Yam, V. W.-W.; Lee, W.-K.; Cheung, K. K.; Lee, H.-K.; Leung, W.-P. Photophysics and Photochemical Reactivities of Organocopper(I) Complexes. Crystal Structure of [Cu2(PPh2Me)4(μ,H1-CCPh)2]. *J. Chem. Soc. Dalton Trans.* **1996**, No. 13, 2889–2891.

(52) Yam, V. W.-W.; Kam-Wing Lo, K.; Man-Chung Wong, K. Luminescent Polynuclear Metal Acetylides. *J. Organomet. Chem.* **1999**, *578* (1), 3–30.

(53) Isse, A. A.; Lin, C. Y.; Coote, M. L.; Gennaro, A. Estimation of Standard Reduction Potentials of Halogen Atoms and Alkyl Halides. *J. Phys. Chem. B* **2011**, *115* (4), 678–684.

(54) Messner, M.; Kozhushkov, S. I.; de Meijere, A. Nickel- and Palladium-Catalyzed Cross-Coupling Reactions at the Bridgehead of Bicyclo[1.1.1]Pentane Derivatives - A Convenient Access to Liquid Crystalline Compounds Containing Bicyclo[1.1.1]Pentane Moieties. *Eur. J. Org. Chem.* **2000**, *2000* (7), 1137–1155.

(55) Toriyama, F.; Cornella, J.; Wimmer, L.; Chen, T.-G.; Dixon, D. D.; Creech, G.; Baran, P. S. Redox-Active Esters in Fe-Catalyzed C–C Coupling. *J. Am. Chem. Soc.* **2016**, *138* (35), 11132–11135.

(56) Kessil LED Lights http://www.kessil.com/aquarium/Saltwater_A160_Tuna_Blue.php (accessed 2017 -12 -11).

(57) Timsina, Y. N.; Biswas, S.; RajanBabu, T. V. Retraction of "Chemoselective Reactions of (E)-1,3-Dienes: Cobalt-Mediated Isomerization to (Z)-1,3-Dienes and Reactions with Ethylene." *J. Am. Chem. Soc.* **2018**, *140* (7), 2700–2700.

(58) Chen, Y.; Zhang, W.; Chen, X.; Wang, J.; Wang, P. G. AGal-Conjugated Anti-Rhinovirus Agents: Chemo-Enzymatic Syntheses and Testing of Anti-Gal Binding. *J. Chem. Soc. Perkin 1* **2001**, *0* (14), 1716–1722.

(59) Mailig, M.; Hazra, A.; Armstrong, M. K.; Lalic, G. Catalytic Anti-Markovnikov Hydroallylation of Terminal and Functionalized Internal Alkynes: Synthesis of Skipped Dienes and Trisubstituted Alkenes. *J. Am. Chem. Soc.* **2017**, *139* (20), 6969–6977.

(60) Uehling, M. R.; Rucker, R. P.; Lalic, G. Catalytic Anti-Markovnikov Hydrobromination of Alkynes. *J. Am. Chem. Soc.* **2014**, *136* (24), 8799–8803.

(61) Grammatikopoulou, M.; Thysiadis, S.; Sarli, V. Gold-Catalyzed Spiro-N,O-Ketal Synthesis. *Org. Biomol. Chem.* **2015**, *13* (4), 1169–1178.

(62) Dang, H.; Cox, N.; Lalic, G. Copper-Catalyzed Reduction of Alkyl Triflates and Iodides: An Efficient Method for the Deoxygenation of Primary and Secondary Alcohols. *Angew. Chem. Int. Ed.* **2014**, *53* (3), 752–756.

(63) Montoro, R.; Wirth, T. Direct Bromination and Iodination of Non-Activated Alkanes by Hypohalite Reagents. *Synthesis* **2005**, *2005* (09), 1473–1478.

(64) Lee, C.-F.; Leigh, D. A.; Pritchard, R. G.; Schultz, D.; Teat, S. J.; Timco, G. A.; Winpenny, R. E. P. Hybrid Organic-Inorganic Rotaxanes and Molecular Shuttles. *Nature* **2009**, *458* (7236), 314–318.

(65) Kim, A. I.; Rychnovsky, S. D. Unified Strategy for the Synthesis of (−)-Elisapterosin B and (−)-Colombiasin A. *Angew. Chem.* **2003**, *115* (11), 1305–1308.

(66) Holstein, P. M.; Vogler, M.; Larini, P.; Pilet, G.; Clot, E.; Baudoin, O. Efficient Pd0-Catalyzed Asymmetric Activation of Primary and Secondary C–H Bonds Enabled by Modular Binepine Ligands and Carbonate Bases. *ACS Catal.* **2015**, *5* (7), 4300–4308.

(67) Rezazadeh, S.; Devannah, V.; Watson, D. A. Nickel-Catalyzed C-Alkylation of Nitroalkanes with Unactivated Alkyl Iodides. *J. Am. Chem. Soc.* **2017**, *139* (24), 8110–8113.

(68) Roslin, S.; Odell, L. R. Palladium and Visible-Light Mediated Carbonylative Suzuki–Miyaura Coupling of Unactivated Alkyl Halides and Aryl Boronic Acids. *Chem. Commun.* **2017**, *53* (51), 6895–6898.

(69) Dudnik, A. S.; Fu, G. C. Nickel-Catalyzed Coupling Reactions of Alkyl Electrophiles, Including Unactivated Tertiary Halides, To Generate Carbon–Boron Bonds. *J. Am. Chem. Soc.* **2012**, *134* (25), 10693–10697.

(70) Adcock, J. L.; Gakh, A. A. Nucleophilic Substitution in 1-Substituted 3-Iodobicyclo[1.1.1]Pentanes. A New Synthetic Route to Functionalized Bicyclo[1.1.1]Pentane Derivatives. *J. Org. Chem.* **1992**, *57* (23), 6206–6210.

(71) Wiberg, K. B.; Pratt, W. E.; Bailey, W. F. Nature of Substituent Effects in Nuclear Magnetic Resonance Spectroscopy. 1. Factor Analysis of Carbon-13 Chemical Shifts in Aliphatic Halides. *J. Org. Chem.* **1980**, *45* (24), 4936–4947.

(72) Thomé, I.; Nijs, A.; Bolm, C. Trace Metal Impurities in Catalysis. *Chem. Soc. Rev.* **2012**, *41* (3), 979–987.

(73) Gonda, Z.; Tolnai, G. L.; Novák, Z. Dramatic Impact of Ppb Levels of Palladium on the "Copper-Catalyzed" Sonogashira Coupling. *Chem. – Eur. J.* **2010**, *16* (39), 11822–11826.

(74) Li, Q.; Hu, W.; Hu, R.; Lu, H.; Li, G. Cobalt-Catalyzed Cross-Dehydrogenative Coupling Reaction between Unactivated C(Sp2)–H and C(Sp3)–H Bonds. *Org. Lett.* **2017**, *19* (17), 4676–4679.

Chapter 3. SYNTHESIS OF ISOMERICALLY PURE (*Z*)-ALKENES FROM TERMINAL ALKYNES AND TERMINAL ALKENES: SILVER-CATALYZED HYDROALKYLATION OF ALKYNES

Portions of this chapter as well as figures, schemes, and tables were adapted or reproduced from the following manuscript, with permission from Lee, M. T.; Goodstein, M. B.; Lalic, G. Synthesis of Isomerically Pure (*Z*)-Alkenes from Terminal Alkynes and Terminal Alkenes: Silver-Catalyzed Hydroalkylation of Alkynes. *J. Am. Chem. Soc*. **2019**, 141, 17086.–17091. Copyright 2019 American Chemical Society.

3.1 **INTRODUCTION**

Alkenes serve as important intermediates in organic synthesis and are often found among pharmaceuticals and other biologically active compounds. The key feature of alkenes is the presence of a π bond, which hinders the rotation about the carbon–carbon σ-bond[1] and confers structural rigidity to alkenes. The hindered rotation also leads to two distinct stereoisomeric forms of disubstituted alkenes, denoted as *E* and *Z*.[2] An efficient synthesis of thermodynamically less stable *Z*-alkenes presents a complex set of challenges that continues to inspire the development of new synthetic methods.

The efficient synthesis of *Z*-alkenes must accomplish three important goals. The most basic goal is to form a double bond. The synthesis should also exert complete control over the double bond geometry, so that only the *Z* isomer of the alkene is formed. The synthesis of diastereopure

products is particularly important considering the difficulties often encountered in the separation of alkene isomers. Finally, a *Z*-alkene should be constructed from two smaller fragments through the formation of a new C–C σ-bond.[3–10] Such a convergent approach to synthesis has long been recognized as key for the efficient buildup of molecular complexity.[11,12] Ideally, all three goals of *Z*-alkene synthesis (π-bond formation, formation of only one isomer, and C–C σ-bond formation) should be accomplished in a single reaction. Unfortunately, this is difficult to achieve using standard catalytic methods for the synthesis of *Z*-alkenes,[13] such as alkyne semireduction,[14,15] cross-coupling reactions,[16] alkene cross metathesis,[17–19] or alkene isomerization.[20–22]

We were intrigued by the idea that the hydroalkylation of alkynes is one reaction that may allow us to accomplish all three goals of *Z*-alkenes synthesis. Hydroalkylation has already proven effective in the synthesis of E-alkenes through the reductive coupling of terminal alkynes with alkyl iodides[23] or alkyl triflates (**Scheme 3.1a**).[24,25] The same approach is also effective when applied to the synthesis of 1,1-disubstituted alkenes (**Scheme 3.1b**).[26–28] Still, hydroalkylation reactions had limited success targeting *Z*-alkenes. *Z*-Selectivity has, so far, been achieved only in an iron-catalyzed radical hydroalkylation, reported by Hu et al. in 2015 (**Scheme 3.1c**). This method is limited to reactions of aryl acetylenes and yields mixtures of E- and *Z*-alkenes with varying selectivity.[29] Unfortunately, other mechanistic paradigms used to accomplish hydroalkylation favor the formation of E-alkenes. As a result, to achieve the synthesis of pure *Z*-alkenes we need a fundamentally new approach to hydroalkylation of alkynes.

Scheme 3.1 Current Methods for the Hydroalkylation of Alkynes

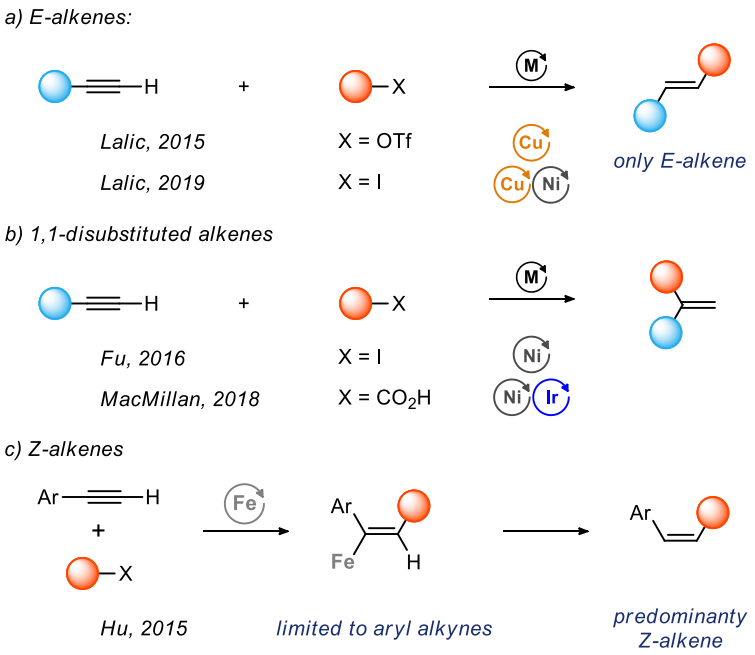

Here, we describe a catalytic method for the synthesis of diastereopure *Z*-alkenes through the coupling of terminal alkynes and alkylboranes. The development of this method was inspired by a 1975 report from H. C. Brown (**Scheme 3.2a**).[30–32] In the report, Brown showed that lithium acetylides readily add to alkylboranes to form borate complexes. Further reaction of the borate with a Brønsted acid leads to a 1,2-metalate shift[33–35] and the formation of both isomers of alkenyl borane, with *Z* being the major isomer. The stereochemical outcome has been attributed to the nature of the 1,2-metalate shift, which is proposed to proceed through a carbocation intermediate.[32] Subsequent protodeboration provides a mixture of *Z*- and *E*-alkenes.[32,36]

We reasoned that in the 1,2-metalate shift described by Brown, the Brønsted acid could be replaced by a cationic complex of a coinage metal (**Scheme 3.2b**). The 1,2-metalate shift promoted by π-acid coordination[37–45] to the alkyne has been shown to require antiperiplanar orientation of the π-acid and the migrating group[46] and would allow exclusive formation of the *Z*-alkene product. Furthermore, the coinage metal complex could be delivered in the form of a metal acetylide that

would replace the lithium acetylide used in the reaction sequence described by Brown. Ultimately, these simple changes would allow us to develop a catalytic process that results in the exclusive formation of *Z*-alkenes.

Scheme 3.2 A New Approach to Hydroalkylation

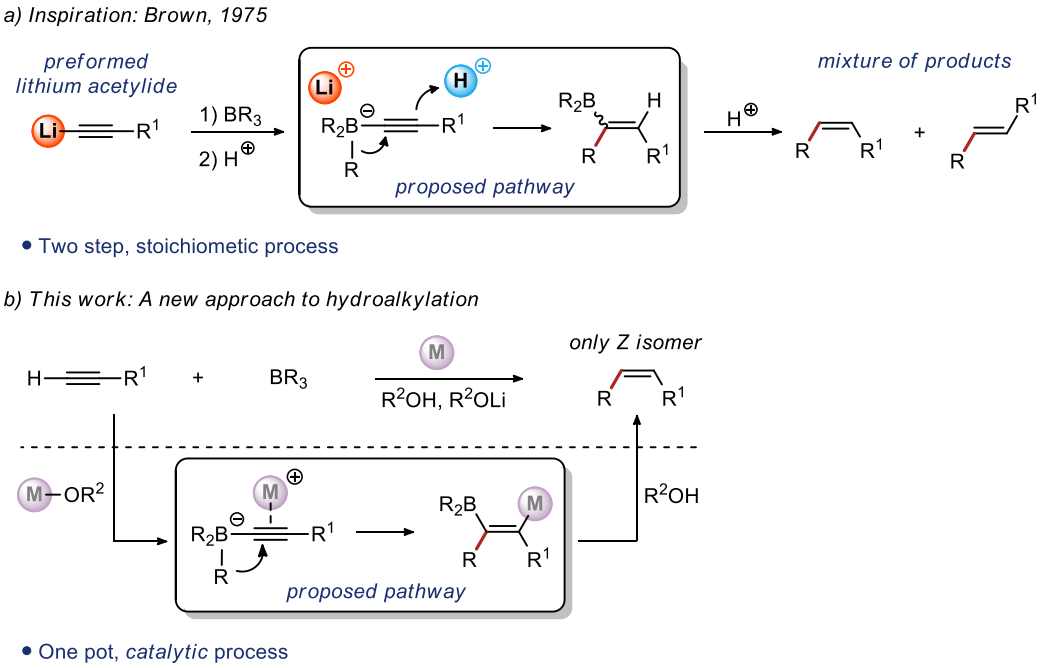

Scheme 3.3 shows the postulated mechanism of such a catalytic reaction. In the presence of an alkoxide base, a coinage metal catalyst promotes acetylide formation, which is followed by addition to the alkylborane. Upon addition, the metal counterion coordinates to the alkyne and promotes the 1,2-metalate shift through π-activation of the alkyne. Finally, alkene formation is accomplished by protodeboration and protodemetalation of the intermediate in the presence of an alcohol additive.

Scheme 3.3 Proposed Catalytic Cycle

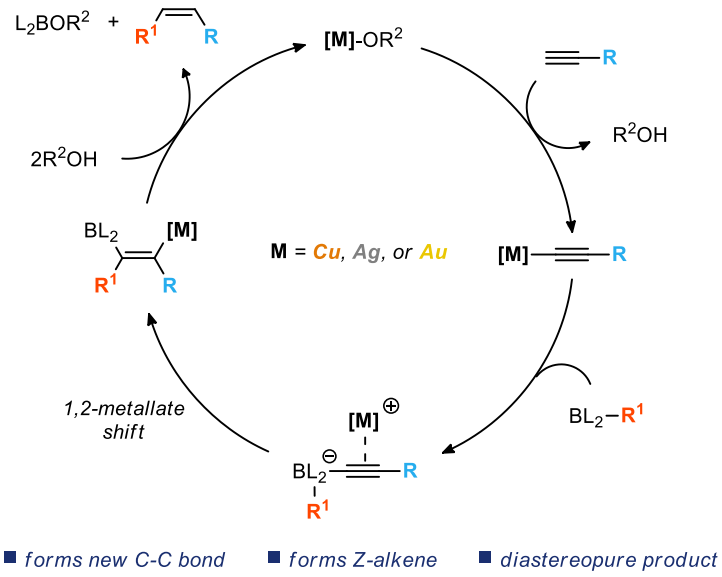

3.2 RESULTS AND DISCUSSION

3.2.1 *Reaction Development*

With the broad strategy outlined in Scheme 3 in mind, we explored the reaction of alkyne **3.1** with alkylborane **3.2** in the presence of a copper, silver, or gold catalyst (**Table 3.1**). Surprisingly, the silver catalyst performed the best, even though silver complexes are expected to be the least π-acidic.[47] Crucially, only the *Z* isomer of alkene product **3.3** was formed in the reaction. Through further optimization of the reaction parameters, we found that a triazole carbene ligand and a nonpolar solvent provided the highest yield of the *Z*-alkene product. Under optimized conditions, complete conversion was achieved using a modest excess (1.3–1.5 equiv) of the alkylborane, which was prepared in situ from an alkene. Standard control experiments confirmed that the catalyst, base, and methanol were all necessary for the reaction.

Table 3.1 Reaction Development

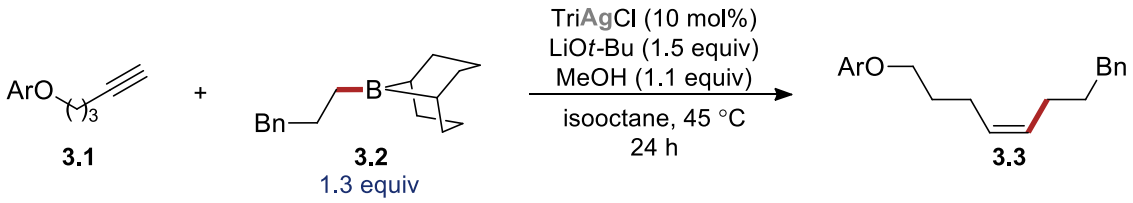

entry	*deviation from above*	*yield*[a]
1	none	92%
2	TriAgCl, toluene as solvent	70%
3	IPrAgCl, toluene as solvent	52%
4	IPrCuCl, toluene as solvent	<5%
5	IPrAuCl, toluene as solvent	0%
6	MeOH as solvent	0%
7	No MeOH	<5%
8	No LiO-*t*Bu	0%
9	No TriAgCl	0%

[a] GC yields are reported. All reactions performed on 0.05 mmol scale. Ar = methyl-4-benzoate

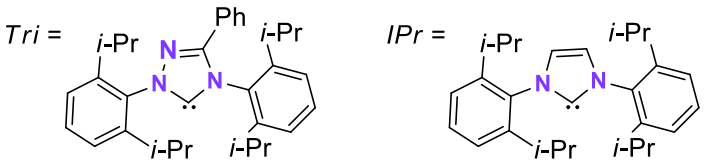

3.2.2 *Substrate Scope*

The new transformation proved to be remarkably general, providing *Z*-alkenes as exclusive products with a wide range of substrates (**Table 3.2**). Functionalized alkyl alkynes could be successfully used in the reaction together with both electron-rich and electron-poor aryl alkynes. Alkylboranes prepared in situ from a variety of terminal alkenes, including 1,1-disubstituted alkenes, could be used as substrates. Furthermore, a wide range of functional groups was tolerated. Alkene products were formed in the presence of alcohols, aldehydes, ketones, esters, nitriles, alkenes, Boc-protected primary and secondary amines, anilines, alkyl bromides, alkyl chlorides, aryl iodides, aryl bromides, aryl boronic esters, epoxides, acetals, and alkyl and silyl ethers. Heterocycles such as pyridine, thiazole, benzimidazole, benzopyrazine, pyrimidine, pyridazine,

thiophene, and furan were also compatible with the reaction conditions. The reaction could be performed on a preparative scale, yielding 1 g of alkene **3.3**. Finally, in the synthesis of alkene 4, careful analysis of the crude reaction mixture by GC and GC/MS using authentic samples of Z and E isomers of the alkene revealed the presence of a very small amount of the E isomer (*Z:E* = 570:1). Similar GC analysis of crude reaction mixtures obtained in the synthesis of **3.3**, **3.17**, **3.35**, **3.39**, and **3.41**, in all cases, indicated the *Z:E* ratio was greater than 300:1 (see section 3.3.5).

Several limitations in the scope of the hydroalkylation reaction were noted. While primary alkyl groups participate in the 1,2-metalate shift, secondary and tertiary alkyl, alkenyl, and aryl groups do not. Free amines, carboxylic acids, and carboxylates are not compatible with the reaction. We also noticed that the presence of an electron-withdrawing group two carbons away from the boron in alkylboranes significantly lowers the yield of the reaction.

Table 3.2 Substrate Scope

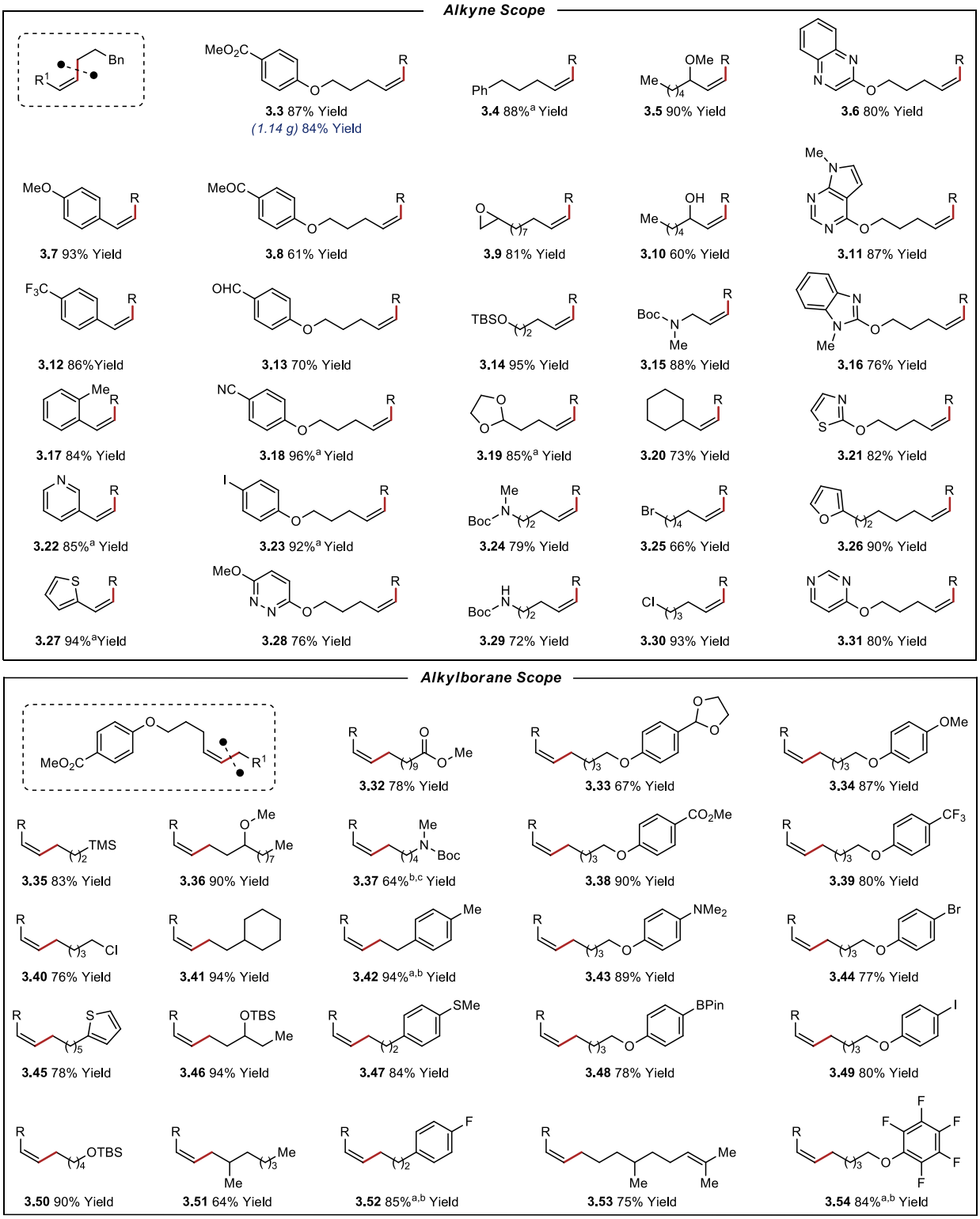

Reactions performed on a 0.5 mmol scale. Reported are yields of isolated products after purification by silica gel chromatography. For Z-selectivity see section 3.4.4. Alkylboranes were prepared in situ by stirring corresponding alkene (1 equiv) and 9-borabicyclo[3.3.1]nonane dimer (0.45 equiv) in toluene (2M) overnight at 60 °C. Reaction Conditions: TriAgCl (10 mol%), alkylborane (1.3 equiv), LiO*t*-Bu (1.5 equiv), MeOH (1.1 equiv), in isooctane (5 mL), 45 °C, 16 h. [a]Reaction Conditions: IPrAgCl (10 mol%), alkyl borane (1.5 equiv), LiO*t*-Bu (2.0 equiv), MeOH (1.1 equiv), in toluene (5 mL), 60 °C, 16 h. [b]R = propylbenzene. [c]Yield determined by ^{1}H NMR.

We have explored the application of the new method in the synthesis of biologically active compounds. Zucapsaicin is used in the treatment of osteoarthritis and neuropathic pain (**Scheme 3.4a**).[48] The formal synthesis[49] of this synthetic analogue of capsaicin was accomplished by the synthesis of **3.57** 82% yield as a single isomer. A formal racemic synthesis of the natural product falcarindiol[50] (**Scheme 3.4b**) was accomplished by preparing alkene **3.60** in 93% yield and 100% *Z*-selectivity. Falcarindiol has been shown to have a range of pharmacologically useful properties, including anticancer activity in breast cancer cells.[51]

Scheme 3.4 Applications to Formal Syntheses of Biologically Active Compounds

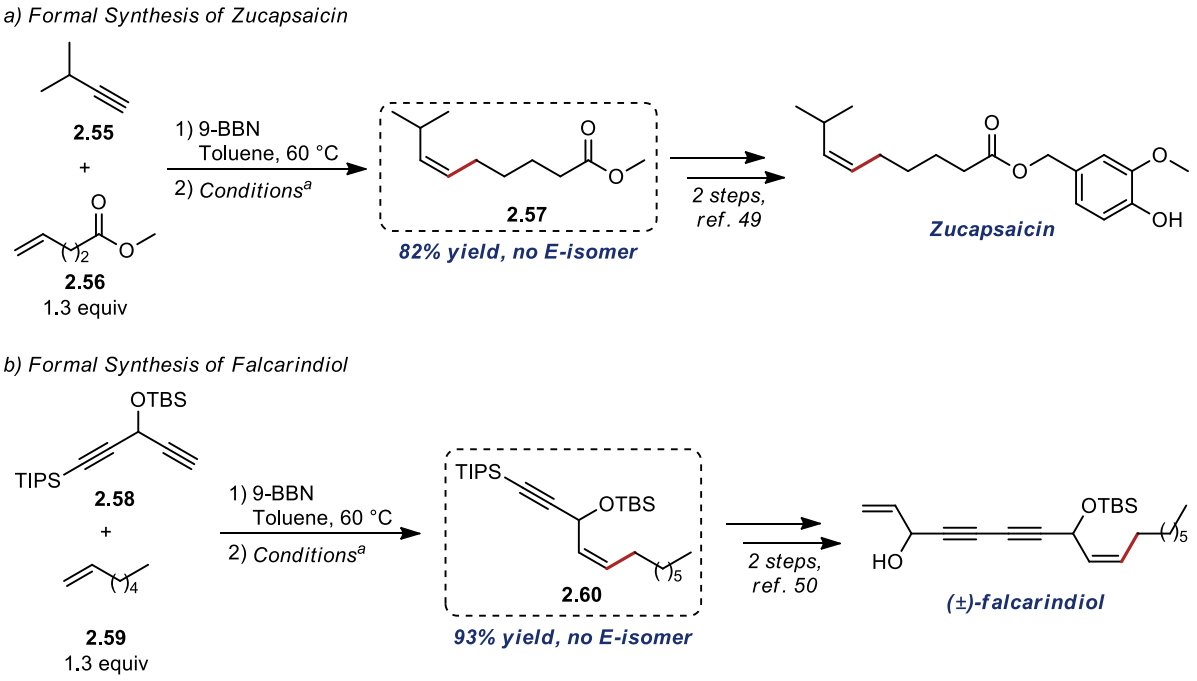

Reactions were performed on a 0.5 mmol scale.[a]Conditions: TriAgCl (10 mol%), Li-O*t*Bu (1.5 equiv), MeOH (1.1 equiv), in Isooctane (5 mL), 45 °C, 16 h.

3.2.3 *Initial Mechanistic Studies*

To probe the mechanism of the reaction, we explored the feasibility of the elementary steps in our postulated catalytic cycle (**Scheme 3.3**). In a stoichiometric reaction, we found that the silver catalyst, in the presence of an alkoxide, readily reacts with a terminal alkyne **3.61** to produce silver

acetylide **3.62** (**Scheme 3.5**). The acetylide rapidly reacts with alkylborane **3.2** to produce borate complex **3.63**. The X-ray structure of this complex (**Figure 3.1**) indicates that the silver cation associated with the borate is coordinated to the alkyne and is therefore poised to promote the 1,2-metalate shift. However, the unfavorable orientation of the migrating alkyl group is consistent with the observed stability of this intermediate. In a control experiment, we confirmed that the silver borate complex is a viable catalyst for the hydroalkylation reaction (see section 3.3.13.2).

Scheme 3.5 Stoichiometric Experiments with Possible Intermediates

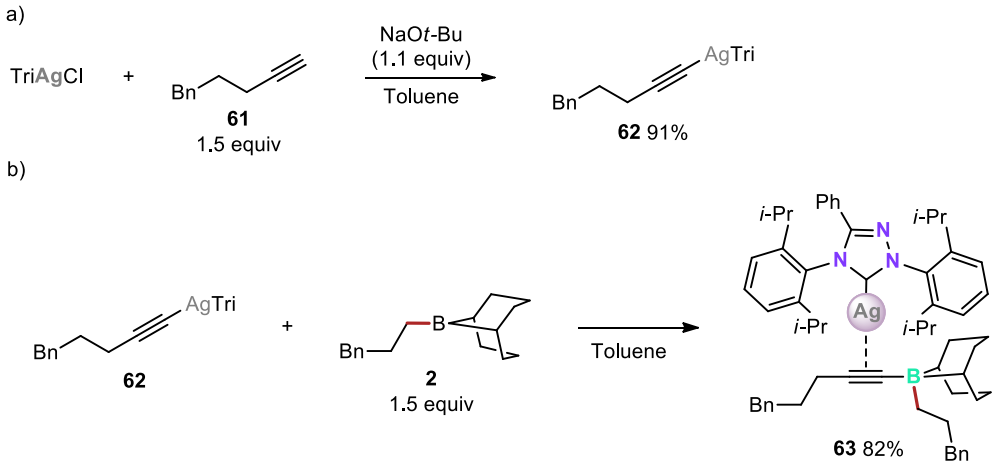

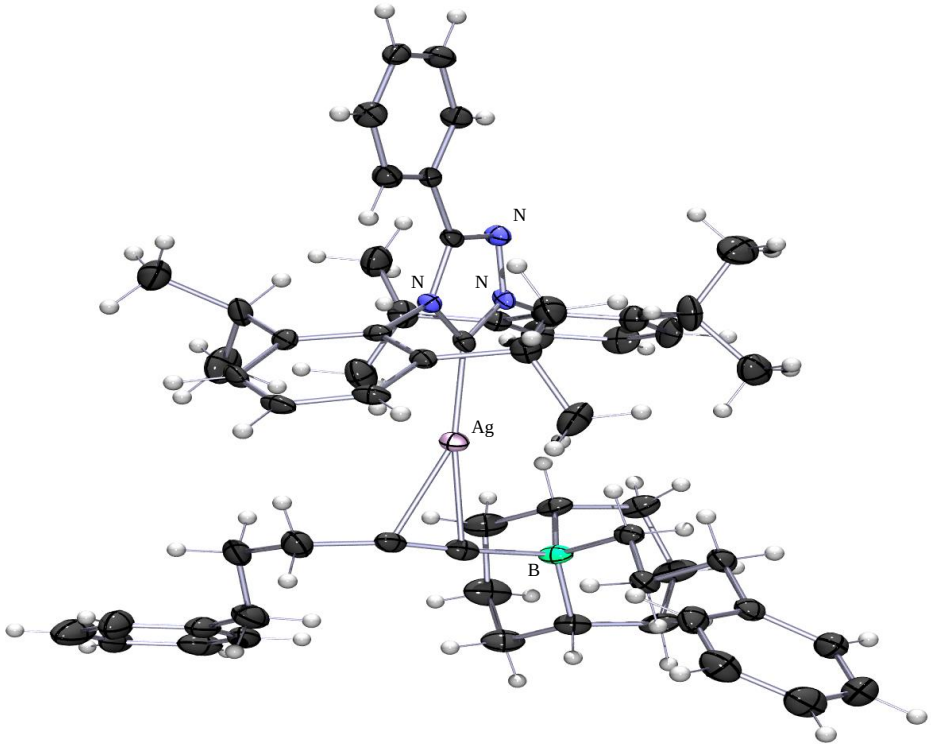

Figure 3.1 POV-Ray rendered ORTEP of the crystal structure of borate complex **3.63** with thermal ellipsoids at 50% probability. Disorder in one phenyl group and one isopropyl group has been omitted for clarity

These experimental observations provide direct support for some of the key aspects of the proposed reaction mechanism shown in **Scheme 3.3** (M = Ag). Further studies are necessary to provide a more detailed understanding of the reaction mechanism, including the steps following the 1,2-metalate shift.

3.3 EXPERIMENTAL

3.3.1 *General Information*

All reactions were performed under a nitrogen atmosphere with flame-dried or oven-dried (120 °C) glassware, using standard Schlenk techniques, or in a glovebox (Nexus II from Vacuum Atmospheres). Column chromatography was performed using a Biotage Iso-1SV flash purification

system with silica gel from Agela Technologies Inc. (60Å, 40-60 μm, 230-400 mesh. Infrared (IR) spectra were recorded on a Perkin Elmer Spectrum RX I spectrometer. IR peak absorbencies are represented as follows: s = strong, m = medium, w = weak, br = broad. ^{1}H- and ^{13}C-NMR spectra were recorded on a Bruker AV-300 or AV-500 spectrometer. ^{1}H NMR chemical shifts (δ) are reported in parts per million (ppm) downfield of TMS and are referenced relative to residual solvent peak ($CDCl_3$ (7.26 ppm)). ^{13}C NMR chemical shifts are reported in parts per million downfield of TMS and are referenced to the carbon resonance of the solvent ($CDCl_3$(77.2 ppm)).^{19}F NMR chemical shifts (δ) are reported in parts per million (ppm) and are referenced relative to the internal standard, hexafluorobenzene. Data are represented as follows: chemical shift, multiplicity (s = singlet, d = doublet, t = triplet, q = quartet, p = pentet, hept = heptet, m = multiplet), coupling constants in Hertz (Hz), intergration. Mass spectra were collected on a JEOL HX-110 mass spectrometer. Gas Chromatography (GC) analysis was performed on a Shimadzu GC-2010 instrument with a flame ionization detector and a SHRXI-5MS column (15 m, 0.25 mm inner diameter, 0.25 μm film thickness). The following temperature program was used: 2 min @ 60 °C, 13 °C/min to 160 °C, 30 °C/min to 250 °C, 5.5 min @ 250 °C.

3.3.2 *Materials*

THF, CH_2Cl_2, ether, benzene, and toluene were degassed and dried by passing through columns of neutral alumina. Anhydrous methanol was purchased from Millipore Sigma and was degassed and stored over 4Å molecular sieves. Isooctane was purchased from Fisher Scientific and was degassed and stored over 4Å molecular sieves. Deuterated solvents were purchased from Cambridge Isotope Laboratories, Inc. and were stored over 4Å molecular sieves prior to use. Commercial reagents were purchased from Millipore Sigma, TCI America, GFS-Chemicals, Ark-

Pharm, Combi-Blocks, Oakwood Chemicals, Strem Chemicals and Alfa Aesar. 9-BBN Dimer was purchased from Millipore Sigma and recrystallized from THF.

3.3.3 *Reaction Development*

All reactions were performed on a 0.05 mmol scale with the stoichiometry shown in

Table 3.1. In a nitrogen-filled glovebox a dram vial was charged with a stir bar, Li*Ot*-Bu (1.5 equiv), catalyst, methyl 4-(pent-4-yn-1-yloxy)benzoate, 1,3,5-trimethoxy benzene (TMB, internal standard), 9-(3-phenylpropyl)-9-borabicyclo[3.3.1]nonane (1.3 equiv), methanol (1.1 equiv) and solvent. The reaction mixture was stirred at 45 °C and monitored by Gas Chromatography for reaction completion. An aliquot was taken every 24 hours.

3.3.4 *Verification of Product Stereochemistry*

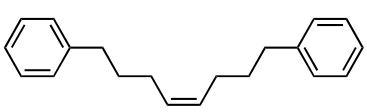

(*Z*)-1,8-diphenyloct-4-ene

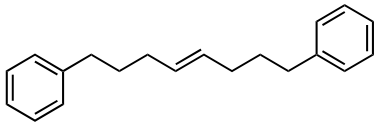

(*E*)-1,8-diphenyloct-4-ene

(*Z*)-1,8-diphenyloct-4-ene (product **3.4)** and (*E*)-1,8-diphenyloct-4-ene (E isomer of **3.4)** have been previously synthesized and characterized [52]. Provided are GC traces of pure (*Z*)-1,8-diphenyloct-4-ene, pure (*E*)-1,8-diphenyloct-4-ene, a mixture of both pure isomers, and a GC trace of the crude reaction mixture of the synthesis of (*Z*)-1,8-diphenyloct-4-ene using our method.

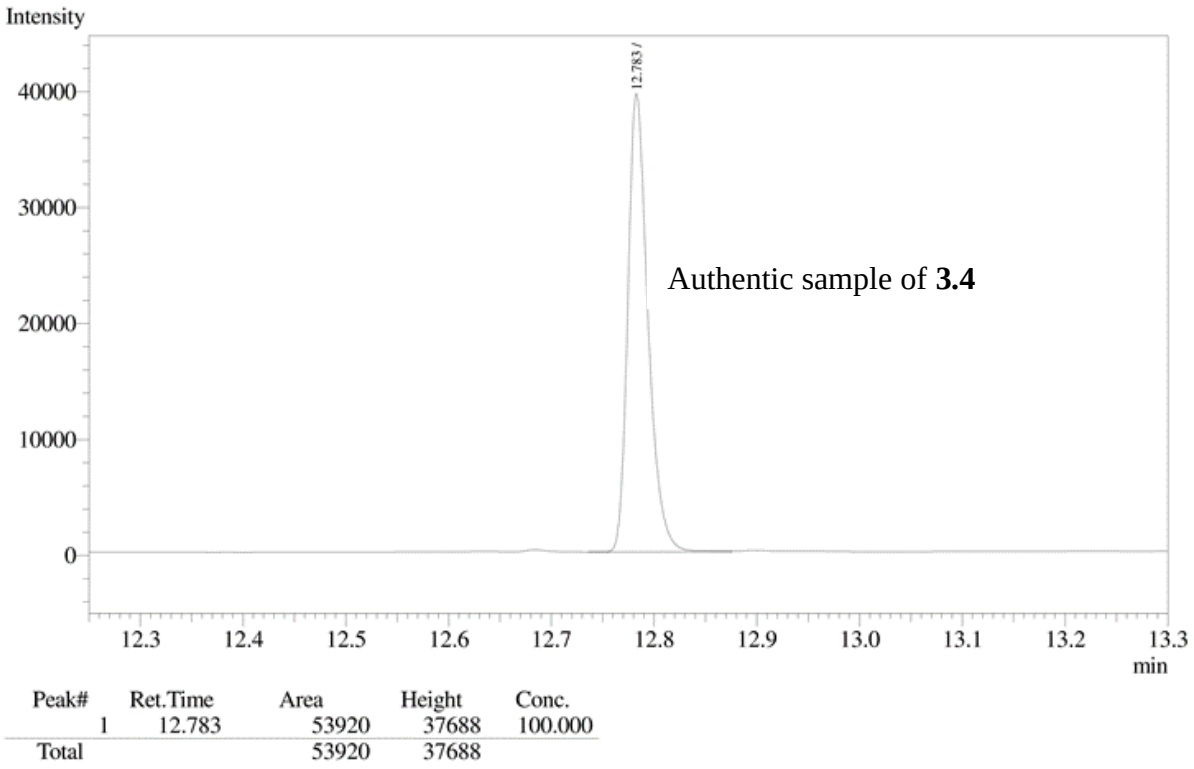

Peak#	Ret.Time	Area	Height	Conc.
1	12.783	53920	37688	100.000
Total		53920	37688	

Figure 3.2 GC trace of isolated (*Z*)-1,8-diphenyloct-4-ene (product **3.4**)

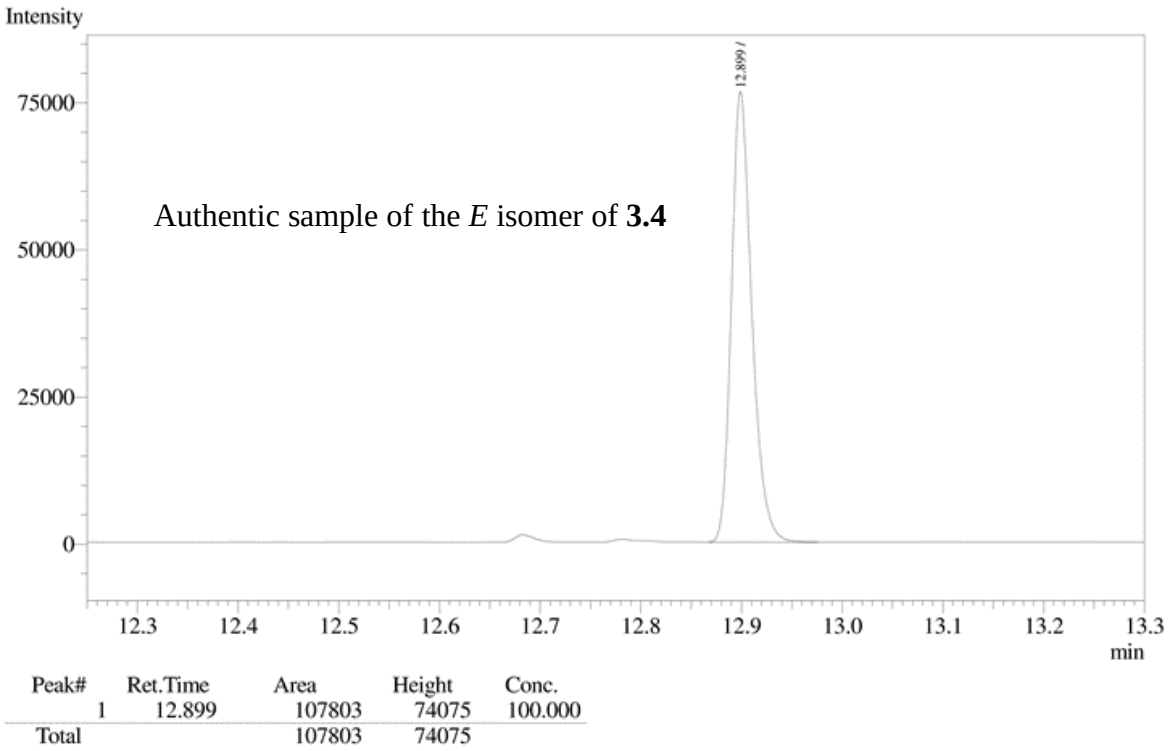

Peak#	Ret.Time	Area	Height	Conc.
1	12.899	107803	74075	100.000
Total		107803	74075	

Figure 3.3 GC trace of isolated (*E*)-1,8-diphenyloct-4-ene (*E* isomer of **3.4**)

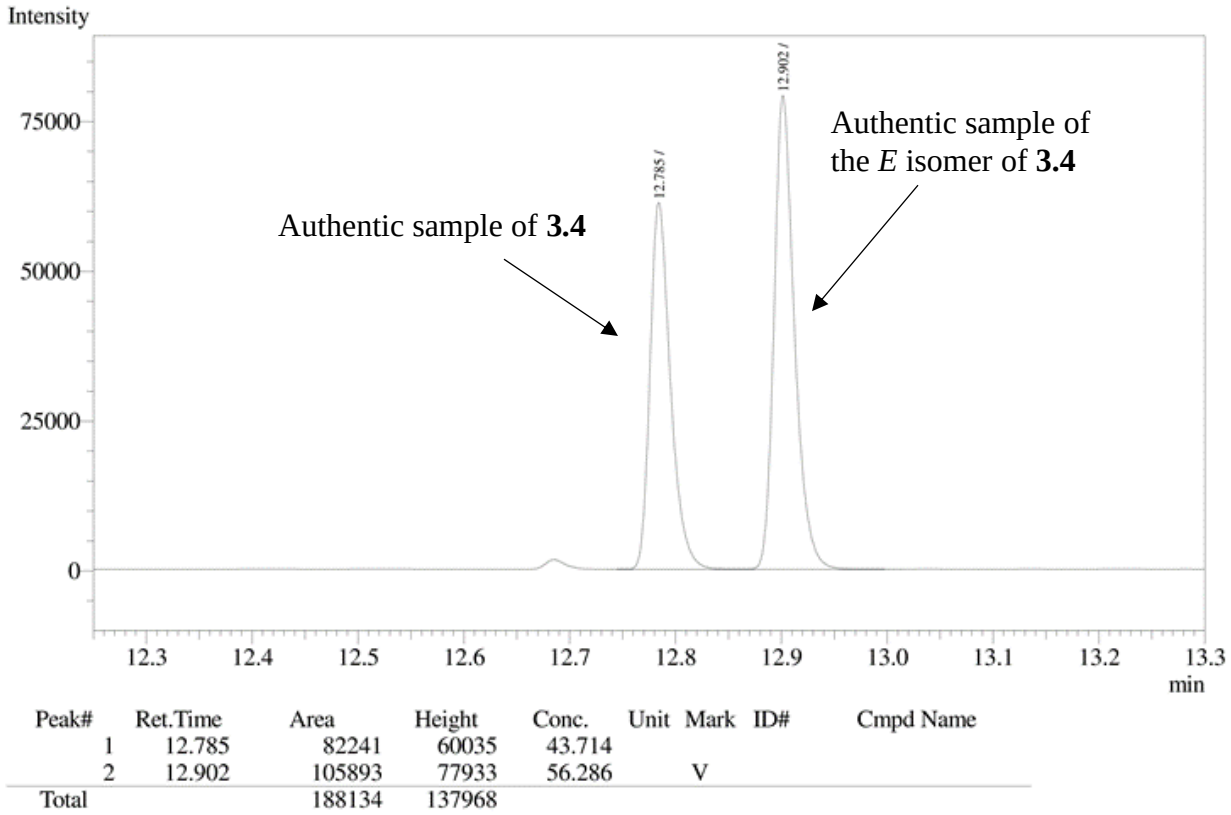

Peak#	Ret.Time	Area	Height	Conc.	Unit	Mark	ID#	Cmpd Name
1	12.785	82241	60035	43.714				
2	12.902	105893	77933	56.286		V		
Total		188134	137968					

Figure 3.4 GC trace of a mixture of the authentic samples of (*Z*)-1,8-diphenyloct-4-ene (product **3.4**) and (*E*)-1,8-diphenyloct-4-ene (E isomer of **3.4**).

E/Z selectivity of the following reaction was determined by GC/FID analysis of an aliquot taken from a crude reaction mixture at the end of the reaction:

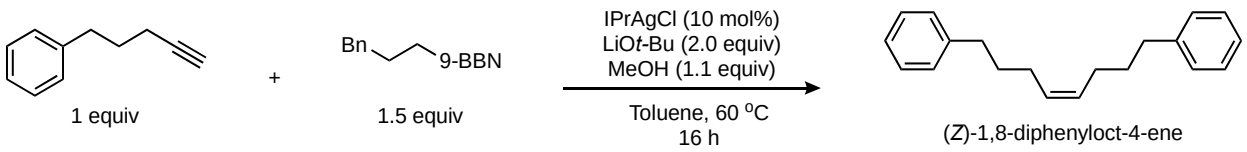

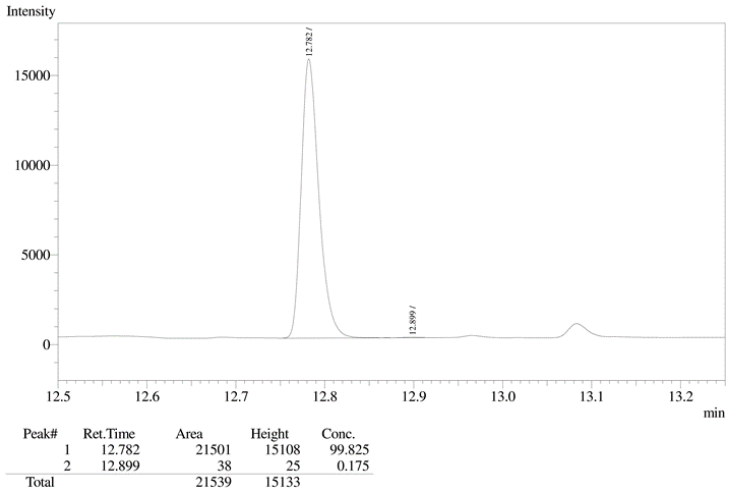

Peak#	Ret.Time	Area	Height	Conc.
1	12.782	21501	15108	99.825
2	12.899	38	25	0.175
Total		21539	15133	

Figure 3.5 GC/FID trace obtained by analysis of the crude reaction mixture of **3.4**

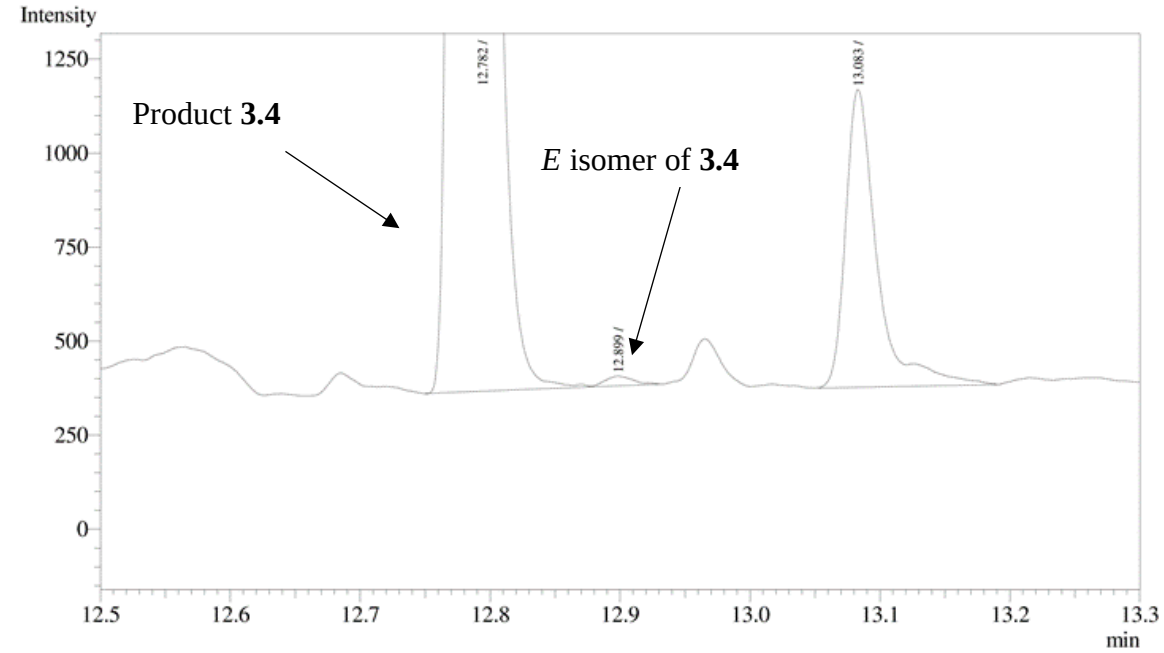

Peak#	Ret.Time	Area	Height	Conc.
1	12.782	21501	15108	99.825
2	12.899	38	25	0.175
Total		21539	15133	

Figure 3.6 Expansion of the product peak from the GC/FID trace obtained by analysis of the crude reaction mixture of **3.4**

Relative concentrations of the two isomers are 570:1 *Z* to *E*.

3.3.5 *Determination of Z/E Selectivity*

The selectivity of the hydroalkylation reaction was determined for several substrates. The *E* isomer of product **3.17** was synthesized according to a known procedure.[6] For other substrates, purified *Z*-alkene products isolated from the hydroalkylation reaction were subjected to a known isomerization procedure[53] to obtain mixtures of *Z* and *E* isomers. These mixtures were then used to determine GC retention times of the *E* isomer in order to analyze the selectivity in the crude reaction mixtures. Analysis was done using a GC/FID instrument.

3.3.5.1 Preparation of samples for the analysis of the reaction selectivity:

After completion of the catalytic reaction, an aliquot of the crude reaction mixture was taken, passed through a plug of silica with ethyl acetate and analyzed by GC.

3.3.5.2 *Z/E* selectivity in the formation of **3.3**:

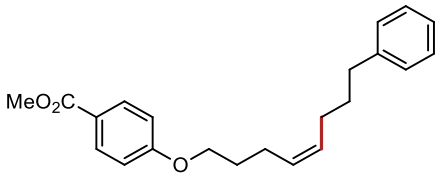

3.3

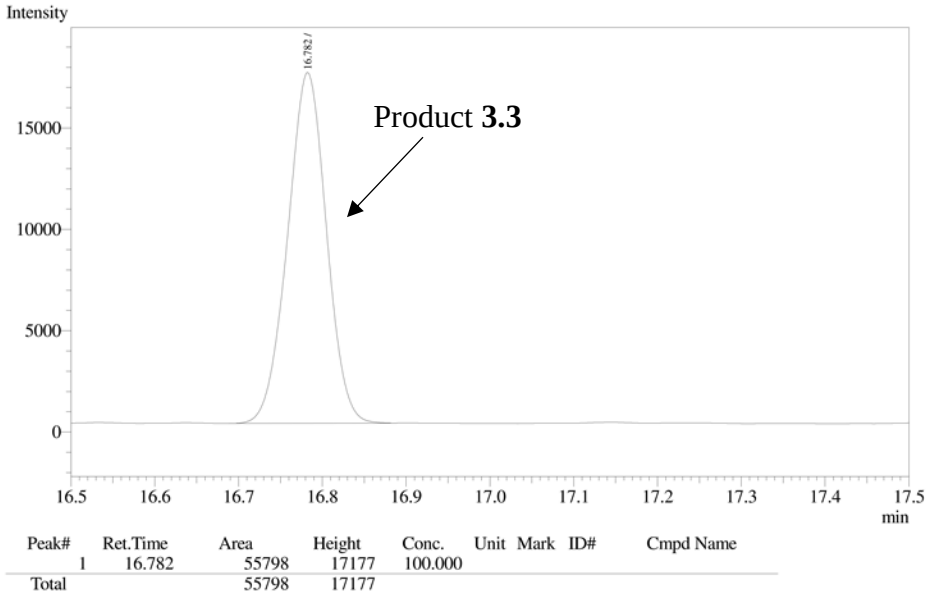

Peak#	Ret.Time	Area	Height	Conc.	Unit	Mark	ID#	Cmpd Name
1	16.782	55798	17177	100.000				
Total		55798	17177					

Figure 3.7 GC trace from the analysis of purified **3.3**

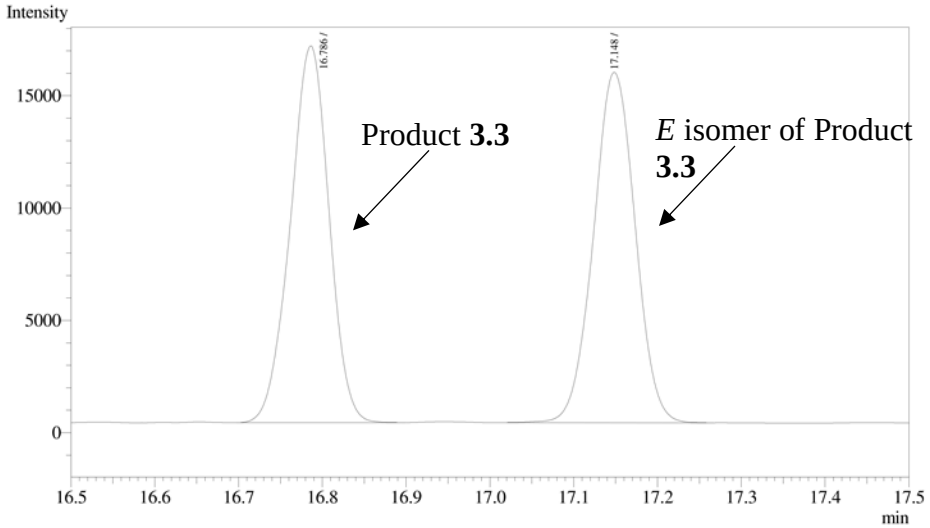

Peak#	Ret.Time	Area	Height	Conc.	Unit	Mark	ID#	Cmpd Name
1	16.786	54011	16692	49.913				
2	17.148	54199	15575	50.087		V		
Total		108210	32267					

Figure 3.8 GC trace from the analysis of **3.3** after isomerization (see 3.3.5.1)

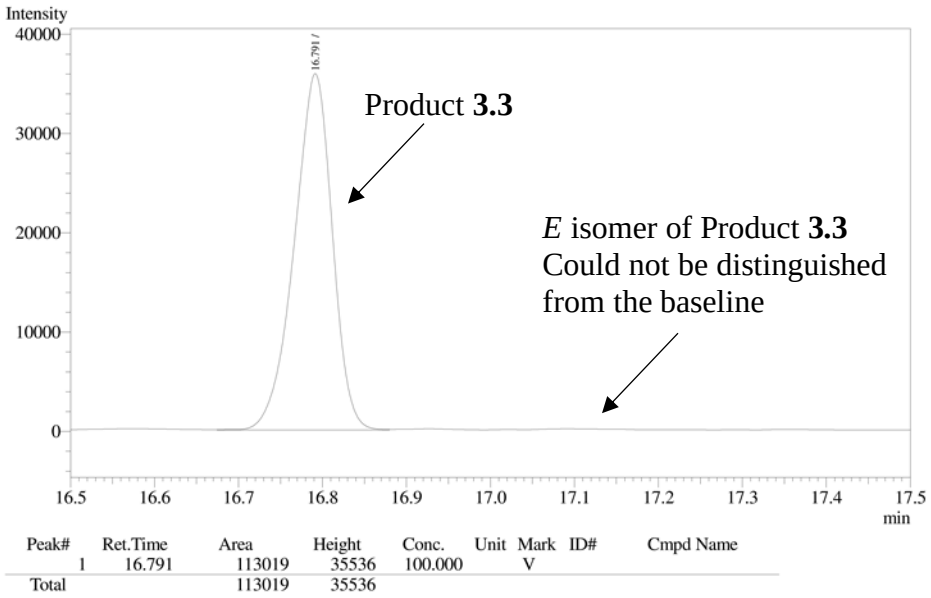

Figure 3.9 GC trace from the analysis of the crude reaction mixture of **3.3**

The *Z:E* ratio >500:1

3.3.5.3 *Z/E* selectivity in the formation of **3.17**:

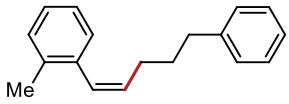

3.17

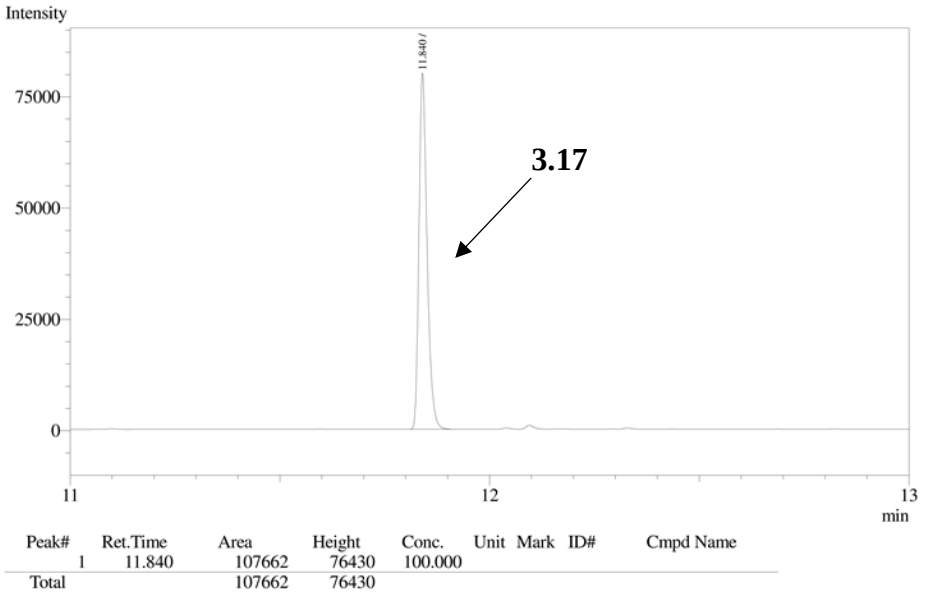

Peak#	Ret.Time	Area	Height	Conc.	Unit	Mark	ID#	Cmpd Name
1	11.840	107662	76430	100.000				
Total		107662	76430					

Figure 3.10 GC-FID trace the analysis of purified **3.17**

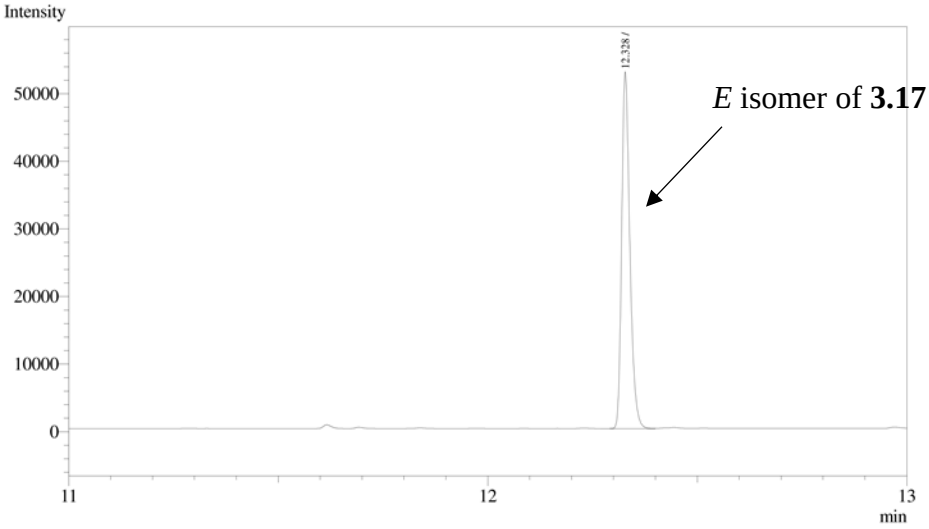

Peak#	Ret.Time	Area	Height	Conc.	Unit	Mark	ID#	Cmpd Name
1	12.328	71526	52087	100.000		V		
Total		71526	52087					

Figure 3.11 GC trace from the analysis of the *E* isomer of **3.17**:

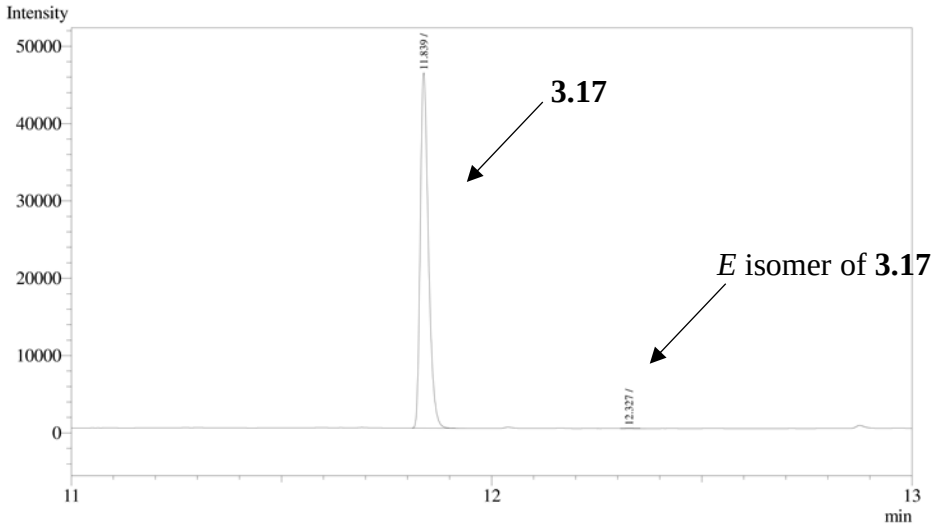

Figure 3.12 GC trace from the analysis of the crude reactoin mixture of **3.17**

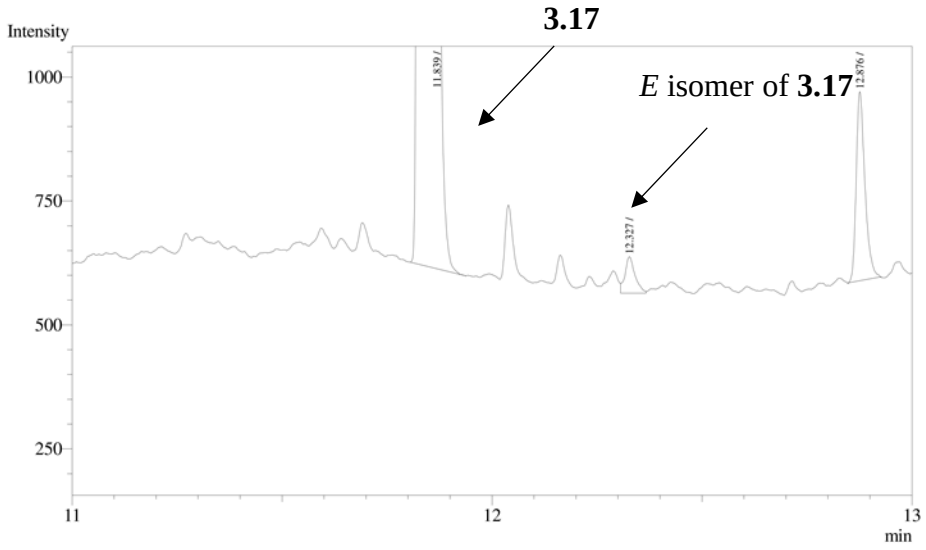

Peak Table - Channel 1

Peak#	Ret.Time	Area	Height	Conc.	Units	Mark	Name
1	11.839	62142	44930	99.808			
2	12.327	119	72	0.192			
Total		62261	45002				

Figure 3.13 Close up of the GC trace from the analysis of a sample from the crude reaction mixture of **3.17**

The ratio of concentrations of the two isomers is 519:1 (*Z:E*).

3.3.5.4 *Z/E* selectivity in the formation of **3.35**:

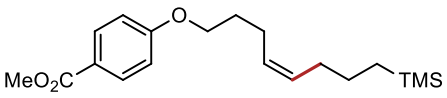

3.35

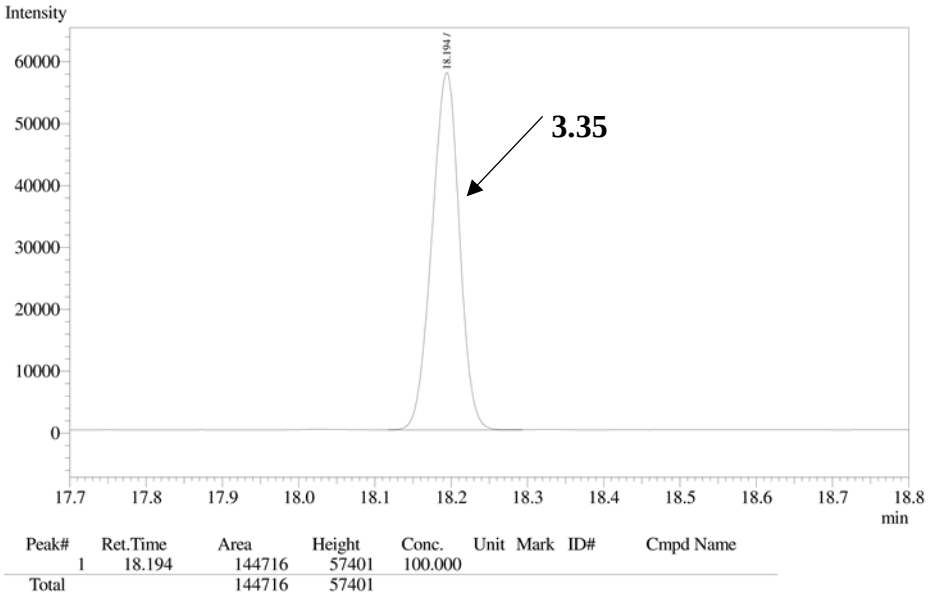

Figure 3.14 GC trace from the analysis of purified **3.35**

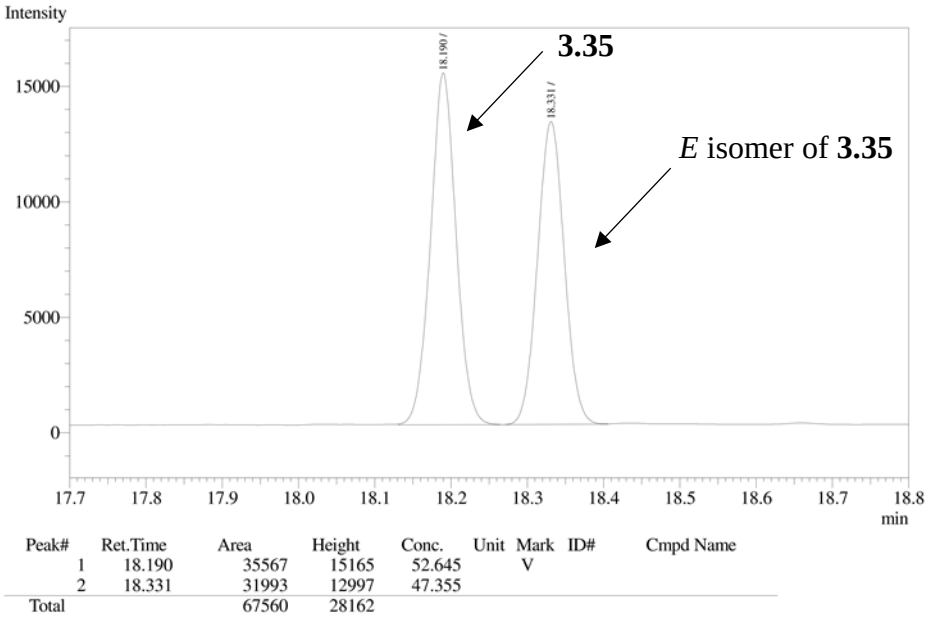

Peak#	Ret.Time	Area	Height	Conc.	Unit	Mark	ID#	Cmpd Name
1	18.190	35567	15165	52.645		V		
2	18.331	31993	12997	47.355				
Total		67560	28162					

Figure 3.15 GC trace from the analysis of a mixture of **3.35** and the *E* isomer of **3. 35**

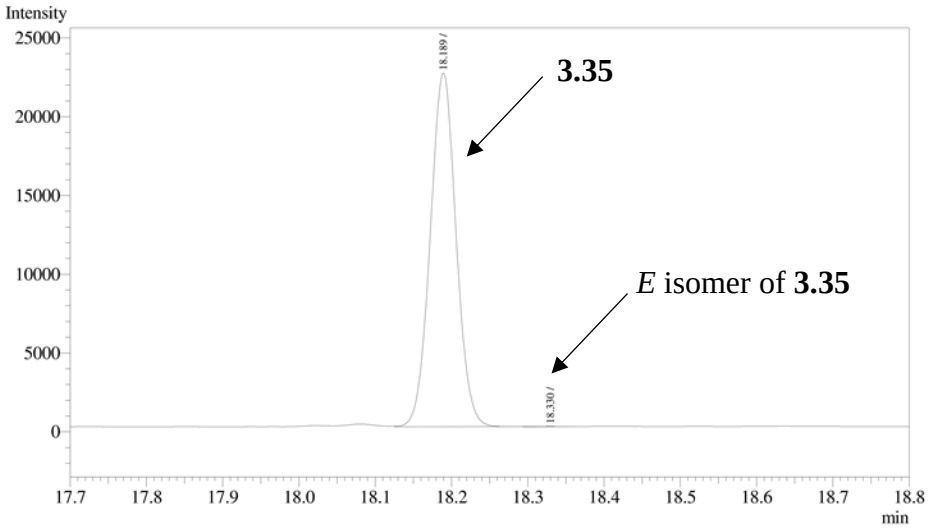

Figure 3.16 GC trace from the analysis of the crude reaction mixture of **3.35**

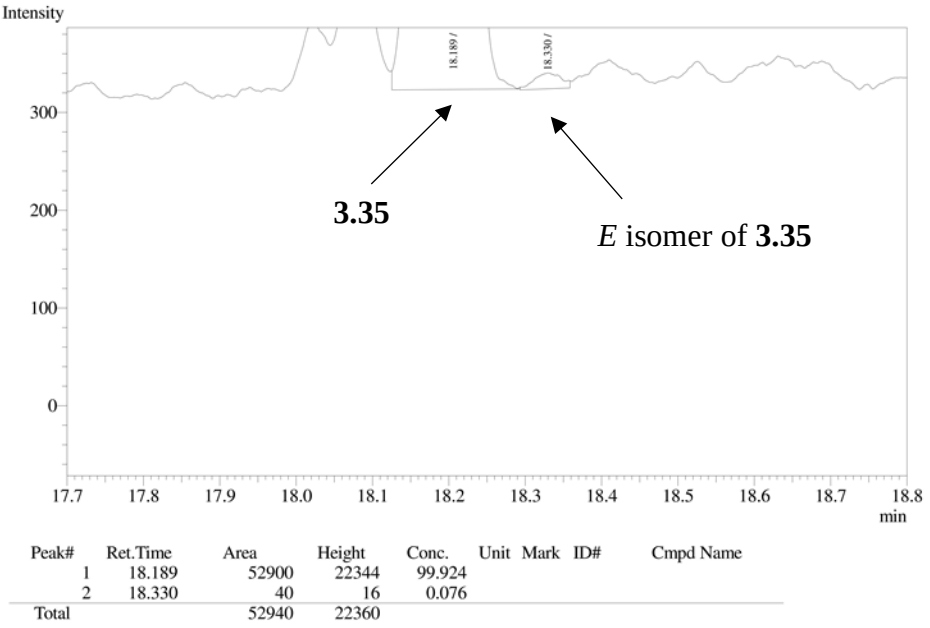

Peak#	Ret.Time	Area	Height	Conc.	Unit	Mark	ID#	Cmpd Name
1	18.189	52900	22344	99.924				
2	18.330	40	16	0.076				
Total		52940	22360					

Figure 3.17 Close up of the GC trace from the analysis of the crude reaction mixture of **3.35**

The ratio of concentrations of the two isomer is >500:1 (*Z:E*).

3.3.5.5 *Z/E* selectivity in the formation of **3.39**:

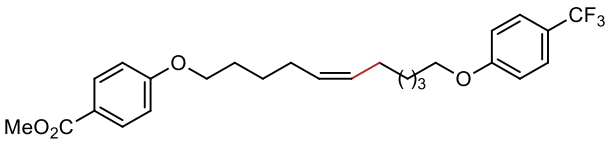

3.39

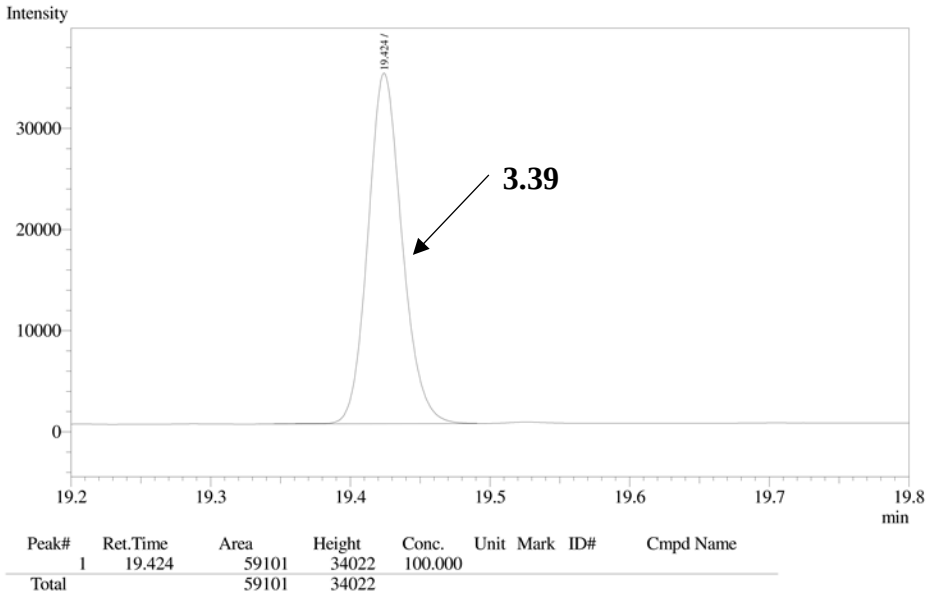

Peak#	Ret.Time	Area	Height	Conc.	Unit	Mark	ID#	Cmpd Name
1	19.424	59101	34022	100.000				
Total		59101	34022					

Figure 3.18 GC trace from the analysis of purified **3.39**

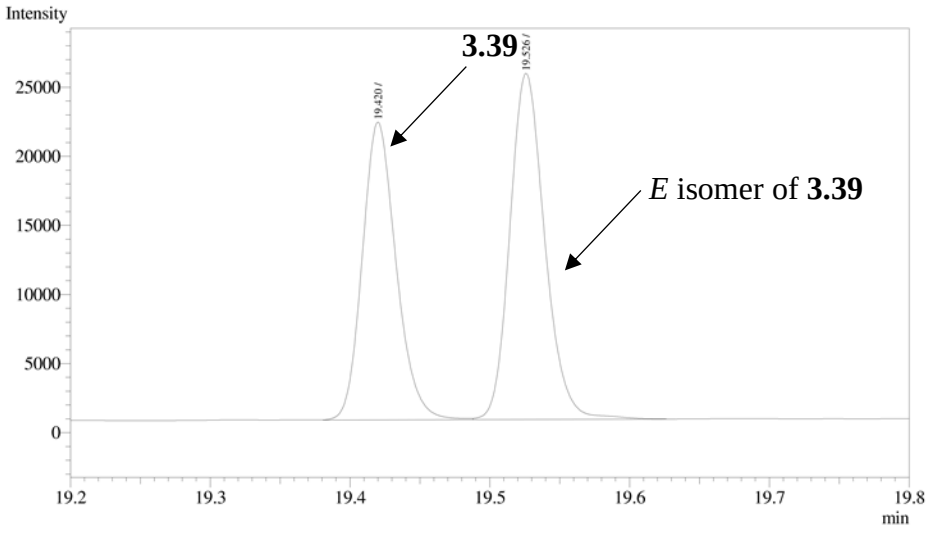

Peak#	Ret.Time	Area	Height	Conc.	Unit	Mark	ID#	Cmpd Name
1	19.420	36345	21331	45.507		V		
2	19.526	43522	24472	54.493		V		
Total		79867	45803					

Figure 3.19 GC trace from the analysis of a mixture of **3.39** and the *E* isomer of **3.39**

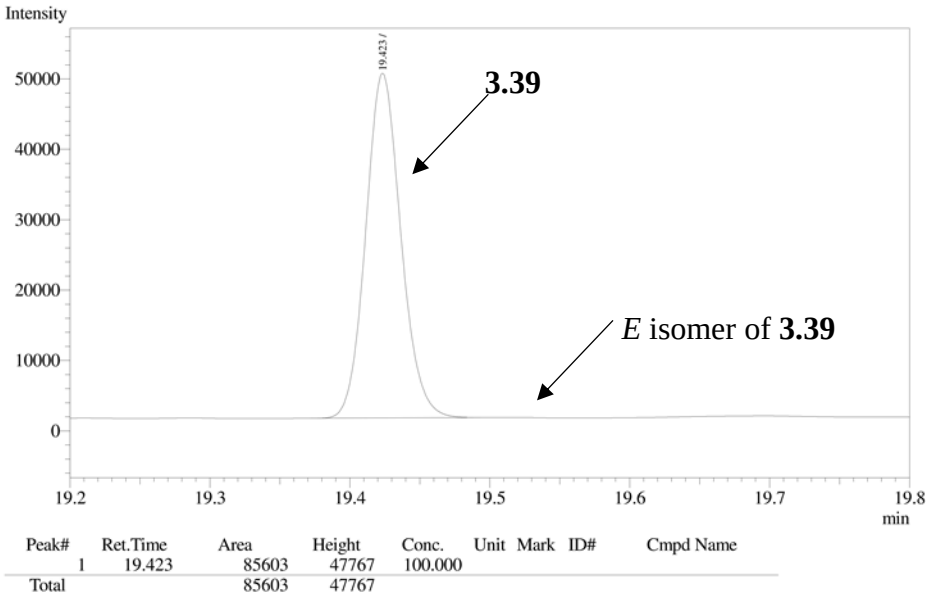

Peak#	Ret.Time	Area	Height	Conc.	Unit	Mark	ID#	Cmpd Name
1	19.423	85603	47767	100.000				
Total		85603	47767					

Figure 3.20 GC trace from the analysis of the crude reaction mixture of **3.39**

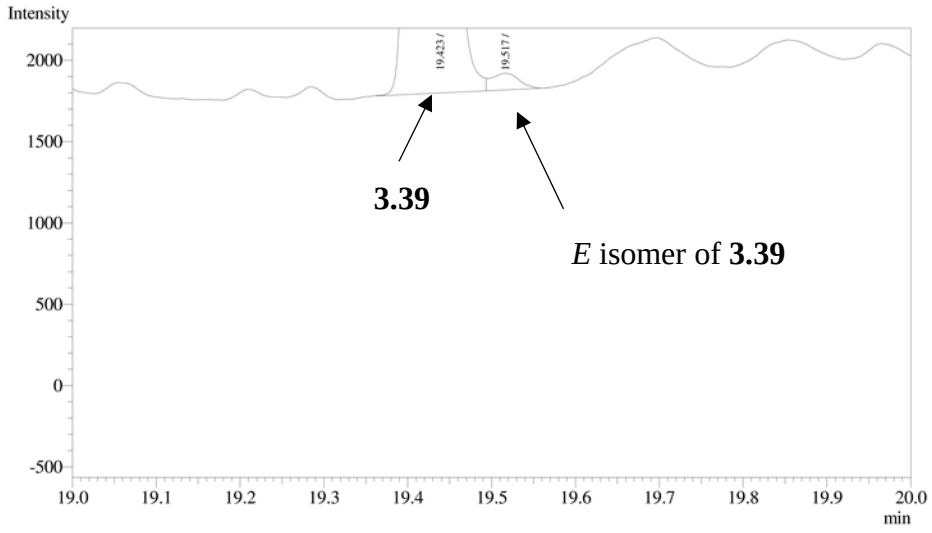

Peak#	Ret.Time	Area	Height	Conc.	Unit	Mark	ID#	Cmpd Name
1	19.423	85905	47802	99.726				
2	19.517	236	101	0.274		V		
Total		86141	47903					

Figure 3.21 Close up of the GC trace from the analysis of the crude reaction mixture of **3.39**

The ratio of concentration of the two isomers is 363:1 (*Z:E*)

3.3.5.6 *Z/E* selectivity in the formation of **3.41**:

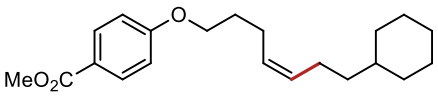

3.41

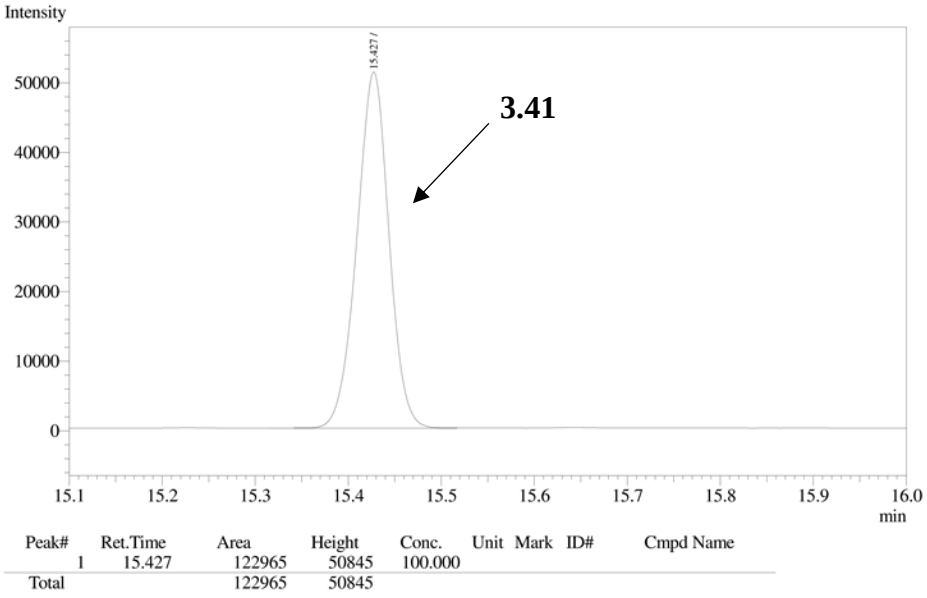

Figure 3.22 GC trace from the analysis of purified **3.41**

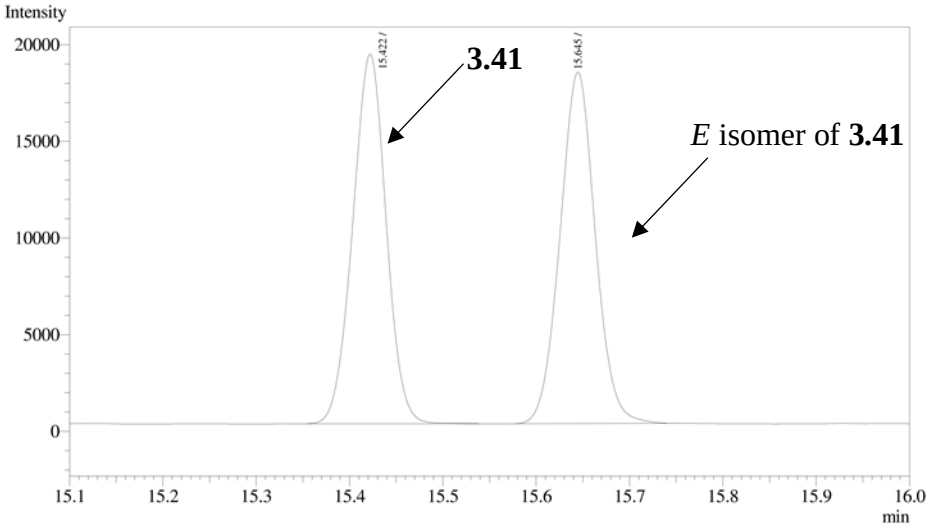

Peak#	Ret.Time	Area	Height	Conc.	Unit	Mark	ID#	Cmpd Name
1	15.422	47731	19054	49.896				
2	15.645	47930	18075	50.104				
Total		95661	37129					

Figure 3.23 GC trace from the analysis of a mixture of **3.41** and the *E* isomer of **3.41**

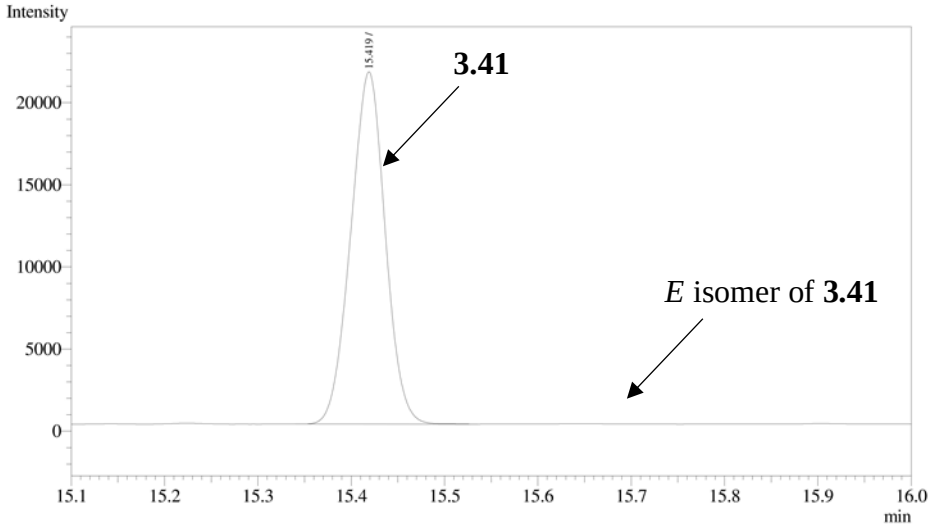

Peak#	Ret.Time	Area	Height	Conc.	Unit	Mark	ID#	Cmpd Name
1	15.419	55168	21261	100.000				
Total		55168	21261					

Figure 3.24 GC trace from the analysis of the crude reaction mixture of **3. 41**

The *Z:E* ratio >500:1

3.3.6 *Synthesis of TriAgCl and IPrAgCl*

The silver catalysts were synthesized using an adapted procedure from Sadighi et. al. that was used for the synthesis of SIPrAgCl.[54]

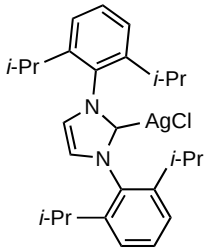

IPrAgCl, complex has been previously characterized.[55]

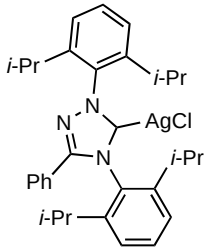

TriAgCl, complex was synthesized from TriHCl,[56] and isolated as a white solid (563.0 mg 77% yield). ^{1}H NMR (300 MHz, $CDCl_3$) δ 7.64 – 7.50 (m, 2H), 7.48 – 7.39 (m, 3H), 7.39 – 7.28 (m, 6H), 2.71 – 2.55 (m, 2H), 2.55 – 2.40 (m, 2H), 1.41 – 1.17 (m, 18H), 1.00 (d, J = 6.8 Hz, 6H). ^{13}C NMR (126 MHz, $CDCl_3$) δ 188.0 (dd, $J(^{109}Ag^{13}C)$ = 265.2 Hz, $J(^{107}Ag^{13}C)$ = 229.2 Hz), 153.6, 153.6, 145.7, 145.3, 134.9, 131.8, 131.7, 131.5, 131.5, 129.1, 128.0, 125.3, 124.4, 29.1, 25.1, 24.5, 23.9, 22.9.

3.3.7 *General Procedure for the Z-Selective Hydroalkylation of Terminal Alkynes*

In a nitrogen filled glovebox, a scintillation vial was charged with a stir bar and LiO*t*-Bu (1.5 or 2.0 equiv). To this was added silver catalyst (0.05 mmol, 0.10 equiv), alkyne (0.50 mmol, 1.0 equiv), alkylborane (1.3 or 1.5 equiv), methanol (17.6 mg, 0.55 mmol, 1.10 equiv), and solvent (5 mL). The reaction mixture was heated and stirred for 16 hours. After 16 hours, an aliquot of the crude reaction mixture was analyzed by GC, and the reaction was quenched with the addition of sodium perborate (150 mg, 0.75 mmol, 1.5 equiv) in 5 mL THF and 5 mL deionized water. The mixture was stirred at room temperature for 1 hour, and then extracted with ether (3 x 10 mL) and dried over $MgSO_4$. The crude mixture was concentrated under reduced pressure and purified by silica gel chromatography.

A: The general procedure was followed using TriAgCl (30.4 mg, 0.05 mmol, 0.10 equiv) as catalyst, 1.5 equivalents of LiO*t*-Bu (60 mg, 0.75 mmol) and 1.3 equivalents of alkylborane (0.65mmol) and the reaction was stirred in isooctane at 45 °C overnight.

B: The general procedure was followed using IPrAgCl (26.7 mg, 0.05 mmol, 0.10 equiv) as catalyst, 2.0 equivalents of LiO*t*-Bu (80 mg, 1.00mmol) and 1.5 equivalents of alkylborane (0.75mmol) and the reaction was stirred in toluene at 60 °C overnight.

Most reactions were performed using general procedure A, however products **3.4**, **3.18**, **3.19, 3.22, 3.23**, **3.27, 3.42**, **3.52**, and **3.54**, were synthesized using general procedure B.

3.3.8 *Characterization of Z-selective Hydroalkylation Products: Alkynes*

9-(3-phenylpropyl)-9-borabicyclo[3.3.1]nonane was used neat and was synthesized according to literature procedure.[57]

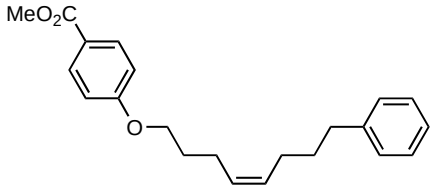

methyl 4-{[(4*Z*)-8-phenyloct-4-en-1-yl]oxy}benzoate (3.3), compound was prepared according to general procedure A. The compound was purified by silica gel chromatography with EtOAc/Hex (0 → 30%) and isolated as a colorless oil (147.6 mg, 87% yield).^{1}H NMR (300 MHz, $CDCl_3$) δ 7.98 (d, *J* = 8.9 Hz, 2H), 7.36 – 7.27 (m, 1H), 7.25 – 7.21 (m, 1H), 7.20 – 7.09 (m, 3H), 6.89 (d, *J* = 8.9 Hz, 2H), 5.64 – 5.31 (m, 2H), 3.99 (t, *J* = 6.3 Hz, 2H), 3.88 (s, 3H), 2.64 – 2.50 (m, 2H), 2.28 – 2.15 (m, 2H), 2.12 – 2.01 (m, 2H), 1.92 – 1.78 (m, 2H), 1.70 – 1.59 (m, 2H).^{13}C NMR (126 MHz, $CDCl_3$) δ 167.0, 163.0, 142.5, 131.7, 130.9, 128.8, 128.5, 128.4, 125.8, 122.5, 114.2, 67.3, 51.9, 35.6, 31.5, 29.1, 26.9, 23.6.GC/MS (EI) calculated for $[M]^{+}$ 338.19, found 338.2. FTIR (neat, cm^{-1}): 2929(m), 2849(m), 2360(m), 1719(s), 1604(s), 1510(s), 1437(s), 1280(s), 1253(s), 1167(s), 1104(s).

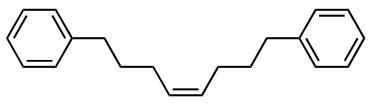

[(4*Z*)-8-phenyloct-4-en-1-yl]benzene (3.4), compound was prepared according to general procedure B. The compound was purified by silica gel chromatography with EtOAc/Hex (0 → 10%) and isolated as a colorless oil (116.3 mg, 88% yield).^{1}H NMR (300 MHz, $CDCl_3$) δ 7.33 –

7.26 (m, 4H), 7.21 – 7.14 (m, 6H), 5.54 – 5.30 (m, 2H), 2.68 – 2.54 (m, 4H), 2.12 – 2.00 (m, 4H), 1.76 – 1.60 (m, 4H).^{13}C NMR (126 MHz, $CDCl_3$) δ 142.6, 130.0, 128.6, 128.4, 125.8, 35.6, 31.6, 27.0. GC/MS (EI) calculated for $[M]^+$ 264.19, found 264.2. FTIR (neat, cm^{-1}): 3061(m), 3005(m), 2931(m), 2856(m), 1602(m) 1495(s), 1452(s), 1217(s), 1030(s), 906(w).

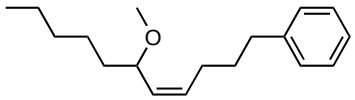

[(4*Z*)-6-methoxyundec-4-en-1-yl]benzene (3.5), compound was prepared according to general procedure A. The compound was purified by silica gel chromatography with EtOAc/Hex (0 → 20%) and isolated as a colorless oil (116.6 mg, 90% yield).^{1}H NMR (300 MHz, $CDCl_3$) δ 7.36 – 7.26 (m, 2H), 7.23 – 7.13 (m, 3H), 5.63 (dt, *J* = 10.9, 7.4 Hz, 1H), 5.23 (dd, *J* = 10.9, 9.2 Hz, 1H), 3.88 (dt, *J* = 9.2, 6.3 Hz, 1H), 3.23 (s, 3H), 2.73 – 2.54 (m, 2H), 2.24 – 2.01 (m, 2H), 1.80 – 1.64 (m, 2H), 1.41 – 1.19 (m, 8H), 0.88 (t, *J* = 6.6 Hz, 3H).^{13}C NMR (126 MHz, $CDCl_3$) δ 142.3, 133.0, 131.4, 128.5, 128.5, 125.9, 76.6, 56.0, 35.7, 35.6, 32.0, 31.6, 27.5, 25.1, 22.8, 14.2. GC/MS (EI) calculated for $[M]^+$ 260.21, found 260.3. FTIR (neat, cm^{-1}): 3025(m), 2929(m), 2857(m), 1603(s), 1496(s), 1452(s), 1332(m), 1124(s), 1097(s).

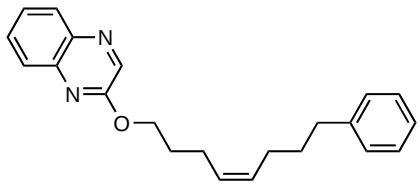

2-{[(4*Z*)-8-phenyloct-4-en-1-yl]oxy}quinoxaline (3.6), compound was prepared according to general procedure A. The compound was purified by silica gel chromatography with EtOAc/Hex (0 → 40%) and isolated as a colorless oil (133.5 mg, 80% yield). ^{1}H NMR (300 MHz, $CDCl_3$) δ 8.46 (s, 1H), 8.01 (dd, *J* = 8.3, 1.5 Hz, 1H), 7.81 (dd, *J* = 8.4, 1.4 Hz, 1H), 7.66 (ddd, *J* = 8.4, 7.0,

1.5 Hz, 1H), 7.55 (ddd, *J* = 8.3, 7.0, 1.4 Hz, 1H), 7.26 – 7.19 (m, 2H), 7.19 – 7.08 (m, 3H), 5.57 – 5.34 (m, 2H), 4.47 (t, *J* = 6.5 Hz, 2H), 2.67 – 2.50 (m, 2H), 2.33 – 2.16 (m, 2H), 2.16 – 2.01 (m, 2H), 1.98 – 1.83 (m, 2H), 1.76 – 1.60 (m, 2H). ^{13}C NMR (75 MHz, $CDCl_3$) δ 157.6, 142.5, 140.6, 139.9, 139.0, 130.7, 130.2, 129.1, 129.0, 128.5, 128.4, 127.3, 126.5, 125.8, 66.0, 35.6, 31.5, 28.8, 27.0, 23.8. GC/MS (EI) calculated for [M]+ 332.19, found 332.2. FTIR (neat, cm^{-1}): 3004(m), 2928(m), 2855(m), 1944(w), 1571(s), 1497(s), 1414(s), 1305(s), 1221(s), 1136(s), 1019(m), 911(s).

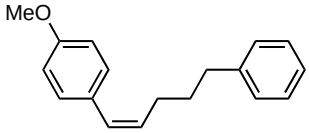

1-methoxy-4-[(1*Z*)-5-phenylpent-1-en-1-yl]benzene (3.7), compound was prepared according to general procedure A. The compound was purified by silica gel chromatography with EtOAc/Hex (0 → 20%) and isolated as a colorless oil (117.9 mg, 93% yield).^{1}H NMR (300 MHz, $CDCl_3$) δ 7.34 – 7.27 (m, 1H), 7.24 – 7.12 (m, 6H), 6.85 (d, *J* = 8.7 Hz, 2H), 6.37 (d, *J* = 11.6 Hz, 1H), 5.60 (dt, *J* = 11.6, 7.2 Hz, 1H), 3.82 (s, 3H), 2.70 – 2.60 (m, 2H), 2.45 – 2.30 (m, 2H), 1.85 – 1.70 (m, 2H).^{13}C NMR (126 MHz, $CDCl_3$) δ 158.3, 142.5, 131.1, 130.5, 130.1, 128.7, 128.6, 128.4, 125.8, 113.7, 55.4, 35.6, 31.9, 28.3. GC/MS (EI) calculated for $[M]^+$ 252.15, found 252.2. FTIR (neat, cm^{-1}):3292(m), 3061(m), 3003(m), 2929(m), 2855(m), 1605(s), 1503(s), 1452(s), 1300(s), 1250(s), 1174(s), 1108(s), 1033(s), 837(s).

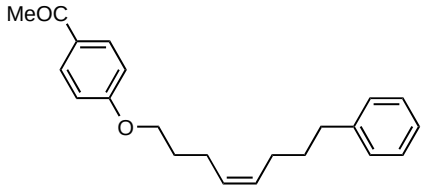

1-(4-{[(4*Z*)-8-phenyloct-4-en-1-yl]oxy}phenyl)ethan-1-one (3.8), compound was prepared according to general procedure A. The compound was purified by silica gel chromatography with EtOAc/Hex (0 → 30%) and isolated as a colorless oil (97.8 mg, 61% yield).^{1}H NMR (300 MHz, $CDCl_3$) δ 7.92 (d, *J* = 8.8 Hz, 2H), 7.28 (s, 1H), 7.23 (s, 1H), 7.20 – 7.08 (m, 3H), 6.91 (d, *J* = 8.8 Hz, 2H), 5.56 – 5.30 (m, 2H), 4.01 (t, *J* = 6.3 Hz, 2H), 2.69 – 2.47 (m, 5H), 2.29 – 2.15 (m, 2H), 2.11 – 1.98 (m, 2H), 1.91 – 1.82 (m, 2H), 1.72 – 1.59 (m, 2H).^{13}C NMR (126 MHz, $CDCl_3$) δ 196.9, 163.2, 142.5, 130.9, 130.7, 130.3, 128.7, 128.5, 128.4, 125.8, 114.2, 67.4, 35.6, 31.5, 29.0, 26.9, 26.4, 23.6.GC/MS (EI) calculated for $[M]^{+}$ 322.19, found 322.2. FTIR (neat, cm^{-1}): 3060(m), 3002(m), 2932(m), 2855(m), 1676(s), 1600(s), 1508(s), 1357(s), 1305(s), 1255(s), 1170(s), 1029(m), 955(s), 833(s).

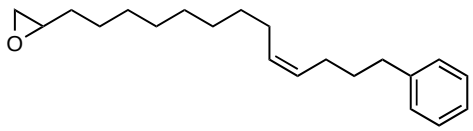

2-[(10*Z*)-14-phenyltetradec-10-en-1-yl]oxirane (3.9), compound was prepared according to general procedure A. The compound was purified by silica gel chromatography with EtOAc/Hex (0 → 20%) and isolated as a colorless oil (122.0 mg, 81% yield).^{1}H NMR (300 MHz, $CDCl_3$) δ 7.31 – 7.26 (m, 2H), 7.21 – 7.14 (m, 3H), 5.51 – 5.26 (m, 2H), 2.95 – 2.85 (m, 1H), 2.78 – 2.72 (m, 1H), 2.66 – 2.57 (m, 2H), 2.46 (dd, *J* = 5.0, 2.7 Hz, 1H), 2.12 – 1.95 (m, 4H), 1.74 – 1.61 (m, 2H), 1.52 – 1.41 (m, 4H), 1.29 (s, 10H).^{13}C NMR (126 MHz, $CDCl_3$) δ 142.7, 130.6, 129.4, 128.5, 128.4, 125.7, 52.5, 47.2, 35.6, 32.6, 31.6, 29.8, 29.7, 29.6, 29.4, 27.4, 27.0, 26.1. GC/MS (EI)

calculated for $[M]^+$ 300.25, found 300.3. FTIR (neat, cm^{-1}): 3001(m), 2926(m), 2853(m), 1725(m), 1603(s), 1495(s), 1453(s), 1258(w), 1029(s).

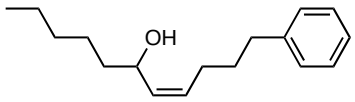

(4*Z*)-1-phenylundec-4-en-6-ol (3.10), compound was prepared according to general procedure A. The compound was purified by silica gel chromatography with EtOAc/Hex (0 → 60%) and isolated as a colorless oil (78.2 mg, 63% yield). ^{1}H NMR (300 MHz, $CDCl_3$) δ 7.35 – 7.27 (m, 2H), 7.24 – 7.12 (m, 3H), 5.64 – 5.26 (m, 2H), 4.44 – 4.29 (m, 1H), 2.75 – 2.55 (m, 2H), 2.24 – 2.00 (m, 2H), 1.78 – 1.64 (m, 2H), 1.59 – 1.38 (m, 2H), 1.35 – 1.22 (m, 6H), 0.88 (t, *J* = 5.5 Hz, 3H). ^{13}C NMR (126 MHz, $CDCl_3$) δ 142.2, 133.3, 131.6, 128.5, 128.4, 125.9, 67.8, 37.6, 35.5, 31.9, 31.4, 27.3, 25.1, 22.7, 14.1. GC/MS (EI) calculated for $[M]^+$ 246.20, found 246.2. FTIR (neat, cm^{-1}): 3349(b), 3025(m), 3004(m), 2929(m), 2857(m), 1603(s), 1496(s), 1453(s), 1378(s), 1303(m), 1123(s), 1028(s), 910(s).

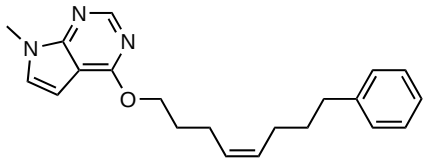

7-methyl-4-{[(4*Z*)-8-phenyloct-4-en-1-yl]oxy}-7H-pyrrolo[2,3-d]pyrimidine (3.11), compound was prepared according to general procedure A. The compound was purified by silica gel chromatography with EtOAc/Hex (0 → 40%) and isolated as a colorless oil (146.7 mg, 87% yield).^{1}H NMR (300 MHz, $CDCl_3$) δ 8.46 (s, 1H), 7.25 – 7.19 (m, 2H), 7.20 – 7.06 (m, 3H), 6.99 (d, *J* = 3.4 Hz, 1H), 6.52 (d, *J* = 3.4 Hz, 1H), 5.58 – 5.33 (m, 2H), 4.51 (t, *J* = 6.6 Hz, 2H), 3.84 (s, 3H), 2.63 – 2.46 (m, 2H), 2.31 – 2.16 (m, 2H), 2.14 – 2.00 (m, 2H), 1.96 – 1.86 (m, 2H), 1.69 –

1.60 (m, 2H).^{13}C NMR (126 MHz, $CDCl_3$) δ 162.9, 151.9, 150.9, 142.4, 130.5, 129.0, 128.4, 128.2, 126.6, 125.6, 105.5, 98.2, 65.7, 35.5, 31.4, 31.4, 28.9, 26.8, 23.7. GC/MS (EI) calculated for $[M]^+$ 335.20, found 335.2. FTIR (neat, cm^{-1}): 3003(m), 2926(m), 2856(m), 1873(w), 1595(s), 1561(s), 1441(s), 1367(s), 1317(s), 1247(s), 1055(s), 1006(m), 888(m).

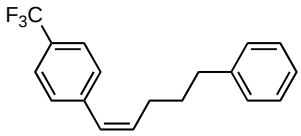

1-[(1*Z*)-5-phenylpent-1-en-1-yl]-4-(trifluoromethyl)benzene (3.12), compound was prepared according to general procedure A. The compound was purified by silica gel chromatography with EtOAc/Hex (0 → 20%) and isolated as a colorless oil (124.3 mg, 86% yield).^{1}H NMR (300 MHz, $CDCl_3$) δ 7.55 (d, *J* = 8.2 Hz, 2H), 7.38 – 7.27 (m, 3H), 7.24 – 7.09 (m, 4H), 6.46 (d, *J* = 11.6 Hz, 1H), 5.80 (dt, *J* = 11.6, 7.4 Hz, 1H), 2.72 – 2.57 (m, 2H), 2.43 – 2.26 (m, 2H), 1.87 – 1.71 (m, 2H)^{13}C NMR (126 MHz, $CDCl_3$) δ 142.1, 141.3, 134.8, 129.0, 128.6 (q, *J* = 27.6 Hz), 128.6, 128.5, 128.2, 126.0, 125.2 (q, *J* = 3.8 Hz), 124.5 (q, *J* = 271.9 Hz), 35.5, 31.6, 28.1.^{19}F NMR (470 MHz, $CDCl_3$) δ -65.4. GC/MS (EI) calculated for $[M]^+$ 290.13, found 290.1. FTIR (neat, cm^{-1}): 3062(m), 3025(m), 2931(m), 2858(m), 1614(s), 1496(s), 1453(s), 1420(m), 1326(s), 1164(s), 1124(s), 1067(s), 1016(s), 837(s).

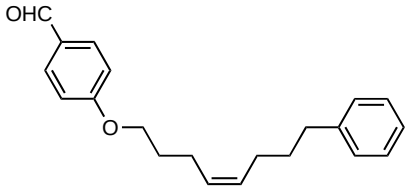

4-{[(4*Z*)-8-phenyloct-4-en-1-yl]oxy}benzaldehyde (3.13), compound was prepared according to general procedure A. The compound was purified by silica gel chromatography with EtOAc/Hex

(0 → 20%) and isolated as a colorless oil (108.2 mg, 70% yield).^{1}H NMR (300 MHz, $CDCl_3$) δ 9.87 (s, 1H), 7.82 (d, *J* = 8.7 Hz, 2H), 7.28 (s, 1H), 7.23 (s, 1H), 7.20 – 7.07 (m, 3H), 6.98 (d, *J* = 8.7 Hz, 2H), 5.57 – 5.30 (m, 2H), 4.03 (t, *J* = 6.3 Hz, 2H), 2.68 – 2.50 (m, 2H), 2.30 – 2.16 (m, 2H), 2.13 – 1.99 (m, 2H), 1.97 – 1.81 (m, 2H), 1.74 – 1.59 (m, 2H).^{13}C NMR (126 MHz, $CDCl_3$) δ 190.9, 164.3, 142.5, 132.1, 131.0, 129.9, 128.7, 128.5, 128.4, 125.8, 114.9, 67.6, 35.6, 31.5, 29.0, 27.0, 23.6. GC/MS (EI) calculated for $[M]^+$ 308.18, found 308.2. FTIR (neat, cm^{-1}): 3016(m), 3003(m), 2924(m), 2854(m), 2735(m), 1694(s), 1590(s), 1574(s), 1497(s), 1393(s), 1310(m), 1257(m), 1158(s), 1029(s), 832(s), 750(s), 698(s).

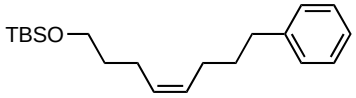

***tert*-butyldimethyl{[(4*Z*)-8-phenyloct-4-en-1-yl]oxy}silane (3.14),** compound was prepared according to general procedure A. The compound was purified by silica gel chromatography with EtOAc/Hex (0 → 20%) and isolated as a colorless oil (150.4 mg, 95% yield). ^{1}H NMR (300 MHz, $CDCl_3$) δ 7.31 – 7.26 (m, 1H), 7.26 – 7.23 (m, 1H), 7.22 – 7.13 (m, 3H), 5.50 – 5.31 (m, 2H), 3.60 (t, *J* = 6.5 Hz, 2H), 2.68 – 2.51 (m, 2H), 2.15 – 2.00 (m, 4H), 1.75 – 1.62 (m, 2H), 1.61 – 1.50 (m, 2H), 0.90 (s, 9H), 0.05 (s, 6H). ^{13}C NMR (126 MHz, $CDCl_3$) δ 142.7, 129.9, 128.6, 128.4, 125.8, 62.8, 35.7, 33.0, 31.6, 27.0, 26.1, 23.7, 18.5, -5.1. GC/MS (EI) calculated for $[M]^+$ 318.24, found 318.3. FTIR (neat, cm^{-1}): 3062(m), 3026(m), 3004(m), 2927(m), 2856(m), 1604(s), 1496(s), 1471(s), 1388(s), 1360(s), 1255(s), 1102(s), 836(s), 774(s), 698(s).

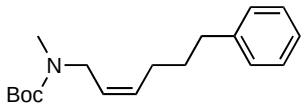

***tert*-butyl N-methyl-N-[(2*Z*)-6-phenylhex-2-en-1-yl]carbamate (3.15),** compound was prepared according to general procedure A. The compound was purified by silica gel chromatography with EtOAc/Hex (0 → 20%) and isolated as a colorless oil (127.7 mg, 88% yield).^{1}H NMR (300 MHz, $CDCl_3$) δ 7.34 – 7.26 (m, 2H), 7.23 – 7.11 (m, 3H), 5.66 – 5.48 (m, 1H), 5.48 – 5.31 (m, 1H), 3.83 (d, *J* = 5.0 Hz, 2H), 2.78 (s, 3H), 2.69 – 2.54 (m, 2H), 2.20 – 2.05 (m, 2H), 1.80 – 1.61 (m, 2H), 1.46 (s, 9H).^{13}C NMR (126 MHz, $CDCl_3$) δ 155.8, 142.2, 132.4, 128.4, 128.4, 125.8, 79.4, 45.2, 35.5, 33.5, 31.4, 28.5, 26.9. GC/MS (EI) calculated for $[M]^+$ 289.20, found 289.4. FTIR (neat, cm^{-1}): 3061(w), 3024(m), 2974(m), 2930(m), 2857(m), 1699(s), 1480(s), 1390(s) 1365(s), 1238(s), 1141(s), 1030(w), 879(s).

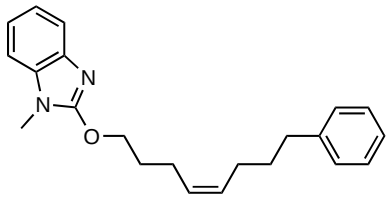

1-methyl-2-{[(4*Z*)-8-phenyloct-4-en-1-yl]oxy}-1H-1,3-benzodiazole (3.16), compound was prepared according to general procedure A. The compound was purified by silica gel chromatography with EtOAc/Hex (0 → 40%) and isolated as a colorless oil (127.6 mg, 76% yield).^{1}H NMR (300 MHz, $CDCl_3$) δ 7.60 – 7.50 (m, 1H), 7.30 – 7.27 (m, 2H), 7.25 – 7.22 (m, 1H), 7.22 – 7.09 (m, 6H), 5.55 – 5.37 (m, 2H), 4.55 (t, *J* = 6.5 Hz, 2H), 3.54 (s, 3H), 2.67 – 2.55 (m, 2H), 2.29 – 2.17 (m, 2H), 2.16 – 2.04 (m, 2H), 1.99 – 1.86 (m, 2H), 1.76 – 1.63 (m, 2H).^{13}C NMR (126 MHz, $CDCl_3$) δ 157.7, 142.5, 140.2, 134.4, 130.8, 128.8, 128.5, 128.4, 125.8, 121.6, 120.9, 117.7, 108.0, 69.8, 35.6, 31.4, 29.1, 28.1, 26.9, 23.7 GC/MS (EI) calculated for $[M]^+$ 334.20,

found 334.2. FTIR (neat, cm^{-1}): 3003(m), 2923(m), 2855(m), 1603(w), 1514(s), 1452(m), 1021(m), 808(s).

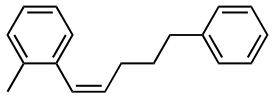

1-methyl-2-[(1*Z*)-5-phenylpent-1-en-1-yl]benzene (3.17), compound was prepared according to general procedure A. The compound was purified by silica gel chromatography with EtOAc/Hex (0 → 10%) and isolated as a colorless oil (99.5 mg, 84% yield).^{1}H NMR (300 MHz, $CDCl_3$) δ 7.35 – 7.27 (m, 2H), 7.25 – 7.11 (m, 7H), 6.51 (d, *J* = 11.5 Hz, 1H), 5.78 (dt, *J* = 11.5, 7.4 Hz, 1H), 2.72 – 2.56 (m, 2H), 2.30 (s, 3H), 2.29 – 2.18 (m, 2H), 1.85 – 1.68 (m, 2H).^{13}C NMR (126 MHz, $CDCl_3$) δ 142.5, 136.9, 136.3, 132.4, 129.9, 129.2, 128.5, 128.5, 128.4, 126.9, 125.8, 125.4, 35.6, 31.8, 28.1, 20.1. GC/MS (EI) calculated for $[M]^+$ 236.16, found 236.2. FTIR (neat, cm^{-1}): 3024(m), 2920(m), 2855(m), 1602(s), 1485(s), 1453(s), 1435(m), 1104(s0, 1083(s), 1030(s).

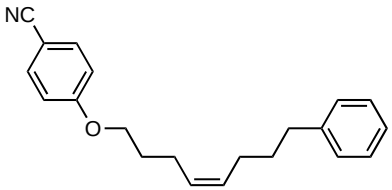

4-{[(4*Z*)-8-phenyloct-4-en-1-yl]oxy}benzonitrile (3.18), compound was prepared according to general procedure B. The compound was purified by silica gel chromatography with EtOAc/Hex (0 → 20%) and isolated as a colorless oil (146.2 mg, 96% yield).^{1}H NMR (300 MHz, $CDCl_3$) δ 7.56 (d, *J* = 8.8 Hz, 2H), 7.34 – 7.26 (m, 1H), 7.26 – 7.23 (m, 1H), 7.21 – 7.10 (m, 3H), 6.91 (d, *J* = 8.8 Hz, 2H), 5.58 – 5.31 (m, 2H), 3.98 (t, *J* = 6.3 Hz, 2H), 2.64 – 2.52 (m, 2H), 2.26 – 2.16 (m, 2H), 2.12 – 2.01 (m, 2H), 1.91 – 1.80 (m, 2H), 1.71 – 1.59 (m, 2H).^{13}C NMR (126 MHz, $CDCl_3$)

δ 162.4, 142.3, 134.0, 130.9, 128.5, 128.4, 128.3, 125.7, 119.3, 115.2, 103.7, 67.4, 35.5, 31.3, 28.8, 26.8, 23.4. GC/MS (EI) calculated for $[M]^+$ 305.18, found 305.1. FTIR (neat, cm^{-1}): 3024(m), 3004(m), 2934(m), 2856(m), 2224(s), 1605(s), 1508(s), 1452(s), 1302(s), 1258(s), 1171(s), 1112(s), 1029(s).

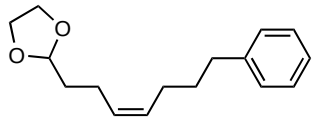

2-[(3*Z*)-7-phenylhept-3-en-1-yl]-1,3-dioxolane (3.19), compound was prepared according to general procedure B. The compound was purified by silica gel chromatography with EtOAc/Hex (0 → 20%) and isolated as a colorless oil (104.4 mg, 85% yield).^{1}H NMR (300 MHz, $CDCl_3$) δ 7.33 – 7.26 (m, 2H), 7.21 – 7.13 (m, 3H), 5.50 – 5.32 (m, 2H), 4.86 (t, *J* = 4.8 Hz, 1H), 4.02 – 3.91 (m, 2H), 3.91 – 3.79 (m, 2H), 2.67 – 2.56 (m, 2H), 2.22 – 2.04 (m, 4H), 1.78 – 1.62 (m, 4H).^{13}C NMR (126 MHz, $CDCl_3$) δ 142.7, 130.2, 129.2, 128.5, 128.4, 125.8, 104.3, 65.0, 35.6, 34.0, 31.5, 26.9, 22.1. GC/MS (EI) calculated for $[M]^+$ 246.16, found 246.2. FTIR (neat, cm^{-1}): 3061(m), 3024(m), 3003(m), 2928(m), 2857(m), 1602(s), 1495(s), 1452(s), 1359(s), 1138(s), 1055(s), 1030(s), 738(s), 699(s).

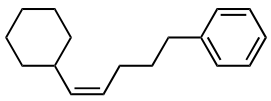

[(4*Z*)-5-cyclohexylpent-4-en-1-yl]benzene (3.20), compound was prepared according to general procedure A. The compound was purified by silica gel chromatography with EtOAc/Hex (0 → 10%) and isolated as a colorless oil (83.7 mg, 73% yield). ^{1}H NMR (300 MHz, $CDCl_3$) δ 7.35 – 7.26 (m, 2H), 7.24 – 7.10 (m, 3H), 5.37 – 5.12 (m, 2H), 2.72 – 2.52 (m, 2H), 2.30 – 2.00 (m, 3H),

1.75 – 1.51 (m, 6H), 1.35 – 0.96 (m, 6H). ^{13}C NMR (126 MHz, $CDCl_3$) δ 142.7, 136.7, 128.6, 128.4, 127.6, 125.8, 110.1, 36.5, 35.6, 33.5, 31.8, 27.2, 26.2, 26.1. GC/MS (EI) calculated for $[M]^+$ 228.19, found 228.2. FTIR (neat, cm^{-1}): 3062(m), 3024(m), 2999(m), 2921(m), 2847(m), 1603(s), 1495(s), 1446(s), 1435(m), 1349(s), 1258(m), 1074(s), 1030(s).

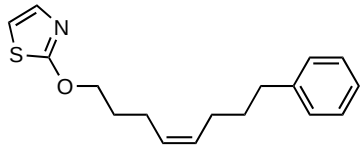

2-{[(4*Z*)-8-phenyloct-4-en-1-yl]oxy}-1,3-thiazole (3.21), compound was prepared according to general procedure A. The compound was purified by silica gel chromatography with EtOAc/Hex (0 → 40%) and isolated as a colorless oil (118.2 mg, 82% yield).^{1}H NMR (300 MHz, $CDCl_3$) δ 7.33 – 7.26 (m, 2H), 7.22 – 7.14 (m, 3H), 7.13 (d, *J* = 3.8 Hz, 1H), 6.67 (d, *J* = 3.8 Hz, 1H), 5.60 – 5.34 (m, 2H), 4.40 (t, *J* = 6.4 Hz, 2H), 2.68 – 2.55 (m, 2H), 2.26 – 2.14 (m, 2H), 2.14 – 2.02 (m, 2H), 1.94 – 1.81 (m, 2H), 1.75 – 1.62 (m, 2H).^{13}C NMR (126 MHz, $CDCl_3$) δ 175.2, 142.5, 137.0, 130.8, 128.6, 128.5, 128.3, 125.7, 110.8, 71.1, 35.5, 31.4, 28.8, 26.9, 23.5. GC/MS (EI) calculated for $[M]^+$ 287.13, found 287.1. FTIR (neat, cm^{-1}): 3003(m), 2931(m), 2855(m), 1523(s), 1461(m), 1380(s), 1308(s), 1236(s), 1162(s), 978(m), 907(m).

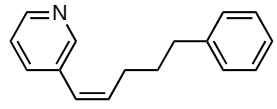

3-[(1*Z*)-5-phenylpent-1-en-1-yl]pyridine (3.22), compound was prepared according to general procedure B. The compound was purified by silica gel chromatography with EtOAc/Hex (0 → 40%) and isolated as a colorless oil (94.6 mg, 85% yield).^{1}H NMR (300 MHz, $CDCl_3$) δ 8.52 (s, 1H), 8.45 (d, *J* = 3.7 Hz, 1H), 7.52 (d, *J* = 7.9 Hz, 1H), 7.25 – 7.09 (m, 5H), 6.39 (d, *J* = 11.7 Hz,

1H), 5.83 (dt, *J* = 11.7, 7.4 Hz, 1H), 2.70 – 2.56 (m, 2H), 2.41 – 2.28 (m, 2H), 1.87 – 1.71 (m, 2H).^{13}C NMR (126 MHz, $CDCl_3$) δ 149.8, 147.4, 142.1, 136.0, 135.2, 133.5, 128.6, 128.5, 126.0, 125.7, 123.3, 35.5, 31.6, 28.2. GC/MS (EI) calculated for $[M]^+$ 223.14, found 223.1. FTIR (neat, cm^{-1}): 3048(m), 3026(m), 2931(m), 2857(m), 1602(s), 1566(s), 1474(s), 1420(s), 1399(s), 1265(s), 1176(s), 1024(s).

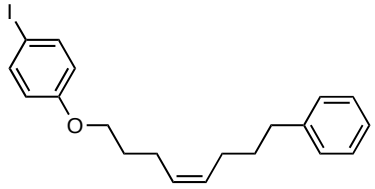

1-iodo-4-{[(4*Z*)-8-phenyloct-4-en-1-yl]oxy}benzene (3.23), compound was prepared according to general procedure B. The compound was purified by silica gel chromatography with EtOAc/Hex (0 → 10%) and isolated as a colorless oil 187.0 mg, 92% yield).^{1}H NMR (300 MHz, $CDCl_3$) δ 7.55 (d, *J* = 8.9 Hz, 2H), 7.32 – 7.27 (m, 2H), 7.23 – 7.11 (m, 3H), 6.67 (d, *J* = 8.9 Hz, 2H), 5.56 – 5.31 (m, 2H), 3.91 (t, *J* = 6.3 Hz, 2H), 2.66 – 2.52 (m, 2H), 2.26 – 2.16 (m, 2H), 2.13 – 2.03 (m, 2H), 1.89 – 1.78 (m, 2H), 1.73 – 1.59 (m, 2H).^{13}C NMR (126 MHz, $CDCl_3$) δ 159.1, 142.5, 138.3, 130.8, 128.9, 128.5, 128.4, 125.8, 117.0, 82.6, 67.2, 35.6, 31.5, 29.1, 27.0, 23.7. GC/MS (EI) calculated for $[M]^+$ 406.08, found 406.1. FTIR (neat, cm^{-1}): 3060(m), 3024(m), 3001(m), 2933(m), 2855(m), 1586(s), 1485(s), 1467(s), 1282(s), 1243(s), 1174(s), 819(s), 698(s).

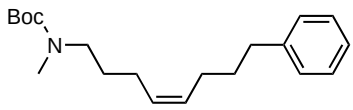

***tert*-butyl N-methyl-N-[(4*Z*)-8-phenyloct-4-en-1-yl]carbamate (3.24),** compound was prepared according to general procedure A. The compound was purified by silica gel chromatography with

EtOAc/Hex (0 → 20%) and isolated as a colorless oil (123.2 mg, 78% yield).^{1}H NMR (300 MHz, $CDCl_3$) δ 7.33 – 7.26 (m, 2H), 7.23 – 7.13 (m, 3H), 5.53 – 5.31 (m, 2H), 3.26 – 3.11 (m, 2H), 2.84 (s, 3H), 2.71 – 2.50 (m, 2H), 2.13 – 1.94 (m, 4H), 1.75 – 1.63 (m, 2H), 1.61 – 1.53 (m, 2H), 1.46 (s, 9H).^{13}C NMR (126 MHz, $CDCl_3$) δ 155.9, 142.5, 130.1, 129.4, 128.5, 128.4, 125.8, 79.2, 48.8, 35.6, 34.2, 31.5, 28.6, 28.6, 26.9, 24.6. GC/MS (EI) calculated for $[M]^+$ 317.24, found 317.2. FTIR (neat, cm^{-1}): 3062(m), 3005(m), 2974(m), 2929(m), 2858(m), 1695(s), 1479(s), 1391(s), 1365(s), 1303(s), 1166(s), 879(s), 754(s).

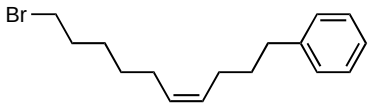

[(4*Z*)-10-bromodec-4-en-1-yl]benzene (3.25), compound was prepared according to general procedure A. The compound was purified by silica gel chromatography with EtOAc/Hex (0 → 10%) and isolated as a colorless oil (96.9 mg, 66% yield).^{1}H NMR (300 MHz, $CDCl_3$) δ 7.36 – 7.26 (m, 2H), 7.22 – 7.12 (m, 3H), 5.49 – 5.29 (m, 2H), 3.40 (t, *J* = 6.8 Hz, 2H), 2.69 – 2.55 (m, 2H), 2.12 – 1.97 (m, 4H), 1.92 – 1.79 (m, 2H), 1.75 – 1.61 (m, 2H), 1.47 – 1.33 (m, 4H).^{13}C NMR (126 MHz, $CDCl_3$) δ 142.6, 130.0, 129.9, 128.6, 128.4, 125.8, 35.6, 34.0, 32.9, 31.6, 29.0, 28.0, 27.2, 27.0. GC/MS (EI) calculated for $[M]^+$ 294.10, found 294.1. FTIR (neat, cm^{-1}): 3060(m), 3002(m), 2930(m), 2855(m), 1602(s), 1495(s), 1452(s), 970(s).

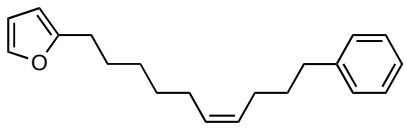

2-[(6*Z*)-10-phenyldec-6-en-1-yl]furan (3.26), compound was prepared according to general procedure A. The compound was purified by silica gel chromatography with EtOAc/Hex (0 →

20%) and isolated as a colorless oil (127.3 mg, 90% yield).^{1}H NMR (300 MHz, $CDCl_3$) δ 7.33 – 7.26 (m, 3H), 7.23 – 7.14 (m, 3H), 6.28 (dd, *J* = 2.9, 2.0 Hz, 1H), 6.00 – 5.95 (m, 1H), 5.47 – 5.32 (m, 2H), 2.62 (t, *J* = 7.6 Hz, 4H), 2.13 – 1.97 (m, 4H), 1.73 – 1.60 (m, 4H), 1.41 – 1.32 (m, 4H).^{13}C NMR (126 MHz, $CDCl_3$) δ 156.3, 142.4, 140.5, 130.1, 129.3, 128.3, 128.1, 125.5, 109.9, 104.4, 35.3, 31.3, 29.3, 28.7, 27.8, 27.0, 26.7. GC/MS (EI) calculated for $[M]^+$ 282.20, found 282.1. FTIR (neat, cm^{-1}): 3025(m), 3002(m), 2928(m), 2855(m), 1655(m), 1597(s), 1507(s), 1460(s), 1350(w), 1147(s), 1079(s), 1007(s), 920(m), 796(s).

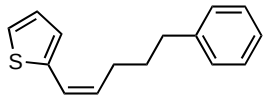

2-[(1*Z*)-5-phenylpent-1-en-1-yl]thiophene (3.27), compound was prepared according to general procedure B. The compound was purified by silica gel chromatography with EtOAc/Hex (0 → 20%) and isolated as a colorless oil (107.4 mg, 94% yield).^{1}H NMR (300 MHz, $CDCl_3$) δ 7.34 – 7.26 (m, 3H), 7.24 – 7.14 (m, 3H), 7.10 (d, *J* = 2.3 Hz, 1H), 7.07 (d, *J* = 5.0 Hz, 1H), 6.40 (d, *J* = 11.6 Hz, 1H), 5.65 (dt, *J* = 11.6, 7.3 Hz, 1H), 2.79 – 2.57 (m, 2H), 2.41 (q, *J* = 7.3 Hz, 2H), 1.91 – 1.73 (m, 2H).^{13}C NMR (126 MHz, $CDCl_3$) δ 142.4, 138.9, 131.7, 128.7, 128.6, 128.4, 125.9, 125.0, 123.5, 122.8, 35.7, 31.6, 28.7. GC/MS (EI) calculated for $[M]^+$ 228.10, found 228.1. FTIR (neat, cm^{-1}): 3061(m), 3024(m), 2923(m), 2855(m), 1602(s), 1494(s), 1452(s), 1350(s), 1251(m), 1149(s), 1080(s), 1029(s).

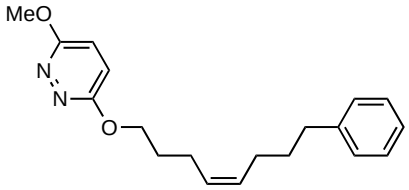

3-methoxy-6-{[(4*Z*)-8-phenyloct-4-en-1-yl]oxy}pyridazine (3.28), compound was prepared according to general procedure A. The compound was purified by silica gel chromatography with EtOAc/Hex (0 → 40%) and isolated as a colorless oil (118.6 mg, 76% yield).^{1}H NMR (300 MHz, $CDCl_3$) δ 7.30 – 7.26 (m, 1H), 7.26 – 7.22 (m, 1H), 7.21 – 7.11 (m, 3H), 6.98 – 6.79 (m, 2H), 5.57 – 5.26 (m, 2H), 4.40 (t, *J* = 6.5 Hz, 2H), 4.04 (s, 3H), 2.66 – 2.52 (m, 2H), 2.25 – 2.13 (m, 2H), 2.13 – 2.00 (m, 2H), 1.92 – 1.81 (m, 2H), 1.75 – 1.57 (m, 2H).^{13}C NMR (75 MHz, $CDCl_3$) δ 162.0, 161.9, 142.6, 130.5, 129.1, 128.5, 128.4, 125.8, 121.6, 121.4, 66.7, 54.6, 35.6, 31.5, 28.9, 26.9, 23.8. GC/MS (EI) calculated for $[M]^+$ 312.18, found 312.2. FTIR (neat, cm^{-1}): 3005(m), 2936(m), 2856(m), 1696(s), 1602(s), 1463(m), 1421(s), 1383(s), 1267(s), 1015(s), 838(s), 750(s), 699(s).

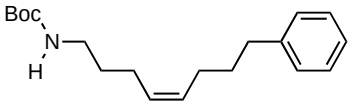

***tert*-butyl N-[(4*Z*)-8-phenyloct-4-en-1-yl]carbamate (3.29),** compound was prepared according to general procedure A. The compound was purified by silica gel chromatography with EtOAc/Hex (0 → 50%) and isolated as a colorless oil (109.7 mg, 72% yield).^{1}H NMR (300 MHz, $CDCl_3$) δ 7.34 – 7.26 (m, 2H), 7.24 – 7.10 (m, 3H), 5.53 – 5.24 (m, 2H), 4.49 (s, 1H), 3.22 – 2.95 (m, 2H), 2.69 – 2.53 (m, 2H), 2.15 – 1.96 (m, 4H), 1.74 – 1.61 (m, 2H), 1.56 – 1.50 (m, 2H), 1.45 (s, 9H).^{13}C NMR (126 MHz, $CDCl_3$) δ 170.4, 142.6, 130.4, 129.2, 128.5, 128.4, 125.8, 79.2, 40.4, 35.6, 31.5, 30.1, 28.6, 26.9, 24.7. GC/MS (EI) calculated for $[M]^+$ 303.22, found 303.1. FTIR (neat,

cm^{-1}): 3438(b), 3355(b), 3005(m), 2927(m), 2857(m), 2247(s), 1694(s), 1524(s), 1455(s), 1363(s), 1250(m), 1168(m), 1030(m), 910(s), 852(m).

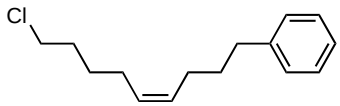

[(4*Z*)-9-chlorononon-4-en-1-yl]benzene (3.30), compound was prepared according to general procedure A. The compound was purified by silica gel chromatography with EtOAc/Hex (0 → 10%) and isolated as a colorless oil (109.6 mg, 93% yield).^{1}H NMR (300 MHz, $CDCl_3$) δ 7.35 – 7.26 (m, 2H), 7.24 – 7.13 (m, 3H), 5.54 – 5.25 (m, 2H), 3.53 (t, *J* = 6.7 Hz, 2H), 2.72 – 2.51 (m, 2H), 2.17 – 1.95 (m, 4H), 1.83 – 1.63 (m, 4H), 1.53 – 1.41 (m, 2H).^{13}C NMR (126 MHz, $CDCl_3$) δ 142.5, 130.2, 129.5, 128.5, 128.4, 125.8, 45.0, 35.5, 32.2, 31.5, 27.0, 26.9, 26.5. GC/MS (EI) calculated for $[M]^+$ 236.13, found 236.1. FTIR (neat, cm^{-1}): 3061(m), 3002(m), 2925(m), 2855(m), 1602(s), 1494(s), 1452(s), 1433(s), 1309(s), 1275(m), 1029(s).

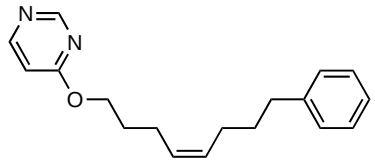

4-{[(4*Z*)-8-phenyloct-4-en-1-yl]oxy}pyrimidine (3.31), compound was prepared according to general procedure A. The compound was purified by silica gel chromatography with EtOAc/Hex (0 → 40%) and isolated as a colorless oil (112.8 mg, 80% yield).^{1}H NMR (300 MHz, $CDCl_3$) δ 8.75 (s, 1H), 8.40 (d, *J* = 5.8 Hz, 1H), 7.32 – 7.27 (m, 1H), 7.25 – 7.21 (m, 1H), 7.20 – 7.12 (m, 3H), 6.70 (dd, *J* = 5.8, 1.1 Hz, 1H), 5.57 – 5.27 (m, 2H), 4.35 (t, *J* = 6.6 Hz, 2H), 2.65 – 2.54 (m, 2H), 2.24 – 2.12 (m, 2H), 2.12 – 2.01 (m, 2H), 1.88 – 1.77 (m, 2H), 1.74 – 1.60 (m, 2H).^{13}C NMR (126 MHz, $CDCl_3$) δ 169.4, 158.9, 157.3, 142.8, 131.0, 129.1, 128.8, 128.7, 126.1, 109.1, 66.3,

35.8, 31.7, 29.0, 27.2, 23.9. GC/MS (EI) calculated for $[M]^+$ 282.17, found 282.1. FTIR (neat, cm^{-1}): 3005(m), 2933(m), 2856(m), 1582(s), 1560(s), 1470(s), 1462(s), 1396(s), 1374(s), 1305(s), 1163(m), 985(s), 834(s), 733(s).

3.3.9 *Characterization of Z-Selective Hydroalkylation Products: Alkylboranes*

Alkylboranes were used as a 2M solution in toluene and were synthesized according to literature procedure the day before use.[57]

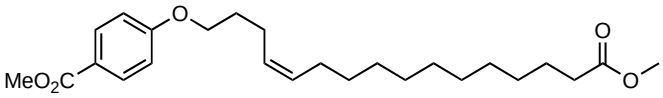

methyl 4-{[(4*Z*)-16-methoxy-16-oxohexadec-4-en-1-yl]oxy}benzoate (3.32), compound was prepared according to general procedure A. The compound was purified by silica gel chromatography with EtOAc/Hex (0 → 30%) and isolated as a colorless oil (163.3 mg, 78% yield).^{1}H NMR (300 MHz, $CDCl_3$) δ 7.97 (d, *J* = 8.9 Hz, 2H), 6.90 (d, *J* = 8.9 Hz, 2H), 5.52 – 5.27 (m, 2H), 4.00 (t, *J* = 6.4 Hz, 2H), 3.88 (s, 3H), 3.66 (s, 3H), 2.30 (t, *J* = 7.6 Hz, 2H), 2.25 – 2.15 (m, 2H), 2.06 – 1.95 (m, 2H), 1.89 – 1.81 (m, 2H), 1.64 – 1.57 (m, 2H), 1.36 – 1.14 (m, 16H).^{13}C NMR (126 MHz, $CDCl_3$) δ 174.4, 166.9, 163.0, 131.6, 131.5, 128.1, 122.4, 114.1, 67.3, 51.9, 51.5, 42.0, 34.2, 29.8, 29.6, 29.5, 29.4, 29.2, 29.1, 27.3, 27.2, 25.0, 23.5. GC/MS (EI) calculated for $[M]^+$ 418.27, found 418.3. FTIR (neat, cm^{-1}): 2998(m), 2925(m), 2853(m), 1726(s), 1720(s), 1605(s), 1511(s), 1434(s), 1279(s), 1253(s), 1167(s), 1104(s), 1024(m), 913(s).

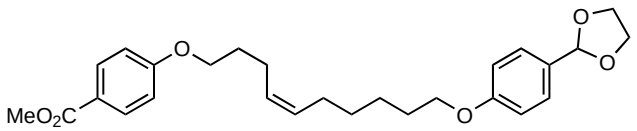

methyl 4-{[(4*Z*)-10-[4-(1,3-dioxolan-2-yl)phenoxy]dec-4-en-1-yl]oxy}benzoate (3.33), compound was prepared according to general procedure A. The compound was purified by silica gel chromatography with EtOAc/Hex (0 → 30%) and isolated as a colorless oil (153.2 mg, 67% yield).^{1}H NMR (300 MHz, $CDCl_3$) δ 7.97 (d, *J* = 8.8 Hz, 2H), 7.38 (d, *J* = 8.6 Hz, 2H), 6.96 – 6.80 (m, 84), 5.75 (s, 1H), 5.50 – 5.30 (m, 2H), 4.17 – 4.05 (m, 2H), 4.03 – 3.98 (m, 2H), 3.92 (t, *J* = 6.5 Hz, 2H), 3.87 (s, 3H), 2.29 – 2.17 (m, 2H), 2.10 – 1.99 (m, 2H), 1.91 – 1.79 (m, 2H), 1.76 – 1.68 (m, 2H), 1.47 – 1.32 (m, 4H).^{13}C NMR (126 MHz, $CDCl_3$) δ 166.9, 163.0, 160.0, 131.6, 131.1, 128.5, 127.9, 122.5, 114.4, 114.1, 103.8, 68.0, 67.3, 65.3, 51.9, 41.9, 29.5, 29.2, 29.0, 27.2, 25.7, 23.6. GC/MS (ESI) calculated for $[M+H]^+$ 455.24, found 455.2. FTIR (neat, cm^{-1}): 3006(m), 2945(m), 2864(m), 1919(w), 1720(s), 1605(s), 1511(s), 1435(s), 1393(s), 1252(m), 1168(s), 912(m), 847(s).

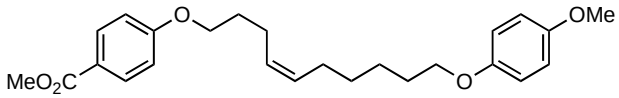

methyl 4-{[(4*Z*)-10-(4-methoxyphenoxy)dec-4-en-1-yl]oxy}benzoate (3.34), compound was prepared according to general procedure A. The compound was purified by silica gel chromatography with EtOAc/Hex (0 → 30%) and isolated as a colorless oil (178.6 mg, 87% yield). ^{1}H NMR (300 MHz, $CDCl_3$) δ 7.97 (d, *J* = 8.9 Hz, 2H), 6.90 (d, *J* = 8.9 Hz, 2H), 6.82 (s, 4H), 5.51 – 5.32 (m, 2H), 4.00 (t, *J* = 6.3 Hz, 2H), 3.91 – 3.82 (m, 5H), 3.76 (s, 3H), 2.29 – 2.18 (m, 2H), 2.05 (q, *J* = 6.5 Hz, 2H), 1.92 – 1.80 (m, 2H), 1.78 – 1.65 (m, 2H), 1.48 – 1.32 (m, 4H). ^{13}C NMR (126 MHz, $CDCl_3$) δ 167.0, 163.0, 153.8, 153.4, 131.7, 131.2, 128.5, 122.5, 115.5, 114.7, 114.2,

68.6, 67.3, 55.8, 51.9, 29.5, 29.4, 29.1, 27.2, 25.8, 23.6. GC/MS (EI) calculated for $[M]^+$ 412.22, found 412.2. FTIR (neat, cm^{-1}): 3053(m), 2986(m), 1711(s), 1606(s), 1502(s), 1421(s), 1262(s), 1169(s), 895(s), 738(s).

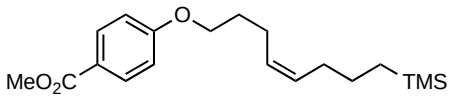

methyl 4-{[(4*Z*)-8-(trimethylsilyl)oct-4-en-1-yl]oxy}benzoate (3.35), compound was prepared according to general procedure A. The compound was purified by silica gel chromatography with EtOAc/Hex (0 → 30%) and isolated as a colorless oil (139.0 mg, 83% yield). ^{1}H NMR (300 MHz, $CDCl_3$) δ 7.98 (d, *J* = 8.8 Hz, 1H), 6.90 (d, *J* = 8.8 Hz, 1H), 5.49 – 5.32 (m, 1H), 4.01 (t, *J* = 6.4 Hz, 1H), 3.88 (s, 1H), 2.32 – 2.16 (m, 1H), 2.10 – 1.97 (m, 1H), 1.86 (p, *J* = 6.7 Hz, 1H), 1.37 – 1.23 (m, 1H), 0.56 – 0.39 (m, 1H), -0.05 (s, 4H). ^{13}C NMR (126 MHz, $CDCl_3$) δ 142.7, 130.2, 129.2, 128.5, 128.4, 125.8, 104.3, 65.0, 35.6, 34.0, 31.5, 26.9, 22.1. GC/MS (EI) calculated for $[M]^+$ 334.20, found 334.2. FTIR (neat, cm^{-1}): 3003(m), 2950(m), 2873(m), 1914(w), 1721(s), 1606(s), 1511(s), 1434(s), 1279(m), 1254(m), 1167(s), 1104(s), 969(s), 844(s).

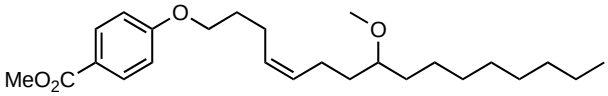

methyl 4-{[(4*Z*)-8-methoxyhexadec-4-en-1-yl]oxy}benzoate (3.36), compound was prepared according to general procedure A. The compound was purified by silica gel chromatography with EtOAc/Hex (0 → 30%) and isolated as a colorless oil (182.8 mg, 90% yield). ^{1}H NMR (300 MHz, $CDCl_3$) δ 7.97 (d, *J* = 8.8 Hz, 2H), 6.90 (d, *J* = 8.8 Hz, 2H), 5.54 – 5.26 (m, 2H), 4.01 (t, *J* = 6.4 Hz, 2H), 3.88 (s, 3H), 3.29 (s, 3H), 3.18 – 3.01 (m, 1H), 2.32 – 2.16 (m, 2H), 2.15 – 2.01 (m, 2H), 1.86 (p, *J* = 6.8 Hz, 2H), 1.54 – 1.35 (m, 4H), 1.27 (s, 12H), 0.88 (t, *J* = 6.6 Hz, 3H). ^{13}C NMR

(126 MHz, $CDCl_3$) δ 167.0, 163.0, 131.7, 131.0, 128.5, 122.5, 114.1, 80.4, 67.4, 56.4, 51.9, 33.5, 33.4, 32.0, 30.0, 29.7, 29.4, 29.1, 25.3, 23.6, 23.1, 22.8, 14.2. GC/MS (EI) calculated for $[M]^+$ 404.29, found 404.3. FTIR (neat, cm^{-1}):3004(m), 2927(m), 2854(m), 1913(w), 1719(s), 1606(s), 1511(s), 1434(s), 1280(s), 1253(s), 1167(s), 1103(s), 1037(m), 970(s), 846(s), 757(s).

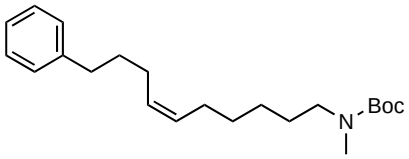

***tert*-butyl N-methyl-N-[(6*Z*)-10-phenyldec-6-en-1-yl]carbamate (3.37),** compound was prepared according to general procedure A. The compound was purified by silica gel chromatography with EtOAc/Hex (0 → 30%) and isolated as a colorless oil (As determined by NMR, 64% yield). ^1H NMR (300 MHz, $CDCl_3$) δ 7.31 – 7.26 (m, 1H), 7.26 – 7.22 (m, 1H), 7.20 – 7.13 (m, 3H), 5.50 – 5.27 (m, 2H), 3.18 (t, *J* = 7.1 Hz, 2H), 2.82 (s, 3H), 2.68 – 2.56 (m, 2H), 2.15 – 1.91 (m, 4H), 1.74 – 1.61 (m, 2H), 1.50 – 1.43 (m, 11H), 1.36 – 1.24 (m, 4H). ^{13}C NMR (126 MHz, $CDCl_3$) δ 156.0, 142.7, 130.3, 129.6, 128.6, 128.4, 125.8, 79.2, 48.9, 35.6, 34.2, 32.2, 31.6, 29.6, 28.6, 27.4, 27.0, 26.5. GC/MS (EI) calculated for $[M]^+$ 345.27, found 345.3. FTIR (neat, cm^{-1}): 3084(w), 3062(w), 3025(m), 3003(m), 2929(s) 2858(s), 1696(s), 1480(m), 1453(m), 1394(s), 1365(s), 1308(m), 1247(m), 1215(m), 1161(s).

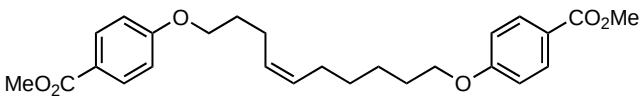

methyl 4-{[(4*Z*)-10-[4-(methoxycarbonyl)phenoxy]dec-4-en-1-yl]oxy}benzoate (3.38), compound was prepared according to general procedure A. The compound was purified by silica gel chromatography with EtOAc/Hex (0 → 30%) and isolated as a colorless oil (198.4 mg, 90%

yield). ^{1}H NMR (300 MHz, $CDCl_3$) δ 7.97 (d, *J* = 8.7 Hz, 4H), 6.95 – 6.80 (m, 4H), 5.51 – 5.31 (m, 2H), 4.04 – 3.92 (m, 4H), 3.88 (s, 3H), 3.87 (s, 3H), 2.31 – 2.16 (m, 2H), 2.05 (q, *J* = 6.4 Hz, 2H), 1.93 – 1.80 (m, 2H), 1.80 – 1.67 (m, 2H), 1.45 – 1.29 (m, 4H). ^{13}C NMR (126 MHz, $CDCl_3$) δ 166.8, 166.8, 162.9, 162.9, 131.6, 130.9, 128.5, 122.4, 122.3, 114.0, 68.0, 67.1, 51.8, 29.4, 29.0, 28.9, 27.1, 25.6, 23.5. GC/MS (EI) calculated for $[M]^+$ 440.22, found 440.3. FTIR (neat, cm^{-1}): 3002(m), 2946(m), 2857(m), 1716(s), 1606(s), 1511(s), 1434(s), 1280(s), 1254(s), 1168(s), 1104(s), 1010(m), 970(m).

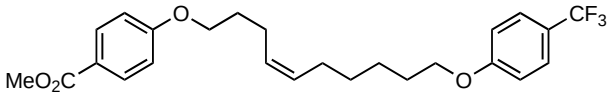

methyl 4-{[(4*Z*)-10-[4-(trifluoromethyl)phenoxy]dec-4-en-1-yl]oxy}benzoate (3.39), compound was prepared according to general procedure A. The compound was purified by silica gel chromatography with EtOAc/Hex (0 → 30%) and isolated as a colorless oil (181.2 mg, 80% yield). ^{1}H NMR (300 MHz, $CDCl_3$) δ 7.97 (d, *J* = 8.6 Hz, 2H), 7.52 (d, *J* = 8.7 Hz, 2H), 7.05 – 6.70 (m, 4H), 5.50 – 5.31 (m, 2H), 4.00 (t, *J* = 6.3 Hz, 2H), 3.94 (t, *J* = 6.5 Hz, 2H), 3.87 (s, 3H), 2.33 – 2.16 (m, 2H), 2.12 – 1.97 (m, 2H), 1.94 – 1.80 (m, 2H), 1.80 – 1.65 (m, 2H), 1.47 – 1.30 (m, 4H). ^{13}C NMR (126 MHz, $CDCl_3$) δ 166.9, 163.0, 161.7, 131.7, 131.0, 128.6, 126.9 (q, *J* = 3.7 Hz), 124.6 (q, *J* = 271.0 Hz), 122.7 (q, *J* =32.8 Hz), 122.5, 114.5, 114.1, 68.2, 67.3, 51.9, 29.5, 29.1, 29.0, 27.2, 25.7, 23.6. ^{19}F NMR (470 MHz, $CDCl_3$) δ -64.4. GC/MS (EI) calculated for $[M]^+$ 450.20, found 450.3. FTIR (neat, cm^{-1}): 3005(m), 2942(m), 2858(m), 1716(s), 1606(s), 1511(s), 1435(s), 1329(s), 1255(s), 1168(s), 1112(m), 1067(s), 1009(s), 836(s).

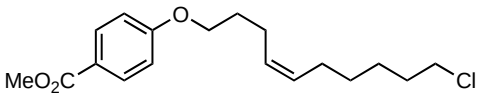

methyl 4-{[(4*Z*)-10-chlorodec-4-en-1-yl]oxy}benzoate (3.40), compound was prepared according to general procedure A. The compound was purified by silica gel chromatography with EtOAc/Hex (0 → 30%) and isolated as a colorless oil (123.1 mg, 76% yield). ^{1}H NMR (300 MHz, $CDCl_3$) δ 7.98 (d, *J* = 8.9 Hz, 2H), 6.90 (d, *J* = 8.9 Hz, 2H), 5.49 – 5.32 (m, 2H), 4.00 (t, *J* = 6.3 Hz, 2H), 3.88 (s, 3H), 3.49 (t, *J* = 6.7 Hz, 2H), 2.30 – 2.15 (m, 2H), 2.09 – 1.96 (m, 2H), 1.93 – 1.79 (m, 2H), 1.78 – 1.63 (m, 2H), 1.42 – 1.26 (m, 4H). ^{13}C NMR (126 MHz, $CDCl_3$) δ 166.9, 162.9, 131.6, 130.9, 128.6, 122.5, 114.1, 67.2, 51.8, 45.0, 32.5, 29.0, 27.1, 26.6, 23.5. GC/MS (EI) calculated for $[M]^+$ 324.15, found 324.2. FTIR (neat, cm^{-1}): 3003(m), 2934(m), 2856(m), 1919(w), 1719(s), 1605(s), 1511(s), 1433(s), 1253(s), 1167(s), 1104(m), 846(s), 770(s).

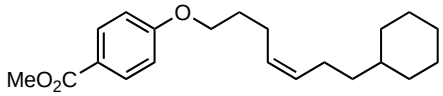

methyl 4-{[(4*Z*)-7-cyclohexylhept-4-en-1-yl]oxy}benzoate (3.41), compound was prepared according to general procedure A. The compound was purified by silica gel chromatography with EtOAc/Hex (0 → 30%) and isolated as a colorless oil (155.2 mg, 94% yield). ^{1}H NMR (300 MHz, $CDCl_3$) δ 7.98 (d, *J* = 8.8 Hz, 2H), 6.90 (d, *J* = 8.8 Hz, 2H), 5.50 – 5.26 (m, 2H), 4.00 (t, *J* = 6.3 Hz, 2H), 3.88 (s, 3H), 2.23 (q, *J* = 7.1 Hz, 2H), 2.09 – 1.94 (m, 2H), 1.85 (p, *J* = 6.8 Hz, 2H), 1.74 – 1.57 (m, 5H), 1.29 – 1.07 (m, 6H), 0.94 – 0.71 (m, 2H). ^{13}C NMR (75 MHz, $CDCl_3$) δ 167.0, 163.0, 131.8, 131.7, 128.0, 122.5, 114.2, 67.4, 51.9, 37.6, 37.4, 33.4, 29.1, 26.8, 26.5, 24.7, 23.6. GC/MS (EI) calculated for $[M]^+$ 330.22, found 330.2. FTIR (neat, cm^{-1}): 3003(m), 2919(m), 2848(m), 1914(w), 1720(s), 1605(s), 1511(s), 1435(m), 1252(s), 1167(s), 971(m) 845(s), 770(s).

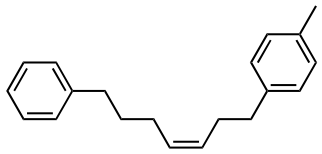

1-methyl-4-[(3*Z*)-7-phenylhept-3-en-1-yl]benzene (3.42), compound was prepared according to general procedure B. The compound was purified by silica gel chromatography with EtOAc/Hex (0 → 10%) and isolated as a colorless oil (123.8 mg, 94% yield). ^{1}H NMR (300 MHz, $CDCl_3$) δ 7.32 – 7.23 (m, 3H), 7.23 – 7.12 (m, 3H), 7.12 – 6.34 (m, 4H), 5.52 – 5.32 (m, 2H), 2.67 – 2.51 (m, 4H), 2.39 – 2.26 (m, 5H), 2.10 – 1.95 (m, 2H), 1.69 – 1.56 (m, 2H). ^{13}C NMR (126 MHz, $CDCl_3$) δ 142.6, 139.1, 135.3, 130.1, 129.4, 129.1, 128.5, 128.5, 128.4, 125.8, 35.7, 35.6, 31.5, 29.5, 27.0, 21.1. GC/MS (EI) calculated for $[M]^+$ 264.19, found 264.2. FTIR (neat, cm^{-1}): 3060(m), 3005(m), 2932(s), 2855(m), 1622(m), 1537(s), 1454(s), 1375(m) 1285(s), 1007(s), 909(m), 739(s).

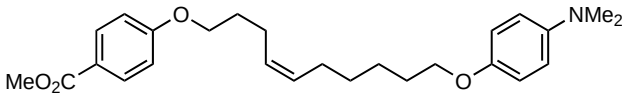

methyl 4-{[(4*Z*)-10-[4-(dimethylamino)phenoxy]dec-4-en-1-yl]oxy}benzoate (3.43), compound was prepared according to general procedure A. The compound was purified by silica gel chromatography with EtOAc/Hex (0 → 40%) and isolated as a colorless oil (189.7 mg, 89% yield). ^{1}H NMR (300 MHz, $CDCl_3$) δ 7.97 (d, *J* = 8.9 Hz, 2H), 6.90 (d, *J* = 8.9 Hz, 2H), 6.82 (d, *J* = 9.1 Hz, 2H), 6.73 (d, *J* = 9.1 Hz, 2H), 5.49 – 5.33 (m, 2H), 4.00 (t, *J* = 6.3 Hz, 2H), 3.95 – 3.77 (m, 5H), 2.86 (s, 6H), 2.31 – 2.16 (m, 2H), 2.11 – 1.97 (m, 2H), 1.92 – 1.76 (m, 2H), 1.76 – 1.63 (m, 2H), 1.47 – 1.31 (m, 4H). ^{13}C NMR (126 MHz, $CDCl_3$) δ 166.9, 163.0, 151.5, 145.8, 131.6, 131.1, 128.4, 122.4, 115.5, 114.9, 114.1, 68.6, 67.3, 51.8, 41.9, 29.5, 29.4, 29.1, 27.2, 25.8, 23.6. GC/MS (EI) calculated for $[M]^+$ 425.26, found 425.3. FTIR (neat, cm^{-1}): 3000(m), 2938(m),

2857(m), 2793(m), 1715(s), 1605(s), 1513(s), 1434(s), 1280(s), 1253(m), 1168(s), 1104(s), 1051(m), 856(s), 816(s).

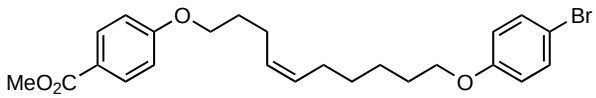

methyl 4-{[(4*Z*)-10-(4-bromophenoxy)dec-4-en-1-yl]oxy}benzoate (3.44), compound was prepared according to general procedure A. The compound was purified by silica gel chromatography with EtOAc/Hex (0 → 30%) and isolated as a colorless oil (177.3 mg, 77% yield). ^{1}H NMR (300 MHz, $CDCl_3$) δ 7.97 (d, *J* = 8.7 Hz, 2H), 7.35 (d, *J* = 8.8 Hz, 2H), 6.89 (d, *J* = 8.7 Hz, 2H), 6.75 (d, *J* = 8.8 Hz, 2H), 5.49 – 5.32 (m, 2H), 4.00 (t, *J* = 6.3 Hz, 2H), 3.94 – 3.77 (m, 5H), 2.31 – 2.17 (m, 2H), 2.05 (q, *J* = 6.2 Hz, 2H), 1.86 (p, *J* = 6.6 Hz, 2H), 1.78 – 1.63 (m, 2H), 1.47 – 1.30 (m, 4H). ^{13}C NMR (126 MHz, $CDCl_3$) δ 167.0, 163.0, 158.3, 132.3, 131.7, 131.1, 128.6, 122.5, 116.4, 114.2, 112.7, 68.2, 67.3, 52.0, 29.5, 29.2, 29.1, 27.2, 25.8, 23.6. GC/MS (EI) calculated for $[M]^+$ 460.12, found 460.1. FTIR (neat, cm^{-1}): 3003(m), 2940(m), 2857(m), 1716(s), 1605(s), 1510(s), 1488(s), 1282(m), 1253(m), 1168(s), 1104(s), 1002(s), 847(s), 738(s).

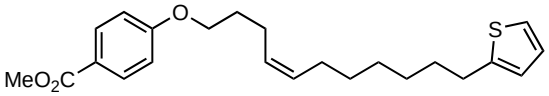

methyl 4-{[(4*Z*)-11-(thiophen-2-yl)undec-4-en-1-yl]oxy}benzoate (3.45), compound was prepared according to general procedure A. The compound was purified by silica gel chromatography with EtOAc/Hex (0 → 30%) and isolated as a colorless oil (150.1 mg, 78% yield). ^{1}H NMR (300 MHz, $CDCl_3$) δ 7.98 (d, *J* = 8.9 Hz, 2H), 7.10 (dd, *J* = 5.1, 1.0 Hz, 1H), 6.99 – 6.83 (m, 3H), 6.80 – 6.71 (m, 1H), 5.53 – 5.28 (m, 2H), 4.00 (t, *J* = 6.3 Hz, 2H), 3.88 (s, 3H), 2.79 (t, *J* = 7.6 Hz, 2H), 2.31 – 2.15 (m, 2H), 2.08 – 1.93 (m, 2H), 1.85 (p, *J* = 6.7 Hz, 2H), 1.72 – 1.58 (m,

2H), 1.37 – 1.22 (m, 6H). ^{13}C NMR (126 MHz, $CDCl_3$) δ 166.9, 162.9, 145.7, 131.6, 131.3, 128.2, 126.7, 123.9, 122.7, 122.4, 114.1, 67.2, 51.8, 31.8, 29.9, 29.6, 29.0, 29.0, 27.2, 23.5. GC/MS (EI) calculated for $[M]^+$ 386.19, found 386.2. FTIR (neat, cm^{-1}): 3002(m), 2928(m), 2853(m), 1720(s), 1605(s), 1510(s), 1434(s), 1253(s), 1167(s), 1104(s), 969(m), 846(s), 770(s), 695(s).

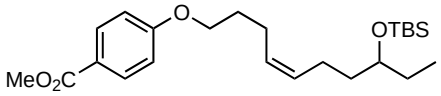

methyl 4-{[(4*Z*)-8-[(*tert*-butyldimethylsilyl)oxy]dec-4-en-1-yl]oxy}benzoate (3.46), compound was prepared according to general procedure A. The compound was purified by silica gel chromatography with EtOAc/Hex (0 → 30%) and isolated as a colorless oil (190.4 mg, 91% yield). ^{1}H NMR (300 MHz, $CDCl_3$) δ 7.97 (d, *J* = 8.7 Hz, 2H), 6.90 (d, *J* = 8.7 Hz, 2H), 5.51 – 5.30 (m, 2H), 4.00 (t, *J* = 6.4 Hz, 2H), 3.88 (s, 3H), 3.56 (p, *J* = 5.6 Hz, 1H), 2.29 – 2.17 (m, 2H), 2.18 – 1.91 (m, 2H), 1.86 (p, *J* = 6.7 Hz, 2H), 1.50 – 1.37 (m, 4H), 0.91 – 0.80 (m, 12H), 0.03 (s, 6H). ^{13}C NMR (126 MHz, $CDCl_3$) δ 166.9, 163.0, 131.6, 131.2, 128.3, 122.5, 114.1, 73.1, 67.3, 51.8, 36.6, 29.7, 29.1, 26.0, 23.6, 23.3, 18.2, 9.6, -4.3, -4.4. GC/MS (EI) calculated for $[M]^+$ 420.27, found 420.2. FTIR (neat, cm^{-1}):3005(m), 2953(m), 2855(m), 1914(w), 1721(s), 1606(s), 1511(s), 1435(m), 1253(m), 1167(s), 1103(m), 1050(m), 835(m), 770(s).

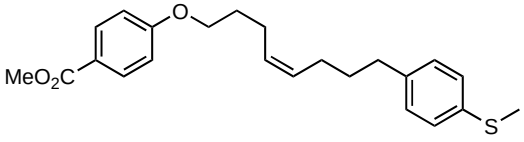

methyl 4-{[(4*Z*)-8-[4-(methylsulfanyl)phenyl]oct-4-en-1-yl]oxy}benzoate (3.47), compound was prepared according to general procedure A. The compound was purified by silica gel chromatography with EtOAc/Hex (0 → 30%) and isolated as a colorless oil (161.0 mg, 84% yield).

^{1}H NMR (300 MHz, $CDCl_3$) δ 7.98 (d, *J* = 8.7 Hz, 2H), 7.17 (d, *J* = 8.1 Hz, 2H), 7.04 (d, *J* = 8.1 Hz, 2H), 6.89 (d, *J* = 8.7 Hz, 2H), 5.51 – 5.33 (m, 2H), 3.99 (t, *J* = 6.3 Hz, 2H), 3.88 (s, 3H), 2.58 – 2.47 (m, 2H), 2.46 (s, 3H), 2.27 – 2.14 (m, 2H), 2.12 – 1.99 (m, 2H), 1.92 – 1.77 (m, 2H), 1.68 – 1.57 (m, 2H). ^{13}C NMR (126 MHz, $CDCl_3$) δ 166.9, 163.0, 139.6, 135.2, 131.7, 130.8, 129.0, 128.8, 127.2, 122.5, 114.1, 67.3, 51.9, 35.0, 31.4, 29.0, 26.8, 23.6, 16.4. GC/MS (EI) calculated for $[M]^+$ 384.18, found 384.2. FTIR (neat, cm^{-1}): 3003(m), 2921(m), 2855(m), 1913(w), 1716(s), 1604(s), 1511(s), 1498(s), 1435(s), 1253(s), 1167(s), 1103(s), 1016(m), 835(s).

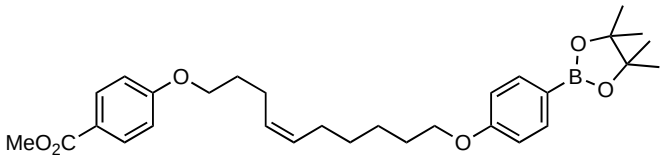

methyl 4-{[(4*Z*)-10-[4-(4,4,5,5-tetramethyl-1,3,2-dioxaborolan-2-yl)phenoxy]dec-4-en-1-yl]oxy}benzoate (3.48), compound was prepared according to general procedure A. The compound was purified by silica gel chromatography with EtOAc/Hex (0 → 50%) and isolated as a colorless oil (198.7 mg, 78% yield). ^{1}H NMR (300 MHz, $CDCl_3$) δ 7.97 (d, *J* = 8.8 Hz, 2H), 7.73 (d, *J* = 8.5 Hz, 2H), 6.93 – 6.82 (m, 4H), 5.50 – 5.31 (m, 2H), 4.00 (t, *J* = 6.3 Hz, 2H), 3.94 (t, *J* = 6.5 Hz, 2H), 3.87 (s, 3H), 2.30 – 2.18 (m, 2H), 2.09 – 2.00 (m, 2H), 1.90 – 1.83 (m, 2H), 1.79 – 1.68 (m, 2H), 1.48 – 1.29 (m, 16H). ^{13}C NMR (126 MHz, $CDCl_3$) δ 166.9, 163.0, 161.8, 136.5, 131.6, 131.1, 128.5, 122.5, 114.1, 113.9, 83.6, 67.7, 67.3, 51.9, 42.0, 29.5, 29.12, 29.0, 27.2, 25.8, 24.9, 23.6. GC/MS (ESI) calculated for $[M+H]^+$ 509.30, found 509.2. FTIR (neat, cm^{-1}): 3305(m), 2977(m), 2937(m), 2858(m), 1913(w), 1720(s), 1604(s), 1511(s), 1434(s), 1252(m), 1142(s), 962(s), 911(s), 846(s), 771(s), 734(s).

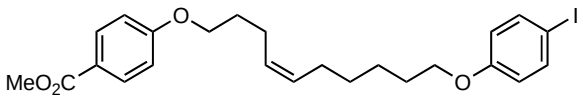

methyl 4-{[(4*Z*)-10-(4-iodophenoxy)dec-4-en-1-yl]oxy}benzoate (3.49), compound was prepared according to general procedure A. The compound was purified by silica gel chromatography with EtOAc/Hex (0 → 30%) and isolated as a colorless oil (202.4 mg, 80% yield). ^{1}H NMR (300 MHz, $CDCl_3$) δ 7.97 (d, *J* = 8.8 Hz, 2H), 7.53 (d, *J* = 8.7 Hz, 2H), 6.90 (d, *J* = 8.8 Hz, 2H), 6.65 (d, *J* = 8.7 Hz, 2H), 5.50 – 5.32 (m, 2H), 4.00 (t, *J* = 6.3 Hz, 2H), 3.92 – 3.79 (m, 5H), 2.29 – 2.16 (m, 2H), 2.05 (q, *J* = 6.1 Hz, 2H), 1.86 (p, *J* = 6.8 Hz, 2H), 1.78 – 1.62 (m, 2H), 1.46 – 1.29 (m, 4H). ^{13}C NMR (126 MHz, $CDCl_3$) δ 166.9, 162.9, 159.0, 138.2, 131.6, 131.0, 128.5, 122.5, 117.0, 114.1, 82.5, 68.0, 67.2, 51.9, 29.5, 29.1, 29.0, 27.2, 25.7, 23.6. GC/MS (ESI) calculated for $[M+H]^+$ 509.11, found 509.0. FTIR (neat, cm^{-1}): 3002(m), 2939(m), 2856(m), 1914(w), 1716(s), 1605(s), 1511(s), 1435(s), 1391(s), 1253(m), 1167(s), 1019(m), 909(s).

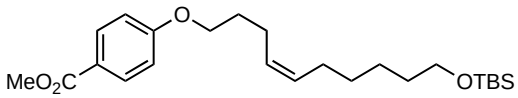

methyl 4-{[(4*Z*)-10-[(*tert*-butyldimethylsilyl)oxy]dec-4-en-1-yl]oxy}benzoate (3.50), compound was prepared according to general procedure A. The compound was purified by silica gel chromatography with EtOAc/Hex (0 → 30%) and isolated as a colorless oil (189.9 mg, 90% yield). ^{1}H NMR (300 MHz, $CDCl_3$) δ 7.98 (d, *J* = 8.8 Hz, 2H), 6.90 (d, *J* = 8.8 Hz, 2H), 5.54 – 5.24 (m, 2H), 4.00 (t, *J* = 6.4 Hz, 2H), 3.88 (s, 3H), 3.57 (t, *J* = 6.6 Hz, 2H), 2.29 – 2.15 (m, 2H), 2.02 (q, *J* = 6.4 Hz, 2H), 1.85 (p, *J* = 6.7 Hz, 2H), 1.52 – 1.42 (m, 2H), 1.35 – 1.25 (m, 4H), 0.89 (s, 9H), 0.04 (s, 6H). ^{13}C NMR (126 MHz, $CDCl_3$) δ 166.9, 162.9, 131.6, 131.2, 128.2, 122.4, 114.1, 67.3, 63.2, 51.8, 32.8, 29.5, 29.0, 27.2, 26.0, 25.5, 23.5, 18.4, -5.3. GC/MS (EI) calculated

for $[M]^+$ 420.27, found 420.4. FTIR (neat, cm^{-1}): 3004(w), 2930(m), 2856(m), 1721(s), 1606(s), 1511(s), 1434(s), 1279(2), 1254(s), 1167(s), 1103(s) 836(s).

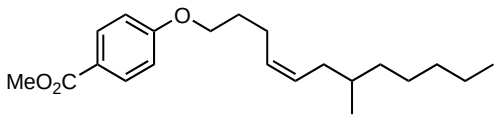

methyl 4-{[(4*Z*)-7-methyldodec-4-en-1-yl]oxy}benzoate (3.51), compound was prepared according to general procedure A. The compound was purified by silica gel chromatography with EtOAc/Hex (0 → 30%) and isolated as a colorless oil (105.6 mg, 64% yield). ^{1}H NMR (300 MHz, $CDCl_3$) δ 7.97 (d, *J* = 8.9 Hz, 2H), 6.90 (d, *J* = 8.9 Hz, 2H), 5.56 – 5.30 (m, 2H), 4.00 (t, *J* = 6.4 Hz, 2H), 3.88 (s, 3H), 2.32 – 2.15 (m, 2H), 2.05 – 1.95 (m, 1H), 1.91 – 1.81 (m, 2H), 1.52 – 1.35 (m, 2H), 1.34 – 1.10 (m, 8H), 0.93 – 0.76 (m, 6H). ^{13}C NMR (126 MHz, $CDCl_3$) δ 167.1, 163.1, 131.7, 130.1, 129.0, 122.5, 114.2, 67.5, 51.9, 36.8, 34.7, 33.5, 32.3, 29.1, 27.0, 23.7, 22.8, 19.7, 14.2. GC/MS (EI) calculated for $[M]^+$ 332.24, found 332.2. FTIR (neat, cm^{-1}): 2998(m), 2925(m), 2857(m), 1913(w), 1720(s), 1606(s), 1511(s), 1433(m), 1253(s), 1167(s), 1103(s), 970(s), 845(s).

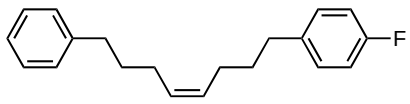

1-fluoro-4-[(4*Z*)-8-phenyloct-4-en-1-yl]benzene (3.52), compound was prepared according to general procedure B. The compound was purified by silica gel chromatography with EtOAc/Hex (0 → 10%) and isolated as a colorless oil (118.6 mg, 84% yield). ^{1}H NMR (300 MHz, $CDCl_3$) δ 7.34 – 7.27 (m, 2H), 7.24 – 7.17 (m, 3H), 7.17 – 7.08 (m, 2H), 7.03 – 6.91 (m, 2H), 5.58 – 5.29 (m, 2H), 2.68 – 2.54 (m, 4H), 2.06 (s, 4H), 1.78 – 1.58 (m, 4H). ^{13}C NMR (126 MHz, $CDCl_3$) δ 161.34 (d, *J* = 243.0 Hz), 142.62, 138.20 (d, *J* = 3.1 Hz), 130.11, 129.83, 129.83 (d, *J* = 7.7 Hz),

128.56, 128.41, 125.82, 115.09 (d, J = 21.0 Hz), 35.61, 34.74, 31.65, 31.54, 26.99, 26.85. ^{19}F NMR (470 MHz, $CDCl_3$) δ -121.0. GC/MS (EI) calculated for $[M]^+$ 282.18, found 282.2. FTIR (neat, cm^{-1}): 3053(m), 2986(m), 2857(m), 2304(m), 1509(s), 1421(m), 1265(s), 895(s), 746(s).

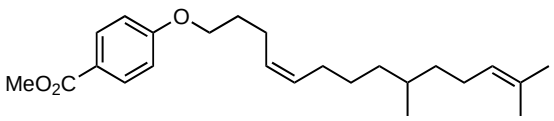

methyl 4-{[(4*Z*)-9,13-dimethyltetradeca-4,12-dien-1-yl]oxy}benzoate (3.53), compound was prepared according to general procedure A. The compound was purified by silica gel chromatography with EtOAc/Hex (0 → 30%) and isolated as a colorless oil (138.7 mg, 75% yield). ^{1}H NMR (300 MHz, $CDCl_3$) δ 7.98 (d, J = 8.7 Hz, 2H), 6.90 (d, J = 8.7 Hz, 2H), 5.50 – 5.30 (m, 2H), 5.09 (t, J = 7.1 Hz, 1H), 4.00 (t, J = 6.4 Hz, 2H), 3.88 (s, 3H), 2.30 – 2.14 (m, 2H), 2.06 – 1.79 (m, 6H), 1.68 (s, 3H), 1.60 (s, 3H), 1.38 – 1.20 (m, 5H), 1.17 – 1.01 (m, 2H), 0.83 (d, J = 6.3 Hz, 3H). ^{13}C NMR (126 MHz, $CDCl_3$) δ 166.9, 163.0, 131.6, 131.5, 131.0, 128.2, 125.1, 122.5, 114.1, 67.3, 51.8, 37.2, 36.7, 32.4, 29.1, 27.6, 27.2, 25.8, 25.6, 23.6, 19.6, 17.7. GC/MS (EI) calculated for $[M]^+$ 372.27, found 372.3. FTIR (neat, cm^{-1}): 3006(m), 2925(m), 2854(m), 1720(s), 1606(s), 1510(s), 1434(s), 1279(s), 1253(s), 1167(s), 1104(s), 910(w), 846(s), 770(s).

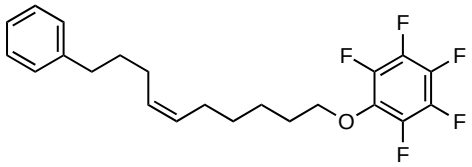

1,2,3,4,5-pentafluoro-6-{[(6*Z*)-10-phenyldec-6-en-1-yl]oxy}benzene (3.54), compound was prepared according to general procedure B. The compound was purified by silica gel chromatography with EtOAc/Hex (0 → 20%) and isolated as a colorless oil (158.8 mg, 80% yield).

^{1}H NMR (300 MHz, $CDCl_3$) δ 7.34 – 7.26 (m, 2H), 7.24 – 7.15 (m, 3H), 5.57 – 5.27 (m, 2H), 4.16 (t, *J* = 6.5 Hz, 2H), 2.71 – 2.56 (m, 2H), 2.17 – 1.98 (m, 4H), 1.87 – 1.61 (m, 4H), 1.56 – 1.36 (m, 4H). ^{13}C NMR (126 MHz, $CDCl_3$) δ 142.7, 130.0, 129.9, 128.5, 128.4, 125.8, 75.9, 35.6, 31.6, 29.9, 29.4, 27.2, 27.0, 25.3. ^{19}F NMR (470 MHz, $CDCl_3$) δ -159.9 (d, *J* = 20.5 Hz), -166.5 (t, *J* = 21.3 Hz), -166.9 (t, *J* = 21.7 Hz). GC/MS (EI) calculated for $[M]^+$ 398.17, found 398.2. FTIR (neat, cm^{-1}): 3310 (m), 3004(m), 2935(m), 2858(m), 2658(w), 2467(w), 1512(s) 1453(m), 1387(s), 1312(s), 1159(s), 1028(m), 997(m), 746(s), 699(s).

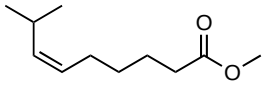

methyl (6*Z*)-8-methylnon-6-enoate (3.57), compound was prepared according to general procedure A. The compound was purified by silica gel chromatography with EtOAc/Hex (0 → 30%) and isolated as a colorless oil (75.1 mg, 82% yield). This compound has been previously synthesized and spectra match the literature values.[49]

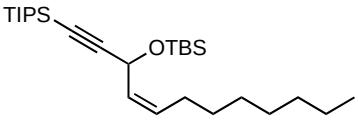

[(4*Z*)-3-[(*tert*-butyldimethylsilyl)oxy]dodec-4-en-1-yn-1-yl]tris(propan-2-yl)silane (3.60), compound was prepared according to general procedure A. The compound was purified by silica gel chromatography with EtOAc/Hex (0 → 30%) and isolated as a colorless oil (209.0 mg, 93% yield). ^{1}H NMR (300 MHz, Chloroform-*d*) δ 5.67 – 5.28 (m, 2H), 5.14 (dd, *J* = 7.8, 1.0 Hz, 1H), 2.09 (q, *J* = 7.2 Hz, 2H), 1.40 – 1.18 (m, 10H), 1.06 (m, 21H), 0.99 – 0.79 (m, 12H), 0.14 (d, *J* = 3.3 Hz, 6H). ^{13}C NMR (126 MHz, $CDCl_3$) δ 131.1, 130.9, 108.7, 84.7, 59.8, 32.0, 29.6, 29.4, 29.4, 27.9, 25.9, 22.8, 18.7, 18.4, 14.2, 11.4, -4.3, -4.5. GC/MS (EI) calculated for $[M]^+$ 345.27, found

345.3. FTIR (neat, cm^{-1}): 3020(w), 2928(s), 2893(s), 2864(s), 2168(w), 1463(m), 1387(w), 1361(w), 1314(w), 1252(m), 1075(s).

3.3.10 *Gram Scale Reaction*

To a flame dried Schlenk flask filled with nitrogen and charged with a stir bar was added LiO*t*-Bu (480.3 mg, 6 mmol, 1.5 equiv). To this was added TriAgCl (243.6 mg, 0.4 mmol, 0.10 equiv), methyl-4-(pent-4-yn-1-yloxy)benzoate (873.0 mg, 4 mmol, 1.0 equiv), and isooctane (40 mL). Then, 9-(3-phenylpropyl)-9-borabicyclo[3.3.1]nonane (2M in toluene, 2.6 mL, 1.3 equiv) and methanol (2M in toluene, 2.2 mL, 1.1 equiv) were added and the reaction mixture was heated to 45 °C in an oil bath for 16 hours. After 16 hours, an aliquot of the crude reaction mixture was analyzed by GC, and the reaction was quenched with the addition of sodium perborate (1.20 g, 12 mmol, 3.0 equiv) in 40 mL THF and 40 mL deionized water. The mixture was stirred at room temperature for 1 hour and then extracted with ether (3 x 100 mL) and dried over $MgSO_4$. The crude mixture was concentrated under reduced pressure and purified by silica gel chromatography.

3.3.11 *Synthesis and Characterization of Alkyne Starting Materials*

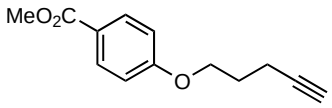

methyl 4-(pent-4-yn-1-yloxy)benzoate (3.1) was prepared according to a known procedure and has been previously characterized.[24]

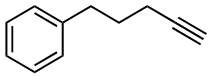

5-phenyl-1-pentyne (3.61) was purchased from GFS Chemical and distilled over calcium hydride under reduced pressure before use.

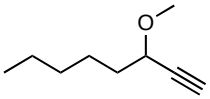

3-methoxyoct-1-yne (3.63) was prepared according to a known procedure and has been previously characterized.[58]

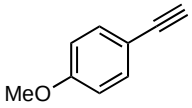

1-ethynyl-4-methoxybenzene (3.64) was purchased from Millipore Sigma and distilled over calcium hydride under reduced pressure before use.

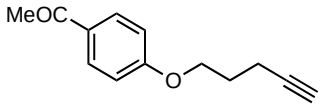

1-[4-(pent-4-yn-1-yloxy)phenyl]ethan-1-one (3.65) was prepared according to a known procedure and has been previously characterized.[59]

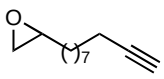

2-(dec-9-yn-1-yl)oxirane (3.66) was prepared according to a known procedure and has been previously characterized.[60]

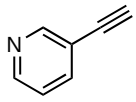

3-ethynylpyridine (3.67) was purchased from Ark Pharm and distilled over calcium hydride under reduced pressure before use.

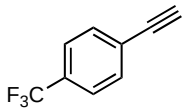

1-ethynyl-4-(trifluoromethyl)benzene (3.68) was purchased from Millipore Sigma and distilled over calcium hydride under reduced pressure before use.

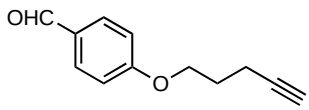

4-(pent-4-yn-1-yloxy)benzaldehyde (3.69) is commercially available from Aurora Building Blocks 2.

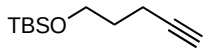

***tert*-butyldimethyl(pent-4-yn-1-yloxy)silane (3.70)** was prepared according to a known procedure and has been previously characterized.[61]

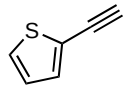

2-ethynylthiophene (3.71) was purchased from Combi-Blocks and distilled over calcium hydride under reduced pressure before use.

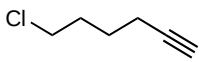

6-chlorohex-1-yne (3.72) was purchased from TCI America and distilled over calcium hydride under reduced pressure before use.

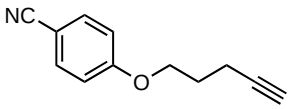

4-(pent-4-yn-1-yloxy)benzonitrile (3.73) was prepared according to a known procedure and has been previously characterized.[59]

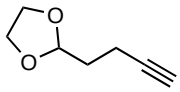

2-(but-3-yn-1-yl)-1,3-dioxolane (3.74) was prepared according to a known procedure and has been previously characterized.[62]

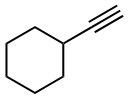

ethynylcyclohexane (3.75) was purchased from Millipore Sigma and distilled over calcium hydride under reduced pressure before use.

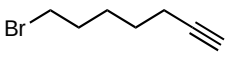

7-bromohept-1-yne (3.76) was prepared according to a known procedure and has been previously characterized.[59]

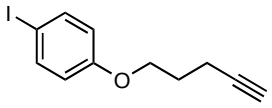

1-iodo-4-(pent-4-yn-1-yloxy)benzene (3.77) was prepared according to a known procedure and has been previously characterized.[59]

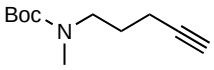

***tert*-butyl N-methyl-N-(pent-4-yn-1-yl)carbamate (3.78)** was prepared according to a known procedure and has been previously characterized.[63]

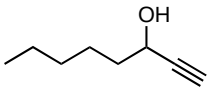

oct-1-yn-3-ol (3.79) was purchased from TCI America and distilled over calcium hydride under reduced pressure before use.

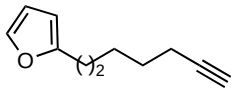

2-(hept-6-yn-1-yl)furan (3.80) was prepared according to a known procedure and has been previously characterized.[64]

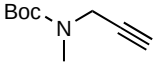

***tert*-butyl N-methyl-N-(prop-2-yn-1-yl)carbamate (3.81)** was prepared according to a known procedure and has been previously characterized.[65]

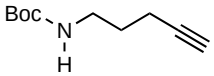

***tert*-butyl N-(pent-4-yn-1-yl)carbamate (3.82)** was prepared according to a known procedure and has been previously characterized.[66]

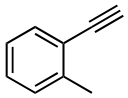

1-ethynyl-2-methylbenzene (3.83) was purchased from Millipore Sigma and distilled over calcium hydride under reduced pressure before use.

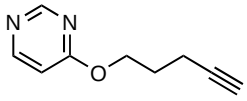

4-(pent-4-yn-1-yloxy)pyrimidine (3.84). A reaction flask charged with a stir bar was flame-dried under vacuum and allowed to cool under nitrogen. The flask was then charged with triphenylphosphine (2.2 g, 24.0 mmol, 1.2 equiv), phenol (7.7 mmol, 1.1 equiv), THF (14.0 mL, 0.5 M) and 4-pentyn-1-ol (654.0 µL, 7.0 mmol, 1.0 equiv). The reaction mixture was cooled to 0 °C with an ice bath. To the cooled reaction mixture was added DIAD (1.6 mL, 8.4 mmol, 1.2 equiv) dropwise. The reaction mixture was allowed to warm to 23 °C and stirred overnight. THF was removed under reduced pressure and the mixture was suspended in hexanes and stirred vigorously for 30 min. The solid triphenylphosphine oxide was removed by passing the mixture through a plug of celite. The solvent was removed under reduced pressure and the crude product was purified by silica gel chromatography. Compound was isolated as a white solid. ^{1}H NMR (300 MHz, $CDCl_3$) δ 8.76 (s, 1H), 8.41 (d, *J* = 5.9 Hz, 1H), 6.72 (dd, *J* = 5.9, 1.0 Hz, 1H), 4.46 (t, *J* = 6.2 Hz, 2H), 2.36 (td, *J* = 7.0, 2.6 Hz, 2H), 2.12 – 1.88 (m, 3H). ^{13}C NMR (75 MHz, $CDCl_3$) δ

169.2, 158.4, 156.8, 108.8, 83.1, 69.2, 65.2, 27.8, 15.3. GC/MS (EI) calculated for $[M]^+$ 162.08, found 162.20.

3-methylbut-1-yne (3.55) was purchased from Millipore Sigma and distilled over calcium hydride under reduced pressure before use.

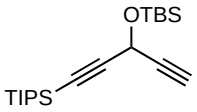

***tert*-butyldimethyl({1-[tris(propan-2-yl)silyl]penta-1,4-diyn-3-yl}oxy)silane (3.58).** The deprotected alcohol of **58** has been previously prepared [67]. TBS protection of the alcohol was performed according to a known literature procedure [61]. The compound was isolated as a yellow oil. ^{1}H NMR (300 MHz, $CDCl_3$) δ 5.22 (d, *J* = 2.3 Hz, 1H), 2.47 (d, *J* = 2.3 Hz, 1H), 1.08 (s, 21H), 0.91 (s, 9H), 0.19 (s, 6H). ^{13}C NMR (75 MHz, $CDCl_3$) δ 104.7, 85.5, 82.0, 71.7, 53.4, 25.8, 18.7, 18.4, 11.4, -4.4. GC/MS (EI) calculated for $[M]^+$ 350.25, found 350.3. FTIR (neat, cm^{-1}): 3313(s), 2944(m), 2865(m), 2716(w), 2176(w), 1623(w), 1464(s), 1287(s), 1252(s), 1087(m), 996(m), 882(s), 836(s), 780(s) 633(m).

General Procedure for the Preparation of Heterocyclic Alkynes:

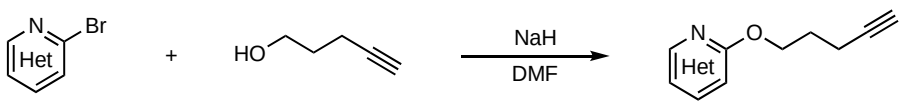

A reaction flask charged with stir bar was flame-dried under vacuum and allowed to cool under nitrogen. The flask was then charged with sodium hydride (1.5 equiv) and DMF (0.1 M).

The reaction mixture was cooled to 0 °C with an ice bath. To the cooled reaction mixture was added 4-pentyn-1-ol (1.5 equiv) and the reaction mixture was allowed to stir for 30 minutes. After the indicated time, heterocyclic bromide (1.0 equiv) was added and the mixture was stirred for 2 hours. After 2 hours, the reaction mixture was quenched with water and extracted with diethyl ether. The extract was concentrated under reduced pressure and the crude product was purified by silica gel chromatography. The following alkynes were prepared using this procedure.

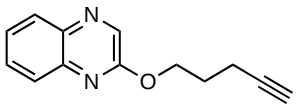

2-(pent-4-yn-1-yloxy)quinoxaline (3.85), compound was isolated as a white solid. ^{1}H NMR (300 MHz, $CDCl_3$) δ 8.46 (s, 1H), 8.01 (d, *J* = 8.1 Hz, 1H), 7.83 (d, *J* = 8.3 Hz, 1H), 7.73 – 7.62 (m, 1H), 7.61 – 7.50 (m, 1H), 4.59 (t, *J* = 6.2 Hz, 2H), 2.44 (td, *J* = 7.0, 2.6 Hz, 2H), 2.09 (p, *J* = 6.6 Hz, 2H), 1.99 (t, *J* = 2.6 Hz, 1H). ^{13}C NMR (75 MHz, $CDCl_3$) δ 157.5, 140.6, 139.8, 139.2, 130.2, 129.2, 127.4, 126.7, 83.4, 69.1, 65.1, 27.9, 15.5. GC/MS (EI) calculated for $[M]^+$ 212.09, found 212.1. FTIR (neat, cm^{-1}): 3245(s), 3058(w), 2960(m), 2852(m), 1849(w), 1573(s), 1466(s), 1416(s), 1314(s), 1223(s), 1141(s), 1029(s), 998(s), 959(s).

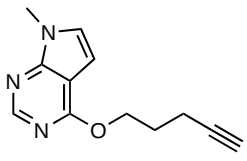

7-methyl-4-(pent-4-yn-1-yloxy)-7H-pyrrolo[2,3-d]pyrimidine (3.86), compound was isolated as a white solid. ^{1}H NMR (300 MHz, $CDCl_3$) δ 8.46 (s, 1H), 7.00 (d, *J* = 3.4 Hz, 1H), 6.51 (d, *J* = 3.4 Hz, 1H), 4.62 (t, *J* = 6.2 Hz, 2H), 3.85 (s, 3H), 2.43 (td, *J* = 7.1, 2.6 Hz, 2H), 2.15 – 2.04 (m, 2H), 1.98 (t, *J* = 2.6 Hz, 1H). ^{13}C NMR (75 MHz, $CDCl_3$) δ 162.8, 152.3, 151.0, 126.8, 105.6,

98.3, 83.5, 69.0, 64.8, 31.4, 28.2, 15.5. GC/MS (EI) calculated for $[M]^+$ 215.11, found 215.1. FTIR (neat, cm^{-1}): 3295(m), 3104(w), 2951(m), 1597(s), 1560(s), 1445(s), 1370(m), 1317(m), 1247(s), 1210(s), 1056(s), 884(m).

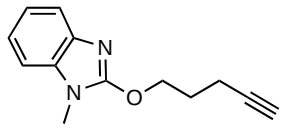

1-methyl-2-(pent-4-yn-1-yloxy)-1H-1,3-benzodiazole (3.87), compound was isolated as a white solid. ^1H NMR (300 MHz, $CDCl_3$) δ 7.57 – 7.50 (m, 1H), 7.20 – 7.11 (m, 3H), 4.65 (t, *J* = 6.2 Hz, 2H), 3.56 (s, 3H), 2.42 (td, *J* = 7.0, 2.6 Hz, 2H), 2.10 (p, *J* = 6.6 Hz, 2H), 1.99 (t, *J* = 2.6 Hz, 1H). ^{13}C NMR (75 MHz, $CDCl_3$) δ 157.4, 140.1, 134.3, 121.5, 120.7, 117.6, 107.9, 83.0, 69.2, 68.7, 28.2, 27.9, 15.2. GC/MS (EI) calculated for $[M]^+$ 214.11, found 214.1. FTIR (neat, cm^{-1}): 3190(m), 2955(m), 2931(m), 1622(s), 1540(s), 1456(s), 1375(s), 1288(s), 1211(s), 1042(s), 975(s), 892(w), 741(s).

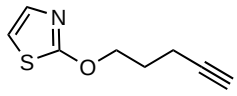

2-(pent-4-yn-1-yloxy)-1,3-thiazole (3.88), compound was isolated as colorless liquid. ^1H NMR (300 MHz, Chloroform-*d*) δ 7.12 (d, *J* = 3.8 Hz, 1H), 6.67 (d, *J* = 3.8 Hz, 1H), 4.51 (t, *J* = 6.1 Hz, 2H), 2.44 – 2.30 (m, 2H), 2.12 – 1.93 (m, 3H). ^{13}C NMR (75 MHz, $CDCl_3$) δ 174.5, 136.7, 111.0, 82.7, 69.7, 69.2, 27.6, 14.9. GC/MS (EI) calculated for $[M]^+$ 167.04, found 167.10.

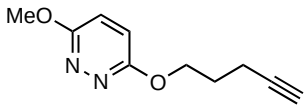

3-methoxy-6-(pent-4-yn-1-yloxy)pyridazine (3.89), compound was isolated as a white solid. ^{1}H NMR (300 MHz, Chloroform-*d*) δ 6.92 – 6.90 (m, 2H), 4.52 (t, *J* = 6.2 Hz, 2H), 4.04 (s, 3H), 2.38 (td, *J* = 7.0, 2.6 Hz, 2H), 2.16 – 1.91 (m, 3H). ^{13}C NMR (75 MHz, $CDCl_3$) δ 161.9, 161.7, 121.4, 121.3, 83.3, 68.9, 65.6, 54.5, 27.8, 15.2. GC/MS (EI) calculated for $[M]^+$192.09, found 192.10. FTIR (neat, cm-1) 3328(s), 2852(s), 2284(s), 1495(s), 1444(s), 1423(s), 1384(s), 1337(m), 1268(s), 1098(m), 1038(s), 1013(s), 949(s), 913(s), 949(s), 913(s), 839(s), 796(m). 729(s).

3.3.12 *Synthesis and Characterization of Alkene Starting Materials for Alkylboranes*

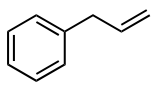

(prop-2-en-1-yl)benzene (3.90) was purchased from Millipore Sigma and distilled over calcium hydride under reduced pressure before use.

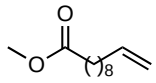

methyl undec-10-enoate (3.91) was prepared according to a known procedure and has been previously characterized.[68]

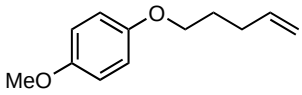

1-methoxy-4-(pent-4-en-1-yloxy)benzene (3.92) was prepared according to a known procedure and has been previously characterized.[69]

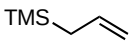

trimethyl(prop-2-en-1-yl)silane (3.93) was purchased from Oakwood Chemicals and distilled over calcium hydride under reduced pressure before use.

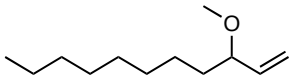

3-methoxyundec-1-ene (3.94) was prepared according to a known procedure and has been previously characterized.[70]

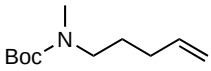

***tert*-butyl N-methyl-N-(pent-4-en-1-yl)carbamate (3.95)** is commercially available from Enamine Building Blocks.

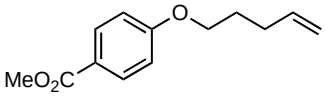

methyl 4-(pent-4-en-1-yloxy)benzoate (3.96) was prepared according to a known procedure and has been previously characterized.[71]

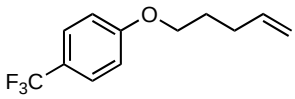

1-(pent-4-en-1-yloxy)-4-(trifluoromethyl)benzene (3.97) was prepared according to a known procedure and has been previously characterized.[72]

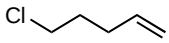

5-chloropent-1-ene (3.98) was purchased from Arctom Chemicals and distilled over calcium hydride under reduced pressure before use.

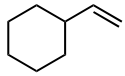

ethenylcyclohexane (3.99) was purchased from Alfa Aesar and distilled over calcium hydride under reduced pressure before use.

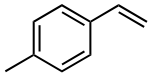

1-ethenyl-4-methylbenzene (3.100) was purchased from TCI America and distilled over calcium hydride under reduced pressure before use.

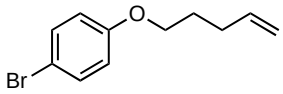

1-bromo-4-(pent-4-en-1-yloxy)benzene (3.101) was prepared according to a known procedure and has been previously characterized.[73]

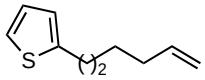

2-(hex-5-en-1-yl)thiophene (3.102) was prepared according to a known procedure and has been previously characterized.[74]

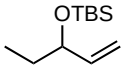

***tert*-butyldimethyl(pent-1-en-3-yloxy)silane (3.103)** was prepared according to a known procedure and has been previously characterized.[75]

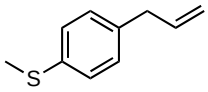

1-(methylsulfanyl)-4-(prop-2-en-1-yl)benzene (3.104) was prepared according to a known procedure and has been previously characterized.[76]

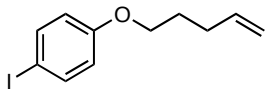

1-iodo-4-(pent-4-en-1-yloxy)benzene (3.105) was prepared according to a known procedure and has been previously characterized.[69]

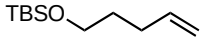

***tert*-butyldimethyl(pent-4-en-1-yloxy)silane (3.106)** was prepared according to a known procedure and has been previously characterized.[77]

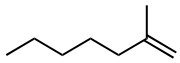

2-methylhept-1-ene (3.107) was purchased from Millipore Sigma and distilled over calcium hydride under reduced pressure before use.

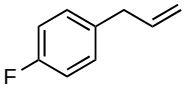

1-fluoro-4-(prop-2-en-1-yl)benzene (3.108) was prepared according to a known procedure and has been previously characterized.[78]

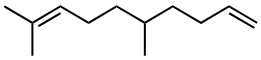

5,9-dimethyldeca-1,8-diene (3.109) was prepared according to a known procedure and has been previously characterized.[79]

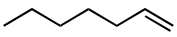

hept-1-ene (3.56) was purchased from Millipore Sigma and distilled over calcium hydride under reduced pressure before use.

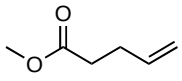

methyl pent-4-enoate (3.59) was prepared according to a known procedure and has been previously characterized.[80]

General Procedure for the Preparation of Different Alkenes:

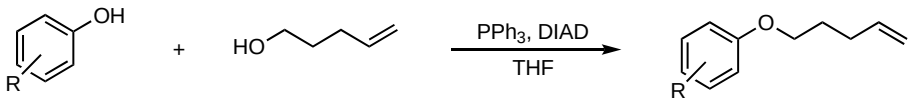

A reaction flask charged with stir bar was flame-dried under vacuum and allowed to cool under nitrogen. The flask was then charged with triphenylphosphine (2.2 g, 24.0 mmol, 1.2 equiv), phenol (7.7 mmol, 1.1 equiv), THF (14.0 mL, 0.5 M) and 4-penten-1-ol (654.0 µL, 7.0 mmol, 1.0 equiv). The reaction mixture was cooled to 0 °C with an ice bath. To the cooled reaction mixture was added DIAD (1.6 mL, 8.4 mmol, 1.2 equiv) dropwise. The reaction mixture was allowed to warm to 23 °C and stirred overnight. THF was removed under reduced pressure and the mixture was suspended in hexanes and stirred vigorously for 30 min. The solid triphenylphosphine oxide was removed by passing the mixture through a plug of celite. The solvent was removed under reduced pressure and the crude product was purified by silica gel chromatography. The following alkenes were prepared using this procedure.

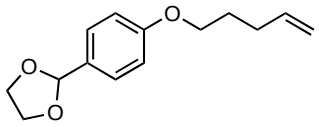

2-[4-(pent-4-en-1-yloxy)phenyl]-1,3-dioxolane (3.110), compound was isolated as a colorless liquid. ^{1}H NMR (300 MHz, $CDCl_3$) δ 7.41 (d, *J* = 8.6 Hz, 2H), 6.91 (d, *J* = 8.6 Hz, 2H), 5.86 (ddt, *J* = 16.9, 10.1, 6.6 Hz, 1H), 5.76 (s, 1H), 5.13 – 4.96 (m, 2H), 4.26 – 3.82 (m, 6H), 2.35 – 2.11 (m, 2H), 2.00 – 1.76 (m, 2H). ^{13}C NMR (75 MHz, $CDCl_3$) δ 159.9, 137.8, 130.1, 127.9, 115.2, 114.5, 103.8, 67.3, 65.3, 30.1, 28.5. GC/MS (EI) calculated for $[M]^+$ 234.13, found 234.1. FTIR (neat, cm^{-1}): 3075(s), 2944(m), 2881(m), 2759(m), 1640(s), 1615(s), 1515(s), 1435(s), 1393(s), 1304(m), 1246(m), 1078(m), 1011(m), 942(m), 829(s).

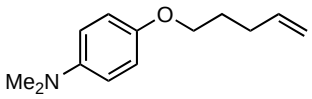

N,N-dimethyl-4-(pent-4-en-1-yloxy)aniline (3.111), compound was isolated as a light yellow liquid. ^{1}H NMR (300 MHz, $CDCl_3$) δ 6.87 (d, *J* = 9.1 Hz, 2H), 6.76 (d, *J* = 9.1 Hz, 2H), 5.88 (ddt, *J* = 16.9, 10.1, 6.6 Hz, 1H), 5.16 – 4.94 (m, 2H), 3.94 (t, *J* = 6.5 Hz, 2H), 2.88 (s, *J* = 10.3 Hz, 6H), 2.31 – 2.14 (m, 2H), 1.95 – 1.75 (m, 2H). ^{13}C NMR (75 MHz, $CDCl_3$) δ 151.6, 145.9, 138.1, 115.7, 115.1, 115.0, 68.1, 41.9, 30.3, 28.8. GC/MS (EI) calculated for $[M]^+$ 205.15, found 205.2. FTIR (neat, cm^{-1}): 3074(m), 2939(m), 2791(m), 1635(m), 1516(s), 1456(s), 1339(w), 1243(s), 1057(m), 947(s), 816(s), 757(s).

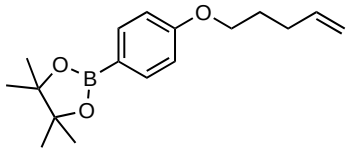

4,4,5,5-tetramethyl-2-[4-(pent-4-en-1-yloxy)phenyl]-1,3,2-dioxaborolane (3.112), compound was isolated as a colorless liquid. ^{1}H NMR (300 MHz, $CDCl_3$) δ 7.77 (d, *J* = 8.6 Hz, 2H), 6.90 (d, *J* = 8.6 Hz, 2H), 5.86 (ddt, *J* = 16.9, 10.2, 6.6 Hz, 1H), 5.16 – 4.92 (m, 2H), 4.00 (t, *J* = 6.4 Hz, 2H), 2.34 – 2.16 (m, 2H), 1.97 – 1.79 (m, 2H), 1.35 (s, 12H). ^{13}C NMR (75 MHz, $CDCl_3$) δ 161.8, 137.9, 136.6, 115.3, 114.0, 83.6, 77.4, 67.1, 30.2, 28.5, 25.0. GC/MS (EI) calculated for $[M]^+$ 288.19, found 288.1. FTIR (neat, cm^{-1}): 3076(m), 2977(m), 2944(m), 1605(s), 1558(s), 1516(s), 1397(s), 1361(s), 1246(s), 1143(s), 1090(s), 962(m), 860(s), 757(s).

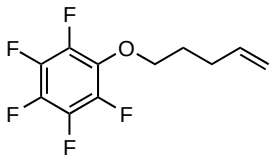

1,2,3,4,5-pentafluoro-6-(pent-4-en-1-yloxy)benzene (3.113), compound was isolated as a colorless liquid. ^{1}H NMR (300 MHz, $CDCl_3$) δ 5.82 (ddt, *J* = 16.9, 10.2, 6.7 Hz, 1H), 5.20 – 4.90 (m, 2H), 4.17 (t, *J* = 6.4 Hz, 2H), 2.37 – 2.15 (m, 2H), 1.97 – 1.77 (m, 2H). ^{13}C NMR (75 MHz, $CDCl_3$) δ 137.4, 115.7, 75.1, 29.7, 29.2. GC/MS (EI) calculated for $[M]^+$ 252.06, found 252.1. FTIR (neat, cm^{-1}): 3082(m), 2947(m), 2663(w), 1829(w), 1643(m), 1538(m), 1511(s), 1456(m), 1313(m), 1161(m), 1026(m), 995(m), 917(m).

3.3.13 *Mechanistic Studies*

3.3.13.1 Synthesis of Silver Borate Complex **3.63**

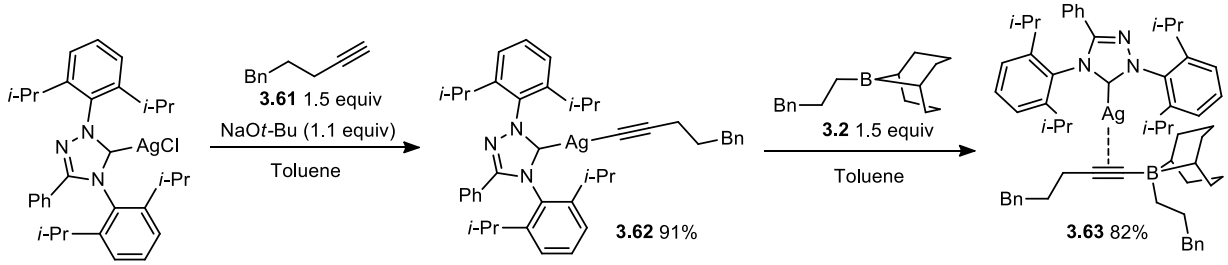

Synthesis of **3.62,** In a nitrogen filled glovebox, a scintillation vial was charged with a stir bar and TriAgCl (91.3 mg, 0.150 mmol, 1.0 equiv). To this was added NaO*t*-Bu (15.9 mg 0.165 mmol, 1.1 equiv), 5-phenyl-1-pentyne (32.4 mg 0.225 mmol, 1.5 equiv) and toluene (3 mL). The reaction mixture was stirred at 25 °C for 2 hours. After, 2 hours, the reaction mixture was filtered through a plug of celite and concentrated. The silver acetylide was then precipitated out with pentane, collected by vacuum filtration and washed several times with pentane. The product was isolated as a white powder (98.2 mg, 91% yield). ^{1}H NMR (300 MHz, $CDCl_3$) δ 7.62 – 7.47 (m, 2H), 7.44 – 7.27 (m, 9H), 7.24 – 7.17 (m, 2H), 7.17 – 7.06 (m, 3H), 2.70 – 2.56 (m, 4H), 2.56 –

2.41 (m, 2H), 2.19 (t, *J* = 7.6 Hz, 2H), 1.81 – 1.68 (m, 2H), 1.43 – 1.27 (m, 12H), 1.24 (d, *J* = 6.9 Hz, 6H), 0.97 (d, *J* = 6.8 Hz, 6H). ^{13}C NMR (126 MHz, $CDCl_3$) δ 153.4, 153.3, 145.7, 145.3, 142.7, 135.2, 131.9, 131.5, 131.2, 128.9, 128.6, 128.1, 128.1, 125.5, 125.1, 124.3, 35.2, 32.0, 29.1, 29.0, 25.1, 24.5, 23.9, 22.8, 20.3

Synthesis of **3.63**, In a nitrogen filled glovebox, a scintillation vial was charged with a stir bar and Silver acetylide **3.62** (39.3 mg, 0.055 mmol, 1.0 equiv). To this was added alkylborane **3.2** (19.8 mg 0.083 mmol, 1.1 equiv) and toluene (3 mL). The reaction mixture was stirred at 25 °C for 1 hours. After 1 hour, the solvent was removed under vacuum and the borate complex was then precipitated out with pentane. It was then collected by vacuum filtration and washed several times with pentane. The complex was isolated as an off-white powder (43.6 mg, 82% yield). Crystallographic information is below. ^{1}H NMR (300 MHz, C_6D_6) δ 7.52 – 7.43 (m, 2H), 7.42 – 7.32 (m, 2H), 7.31 – 7.17 (m, 5H), 7.15 – 7.04 (m, 7H), 7.03 – 6.94 (m, 2H), 6.87 – 6.69 (m, 3H), 2.97 – 2.83 (m, 2H), 2.83 – 2.69 (m, 2H), 2.65 – 2.20 (m, 10H), 2.04 (s, 8H), 1.90 – 1.73 (m, 2H), 1.42 – 1.24 (m, 14H), 1.15 (d, *J* = 6.8 Hz, 6H), 0.87 – 0.63 (m, 10H).

3.3.13.2 Catalytic Competency of the Borate Complex

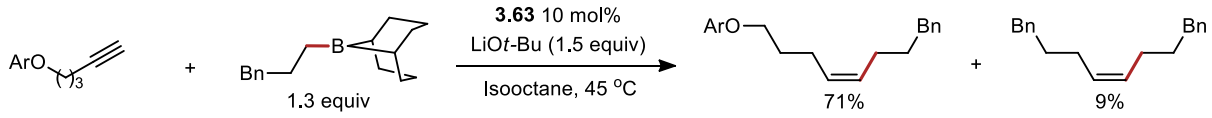

Ar = methyl-4-benzoate

In a nitrogen filled glovebox, a dram vial was charged with a stir bar and LiO*t*-Bu (6.0 mg, 0.075 mmol, 1.5 equiv). To this was added Borate complex **3.63** (4.9 mg 0.005 mmol, 0.005 equiv), alkyne **3.1** (10.9 mg 0.05 mmol, 1.0 equiv), alkylborane **3.2** (15.6 mg, 0.065 mmol, 1.3 equiv), methanol (1.8 mg, 0.055 mmol, 1.10 equiv), isooctane (0.5 mL) and internal standard, TMB (4.2

mg, 0.05 mmol, 0.5 equiv). The reaction mixture was heated at 45°C and an aliquot of the crude reaction mixture was analyzed by GC after 16h.

3.3.14 *X-Ray Cyrstallography*

3.3.14.1 Crystallization of **3.63** for X-Ray Crystallography

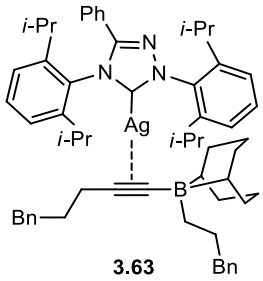

3.63

In a nitrogen filled glove box, a dram vial was charged with borate complex **3.63** (14.6 or 13.4 mg, 0.015 mmol, 1 equiv). The solid was then crystallized from benzene and pentane.

3.3.14.2 Crystallographic Data for **3.63**

A colorless prism, measuring 0.09 x 0.07 x 0.04 mm^3 was mounted on a loop with oil. Data was collected at -173°C on a Bruker APEX II single crystal X-ray diffractometer, Mo-radiation. Crystal-to-detector distance was 40 mm and exposure time was 60 seconds per frame for all sets. The scan width was 0.5°. Data collection was 99.7% complete to 25° in ϑ. A total of 25311 merged reflections were collected covering the indices, -23<=h<=23, -17<=k<=17, -29<=l<=29. 12944 reflections were symmetry independent and the R_{int} = 0.1029 reflects the small sample size. Indexing and unit cell refinement indicated a primitive monoclinic lattice. The space group was found to be P 2_1/n (No. 14).

The data was integrated and scaled using SAINT,[81] SADABS[82] within the APEX2[83] software package by Bruker.

Solution by direct methods (SHELXT[84] or SIR97[85,86]) produced a complete heavy atom phasing model consistent with the proposed structure. The structure was completed by difference Fourier synthesis with SHELXL97.[87–89] Scattering factors are from Waasmair and Kirfel.[90] Hydrogen atoms were placed in geometrically idealised positions and constrained to ride on their parent atoms with C---H distances in the range 0.95-1.00 Angstrom. Isotropic thermal parameters U_{eq} were fixed such that they were $1.2U_{eq}$ of their parent atom Ueq for CH's and $1.5U_{eq}$ of their parent atom U_{eq} in case of methyl groups. All non-hydrogen atoms were refined anisotropically by full-matrix least-squares.

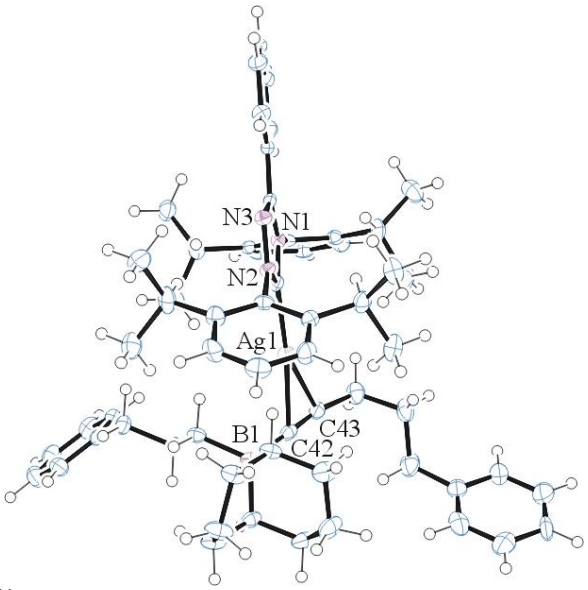

Figure 3.25. ORTEP[91] of the structure of boronate complex **3.63** with thermal ellipsoids at the 50% probability level. Disorder omitted for clarity. One phenyl and one *i*-Pr unit are disordered.

Table 3.3 Crystallographic Data: TriAg Boronate Complex **3.63**

Empirical formula	C60 H75 Ag B N3	
Formula weight	956.91	
Temperature	99(2) K	
Wavelength	0.71073 Å	
Crystal system	Monoclinic	
Space group	P 2_1/n	
Unit cell dimensions	a = 17.5111(18) Å	α= 90°.
	b = 13.3239(14) Å	β= 94.480(4)°.
	c = 22.382(2) Å	γ = 90°.
Volume	5206.2(9) $Å^3$	
Z	4	
Density (calculated)	1.221 Mg/m^3	
Absorption coefficient	0.427 mm^{-1}	
F(000)	2032	
Crystal size	0.090 x 0.070 x 0.040 mm^3	
Theta range for data collection	1.424 to 28.373°.	
Index ranges	-23<=h<=23, -17<=k<=17, -29<=l<=29	
Reflections collected	25311	
Independent reflections	12944 [R(int) = 0.1029]	
Completeness to theta = 25.000°	99.7 %	
Refinement method	Full-matrix least-squares on F^2	
Data / restraints / parameters	12944 / 33 / 596	

Goodness-of-fit on F^2	0.946
Final R indices [I>2sigma(I)]	R1 = 0.0480, wR2 = 0.0793
R indices (all data)	R1 = 0.1377, wR2 = 0.1037
Largest diff. peak and hole	0.544 and -0.661 e.$Å^{-3}$

3.4 REFERENCES FOR CHAPTER 3

(1) Rabinovitch, B. S.; Michel, K.-W. The Thermal Unimolecular Cis-Trans Isomerization of Cis-Butene-21. *J. Am. Chem. Soc.* **1959**, *81* (19), 5065–5071.

(2) Blackwood, J. E.; Gladys, C. L.; Loening, K. L.; Petrarca, A. E.; Rush, J. E. Unambiguous Specification of Stereoisomerism about a Double Bond. *J. Am. Chem. Soc.* **1968**, *90* (2), 509–510.

(3) Park, B. Y.; Nguyen, K. D.; Chaulagain, M. R.; Komanduri, V.; Krische, M. J. Alkynes as Allylmetal Equivalents in Redox-Triggered C–C Couplings to Primary Alcohols: (Z)-Homoallylic Alcohols via Ruthenium-Catalyzed Propargyl C–H Oxidative Addition. *J. Am. Chem. Soc.* **2014**, *136* (34), 11902–11905.

(4) Kong, J. R.; Krische, M. J. Catalytic Carbonyl Z-Dienylation via Multicomponent Reductive Coupling of Acetylene to Aldehydes and α-Ketoesters Mediated by Hydrogen: Carbonyl Insertion into Cationic Rhodacyclopentadienes. *J. Am. Chem. Soc.* **2006**, *128* (50), 16040–16041.

(5) Thomas, B. N.; Moon, P. J.; Yin, S.; Brown, A.; Lundgren, R. J. Z-Selective Iridium-Catalyzed Cross-Coupling of Allylic Carbonates and α-Diazo Esters. *Chem. Sci.* **2017**, *9* (1), 238–244.

(6) Armstrong, M. K.; Goodstein, M. B.; Lalic, G. Diastereodivergent Reductive Cross Coupling of Alkynes through Tandem Catalysis: Z- and E-Selective Hydroarylation of Terminal Alkynes. *J. Am. Chem. Soc.* **2018**, *140* (32), 10233–10241.

(7) Hodgson, D. M.; Arif, T. Convergent Synthesis of Trisubstituted Z-Allylic Esters by Wittig−Schlosser Reaction. *Org. Lett.* **2010**, *12* (18), 4204–4207.

(8) Dong, D.-J.; Li, H.-H.; Tian, S.-K. A Highly Tunable Stereoselective Olefination of Semistabilized Triphenylphosphonium Ylides with N-Sulfonyl Imines. *J. Am. Chem. Soc.* **2010**, *132* (14), 5018–5020.

(9) Reichard, H. A.; Micalizio, G. C. Metallacycle-Mediated Cross-Coupling with Substituted and Electronically Unactivated Alkenes. *Chem. Sci.* **2011**, *2* (4), 573–589.

(10) Das, M.; O'Shea, D. F. Z-Stereoselective Aza-Peterson Olefinations with Bis(Trimethylsilane) Reagents and Sulfinyl Imines. *Org. Lett.* **2016**, *18* (2), 336–339.

(11) Velluz, L.; Valls, J.; Nominé, G. Recent Advances in the Total Synthesis of Steroids. *Angew. Chem. Int. Ed. Engl.* **1965**, *4* (3), 181–200.

(12) Hendrickson, J. B. Systematic Synthesis Design. 6. Yield Analysis and Convergency. *J. Am. Chem. Soc.* **1977**, *99* (16), 5439–5450.

(13) Siau, W.-Y.; Zhang, Y.; Zhao, Y. Stereoselective Synthesis of Z-Alkenes. In *Stereoselective Alkene Synthesis*; Wang, J., Ed.; Topics in Current Chemistry; Springer Berlin Heidelberg: Berlin, Heidelberg, 2012; pp 33–58.

(14) Oger, C.; Balas, L.; Durand, T.; Galano, J.-M. Are Alkyne Reductions Chemo-, Regio-, and Stereoselective Enough To Provide Pure (Z)-Olefins in Polyfunctionalized Bioactive Molecules? *Chem. Rev.* **2013**, *113* (3), 1313–1350.

(15) Munslow, I. J. Alkyne Reductions. In *Modern Reduction Methods*; John Wiley & Sons, Ltd, 2008; pp 363–385.

(16) Meijere, A. de; Bräse, S.; Oestreich, M. *Metal-Catalyzed Cross-Coupling Reactions and More*; John Wiley & Sons, Ltd, 2013.

(17) Keitz, B. K.; Endo, K.; Patel, P. R.; Herbert, M. B.; Grubbs, R. H. Improved Ruthenium Catalysts for Z-Selective Olefin Metathesis. *J. Am. Chem. Soc.* **2012**, *134* (1), 693–699.

(18) Meek, S. J.; O'Brien, R. V.; Llaveria, J.; Schrock, R. R.; Hoveyda, A. H. Catalytic Z - Selective Olefin Cross-Metathesis for Natural Product Synthesis. *Nature* **2011**, *471* (7339), 461–466.

(19) Xu, C.; Shen, X.; Hoveyda, A. H. In Situ Methylene Capping: A General Strategy for Efficient Stereoretentive Catalytic Olefin Metathesis. The Concept, Methodological Implications, and Applications to Synthesis of Biologically Active Compounds. *J. Am. Chem. Soc.* **2017**, *139* (31), 10919–10928.

(20) Singh, K.; Staig, S. J.; Weaver, J. D. Facile Synthesis of Z-Alkenes via Uphill Catalysis. *J. Am. Chem. Soc.* **2014**, *136* (14), 5275–5278.

(21) Chen, C.; Dugan, T. R.; Brennessel, W. W.; Weix, D. J.; Holland, P. L. Z-Selective Alkene Isomerization by High-Spin Cobalt(II) Complexes. *J. Am. Chem. Soc.* **2014**, *136* (3), 945–955.

(22) Metternich, J. B.; Gilmour, R. A Bio-Inspired, Catalytic E → Z Isomerization of Activated Olefins. *J. Am. Chem. Soc.* **2015**, *137* (35), 11254–11257.

(23) Hazra, A.; Chen, J.; Lalic, G. Stereospecific Synthesis of E-Alkenes through Anti-Markovnikov Hydroalkylation of Terminal Alkynes. *J. Am. Chem. Soc.* **2019**, *141* (32), 12464–12469.

(24) Uehling, M. R.; Suess, A. M.; Lalic, G. Copper-Catalyzed Hydroalkylation of Terminal Alkynes. *J. Am. Chem. Soc.* **2015**, *137* (4), 1424–1427.

(25) Suess, A. M.; Uehling, M. R.; Kaminsky, W.; Lalic, G. Mechanism of Copper-Catalyzed Hydroalkylation of Alkynes: An Unexpected Role of Dinuclear Copper Complexes. *J. Am. Chem. Soc.* **2015**, *137* (24), 7747–7753.

(26) Lu, X.-Y.; Liu, J.-H.; Lu, X.; Zhang, Z.-Q.; Gong, T.-J.; Xiao, B.; Fu, Y. 1,1-Disubstituted Olefin Synthesis via Ni-Catalyzed Markovnikov Hydroalkylation of Alkynes with Alkyl Halides. *Chem. Commun.* **2016**, *52* (30), 5324–5327.

(27) Till, N. A.; Smith, R. T.; MacMillan, D. W. C. Decarboxylative Hydroalkylation of Alkynes. *J. Am. Chem. Soc.* **2018**, *140* (17), 5701–5705.

(28) Wang, Z.; Yin, H.; Fu, G. C. Catalytic Enantioconvergent Coupling of Secondary and Tertiary Electrophiles with Olefins. *Nature* **2018**, *563* (7731), 379–383.

(29) Cheung, C. W.; Zhurkin, F. E.; Hu, X. Z-Selective Olefin Synthesis via Iron-Catalyzed Reductive Coupling of Alkyl Halides with Terminal Arylalkynes. *J. Am. Chem. Soc.* **2015**, *137* (15), 4932–4935.

(30) Brown, H. C.; Levy, A. B.; Midland, M. M. Reaction of Lithium Ethynyl- and Ethenyltrialkylborates with Acid. Valuable Route to the Markovnikov Alkenyl- and Alkylboranes. *J. Am. Chem. Soc.* **1975**, *97* (17), 5017–5018.

(31) Zweifel, George.; Arzoumanian, Henri.; Whitney, C. C. A Convenient Stereoselective Synthesis of Substituted Alkenes via Hydroboration-Iodination of Alkynes. *J. Am. Chem. Soc.* **1967**, *89* (14), 3652–3653.

(32) Miyaura, N.; Yoshinari, T.; Itoh, M.; Suzuki, A. Reaction of Lithium Alkynyltrialkylborates with Propionic Acid. General and Convenient Syntheses of Internal and Terminal Olefins Using Organoboranes. *Tetrahedron Lett.* **1974**, *15* (34), 2961–2964.

(33) Matteson, D. S.; Mah, R. W. H. Neighboring Boron in Nucleophilic Displacement. *J. Am. Chem. Soc.* **1963**, *85* (17), 2599–2603.

(34) Aggarwal, V. K.; Fang, G. Y.; Ginesta, X.; Howells, D. M.; Zaja, M. Toward an Understanding of the Factors Responsible for the 1,2-Migration of Alkyl Groups in Borate Complexes. *Pure Appl. Chem.* **2006**, *78* (2), 215–229.

(35) Namirembe, S.; Morken, J. P. Reactions of Organoboron Compounds Enabled by Catalyst-Promoted Metalate Shifts. *Chem. Soc. Rev.* **2019**, *48* (13), 3464–3474.

(36) Binger, P.; Benedikt, G.; Rotermund, G. W.; Köster, R. Borverbindungen, XV. Alkalimetall-Alkyl-1-Alkinyl-Boranate. *Justus Liebigs Ann. Chem.* **1968**, *717* (1), 21–40.

(37) Zhang, L.; Lovinger, G. J.; Edelstein, E. K.; Szymaniak, A. A.; Chierchia, M. P.; Morken, J. P. Catalytic Conjunctive Cross-Coupling Enabled by Metal-Induced Metallate Rearrangement. *Science* **2016**, *351* (6268), 70–74.

(38) Edelstein, E. K.; Namirembe, S.; Morken, J. P. Enantioselective Conjunctive Cross-Coupling of Bis(Alkenyl)Borates: A General Synthesis of Chiral Allylboron Reagents. *J. Am. Chem. Soc.* **2017**, *139* (14), 5027–5030.

(39) Lovinger, G. J.; Morken, J. P. Ni-Catalyzed Enantioselective Conjunctive Coupling with C(Sp3) Electrophiles: A Radical-Ionic Mechanistic Dichotomy. *J. Am. Chem. Soc.* **2017**, *139* (48), 17293–17296.

(40) Chierchia, M.; Law, C.; Morken, J. P. Nickel-Catalyzed Enantioselective Conjunctive Cross-Coupling of 9-BBN Borates. *Angew. Chem. Int. Ed.* **2017**, *56* (39), 11870–11874.

(41) Myhill, J. A.; Wilhelmsen, C. A.; Zhang, L.; Morken, J. P. Diastereoselective and Enantioselective Conjunctive Cross-Coupling Enabled by Boron Ligand Design. *J. Am. Chem. Soc.* **2018**, *140* (45), 15181–15185.

(42) Ishida, N.; Shimamoto, Y.; Murakami, M. Stereoselective Synthesis of (E)-(Trisubstituted Alkenyl)Borinic Esters: Stereochemistry Reversed by Ligand in the Palladium-Catalyzed Reaction of Alkynylborates with Aryl Halides. *Org. Lett.* **2009**, *11* (23), 5434–5437.

(43) Ishida, N.; Narumi, M.; Murakami, M. Synthesis of Amine−Borane Intramolecular Complexes through Palladium-Catalyzed Rearrangement of Ammonioalkynyltriarylborates. *Org. Lett.* **2008**, *10* (6), 1279–1281.

(44) Ishida, N.; Miura, T.; Murakami, M. Stereoselective Synthesis of Trisubstituted Alkenylboranes by Palladium-Catalysed Reaction of Alkynyltriarylborates with Aryl Halides. *Chem. Commun.* **2007**, No. 42, 4381–4383.

(45) Shimamoto, Y.; Sunaba, H.; Ishida, N.; Murakami, M. Regioselective Construction of Indene Skeletons by Palladium-Catalyzed Annulation of Alkynylborates with o-Iodophenyl Ketones. *Eur. J. Org. Chem.* **2013**, *2013* (8), 1421–1424.

(46) Sebald, A.; Wrackmeyer, B. Novel Synthesis of Platinum(II) Alkenyl Compounds via Organoboration of Platinum(II) Acetylides. *J. Chem. Soc. Chem. Commun.* **1983**, No. 6, 309–310.

(47) Shapiro, N. D.; Toste, F. D. Synthesis and Structural Characterization of Isolable Phosphine Coinage Metal π-Complexes. *Proc. Natl. Acad. Sci.* **2008**, *105* (8), 2779–2782.

(48) Sałat, K.; Jakubowska, A.; Kulig, K. Zucapsaicin for the Treatment of Neuropathic Pain. *Expert Opin. Investig. Drugs* **2014**, *23* (10), 1433–1440.

(49) Kaga, H.; Miura, M.; Orito, K. A Facile Procedure for Synthesis of Capsaicin. *J. Org. Chem.* **1989**, *54* (14), 3477–3478.

(50) Mann, T. J.; Speed, A. W. H.; Schrock, R. R.; Hoveyda, A. H. Catalytic Z-Selective Cross-Metathesis with Secondary Silyl- and Benzyl-Protected Allylic Ethers: Mechanistic Aspects and Applications to Natural Product Synthesis. *Angew. Chem. Int. Ed.* **2013**, *52* (32), 8395–8400.

(51) Lu, T.; Gu, M.; Zhao, Y.; Zheng, X.; Xing, C. Autophagy Contributes to Falcarindiol-Induced Cell Death in Breast Cancer Cells with Enhanced Endoplasmic Reticulum Stress. *PLOS ONE* **2017**, *12* (4), e0176348.

(52) Molander, G. A.; Argintaru, O. A. Stereospecific Ni-Catalyzed Cross-Coupling of Potassium Alkenyltrifluoroborates with Alkyl Halides. *Org. Lett.* **2014**, *16* (7), 1904–1907.

(53) Biermann, U.; Butte, W.; Koch, R.; Fokou, P. A.; Türünç, O.; Meier, M. A. R.; Metzger, J. O. Initiation of Radical Chain Reactions of Thiol Compounds and Alkenes without Any Added Initiator: Thiol-Catalyzed Cis/Trans Isomerization of Methyl Oleate. *Chem. – Eur. J.* **2012**, *18* (26), 8201–8207.

(54) Laitar, D. S.; Müller, P.; Gray, T. G.; Sadighi, J. P. A Carbene-Stabilized Gold(I) Fluoride: Synthesis and Theory. *Organometallics* **2005**, *24* (19), 4503–4505.

(55) Yu, X.-Y.; Patrick, B. O.; James, B. R. New Rhodium(I) Carbene Complexes from Carbene Transfer Reactions. *Organometallics* **2006**, *25* (9), 2359–2363.

(56) Yatham, V. R.; Harnying, W.; Kootz, D.; Neudörfl, J.-M.; Schlörer, N. E.; Berkessel, A. 1,4-Bis-Dipp/Mes-1,2,4-Triazolylidenes: Carbene Catalysts That Efficiently Overcome Steric Hindrance in the Redox Esterification of α- and β-Substituted α,β-Enals. *J. Am. Chem. Soc.* **2016**, *138* (8), 2670–2677.

(57) Rucker, R. P.; Whittaker, A. M.; Dang, H.; Lalic, G. Synthesis of Tertiary Alkyl Amines from Terminal Alkenes: Copper-Catalyzed Amination of Alkyl Boranes. *J. Am. Chem. Soc.* **2012**, *134* (15), 6571–6574.

(58) Hintermann, L.; Kribber, T.; Labonne, A.; Paciok, E. Aldol Synthesis by Anti-Markovnikov Hydration of Propargyloxy Substrates: Feasibility, Stereospecifity, and Reiterative Alkynylation-Hydration. *Synlett* **2009**, (15), 2412–2416.

(59) Mailig, M.; Hazra, A.; Armstrong, M. K.; Lalic, G. Catalytic Anti-Markovnikov Hydroallylation of Terminal and Functionalized Internal Alkynes: Synthesis of Skipped Dienes and Trisubstituted Alkenes. *J. Am. Chem. Soc.* **2017**, *139* (20), 6969–6977.

(60) Uehling, M. R.; Rucker, R. P.; Lalic, G. Catalytic Anti-Markovnikov Hydrobromination of Alkynes. *J. Am. Chem. Soc.* **2014**, *136* (24), 8799–8803.

(61) Balas, L.; Bertrand-Michel, J.; Viars, F.; Faugere, J.; Lefort, C.; Caspar-Bauguil, S.; Langin, D.; Durand, T. Regiocontrolled Syntheses of FAHFAs and LC-MS/MS Differentiation of Regioisomers. *Org. Biomol. Chem.* **2016**, *14* (38), 9012–9020.

(62) Abdel Ghani, S. B.; Chapman, J. M.; Figadère, B.; Herniman, J. M.; Langley, G. J.; Niemann, S.; Brown, R. C. D. Total Synthesis and Stereochemical Assignment of *Cis* -Uvariamicin I and *Cis* -Reticulatacin. *J. Org. Chem.* **2009**, *74* (18), 6924–6928.

(63) Lawson, E. C. Preparation of Indoylpropylaminobutanamide Derivatives and Analogs for Use as DPP-1 Inhibitors. U.S. Patent WO 2011/075634 A1, June 23, 2011.

(64) Harwood, L. M.; Leeming, S. A.; Isaacs, N. S.; Jones, G.; Pickard, J.; Thomas, R. M.; Watkin, D. The High Pressure Mediated Intramolecular Diels-Alder Reaction of Furans: Factors Controlling Cycloaddition with Monoactivated Dienophiles. *Tetrahedron Lett.* **1988**, *29* (39), 5017–5020.

(65) Tayama, E.; Toma, Y. Stereoselective Preparation of (1Z)- and (1E)-N-Boc-1-Amino-1,3-Dienes by Stereospecific Base-Promoted 1,4-Elimination. *Tetrahedron* **2015**, *71* (4), 554–559.

(66) Reed, N. L.; Herman, M. I.; Miltchev, V. P.; Yoon, T. P. Photocatalytic Oxyamination of Alkenes: Copper(II) Salts as Terminal Oxidants in Photoredox Catalysis. *Org. Lett.* **2018**, *20* (22), 7345–7350.

(67) Cocq, K.; Saffon-Merceron, N.; Coppel, Y.; Poidevin, C.; Maraval, V.; Chauvin, R. *Carbo* -Naphthalene: A Polycyclic *Carbo* -Benzenoid Fragment of α-Graphyne. *Angew. Chem. Int. Ed.* **2016**, *55* (48), 15133–15136.

(68) Narra, N.; Kaki, S. S.; Prasad, R. B. N.; Misra, S.; Dhevendar, K.; Kontham, V.; Korlipara, P. V. Synthesis and Evaluation of Anti-Oxidant and Cytotoxic Activities of Novel 10-Undecenoic Acid Methyl Ester Based Lipoconjugates of Phenolic Acids. *Beilstein J. Org. Chem.* **2017**, *13*, 26–32.

(69) Chen, C.; Luo, Y.; Fu, L.; Chen, P.; Lan, Y.; Liu, G. Palladium-Catalyzed Intermolecular Ditrifluoromethoxylation of Unactivated Alkenes: CF_3 O-Palladation Initiated by Pd(IV). *J. Am. Chem. Soc.* **2018**, *140* (4), 1207–1210.

(70) Park, S. R.; Kim, C.; Kim, D.; Thrimurtulu, N.; Yeom, H.-S.; Jun, J.; Shin, S.; Rhee, Y. H. Entry to β-Alkoxyacrylates via Gold-Catalyzed Intermolecular Coupling of Alkynoates and Allylic Ethers. *Org. Lett.* **2013**, *15* (6), 1166–1169.

(71) Wilkinson, M. C.; Higson, M. Improved Preparation of an Epoxy Substituted Reactive Mesogen. *Org. Process Res. Dev.* **2017**, *21* (1), 75–78.

(72) Wang, X.; Wu, Y. Direct Oxidative Isoperfluoropropylation of Terminal Alkenes *via* Hexafluoropropylene (HFP) and Silver Fluoride. *Chem. Commun.* **2018**, *54* (15), 1877–1880.

(73) Danon, J. J.; Krüger, A.; Leigh, D. A.; Lemonnier, J.-F.; Stephens, A. J.; Vitorica-Yrezabal, I. J.; Woltering, S. L. Braiding a Molecular Knot with Eight Crossings. *Science* **2017**, *355* (6321), 159–162.

(74) Ponomarenko, S. A.; Borshchev, O. V.; Meyer-Friedrichsen, T.; Pleshkova, A. P.; Setayesh, S.; Smits, E. C. P.; Mathijssen, S. G. J.; de Leeuw, D. M.; Kirchmeyer, S.; Muzafarov, A. M. Synthesis of Monochlorosilyl Derivatives of Dialkyloligothiophenes for Self-Assembling Monolayer Field-Effect Transistors. *Organometallics* **2010**, *29* (19), 4213–4226.

(75) Midland, M. M.; Koops, R. W. Asymmetric Hetero Diels-Alder Reaction of .Alpha.-Alkoxy Aldehydes with Activated Dienes. The Scope of Lewis Acid Chelation-Controlled Cycloadditions. *J. Org. Chem.* **1990**, *55* (17), 5058–5065.

(76) Lazzaroni, S.; Dondi, D.; Fagnoni, M.; Albini, A. Photochemical Arylation Reactions by 4-Chlorothioanisole. *Eur. J. Org. Chem.* **2007**, *2007* (26), 4360–4365.

(77) Solinski, A. E.; Koval, A. B.; Brzozowski, R. S.; Morrison, K. R.; Fraboni, A. J.; Carson, C. E.; Eshraghi, A. R.; Zhou, G.; Quivey, R. G.; Voelz, V. A.; Buttaro, B. A.; Wuest, W. M. Diverted Total Synthesis of Carolacton-Inspired Analogs Yields Three Distinct Phenotypes in *Streptococcus Mutans* Biofilms. *J. Am. Chem. Soc.* **2017**, *139* (21), 7188–7191.

(78) Guo, Y.; Shen, Z. Palladium-Catalyzed Allylic C–H Oxidation under Simple Operation and Mild Conditions. *Org. Biomol. Chem.* **2019**, *17* (12), 3103–3107.

(79) Ueno, Y.; Sano, H.; Okawara, M. Deoxygenation of Allylic Alcohols to Terminal Olefins via Stannylation/Destannylation. *Tetrahedron Lett.* **1980**, *21* (18), 1767–1770.

(80) Bauer, J. M.; Frey, W.; Peters, R. Asymmetric Cascade Reaction to Allylic Sulfonamides from Allylic Alcohols by Palladium(II)/Base-Catalyzed Rearrangement of Allylic Carbamates. *Angew. Chem. Int. Ed.* **2014**, *53* (29), 7634–7638.

(81) Bruker. *SAINT*; BrukerAXS Inc: Madison, Wisconsin, USA, 2007.

(82) Bruker. *SADABS*; BrukerAXS Inc: Madison, Wisconsin, USA, 2007.

(83) Bruker. *APEX2*; BrukerAXS Inc: Madison, Wisconsin, USA, 2007.

(84) Sheldrick, G. M. SHELXT – Integrated Space-Group and Crystal-Structure Determination. *Acta Crystallogr. Sect. Found. Adv.* **2015**, *71* (1), 3–8.

(85) Altomare, A.; Burla, M. C.; Camalli, M.; Cascarano, G. L.; Giacovazzo, C.; Guagliardi, A.; Moliterni, A. G. G.; Polidori, G.; Spagna, R. SIR97: A New Tool for Crystal Structure Determination and Refinement. *J. Appl. Crystallogr.* **1999**, *32* (1), 115–119.

(86) Altomare, A.; Cascarano, G.; Giacovazzo, C.; Guagliardi, A. Completion and Refinement of Crystal Structures with SIR92. *J. Appl. Crystallogr.* **1993**, *26* (3), 343–350.

(87) G. M. Sheldrick. *SHELXL-97, Program for the Refinement of Crystal Structures*; University of Göttingen: Germany, 1997.

(88) Sheldrick, G. M. Crystal Structure Refinement with SHELXL. *Acta Crystallogr. Sect. C Struct. Chem.* **2015**, *71* (1), 3–8.

(89) S. Mackay; C. Edwards; A. Henderson; C. Gilmore; K. Shankland. *MaXus: A Computer Program for the Solution and Refinement of Crystal Structures from Diffraction Data*; University of Glasgow: Scotland, 1997.

(90) Waasmaier, D.; Kirfel, A. New Analytical Scattering-Factor Functions for Free Atoms and Ions. *Acta Crystallogr. A* **1995**, *51* (3), 416–431.

(91) Farrugia, L. J. ORTEP-3 for Windows - a Version of ORTEP-III with a Graphical User Interface (GUI). *J. Appl. Crystallogr.* **1997**, *30* (5), 565–565.

Chapter 4. MECHANISM OF THE *Z*-SELECTIVE HYDROALKYLATION OF TERMINAL ALKYNES

4.1 **INTRODUCTION**

Alkenes are an important class of organic molecules present among biologically active compounds and in variety of synthetic intermediates. The key structural feature of alkenes is the presence of a π-bond, which hinders the free rotation around the carbon-carbon σ-bond and imparts conformational rigidity to a molecule. The hindered rotation often leads to two distinct diastereomeric arrangements of substituents around the double bond – commonly denoted as E and Z isomers. The ubiquitous nature of alkenes has led to development of a wide range of methods for their synthesis with special attention paid to controlling the stereochemistry of the π-bond.

Recently, the hydroalkylation of alkynes has emerged as a new and powerful approach to the synthesis of alkenes. While the approach encompasses a mechanistically diverse set of transformations, they all involve the addition of a hydrogen and an alkyl group to a π-bond of an alkyne. The approach is convergent,[1,2] as it results in the formation of a new C-C σ-bond. It is also highly versatile and allows access to various isomers of alkenes (**Scheme 4.1a**). By controlling the regioselectivity of the addition (Markovnikov vs anti-Markovnikov) different structural isomers of an alkene can be formed from the same alkyne precursor. For example, terminal alkynes can be used as a precursor to both 1,1-disubstituted alkenes[3,4] and 1,2-disubtituted alkenes.[5-10] Several methods have also been developed for the synthesis of trisubstituted alkenes through the hydroalkylation of internal alkynes, although controlling the regioselectivity in this case is still a challenge.[4,11-15] Another feature of hydroalkylation reactions is that they establish the double bond

geometry of the resulting alkene, and either the E or Z isomer of a 1,2-disubstitute alkene can be accessed from the same terminal alkyne. As a result, significant effort has been devoted to controlling the relative stereochemistry of the hydroalkylation (syn vs anti) that ultimately determines the E/Z selectivity of the alkene formation.

Scheme 4.1 Approaches to the Hydroalkylation of Terminal Alkynes

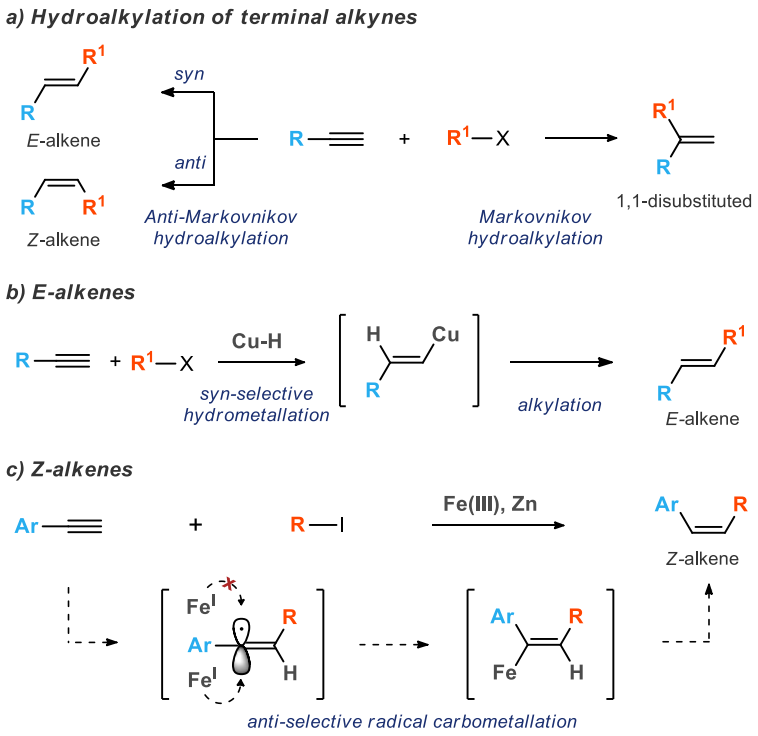

The formation of *E*-1,2-Disubstituted alkenes require syn hydroalkylation reactions. The development of such reactions has heavily relied on the well-established syn selectivity of alkyne insertion into metal hydrides (**Scheme 4.1b**). The syn selective hydrocupration[16,17] of terminal alkynes has often been used to access *E*-alkenyl copper intermediates with high selectivity. Subsequent alkylation of these intermediates provides *E*-alkenes. The alkylation has been accomplished in several ways including a direct alkylation with strong alkyl electrophiles,[6] an alkylation promoted by a nickel catalyst,[7] and an alkylation promoted by a SET (single electron

transfer) oxidation of the alkenyl copper intermediate.[8] Regardless of the methods used for alkylation, in all reactions, the *E*-selectivity is established in the hydrocupration step.

The synthesis of *Z*-alkenes from terminal alkynes has been more challenging. The key problem is the lack of obvious strategies for anti-selective additions to π-bonds that can be adapted to catalytic hydroalkylations. For example, while the anti-selective *hydroarylation* of alkynes has been known since 1998,[18,19] the underlying mechanism[20] did not allow the development of the analogous hydroalkylation reaction. Only later, in 2015, was the first catalytic *Z*-selective hydroalkylation of alkynes reported by Hu et al. (**Scheme 4.1c**).[5] Their innovative approach involves a reaction of activated aryl alkynes[21] with alkyl iodides in the presence of an iron catalyst and zinc reductant. The method relies on the anti-selectivity previously observed[22,23] in radical additions to alkynes.[24] The diastereodetermining step is the capture of the alkenyl radical by the iron catalyst (**Scheme 4.1c**). The formation of the metal-carbon bond occurs preferentially from the less hindered side of the linear alkenyl radical intermediate and establishes the cis arrangement of the aryl and alkyl groups. Driven by steric interactions,[23] the selectivity varies with the size of the alkyl group delivered and is the highest with tertiary alkyl groups. When primary alkyl iodides are used, *Z*-selectivity is generally lower than 10:1. A similar approach was later explored by Nishikata et al. with similar results.[9]

In 2019, our group reported a new method for the *Z*-selective hydroalkylation of alkynes (**Scheme 4.2a**).[10] In the presence of a silver catalyst, supported by a sterically demanding Tri[25] or IPr[26] NHC ligand (see **Scheme 4.2a** for structures), alcohol, and an alkoxide base, simple terminal alkynes react with alkylboranes to produce *Z*-alkenes. The reaction has an excellent substrate scope and can be performed in the presence of alcohols, aldehydes, ketones, nitriles, esters, aryl halides and many other functional groups. The most remarkable feature of the reaction, however, is the

consistently high *Z*-selectivity. Analysis of crude reaction mixtures revealed that *Z*-selectivity is greater than 300:1.

The surprisingly high selectivity of the reaction, together with the unusual way in which we discovered it, sparked our interest in understanding the reaction mechanism.[27] The initial experiments in which we observed *Z*-selective hydroalkylation were part of our pursuit of a carbometallation reaction (**Scheme 4.2b**). We anticipated the formation of a 1,1-disubstituted alkene through alkyne insertion into an alkyl silver intermediate (carbometallation), followed by protodeargentation of the alkenyl metal intermediate, as shown in **Scheme 4.2b**. However, we observed a *Z*-alkene as the major product of the reaction.

Scheme 4.2 Prior Work and Initial Motivation

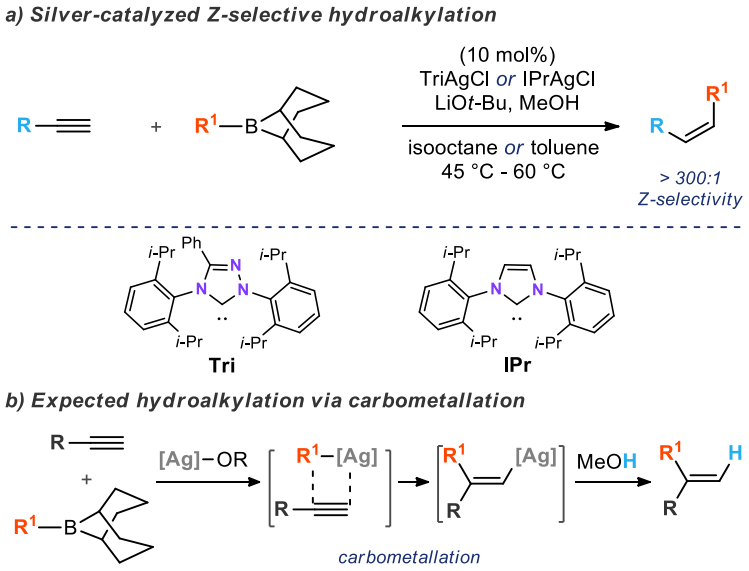

Our initial mechanistic hypothesis was a minor perturbation of the reaction sequence we had been expecting. Instead of the two electron carbometallation of the alkyne, we postulated a radical carbometallation mechanism, similar to the one proposed by Hu,[5] for the iron catalyzed hydroalkylation of alkynes (**Scheme 4.3**). According to this mechanism, the initial transmetalation (step 1) leads to the formation of the alkyl silver complex (**4.2**). Homolysis of the C-Ag bond is

followed by the addition of the alkyl radical to the alkyne (step 2) and capture of the resulting alkenyl radical (**4.3**) by the silver catalyst (step 3). Protodeargentation of alkenyl silver intermediate **4.4** by the alcohol regenerates the silver alkoxide (**4.1**) (step 4). The key steps in this mechanism, the radical carboargentation of the alkyne, was previously proposed by Terao et al. in their work on an anti-selective silver-catalyzed carbomagnesiation.[28]

Scheme 4.3 Initial Mechanistic Proposal: Radical Pathway

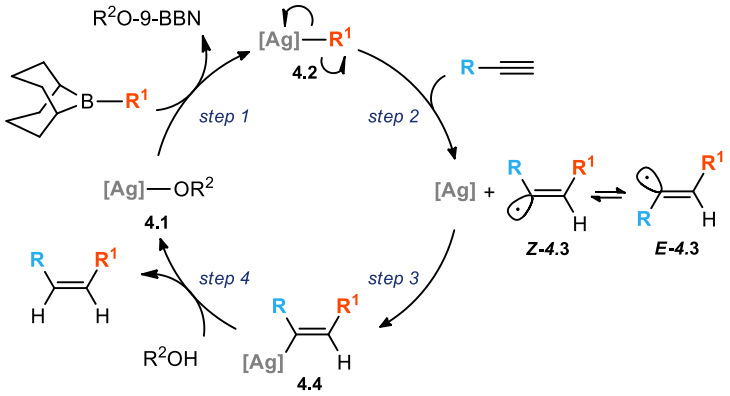

The main strength of our initial hypothesis was that, in the absence of meaningful alternatives, it provided a plausible explanation for the observed *Z*-selectivity. In analogy to Hu's mechanism,[5] the reaction of the alkenyl radical intermediate with the silver catalyst would be diastereodetermining. In our case, the unstabilized alkenyl radical would exist in a fast E/Z equilibrium (***Z*-4.3** to ***E*-4.3**).[29,30] In a typical Curtin-Hammett situation, the capture of the *Z*-alkenyl radical would kinetically dominate. Protonation of the alkenyl metal intermediate would then yield the *Z*-alkene.

Taking the mechanistic hypothesis outlined in Scheme 3 as a starting point, we explored the mechanism of the *Z*-selective hydroalkylation. In this article, we provide a full account of this study,[16] which did not support our original hypothesis and instead revealed an unprecedented new mechanism for the catalytic *Z*-selective hydroalkylation of alkynes. Our study also explored the

elementary steps of the new catalytic cycle, their relative rates, and their contributions to the overall kinetics of the reaction. Finally, the study provided insight into the origin of the unusually high diastereoselectivity of the reaction.

4.2 RESULTS

4.2.1 *Probing the Radical Mechanism Hypothesis*

We began our study by probing the feasibility of the key elementary step of the radical mechanism presented in Scheme 3. We prepared silver alkyl complex **4.5**[31] and exposed it to a simple terminal alkyne (**4.6**) at an elevated temperature (**Scheme 4.4a**). Based on the work of Terao et al.[28] we expected the formation of alkenyl silver complex **4.7** resulting from a formal anti addition. However, we did not observe the formation of the alkenyl silver complex as the starting materials were consumed. Considering that the alkenyl silver complex may not be sufficiently stable, we performed the same experiment in the presence of the alcohol used in the catalytic reaction (**Scheme 4.4b**). Again, upon complete consumption of the starting materials we did not observe the formation of the expected alkene. Instead, we observed the fast formation of ethane (not quantified) and slower formation of silver acetylide **4.8** (98% yield after 18 h). These experiments suggest that the homolysis of the alkyl silver complex and the radical addition to the alkyne are not competitive with protonation of the alkyl silver complex by an alcohol.

Scheme 4.4 Probing the Radical Based Pathway Hypothesis

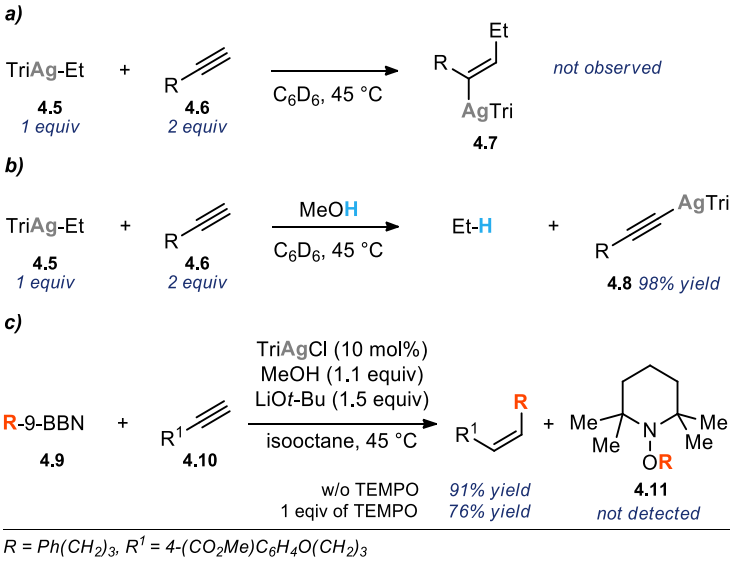

Further exploring the possibility of a mechanism with radical intermediates, we performed the catalytic reaction in the presence of TEMPO (**Scheme 4.4c**). In line with the results of the stoichiometric experiments, we found that a full equivalent of TEMPO had only a minor effect on the yield of the reaction, and we did not observe the formation of the TEMPO adduct **4.11**. This result further strengthened the conclusion that the mechanism presented in Scheme 3 is not a viable mechanism of the *Z*-selective hydroalkylation reaction.

4.2.2 *Formation and Reactivity of Silver Acetylide*

Prompted by the results shown in **Scheme 4.4a** and **b**, we focused on the formation and the reactivity of silver acetylides.[32-34] We found that in the presence of an alkoxide, the IPr supported silver catalyst quickly reacts with a terminal alkyne (**4.6**) to form silver acetylide **4.12** (**Scheme 4.5a**).

Scheme 4.5 Exploration of Silver Acetylide as an Intermediate

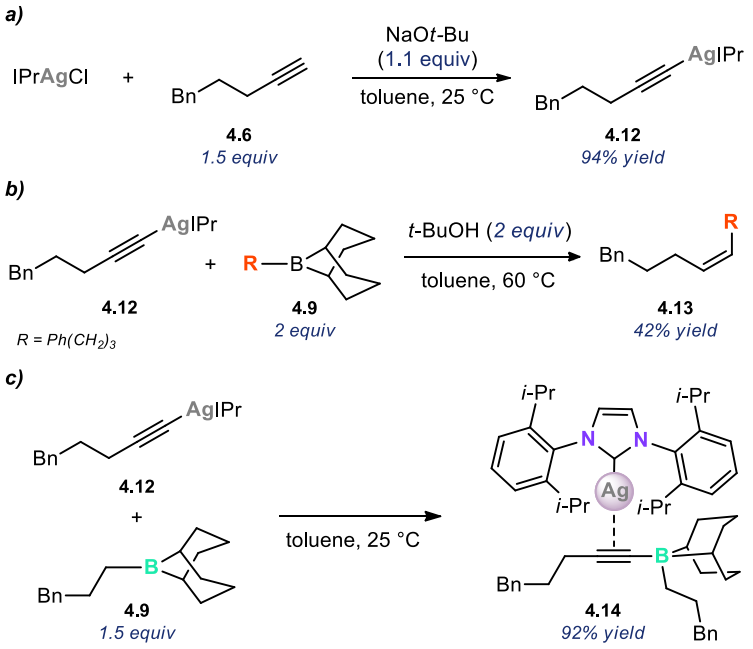

We also discovered that the reaction of acetylide **4.12** and alkylborane **4.9**, in the presence of an alcohol, gave the expected *Z*-alkene (**4.13**) in 42% yield (**Scheme 4.5b**). These experiments suggested the acetylide as a plausible intermediate in the formation of the *Z*-alkene. Hoping to intercept intermediates on the path to the *Z*-alkene we explored the reaction of the silver acetylide with an alkylborane in the absence of the alcohol. In situ ^{1}H NMR analysis of the reaction mixture indicated the fast formation of a new species that could be precipitated by the addition of pentane (**Scheme 4.5c**). This white precipitate, after filtration and careful recrystallization, provided X-ray quality crystals. The X-ray crystal structure revealed an interesting boronate complex (**4.14**) resulting from the addition of the silver acetylide to the alkylborane (**Figure 4.1a**). In this complex, the silver cation serves as a counterion to the negatively charged boronate and is coordinated to the alkyne. Qualitatively, the same results were also observed with the TriAgCl catalyst, including the formation of boronate complex **4.15**, which has also been characterized by X-ray crystallography (**Figure 4.1b**.).[10]

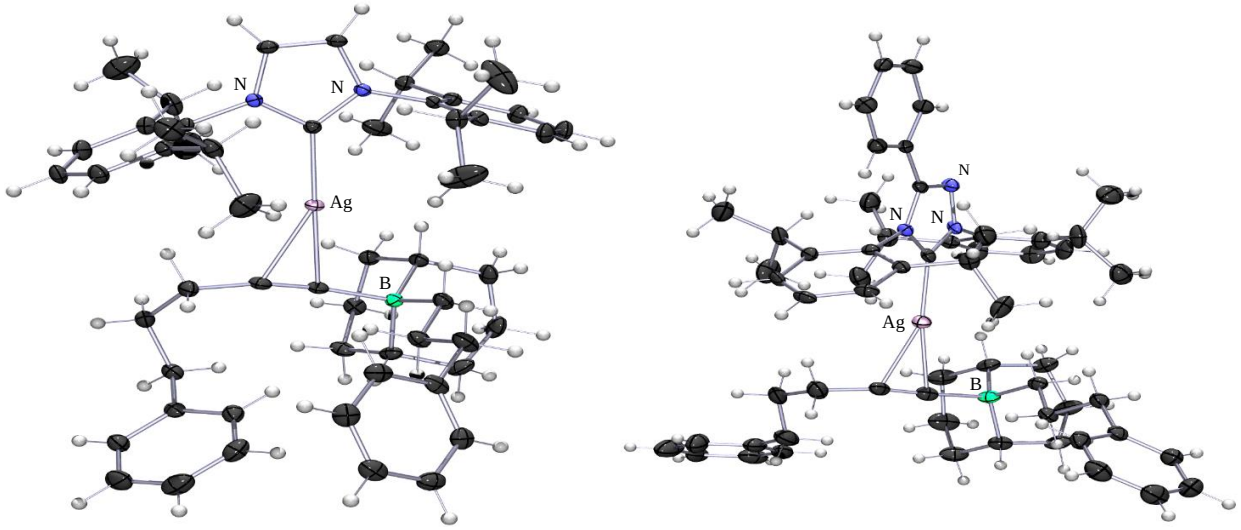

Figure 4.1 POV-Ray rendered ORTEPs of crystal structures of isolated silver complexes with thermal ellipsoids at 50% probability. a) Silver boronate complex **4.14**. b) Triazole supported silver boronate complex **4.15**

4.2.3 *An Alternative Mechanism*

The structure of the boronate complexes pointed us toward an alternative mechanism of the *Z*-selective hydroalkylation. Considering the known chemistry of alkynyl boronate complexes[35,36] (see section 4.3) and the known properties of 1,2-metallate rearrangements of boronate complexes,[37-39] we proposed the alternative mechanism shown in **Scheme 4.6**.[10] The key steps of the new catalytic cycle are the addition of the silver acetylide (**4.16**) to the alkylborane, which forms the boronate complex (**4.17**), and the subsequent 1,2-metallate shift, which yields the tetrasubstituted alkene intermediate (**4.18**). Protodeboration and protodeargentation of alkene **4.18** yield the desired *Z*-alkene product.

Scheme 4.6 An Alternative Mechanism

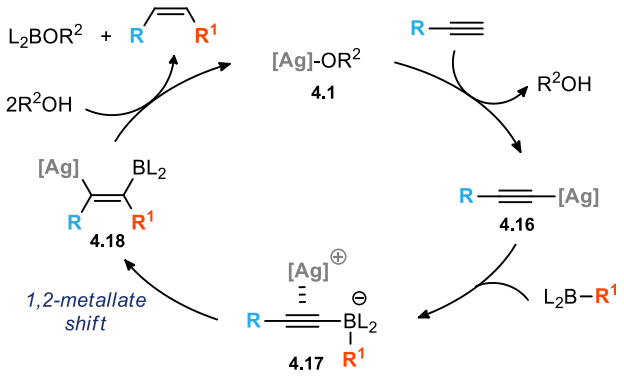

The proposed catalytic cycle presented in **Scheme 4.6** provided new directions for our mechanistic study. We were interested in further exploring the 1,2-metallate shift and the steps involved in the conversion of the tetrasubstituted intermediate to the *Z*-alkene. We were also interested in understanding the relative rates of the individual steps and their contribution to the overall kinetics of the reaction. We were hoping that the analysis of the reaction kinetics would allow us to identify the resting state of the catalyst and the rate determining step of the reaction.

4.2.4 *Silver Promoted 1,2-Metallate Rearrangement*

We decided to explore the 1,2-metallate rearrangement computationally with DFT calculations (**Scheme 4.7**).[13] We were able to identify a pathway for the rearrangement of simplified boronate complex **4.19** to **4.20**. Initially, there is a rotation around the (sp)C-B bond that changes the dihedral angle between Et and Ag from ~60° to ~180° (**Scheme 4.7**).[21] We located a transition state (see **Figure 4.2**) between this rotamer of the boronate complex (**4.19**) and the proposed tetrasubstituted alkene (**4.20**). The IRC calculation confirms the 1,2-metallate rearrangement pathway. The calculated reaction parameters indicated that the rearrangement is a slightly endergonic and likely, a highly reversible process. While the rearrangement is essentially thermoneutral, there is a significant activation barrier (24.6 kcal/mol) associated with it.

Scheme 4.7 1,2-Metallate Rearrangement

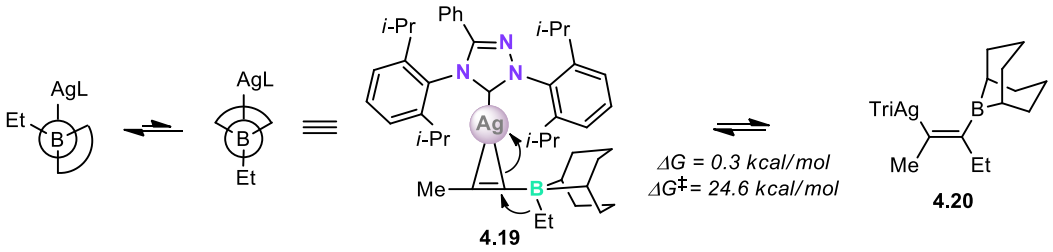

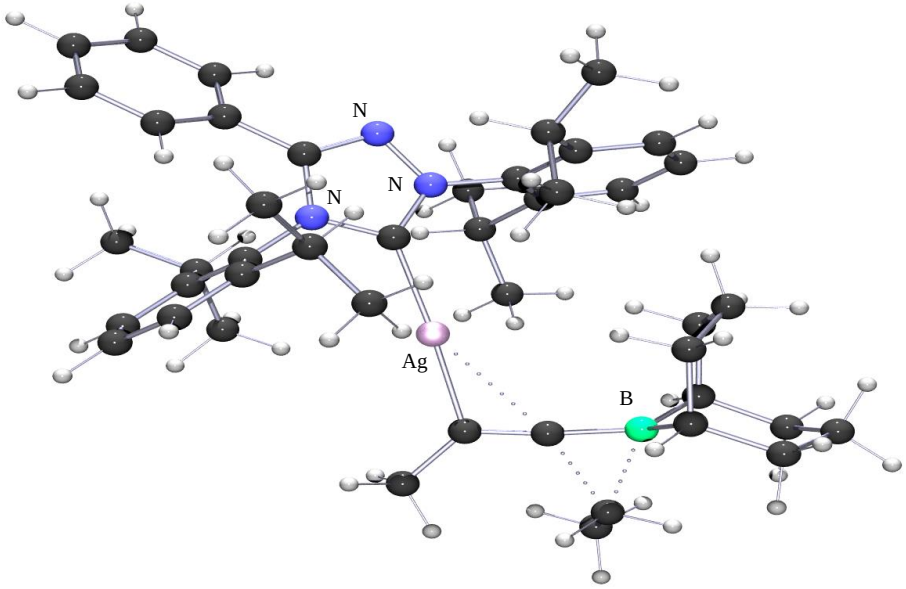

Figure 4.2 POV-Ray rendering of the calculated structure of the 1,2-metallate rearrangement transition state

4.2.5 *Protodeboration and Protodeargentation Studies*

Following the proposed catalytic cycle, we focused on the protodemetallation steps involved in the conversion of the tetrasubstituted alkene intermediate (**4.18**) into the *Z*-alkene. The initial experiments suggested that both methanol and tert-butanol can affect protodeboration of alkenyl-9-BBN **4.21** (**Scheme 4.8**). Surprisingly, we found that an alkoxide, which is present in our catalytic reaction, fully suppresses protodeboration of the alkenyl borane by either alcohol (**Scheme 4.8a**). We found support for this result in work by Brown et al. They reported that even 5 mol% of sodium methoxide is sufficient to suppress stoichiometric protodeboration of alkenyl

boranes.[40] While we do not understand the effect that the base has on protodeboration, this effect clearly suggests a different mechanism for the conversion of **4.21** into Z-alkene **4.22**.

Scheme 4.8 Protodeboration Reaction

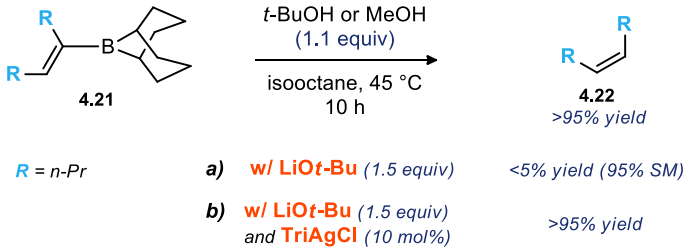

While searching for an alternative pathway to protodeboration, we found that the silver catalyst may play an important role. As shown in **Scheme 4.8b**, addition of 10 mol% of the silver catalyst to a mixture of alcohol, alkoxide, and the alkenylborane, leads to quantitative protodeboration and the formation of *Z*-alkene **4.22**. A similar silver-catalyzed protodeboration has been proposed in a recent computational study.[27]

We further investigated this process by in situ ^{1}H NMR. As shown in **Scheme 4.9** the addition of silver alkoxide[23] to alkenyl borane **4.23** (**Scheme 4.9a**) leads to the fast formation of a new species (**Scheme 4.9b**). Independent synthesis and X-ray crystallographic analysis confirmed that the new species is alkenyl silver complex **4.24**. Surprisingly, there are very few reports of transmetalation of organoboron compounds with silver complexes.[41] Furthermore, it is worth noting that **4.24** is the first example of an isolated and characterized alkenyl silver complex reported in the literature (see**Figure 4.3**).[31,42-44] Protected from air and light, the complex is stable at -35 °C for days. However, when exposed to MeOH, **4.24** is rapidly converted to the expected *Z*-alkene (**4.25**) (**Scheme 4.9c**).

Scheme 4.9 Transmetalation Protodeargentation Sequence

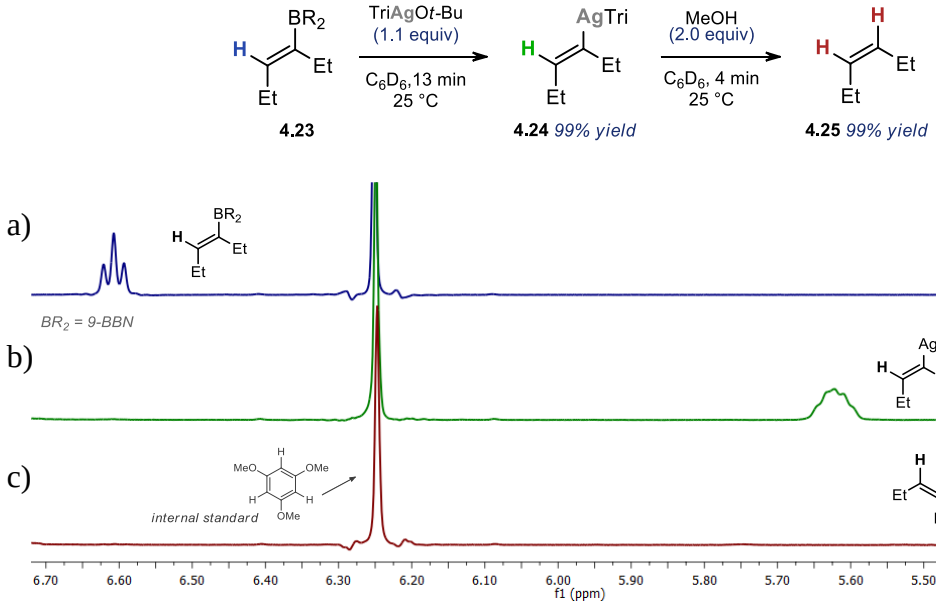

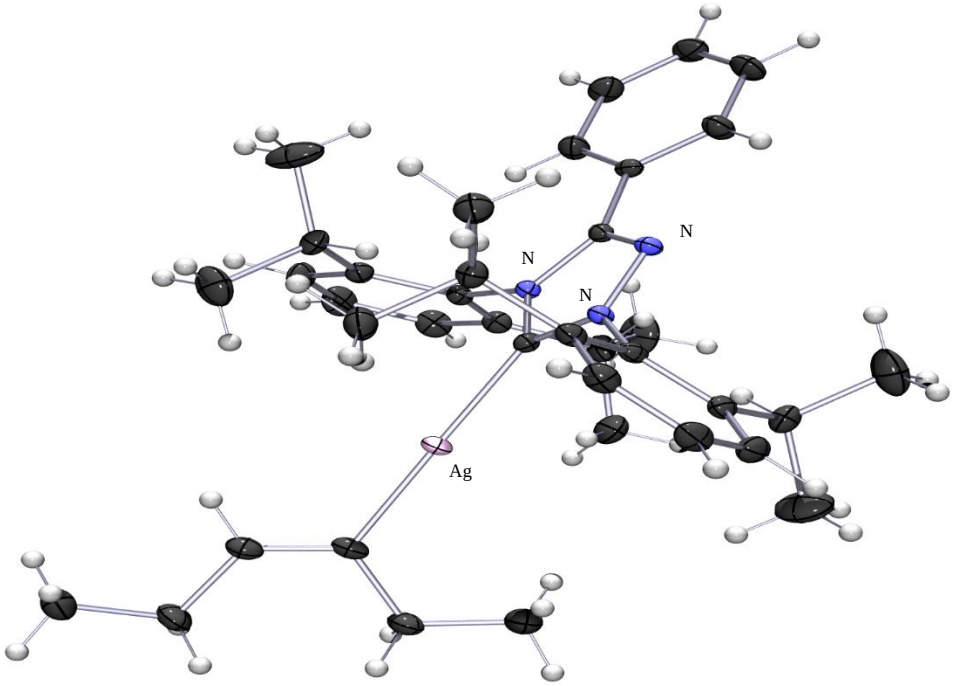

Figure 4.3 POV-Ray rendered ORTEP of the crystal structure of alkenyl silver complex **4.24** with thermal ellipsoids at 50% probability.

4.2.6 *Reaction Kinetics and KIE Experiments*

Having established the feasibility of the elementary steps involved in the proposed catalytic cycle we turned to the reaction kinetics.[26] In initial experiments, we observed that the rate of the hydroalkylation reaction remains essentially the same throughout the reaction (**Figure 4.4**). The rate doubled with the doubling of the catalyst loading ($rate_{10\ mol\%} = 3.85x10^{-2}$ mol/s vs. $rate_{20\ mol\%} = 7.53x10^{-2}$ mol/s), which confirmed that the reaction is first order in the catalyst. The simplest explanation for the constant rate was that the concentration of neither reactant was in the rate law.

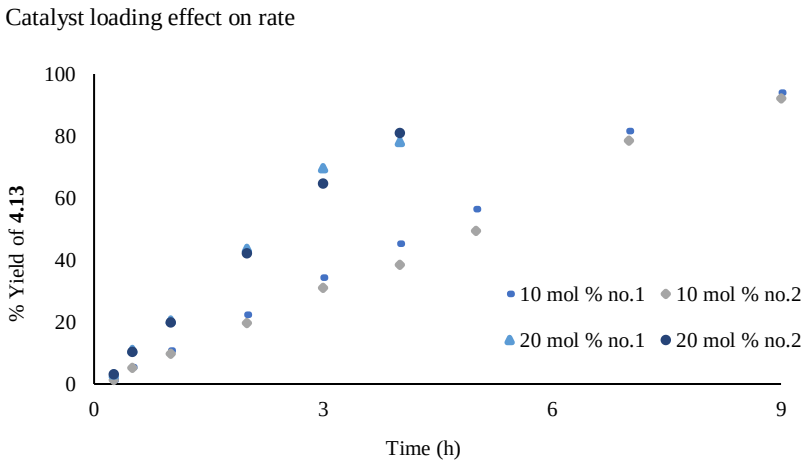

Figure 4.4 Catalyst loading effect on rate. Reaction conditions: IPrAgCl catalyst (0.1 or 0.2 equiv), LiO*t*-Bu (2.0 equiv), alkyne 6 (1.0 equiv), alkylborane 9 (1.5 equiv), methanol (1.1 equiv), and toluene (1 mL).

Measuring the rate of the reaction at various initial concentrations of alkylborane confirmed that the reaction is zeroth order in alkylborane (**Figure 4.5**).[27] Unfortunately, the reaction was not well behaved when we tried to vary the concentration of the alkyne. However, the constant rate even at high conversions makes the rate dependance on the alkyne unlikely.

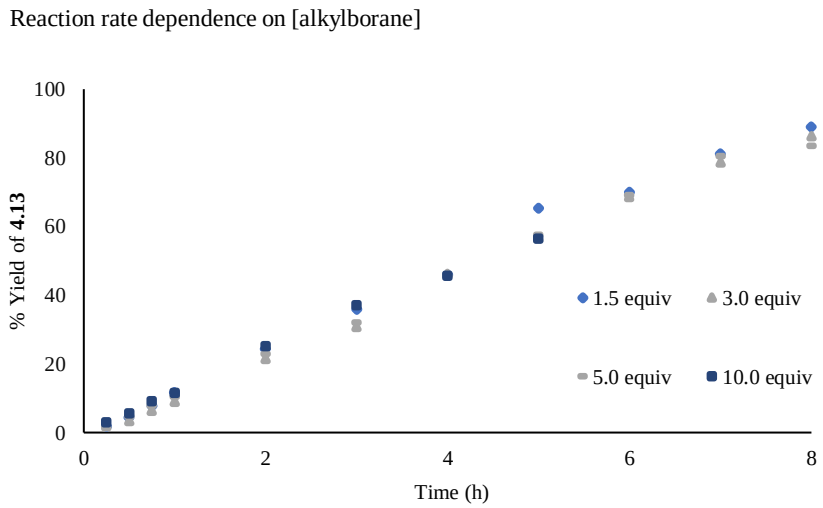

Figure 4.5 Reaction rate dependence on [alkylborane]. Reaction conditions: IPrAgCl catalyst (0.1 equiv), LiO*t*-Bu (2.0 equiv), alkyne 6 (1.0 equiv), alkylborane 9 (1.5, 3.0, 5.0, or 10.0 equiv), methanol (1.1 equiv), and toluene (1 mL).

Probing the contribution of alkyne to the reaction rate, we measured a KIE using independent rate measurements for reactions of the proteo and the deutero alkyne (**4.13** and **4.13-D**) in the presence of proteo and deutero methanol, respectively (**Scheme 4.10**a). The KIE of 1.06 suggests that neither the acetylide formation nor the proton transfers in the protodemetallation steps are the rate determining step of the reaction.

Further KIE experiments were performed to establish the KIE associated with the conversion of the boronate complex (**4.14**) to the *Z*-alkene. In the competition experiment shown in **Scheme 4.10b**, we measured a KIE of 5.8. Because we cannot distinguish the two alkene protons, this value reflects the average KIE in protodemetallation steps at the two positions. In a separate competition experiment, we also measured the intrinsic kinetic isotope effect for protodeargentation of an alkenyl silver complex and obtained KIE of 5.3 (**Scheme 4.10c**).[28] These values further strengthened the conclusion that the protodemetallation steps were not turnover limiting in the catalytic reaction.

Scheme 4.10 KIE Experiments

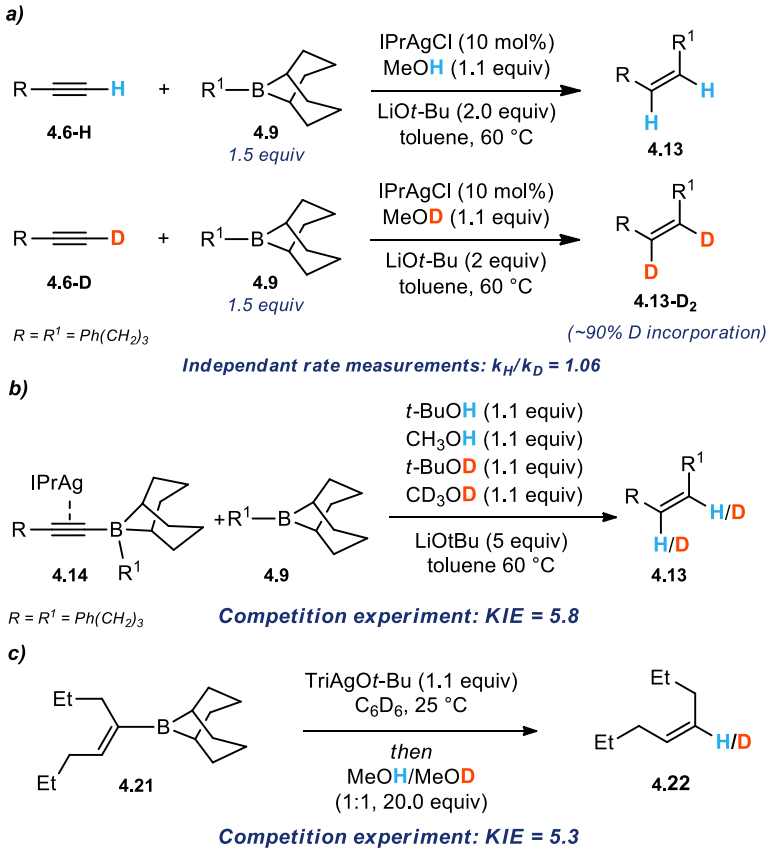

4.2.7 *Boronate Formation*

The results of the kinetics experiments led us to explore the possibility that the boronate complex is the resting state of the catalyst, while the rearrangement is the turnover limiting step. We probed the catalytic reaction performed with 20% catalyst loading by in situ ^{1}H NMR (**Figure 4.6a**). We did not observe the characteristic peak at 2.7 ppm associated with boronate complex **4.14** (**Figure 4.6b**). We later found that the addition of an alkylborane to the solution of the boronate complex removes the characteristic peak at 2.7 ppm seen in the ^{1}H NMR of the boronate complex (**Figure 4.6c**). Furthermore, the resulting ^{1}H NMR spectrum (**Figure 4.6c**) contains features similar to those found in the ^{1}H NMR spectrum obtained by in situ monitoring of a catalytic reaction (**Figure 4.6a**). We interpreted these results as an indication of the reversible

formation of the boronate complex that results in an exchange between the alkylborane part in the boronate complex and the free alkylborane. We also observed that, at a lower temperature, the characteristic peak at 2.7 ppm reemerges, providing further indication of a dynamic system (**Figure 4.6d**).

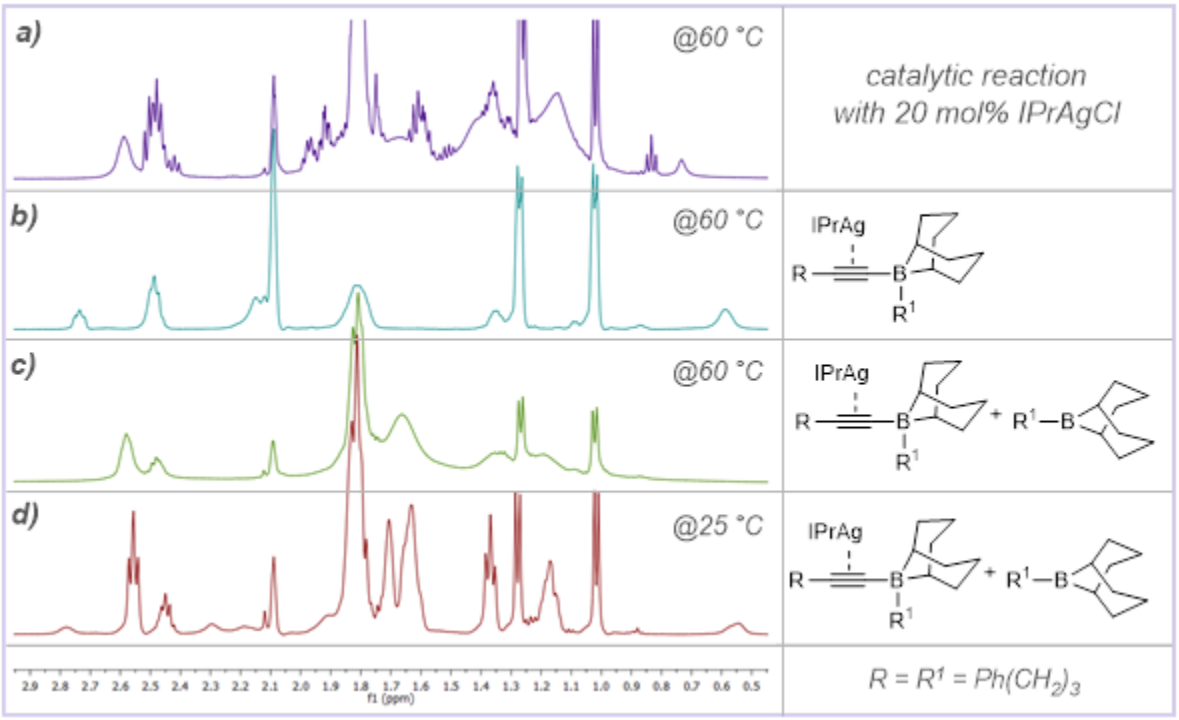

Figure 4.6 In situ ^{1}H NMR spectra. a) catalytic reaction with 20 mol% catalyst; b) boronate complex 14; c) a mixture of 14 and 9 at 60 °C; d) a mixture of 14 and 9 at 25 °C.

To test our idea about the reversible formation of the boronate complex, we performed an exchange experiment shown in **Scheme 4.11** Alkylborane Exchange Experiment. Using **4.14** and 2 equivalents of another alkylborane (**4.26**), we observed the formation of both alkene products. Even at relatively low conversion (37% combined yield of **4.13** and **4.27**), product **4.27** was formed in excess, reflecting the stoichiometry of alkylborane **4.26** relative to boronate complex **4.14** at the outset of the experiment.

The result of this experiment confirms the fast and reversible formation of the boronate complex under the conditions relevant to the catalytic reaction. This observation is also in

agreement with the results of NMR monitoring of both the stoichiometric formation of the boronate complex and the catalytic reaction.

Scheme 4.11 Alkylborane Exchange Experiment

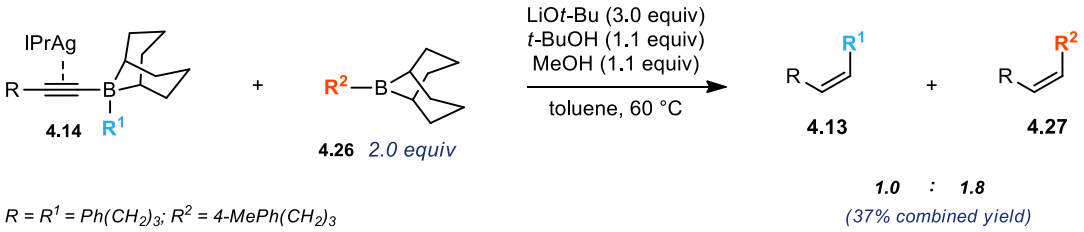

4.3 DISCUSSION

We began our study with the mechanism outlined in Scheme 3, as the only available mechanistic hypothesis consistent with the Z-selectivity of the hydroalkylation reaction. A combination of stoichiometric experiments and radical trap experiments quickly allowed us to discard this initial proposal. It is worth pointing out several other observations that also made us question the initial hypothesis. Previous examples of radical based carbometallation of alkynes required aryl alkynes as substrates because they form stabilized alkenyl radical intermediates upon the radical addition. Our reaction, on the other hand, performed well with simple alkyl-substituted alkynes. Another notable difference was an unusually high diastereoselectivity, even when small alkyl groups were delivered in the hydroalkylation reaction. This contrasts other notable reports in which excellent selectivity was only observed with the addition of tertiary alkyl radicals,[5] although some examples of radical carbostannylation of alkynes with high selectivity have been reported.[45,46]

The initial work on the radical carbometallation mechanism prompted us to explore the reactivity of the silver acetylides which had emerged as readily formed intermediates. The stoichiometric reaction of silver acetylide with alkylborane provided the desired *Z*-alkene (**Scheme**

4.5b) and pointed us toward and alternative reaction mechanism featuring alkynyl boronate complex **4.14**. Exploring literature reports of acetylide addition to alkylboranes, we found reports by Brown et al.[35] and Suzuki et al.[36] describing lithium acetylide addition to alkylboranes (**Scheme 4.12**). In these reports, they also described a Bronstead acid promoted rearrangement of the boronate[47] and the formation of the alkene with moderate to high *Z*-selectivity (**Scheme 4.12**).

Scheme 4.12 Literature Reports of Acetylide Addition to Alkylboranes

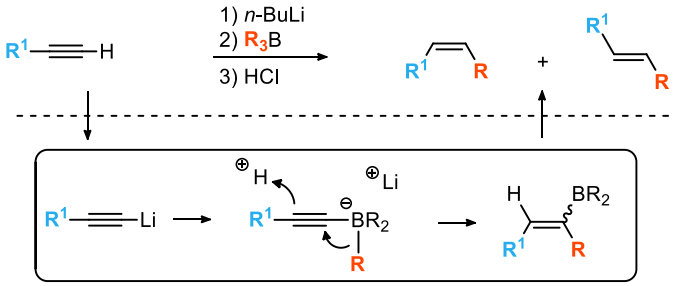

Interestingly, the rearrangement of the alkynyl boronate complex was originally proposed to involve a carbo cation intermediate.[36] However, a significant body of work has since been devoted to 1,2-metallate shifts that occur upon electrophilic activation of a π-bond of an alkenyl or alkynyl boronate complexe. The 1,2-metallate shift is generally considered to be concerted with a requirement for the antiperiplanar orientation of the electrophile activating the π-bond relative to the migrating group on boron.[39]

In combination with the literature precedents by Brown and Suzuki, our findings led us to propose the mechanism shown in Scheme 6. The overall catalytic cycle is remarkably similar to the reaction sequence reported by Brown and Suzuki (**Scheme 4.12**). The main difference is that the silver catalyst, with a mixture of an alkoxide and an alcohol, replaces both the strong base used in the formation of the acetylide and the strong Bronstead acid used to promote the 1,2-metallate shift and protodeboration. As a result, the whole reaction sequence can be performed as a single catalytic transformation.

The key feature of the alternative mechanism is that it provides a straightforward explanation for the excellent *Z*-selectivity of the reaction. The 1,2-metallate shift induced by π activation of unsaturated boronates by transition metal catalysts is well established. Initially explored by Murakami,[48] this approach has been fully developed by Morken.[38] Morken's work has also demonstrated that the 1,2-metallate shift results in the *anti* addition of the migrating group and the metal catalyst across the activated π bond.[49,50] The same *anti* relationship is evident in the transition state we identified for the 1,2-metalate shift, (**Scheme 4.7b**). A recent computational study attributes the preference for the *anti* addition to an unfavorable Pauli repulsion found in the analogous *syn* addition process.[27] Regardless of the exact origin, the strong preference for the *anti* relationship between the catalyst and the migrating group provides a simple explanation for the excellent Z-selectivity observed our hydroalkylation reaction.

One interesting feature of the 1,2-metallate shift in our reaction is that 9-BBN group behaves as a nonmigrating group. Previous examples of 1,2-metallate shift in electrophilically activated alkynyl boronate complexes featured exclusive migration of an alkyl group that is a part of 9-BBN.[51] Furthermore, in a majority of known examples of 1,2-metalaltes shifts, when present, 9-BBN group migrates preferentially.[39] Known examples of 1,2-metallate shifts in which 9-BBN is a nonmigrating group are initiated by the presence of a relatively weak leaving group at the α carbon.[52-54] The late transition state of such rearrangements has been offered as a possible explanation for unusual behavior of 9-BBN group.[39] The same explanation may apply to the essentially thermoneutral 1,2-metallate shift featured in our reaction.

The rest of our study focused on more detailed exploration of the basic mechanism presented in **Scheme 4.6**. The summary of our findings is presented in the catalytic cycle shown in **Scheme 4.13**. The main difference, compared to the mechanism shown in **Scheme 4.6**, is that

the protodeboration of intermediate **4.31** is likely promoted by the silver catalyst. Our stoichiometric experiments suggest a pathway that involves rapid transmetalation with a silver alkoxide, followed by rapid protodeargentation. Subsequent experiments in our study did not further alter the steps involved in the catalytic cycle, and instead, provided a better understanding of their relative rates.

Scheme 4.13 Proposed Mechanism for *Z*-Selective Hydroalkylation

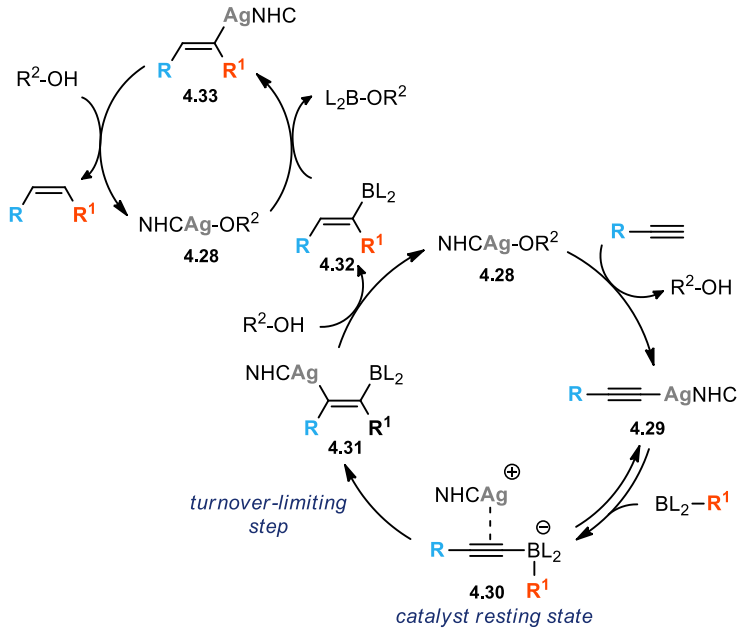

Kinetics studies and the KIE experiments focused on identifying the turnover-limiting step and the resting state of the catalyst. The constant rate throughout the course of the reaction and the zeroth order of the reaction in alkylborane, together, suggest that neither alkyne nor the alkylborane are involved in the turnover limiting step. The results of the KIE experiments strongly suggest that none of the proton transfer steps are turnover-limiting. The only two remaining steps that could be turnover limiting are the transmetalation from the alkenyl boron intermediate to silver and the 1,2-metallate shift. Considering the fast transmetalation we observed in our stoichiometric reaction, the turnover limiting step is more likely to be the 1,2-metallate shift. This conclusion is consistent

with the results of the kinetics study. The unimolecular nature of the rearrangement makes it insensitive to the concentration of any component of the reaction other than the concentration of the borate complex, which in turn is limited by the amount of the available silver catalyst. In this scenario, the thermoneutral 1,2-metallate shift is rendered irreversible by the fast protodeargentation of the product of the 1,2-metallate shift (**4.31**), consistent with the results of stoichiometric protodeargentation experiments (**Scheme 4.9**). An important implication is that the 1,2-metallate shift would also be a diastereodeterming step of the reaction.

If our analysis is correct and the 1,2-metallate shift is turnover-limiting, we would expect boronate complex to be the resting state of the catalyst. Consequently, we would expect that at a sufficiently high catalyst loading we could observe the complex by monitoring the reaction in situ. However, the results of in situ NMR experiments and the alkylborane exchange experiment are consistent with a fast equilibrium between boronate complex **4.30** and silver acetylide **4.29**. This observation, together with the fact that the reaction rate does not depend on the concentration of the alkylborane, requires a high equilibrium constant for the formation of the boronate complex. With a sufficiently high equilibrium constant, the reaction would be fully saturated in the alkylborane across a range of concentrations encountered during the reaction. Therefore, any increase in the initial alkylborane concentration does not increase the concentration of the boronate complex or the overall rate of the reaction.

4.4 CONCLUSION

We have discovered a new hydroalkylation reaction that allows reductive coupling of terminal alkynes and alkylboranes and results in a highly selective formation of the Z-alkene. The established mechanisms for hydroalkylation of alkynes seemed inadequate in explaining the

features of the new reaction. We explored the reaction mechanism and found that the available mechanistic paradigms were not relevant in our reaction. In the process, we learned enough to propose a new reaction mechanism that is consistent with all the features of our reaction and provides a straightforward explanation for its unusual diastereoselectivity. Furthermore, our study provided a detailed understanding of other steps involved in the catalytic cycle, including the silver catalyzed protodeboration of the key intermediate. Within the new mechanistic framework, we were able to identify the turnover limiting step and the likely resting state of the catalyst. We believe that these findings will be valuable in further exploration of this and related reactions.

4.5 EXPERIMENTAL

4.5.1 *General Information*

All reactions were performed under a nitrogen atmosphere with flame-dried or oven-dried (120 °C) glassware, using standard Schlenk techniques, or in a glovebox (Nexus II from Vacuum Atmospheres). Column chromatography was performed using a Biotage Iso-1SV flash purification system with silica gel from Agela Technologies Inc. ^{1}H- and ^{13}C-NMR spectra were recorded on a Bruker AV-300 or AV-500 spectrometer. ^{1}H NMR chemical shifts (δ) are reported in parts per million (ppm) downfield of TMS and are referenced relative to residual solvent peak ($CDCl_3$ (7.26 ppm), C_6D_6 (7.16 ppm), or toluene-d_8 (2.09 ppm). ^{13}C NMR chemical shifts are reported in parts per million downfield of TMS and are referenced to the carbon resonance of the solvent ($CDCl_3$(77.2 ppm), or C_6D_6 (128.1 ppm)). Data are represented as follows: chemical shift, multiplicity (s = singlet, d = doublet, t = triplet, q = quartet, p = pentet, hept = heptet, m = multiplet), coupling constants in Hertz (Hz), intergration. Mass spectra were collected on a JEOL HX-110 mass spectrometer. Gas Chromatography (GC) analysis was performed on a Shimadzu GC-2010

instrument with a flame ionization detector and a SHRXI-5MS column (15 m, 0.25 mm inner diameter, 0.25 µm film thickness). The following temperature program was used: 2 min @ 60 °C, 13 °C/min to 160 °C, 30 °C/min to 250 °C, 5.5 min @ 250 °C.

4.5.2 *Materials*

THF, CH_2Cl_2, ether, benzene, pentane, and toluene were degassed and dried by passing through columns of neutral alumina. Anhydrous methanol, deuterated methanol, and deuterated *tert*- were purchased from Millipore Sigma, degassed and stored over 4Å molecular sieves. Isooctane was purchased from Fisher Scientific and was degassed and stored over 4Åmolecular sieves. Deuterated NMR solvents were purchased from Cambridge Isotope Laboratories, Inc. and were either used as received or degassed and stored over 4Å molecular sieves prior to use. Commercial reagents were purchased from Millipore Sigma, TCI America, GFS-Chemicals, Ark-Pharm, Combi-Blocks, Oakwood Chemicals, Strem Chemicals and Alfa Aesar. 9-BBN Dimer was purchased from Millipore Sigma and recrystallized from THF.

4.5.3 *Experimental Procedures*

4.5.3.1 Reactions with Alkyl Silver Complex (5)

4.5.3.1.1 Without Methanol

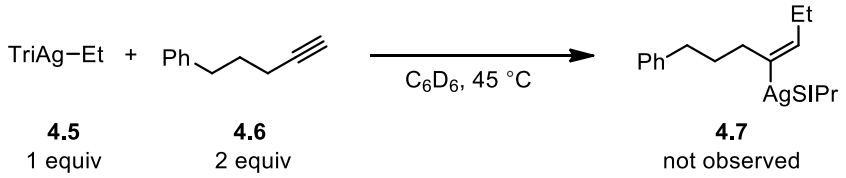

In a nitrogen filled glovebox, alkyl silver complex **4.5** (6.0 mg, 0.01 mmol, 1 equiv.) was added using 3 x 100 uL C_6D_6 to a J-Young tube. To this was added 100 uL of an 8.4 mg/mL solution of internal standard, trimethoxy benzene (TMB), (0.8mg, 0.05 mmol, 0.5 equiv.) in C_6D_6. An NMR spectrum of this solution was then recorded. The J-Young tube was then returned to the glovebox and 100 uL of a 28.8 mg/mL solution of alkyne **4.6** (2.9 mg 0.02 mmol, 2.0 equiv.) in C_6D_6 was added. An NMR spectrum of this mixture was then recorded. The J-Young tube was heated at 45°C for 20 min and another NMR spectrum was recorded.

4.5.3.1.2 With Methanol

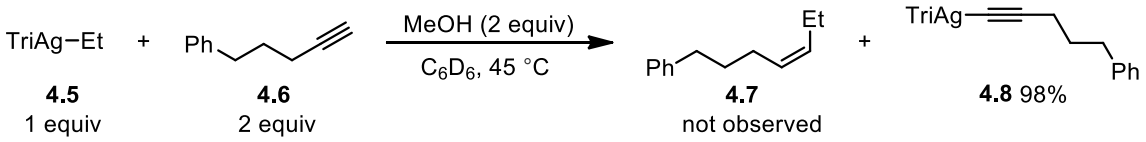

In a nitrogen filled glovebox, alkyl silver complex **4.5** (6.0 mg, 0.01 mmol, 1 equiv.) was added using 3 x 100 uL C_6D_6 to a J-Young tube. To this was added 100 uL of an 8 mg/mL solution of internal standard, TMB (0.8mg, 0.005 mmol, 0.5 equiv.) in C_6D_6. An NMR spectrum of this solution was then recorded. The J-Young tube was then returned to the glovebox and 50 uL of a 57.6 mg/mL solution of alkyne **4.6** (2.9 mg 0.02 mmol, 2.0 equiv.) in C_6D_6 was added. This was followed by 50 uL of a 10.2 mg/mL solution of MeOH (0.5 mg, 0.015 mmol, 1.5 equiv.) in C_6D_6

and an NMR spectrum was then recored. The J-Young tube was then heated at 45°C and NMR spectra were obtained after 1 hour (70% yield of TriAg acetylide **4.8**) and 18 hours (98% yield of TriAg Acetylide **4.8**).

4.5.3.2 Effect of TEMPO on the Catalytic Reaction

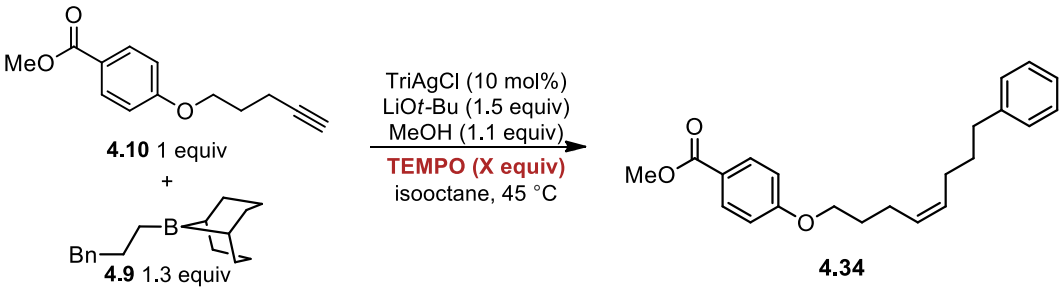

TEMPO (X equiv)	0.0	0.2	0.5	1.0	2.5
yield of XX	91%	91%	87%	76%	37%

In a nitrogen filled glovebox, a series of five 1-dram vials were each charged with a stir bar and LiO*t*-Bu (6.0 mg, 0.075 mmol, 1.5 equiv). To these was added TriAgCl catalyst (3.0 mg, 0.005 mmol, 0.10 equiv), and alkyne **4.10** (10.9 mg 0.050 mmol, 1.0 equiv). To this was added TMB (4.2 mg, 0.025 mmol, 0.5 equiv) with 3x100 uL isooctane, 50 uL of a 31.2 mg/mL solution of alkylborane **4.9** (15.6 mg, 0.065 mmol, 1.3 equiv), and 50 uL of a warmed (just enough to dissolve the methanol) solution of 35.2 mg/mL methanol (1.8 mg, 0.055 mmol, 1.10 equiv) in isooctane. The specified amount of TEMPO was then added to each reaction as 100 uL of the needed stock solution in isooctane. The reaction mixtures were heated to 45 °C and stirred overnight. After 16 hours, 25 uL aliquots of the crude reaction mixtures were pushed through short plugs of silica with ethyl acetate and analyzed by GC.

4.5.3.3 Reaction of Silver Acetylide with Alkylborane and t-BuOH

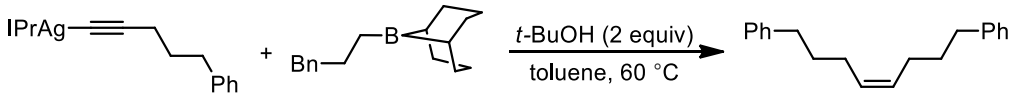

4.12 1 equiv | **4.9** 2 equiv | **4.13** 42%

In a nitrogen filled glovebox, a 1-dram vial was charged with a stir bar and silver acetylide complex **4.12** (32.0 mg, 0.05 mmol, 1 equiv.). To this was added 100 uL of a 42.0 mg/mL solution of internal standard, trimethoxy benzene (TMB), (4.2 mg, 0.025 mmol, 0.5 equiv.) in toluene. This was followed by alkylborane **4.9** (24.0 mg 0.10 mmol, 2.0 equiv.) using 3 portions of 100 uL toluene. Finally, 100 uL of a 74.1 mg/mL solution of *t*-BuOH (7.4 mg, 0.10 mmol, 2.0 equiv) in toluene was added. The reaction mixture was heated to 60 °C and stirred overnight. The next day a 25 uL aliquot of the crude reaction mixture was pushed through a short plug of silica with ethyl acetate and analyzed by GC.

4.5.3.4 Protodeboration Studies

A stock solution of 116.1 mg/mL alkenyl borane **4.21** and 42.0 mg/mL TMB in isooctane was prepared and used for the following experiments.

4.5.3.4.1 MeOH or t-BuOH

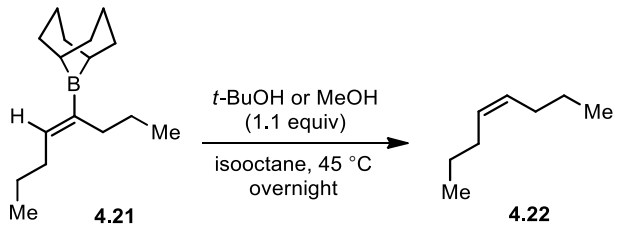

4.21 | **4.22** quantitative

In a nitrogen filled glovebox, two 1-dram vials were charged with a stir bar and 300 uL isooctane was added. To these was added 100 uL of the stock solution of alkenyl borane **4.21** (11.6 mg, 0.05 mmol, 1.0 equiv.) and TMB (4.2 mg, 0.05 mmol, 0.5 equiv). To this was added 100 uL

of either a warmed 17.6 mg/mL solution of MeOH (1.8 mg, 0.055 mmol, 1.1 equiv) in isooctane or a 40.8 mg/mL solution of *t*-BuOH (4.1 mg, 0.055 mmol, 1.1 equiv) in isooctane. The reaction mixture was heated to 45 °C and stirred overnight. The next day an aliquot of the crude reaction mixture was added to C_6D_6 in the glovebox and then a crude NMR spectrum was recorded.

4.5.3.4.2 LiOt-Bu and Alcohol

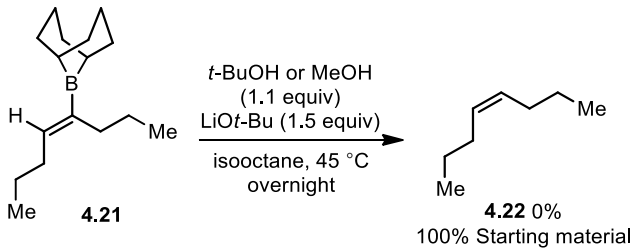

In a nitrogen filled glovebox, two 1-dram vials were charged with a stir bar and LiO*t*-Bu (6.0 mg, 0.075 mmol, 1.5 equiv) and then 300 uL isooctane was added. To this was added 100 uL of the stock solution of alkenyl borane **4.21** (11.6 mg, 0.05 mmol, 1.0 equiv.) and TMB (4.2 mg, 0.05 mmol, 0.5 equiv). To this was added 100 uL of either a warmed 17.6 mg/mL solution of MeOH (1.8 mg, 0.055 mmol, 1.1 equiv) in isooctane or a 40.8 mg/mL solution of *t*-BuOH (4.1 mg, 0.055 mmol, 1.1 equiv) in isooctane. The reaction mixture was heated to 45 °C and stirred overnight. The next day an aliquot of the crude reaction mixture was added to C_6D_6 in the glovebox and then a crude NMR spectrum was recorded.

4.5.3.4.3 With TriAgCl, Base, and Alcohol

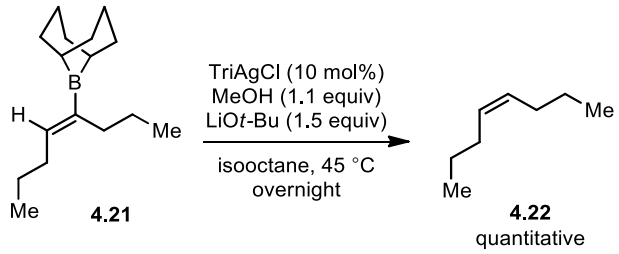

In a nitrogen filled glovebox, a 1-dram vial was charged with a stir bar, TriAgCl (3.0 mg, 0.005 mmol, 0.10 equiv), and LiO*t*-Bu (6.0 mg, 0.075 mmol, 1.5 equiv) and then 300 uL isooctane was added. To this was added 100 uL of the stock solution of alkenyl borane **4.21** (11.6 mg, 0.05 mmol, 1.0 equiv.) and TMB (4.2 mg, 0.05 mmol, 0.5 equiv). To this was added 100 uL of a warmed 17.6 mg/mL solution of MeOH (1.8 mg, 0.055 mmol, 1.1 equiv) in isooctane. The reaction mixture was heated to 45 °C and stirred overnight. The next day an aliquot of the crude reaction mixture was added to C_6D_6 in the glovebox and then a crude NMR spectrum was recorded.

4.5.3.5 Transmetalation and Protodeargentation Study

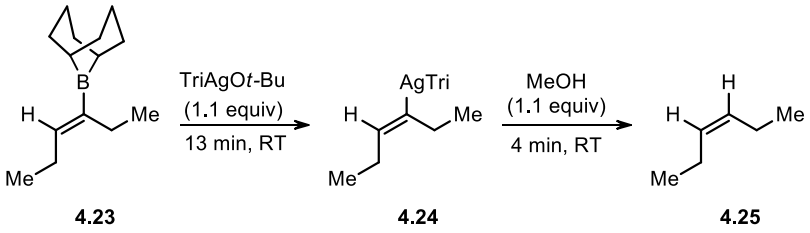

In a nitrogen filled glovebox, a 1-dram vial was charged with a stir bar and TriAgOtBu (14.2 mg, 0.022 mmol, 1.1 equiv) and then 350 uL C_6D_6 was added. To this was added 100 uL of a stock solution of 40.8 mg/mL alkenyl borane **4.23** (4.1 mg, 0.02 mmol, 1.0 equiv.) and 16.8 mg/mL TMB (1.6 mg, 0.01 mmol, 0.5 equiv). The reaction was then stirred 5 min at 25 °C and transferred to an NMR tube. While stirring, 50 uL of a 14.0 mg/mL solution of MeOH (0.7 mg, 0.022 mmol, 1.1 equiv) in C_6D_6 was drawn into a syringe. After being transferred to an NMR tube,

NMR tube and syringe were taken to the NMR facility and an NMR spectrum was recorded (8 min later). After ejection, the methanol solution was added by injecting the needle through the cap and covering with parafilm. A second spectrum was then obtained (4 min after methanol addition).

4.5.3.6 Reaction Kinetics

4.5.3.6.1 10 mol% and 20 mol% TriAgCl

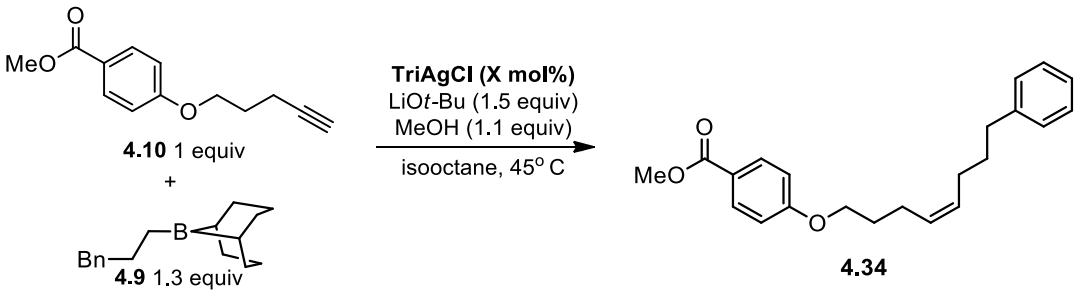

In a nitrogen filled glovebox, four 1-dram vials were each charged with a stir bar and TriAgCl catalyst (duplicates of either 6.10 mg, 0.01 mmol, 0.10 equiv or 12.2 mg, 0.02 mmol, 0.20 equiv). To these was added LiO*t*-Bu (12.0 mg, 0.15 mmol, 1.5 equiv), alkyne **4.10** (21.8 mg 0.10 mmol, 1.0 equiv) and TMB (8.4 mg, 0.05 mmol, 0.5 equiv). To this was added 600 uL isooctane, alkylborane **4.9** (31.2 mg, 1.3 mmol, 1.3 equiv) using 3x100 uL isooctane, and 100 uL of a warmed solution (to dissolve MeOH) of 35.2 mg/mL methanol (3.5 mg, 0.11 mmol, 1.10 equiv) in isooctane. 25 uL aliquots of the crude reaction mixtures were pushed through short plugs of silica with ethyl acetate at the reported times and analyzed by GC.

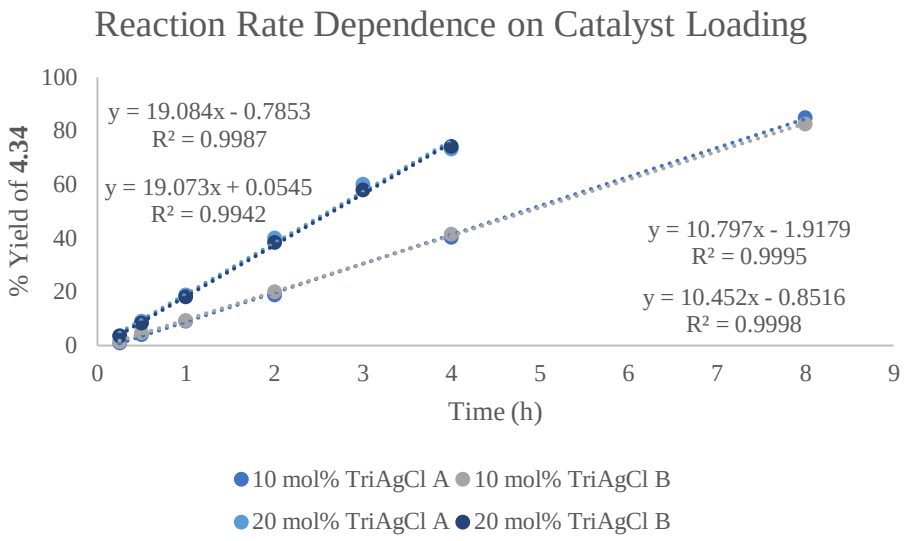

Figure 4.7 Graph of the reaction rate dependence on TriAgCl catalyst loading

Rates (average of duplicate measurements)

10 mol% TriAgCl – $Rate = 3.82x10^{-2}\,\frac{mol}{s}$

20 mol% TriAgCl – $Rate = 6.87x10^{-2}\,\frac{mol}{s}$

4.5.3.6.2 10 mol% and 20 mol% IPrAgCl

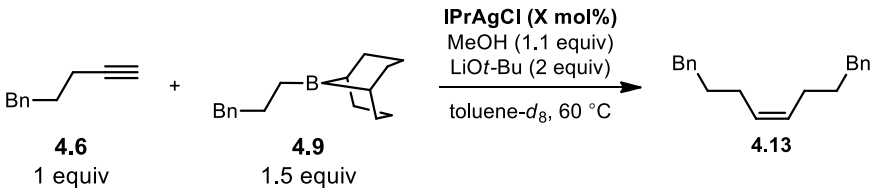

In a nitrogen filled glovebox, four 1-dram vials were each charged with a stir bar and IPrAgCl catalyst (duplicates of either 5.30 mg, 0.01 mmol, 0.10 equiv or 10.6 mg, 0.02 mmol, 0.20 equiv). To these was added LiO*t*-Bu (16.0 mg, 0.2 mmol, 2.0 equiv) and 500 uL toluene. To this was added 100 uL of a stock solution of 144.2 mg/mL alkyne **4.6** (14.4 mg, 0.10 mmol, 1.0 equiv) and 84.1 mg/mL TMB (8.4 mg, 0.05 mmol, 0.5 equiv) in toluene, alkylborane **4.9** (36.0 mg, 0.15 mmol, 1.5 equiv) using 3x100 uL toluene, and 100 uL of a solution of 35.2 mg/mL

methanol (3.5 mg, 0.11 mmol, 1.1 equiv) in toluene. 25 uL aliquots of the crude reaction mixtures were pushed through short plugs of silica with ethyl acetate at the reported times and analyzed by GC.

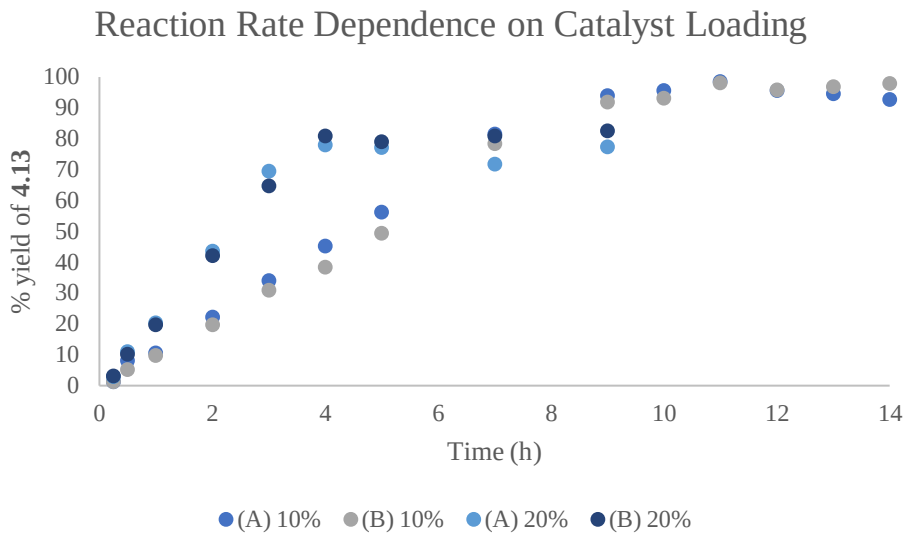

Figure 4.8 Graph of the reaction rate dependence on IPrAgCl catalyst loading: all points

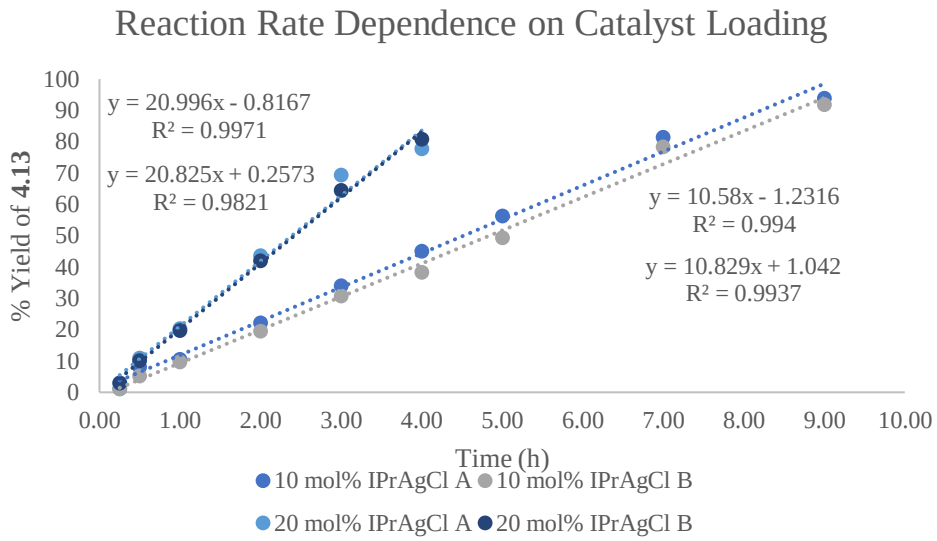

Figure 4.9 Graph of the reaction rate dependence on IPrAgCl catalyst loading: truncated

Rates (average of duplicate measurements and based on graph after removal of data points in which yield stops increasing)

10 mol% IPrAgCl – $Rate = 3.85x10^{-2}\,\frac{mol}{s}$

20 mol% IPrAgCl – $Rate = 7.53x10^{-2}\,\frac{mol}{s}$

*4.5.3.6.3 1.5, 3.0, 5.0, and 10 Equivalents Alkylborane **4.9***

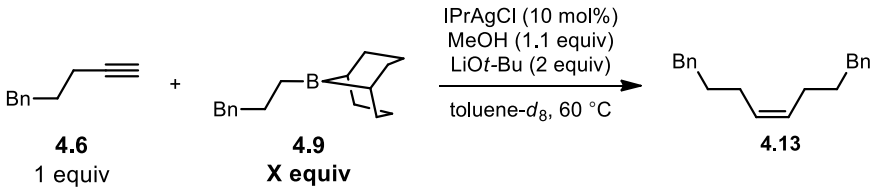

In a nitrogen filled glovebox, four 1-dram vials were each charged with a stir bar and IPrAgCl catalyst (5.30 mg, 0.01 mmol, 0.10 equiv). To these was added LiO*t*-Bu (16.0 mg, 0.2 mmol, 2.0 equiv) and 500 uL toluene. To this was added 100 uL of a stock solution of 144.2 mg/mL alkyne **4.6** (14.4 mg, 0.10 mmol, 1.0 equiv) and 84.1 mg/mL TMB (8.4 mg, 0.05 mmol, 0.5 equiv), alkylborane **4.9** (1.5, 3.0, 5,0, or 10.0 equiv) using 3x100 uL toluene, and 100 uL of a solution of 35.2 mg/mL methanol (3.5 mg, 0.11 mmol, 1.10 equiv) in toluene. 25 uL aliquots of the crude reaction mixtures were pushed through short plugs of silica with ethyl acetate at the reported times and analyzed by GC.

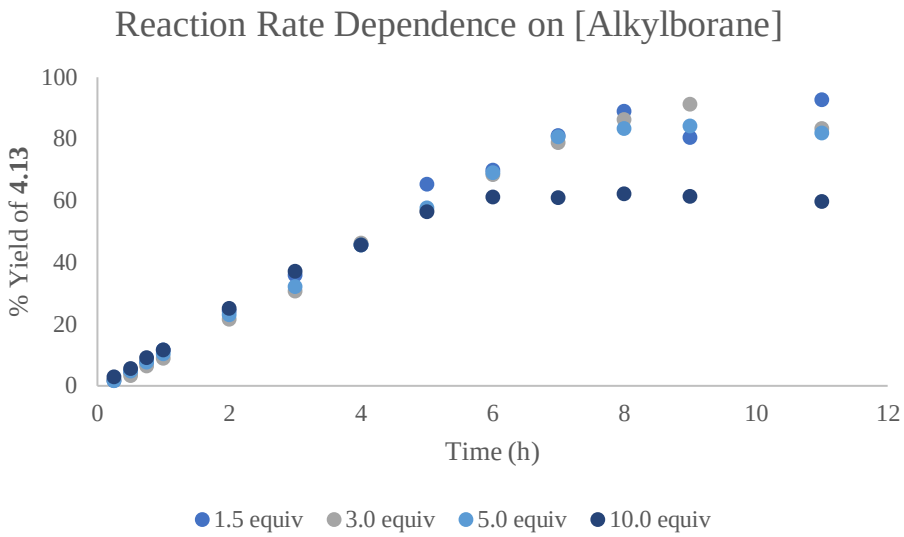

Figure 4.10 Graph of the reaction rate dependence on [alkylborane]: all points

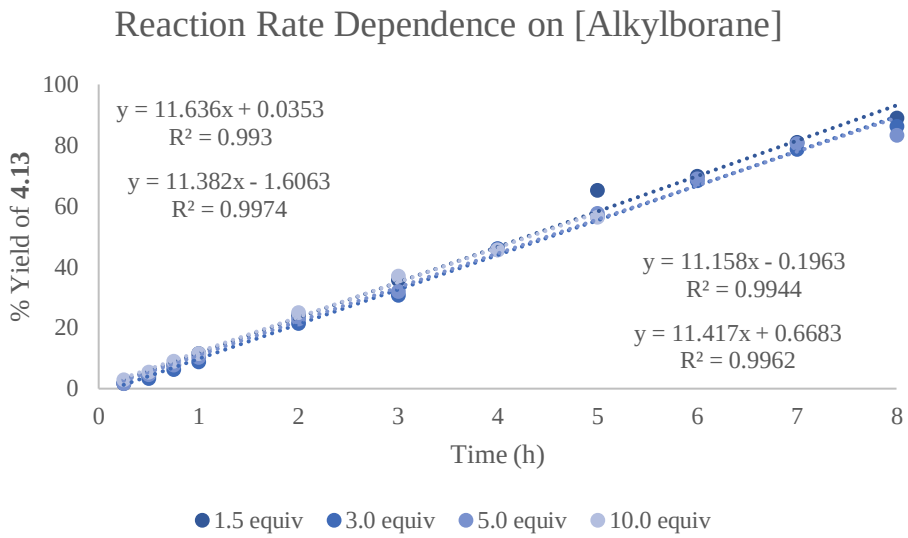

Figure 4.11 Graph of the reaction rate dependence on [alkylborane]: truncated

Rates (based on graph after removal of data points in which yield stops increasing)

1.5 equivalents alkylborane – $Rate = 4.19x10^{-2}\,\frac{mol}{s}$

3.0 equivalents alkylborane – $Rate = 4.10x10^{-2}\,\frac{mol}{s}$

5.0 equivalents alkylborane – $Rate = 4.02x10^{-2}\,\frac{mol}{s}$

10.0 equivalents alkylborane – $Rate = 4.11x10^{-2}\,\frac{mol}{s}$

4.5.3.7 KIE Experiments

All glassware used with CD_3OD or *t*-BuOD for KIE experiments was rinsed with D_2O and oven-dried (120 °C) overnight.

4.5.3.7.1 Independent Rate Measurements

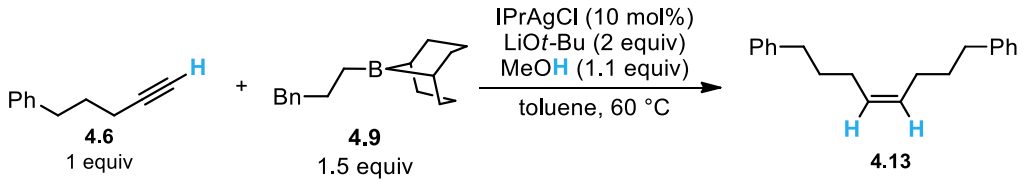

In a nitrogen filled glovebox, a 1-dram vial was charged with a stir bar and IPrAgCl catalyst (5.3 mg, 0.01 mmol, 0.10 equiv). To this was added LiO*t*-Bu (16.0 mg, 0.2 mmol, 2.0 equiv) and 500 uL toluene. To this was added 100 uL of a stock solution of 144.2 mg/mL alkyne **4.6** (14.4 mg, 0.10 mmol, 1.0 equiv) and 84.1 mg/mL TMB (8.4 mg, 0.05 mmol, 0.5 equiv). Then alkylborane **4.9** (36.0 mg, 0.15 mmol, 1.5 equiv) using 3x100 uL toluene, and 100 uL of a solution of 35.2 mg/mL methanol (3.5 mg, 0.11 mmol, 1.1 equiv) in toluene were added. A series of 25 uL aliquots of the crude reaction mixtures were pushed through short plugs of silica with ethyl acetate and analyzed by GC.

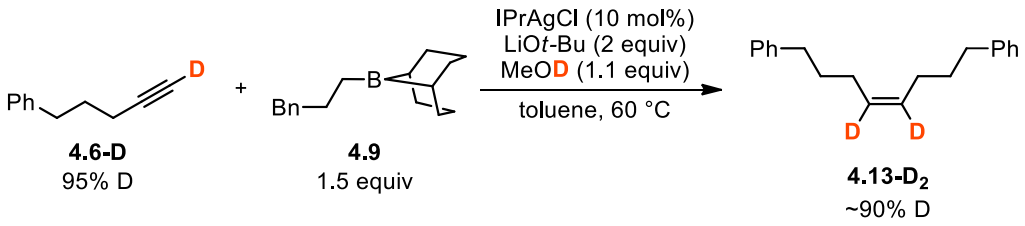

The same experiment was run using deuterated alkyne, CD_3OD and glassware that had been washed with D_2O and dried overnight in an oven (120 °C). Deuterium incorporation into the product was determined by GC/MS for several samples.

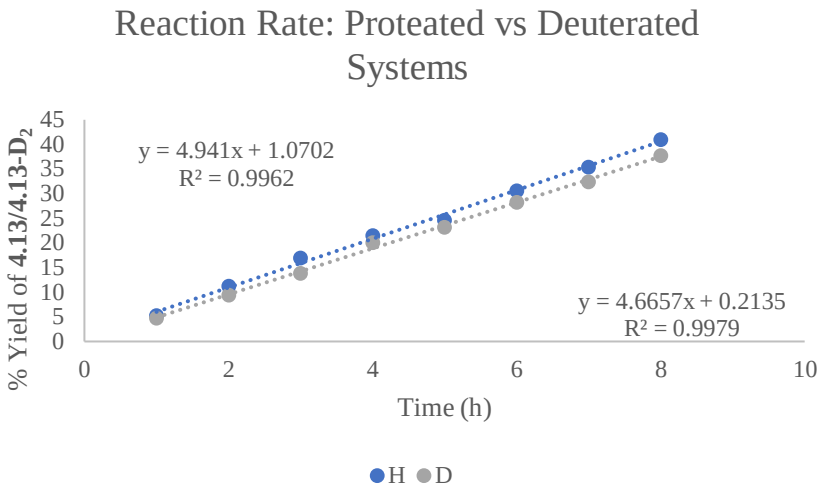

Figure 4.12 Graph for the KIE experiment: independent rate measurements

$$KIE = \frac{k_{obsH}}{k_{obsD}} = \frac{1.78x10^{-2}\frac{mol}{s}}{1.68x10^{-2}\frac{mol}{s}} = 1.06$$

The following data is for calculating deuterium incorporation at 20, 38, and 69% product yield

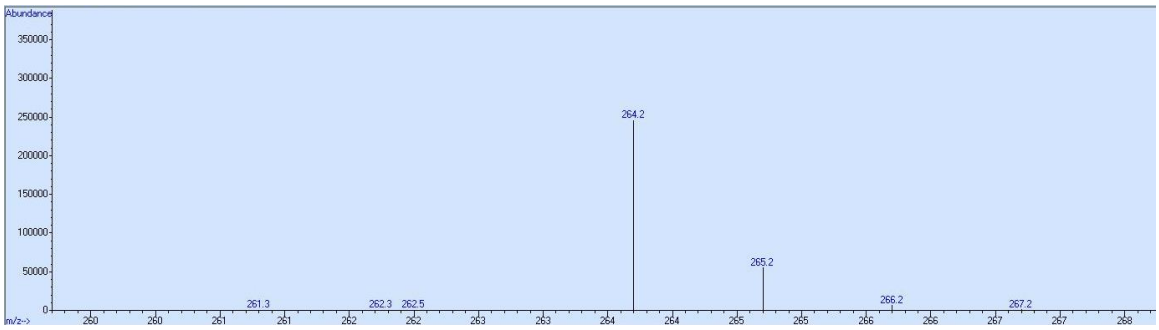

Figure 4.13 Mass spectrum of the reaction with proteated substrate at 21% yield

Table 4.1 Tabulated MS Data: Proteated Substrate at 21% Yield

M/Z	Abundance	Relative % H
263	0	
264.2	245694	80.1
265.2	55086	18.0
266.2	6050	2.0

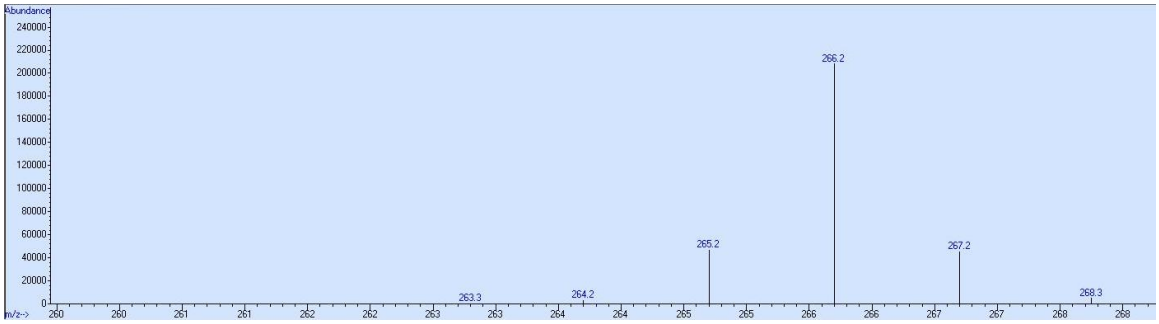

Figure 4.14 Mass spectrum of the reaction with deuterated substrate at 20% yield

Table 4.2 Tabulated MS Data: Deuterated Substrate at 20% Yield

M/Z	Abundance	Relative %	%D
263	0	0	
264.2	3164	1.0	
265.2	46620	15.1	7.4
266.2	208012	67.5	64.1
267.2	45402	14.7	14.4
268.3	4955	1.6	1.6

Total deuterium incorporation into product = 88%

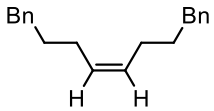

$[M_{HH}]$
0%D

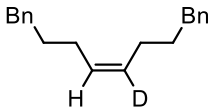

$[M_{HD}]$
50%D

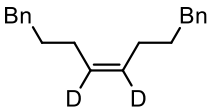

$[M_{DD}]$
100%D

Since we are looking at the overall deuteration of two independent positions, we looked at the analysis from the perspective that a monodeuterated substrate, $[M_{HD}]$, would be 50% deuterated

and a fully deuterated substrate, $[M_{DD}]$, would be 100% deuterated. This results in being able to think about %D being the amount of fully deuterated molecules.

Since there is no $[M_{HH}\text{-}1]^+$ peak in the fully proteated substrate, the M/Z=264.2 peak in the experiment with deuterated reagents is assumed to be composed entirely of fully proteated substrate, $[M_{HH}]^+$. The M/Z=265.2 peak is assumed to be composed of $[M_{HH}+1]^+$ and $[M_{HD}]^+$. Similarly, the M/Z peak at 266.2 is assumed be composed of $[M_{HH}+2]^+$, $[M_{HD}+1]^+$, and $[M_{DD}]^+$. The M/Z peak at 267.2 is assumed be composed of $[M_{HD}+2]^+$, and $[M_{DD}+1]^+$. The peak at M/Z=268.3 is assumed to be composed entirely of $[M_{DD}+2]^+$.

The contributions of $[M_{HH}+1]^+$ and $[M_{HH}+2]^+$ to the respective $[M_{HD}]^+$ and $[M_{HD}+1]^+$ peaks were determined using the assumption that the ratios of $[M_{HH}]^+$ to $[M_{HH}+1]^+$ and $[M_{HH}+2]^+$ would be the same in both the proteated and deuterated experiments. An additional assumption was made that the ratios of $[M_{HD}]^+$ to $[M_{HD}+1]^+$ and $[M_{HD}+2]^+$ would match those of the $[M_{HH}]^+$. These ratios were then used to find and subtract out their expected contributions to subsequent peaks.

For example, the %D in M/Z=265.2 was found using the following equation:

$$\%D_{265.2} = \left(\%_{265.2} - \%_{264.2} \times \frac{\%H_{265.2}}{\%H_{264.2}}\right)/2 \tag{4.1}$$

The %D in M/Z=266.2 was found using the following equation:

$$\%D_{266.2} = \%_{266.2} - \left(\%_{264.2} \times \frac{\%H_{266.2}}{\%H_{264.2}}\right) - \left(2 \times \%D_{265.2} \times \frac{\%H_{265.2}}{\%H_{264.2}}\right) \tag{4.2}$$

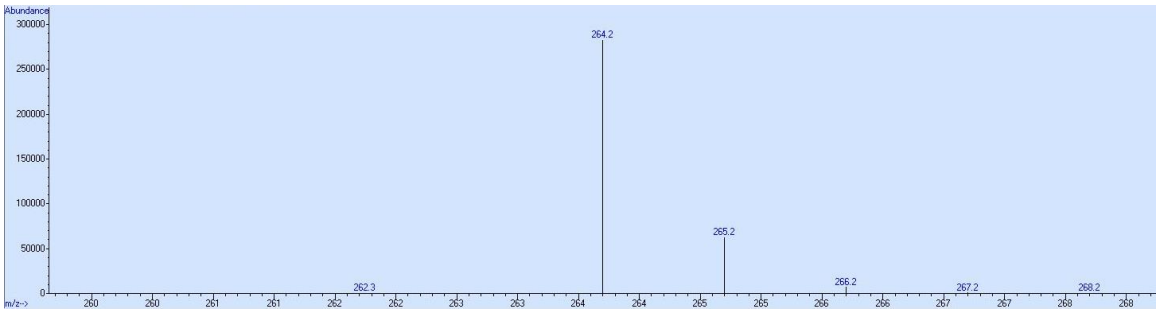

Figure 4.15 Mass spectrum of the reaction with proteated substrate at 41% yield

Table 4.3 Tabulated MS Data: Proteated Substrate at 41% Yield

M/Z	Abundance	Relative % H
263	0	
264.2	282619	80.3
265.2	62501	17.8
266.2	6769	1.9

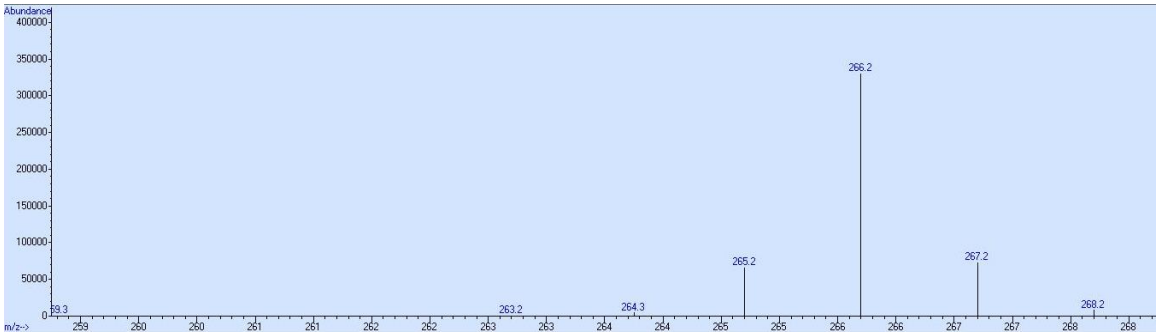

Figure 4.16 Mass spectrum of the reaction with deuterated substrate at 38% yield

Table 4.4 Tabulated MS Data: Deuterated Substrate at 38% Yield

M/Z	Abundance	Relative %	%D
263	0	0	
264.2	4398	0.9	
265.2	65910	13.7	6.8
266.2	329632	68.6	65.6
267.2	72924	15.2	14.8
268.3	7754	1.6	1.6

Total deuterium incorporation into product = 89%

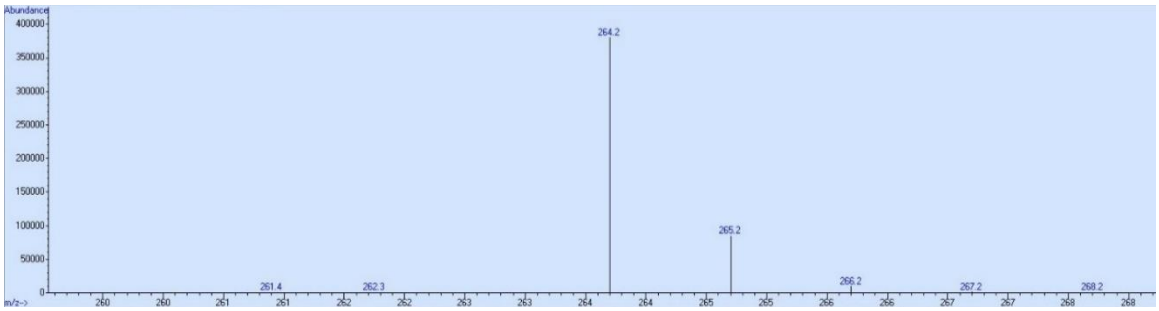

Figure 4.17 Mass spectrum of the reaction with proteated substrate at 69% yield

Table 4.5 Tabulated MS Data: Proteated Substrate at 69% Yield

M/Z	Abundance	Relative % H
263	0	0
264.2	380130	80.2
265.2	84691	17.9
266.2	9157	1.9

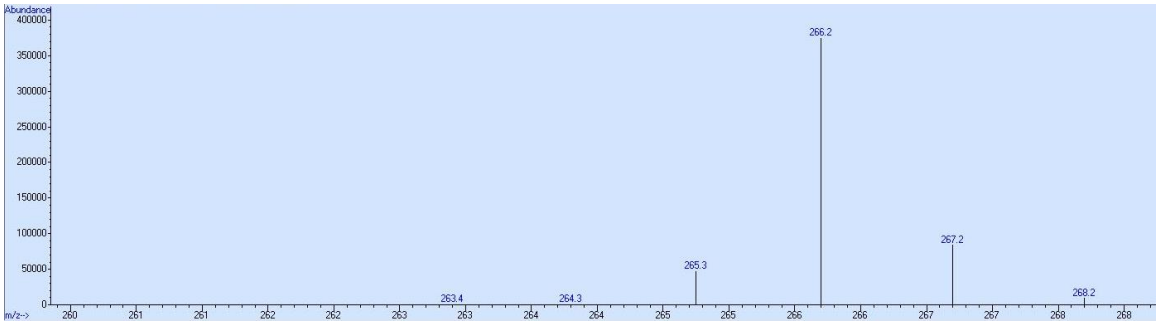

Figure 4.18 Mass spectrum of the reaction with deuterated substrate at 69% yield

Table 4.6 Tabulated MS Data: Deuterated Substrate at 69% Yield

M/Z	Abundance	Relative %	%D
263	0	0	
264.2	138	0.0	
265.2	47096	9.2	4.6
266.2	374221	72.8	70.8
267.2	83573	16.3	16.0
268.3	8905	1.7	1.7

Total deuterium incorporation into product = 93%

4.5.3.7.2 Competition Experiment with IPrAg Boronate complex

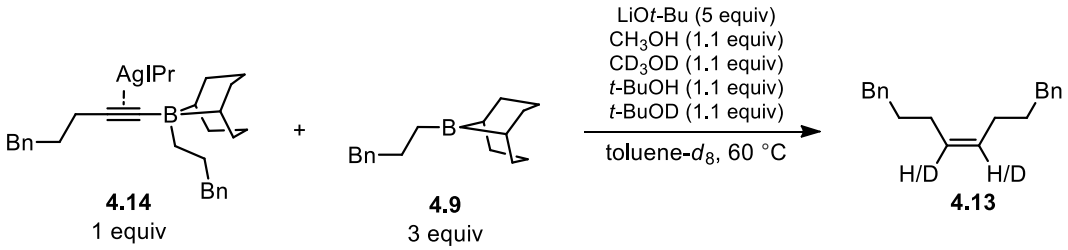

In a nitrogen filled glovebox, a 1-dram vial was charged with a stir bar and IPrAg boronate complex **4.14** (21.4 mg, 0.025 mmol, 1 equiv.). To this was added LiO*t*-Bu (10.0 mg, 0.125 mmol, 5 equiv), 50 uL of a 42.0 mg/mL solution of TMB (2.1 mg, 0.013 mmol, 0.5 equiv.) in toluene. This was followed by 100 uL of a 180.0 mg/mL solution of alkylborane **4.9** (18.0 mg 0.075 mmol, 3.0 equiv.) in toluene. Finally, 100 uL of a solution containing 8.8 mg/mL MeOH (0.9 mg, 0.028 mmol, 1.1 equiv), 9.9 mg/mL CD_3OD (1.0 mg, 0.028 mmol, 1.1 equiv), 20.4 mg/mL *t*-BuOH (2.0 mg, 0.028 mmol, 1.1 equiv), and 20.7 mg/mL *t*-BuOD (2.1 mg, 0.028 mmol, 1.1 equiv) in toluene was added. The reaction mixture was heated to 60°C and 25 uL aliquots of the crude reaction mixtures were pushed through short plugs of silica with ethyl acetate and analyzed by GC/MS for deuterium incorporation.

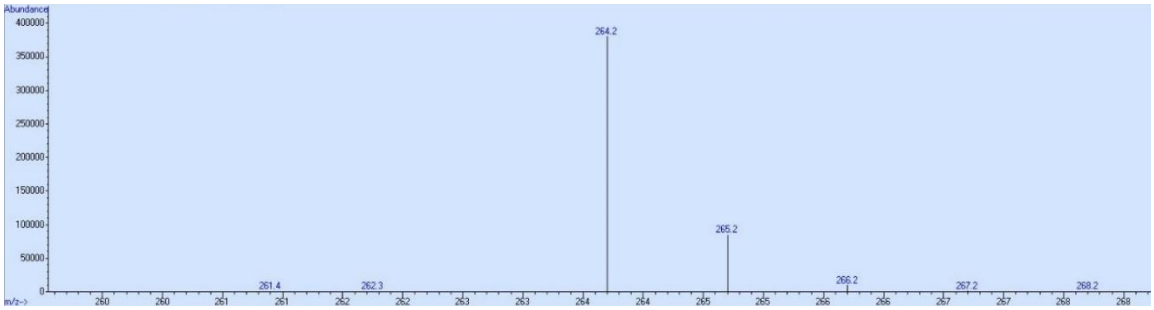

Figure 4.19 Mass spectrum of proteated substrate **4.13**

Table 4.7 Tabulated MS Data: Proteated Substrate **4.13**

M/Z	Abundance	Relative % H
263	0	0
264.2	380130	80.2
265.2	84691	17.9
266.2	9157	1.9

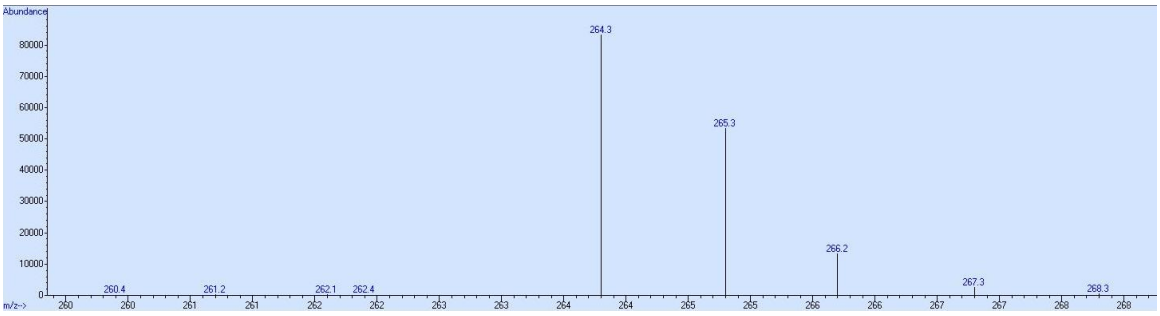

Figure 4.20 Mass spectrum of the competition experimment at 7% product formation

Table 4.8 Tabulated MS Data: Competition Experimment at 7% Product Formation

M/Z	Abundance	Relative %	%D
263	0	0	0
264.2	83116	54.5	0
265.2	53308	34.9	11.4
266.2	13185	8.6	2.2
267.3	2551	1.7	0.8
268.3	399	0.3	0.3

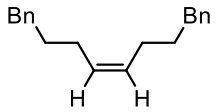

$[M_{HH}]$
0%D

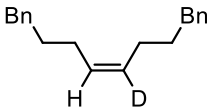

$[M_{HD}]$
50%D

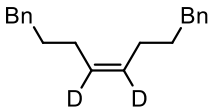

$[M_{DD}]$
100%D

Since we are looking at the overall deuteration of two independent positions, we looked at the analysis from the perspective that a monodeuterated substrate, $[M_{HD}]$, would be 50% deuterated and a fully deuterated substrate, $[M_{DD}]$, would be 100% deuterated. This results in being able to

think about %D being the amount of fully deuterated molecules, which makes 100%-%D represent the amount of fully proteated molecules. Thus

$$KIE = \frac{100\% - \%D}{\%D} \tag{4.3}$$

Since there is no $[M_{HH}\text{-}1]^+$ peak in the fully proteated substrate, the M/Z=264.2 peak in the competition experiment is assumed to be composed entirely of fully proteated substrate, $[M_{HH}]^+$. The M/Z=265.2 peak in the competition experiment is assumed to be composed of $[M_{HH}+1]^+$ and $[M_{HD}]^+$. Similarly, the M/Z peak at 266.2 is assumed be composed of $[M_{HH}+2]^+$, $[M_{HD}+1]^+$, and $[M_{DD}]^+$. The M/Z peak at 267.2 is assumed be composed of $[M_{HD}+2]^+$, and $[M_{DD}+1]^+$. The peak at M/Z=268.3 is assumed to be composed entirely of $[M_{DD}+2]^+$.

The contributions of $[M_{HH}+1]^+$ and $[M_{HH}+2]^+$ to the respective $[M_{HD}]^+$, $[M_{HD}+1]^+$, and $[M_{DD}]^+$ peaks were determined using the assumption that the ratios of $[M_{HH}]^+$ to $[M_{HH}+1]^+$ and $[M_{HH}+2]^+$ would be the same in both experiments. An additional assumption was made that the ratios of $[M_{HD}]^+$ to $[M_{HD}+1]^+$ and $[M_{HD}+2]^+$ would match those of the $[M_{HH}]^+$. These ratios were then used to find and subtract out their expected contributions to subsequent peaks.

For example, the %D in M/Z=265.2 was found using the following equation:

$$\%\mathrm{D}_{265.2} = \left(\%_{265.2} - \%_{264.2} \times \frac{\%\mathrm{H}_{265.2}}{\%\mathrm{H}_{264.2}}\right)/2 \tag{4.4}$$

The %D in M/Z=266.2 was found using the following equation:

$$\%\mathrm{D}_{266.2} = \%_{266.2} - \left(\%_{264.2} \times \frac{\%\mathrm{H}_{266.2}}{\%\mathrm{H}_{264.2}}\right) - \left(2 \times \%\mathrm{D}_{265.2} \times \frac{\%\mathrm{H}_{265.2}}{\%\mathrm{H}_{264.2}}\right) \tag{4.5}$$

Overall: $KIE = \frac{85.3\%}{14.7\%} = 5.8$

This value represents the average of the two separate KIE effects for the two protonation events.

4.5.3.7.3 Competition Experiment for Protodeargentation

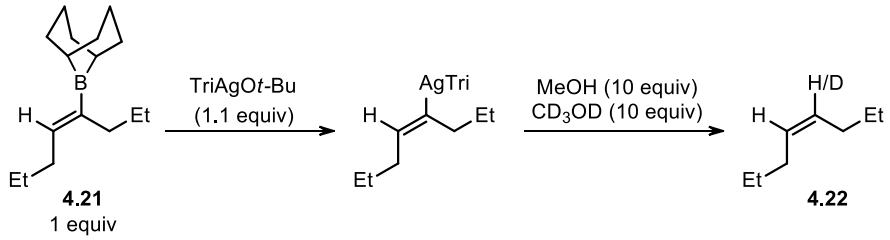

In a nitrogen filled glovebox, a 1-dram vial was charged with a stir bar and TriAgO*t*-Bu (106.7 mg, 0.165 mmol, 1.1 equiv.). To this was added TMB (12.6 mg, 0.075 mmol, 0.5 equiv.) using 3x250 uL C_6D_6. This was followed by octenyl borane **4.21** (34.8 mg 0.15 mmol, 1.0 equiv.) using 3x300 uL C_6D_6. After stirring for 10 min, 450 uL of this solution was transferred to an NMR tube and used to confirm complete transmetalation. Another 500 uL was added to a 100 uL solution containing MeOH (48.1 mg, 1.5 mmol, 10 equiv) and CD_3OD (54.1 mg, 1.5 mmol, 10 equiv) in C_6D_6. This was then added to an NMR tube to confirm complete protodeargentation. Similarly, another 500 uL was added to a 100 uL solution of MeOH (96.1 mg, 3.0 mmol, 20 equiv) in C_6D_6 and protodeargentation was checked by NMR. 25 uL aliquots of the competition experiment and control experiment were pushed through short plugs of silica with ethyl acetate and analyzed by GC/MS to determine deuterium incorporation.

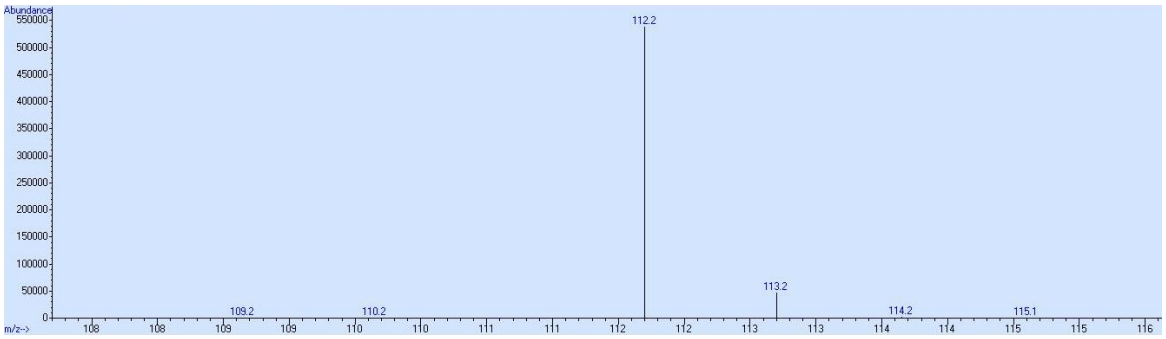

Figure 4.21 Mass spectrum of the control experiment

Table 4.9 Tabulated MS Data: Control Experiment

M/Z	Abundance	Relative % H
111	0	0
112.2	537845	91.7
113.2	46705	8.0
114.2	1918	0.3

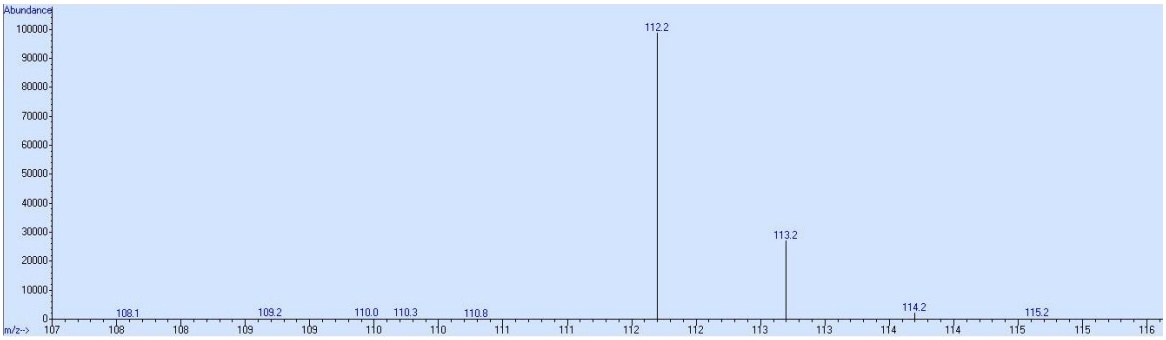

Figure 4.22 Mass spectrum of the alkenyl silver quenching competition experimment

Table 4.10 Tabulated MS Data: Alkenyl Silver Quenching Competition Experimment

M/Z	Abundance	Relative % D/H	%D
111	0	0	0
112.2	98652	77.2	0
113.2	26989	21.1	14.4
114.2	1991	1.6	1.3
115.2	24.2	0	0

Calculation of Deuterium Incorporation

Since there is no $[M_H\text{-}1]^+$ peak in the control, the M/Z=112.2 peak in the competition experiment is assumed to be composed entirely of fully proteated substrate, $[M_H]^+$. The M/Z=113.2 peak in the competition experiment is assumed to be composed of $[M_H+1]^+$ and $[M_D]^+$. Similarly, the M/Z peak at 114.2 is assumed be composed of $[M_H+2]^+$ and $[M_D+1]^+$. The peak at M/Z=115.2 is assumed to be composed entirely of $[M_D+2]^+$.

The contributions of $[M_H+1]^+$ and $[M_H+2]^+$ to the respective $[M_D]^+$ and $[M_D+1]^+$ peaks were determined using the assumption that the ratios of $[M_H]^+$ to $[M_H+1]^+$ and $[M_H+2]^+$ would be the same in both experiments. These ratios were then used to find and subtract out the expected contribution from proteated substrates.

For example, the %D in M/Z=113.2 was found using the following equation:

$$\%D_{113.2} = \%D/H_{113.2} - \%D/H_{112.2}\left(\frac{\%H_{113.2}}{\%H_{112.2}}\right) \quad (4.6)$$

Overall: $KIE = \frac{84.3\%}{15.7\%} = 5.3$

4.5.3.8 Resting State NMR Experiment

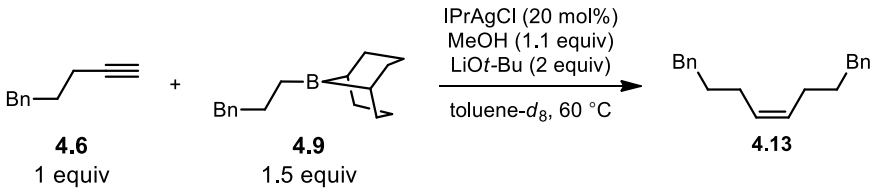

4.6 1 equiv | **4.9** 1.5 equiv | **4.13**

In a nitrogen filled glovebox, a 1-dram vial was charged with a stir bar and IPrAgCl catalyst (10.6 mg, 0.02 mmol, 0.20 equiv). To this was added LiO*t*-Bu (16.0 mg, 0.2 mmol, 2.0 equiv) and 500 uL toluene-d_8. To this was added 100 uL of a stock solution of 144.2 mg/mL alkyne **4.6** (14.4 mg, 0.10 mmol, 1.0 equiv) and 84.1 mg/mL TMB (8.4 mg, 0.05 mmol, 0.5 equiv) in toluene-d_8, alkylborane **4.9** (36.0 mg, 0.15 mmol, 1.5 equiv) using 3x100 uL toluene-d_8, and 100 uL of a

solution of 35.2 mg/mL methanol (3.5 mg, 0.11 mmol, 1.10 equiv) in toluene-d_8. After stirring for 2 hours at 60 °C, an aliquot for GC analysis was taken and 500 uL (half) of the reaction was added to a J-Young tube. The J-Young tube was then placed in a preheated (60 °C) NMR spectrometer and allowed to reach temperature for 5 minutes. A spectrum was then acquired. Several subsequent NMR spectra were taken to ensure the reaction was progressing in the J-Young tube. The J-Young tube was later returned to the glovebox and 25 uL aliquots of it and the other half that remained stirring in the glovebox were pushed through short plugs of silica with ethyl acetate and analyzed by GC to ensure equivalency.

4.5.3.9 Variable Temperature NMR Experiments

*4.5.3.9.1 IPrAg Complex **4.14***

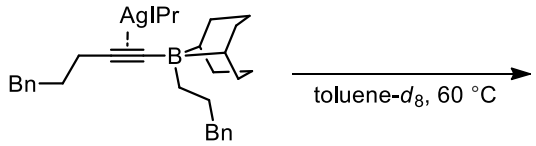

4.14

In a nitrogen filled glovebox, a 1-dram vial was charged with IPrAg complex **4.14** (8.8 mg, 0.01 mmol, 1.0 equiv) (amount at 20% catalyst loading in reaction) and 500 uL toluene-d_8 was used to transfer it to a J-Young tube. The J-Young tube was then placed in a preheated (60 °C) NMR spectrometer and allowed to reach temperature for 5 minutes. A spectrum was then acquired.

*4.5.3.9.2 IPrAg Complex **4.14** and alkylborane **4.9***

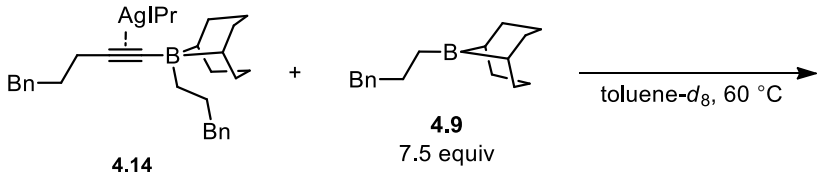

In a nitrogen filled glovebox, a 1-dram vial was charged with IPrAg complex **4.14** (8.8 mg, 0.01 mmol, 1.0 equiv) (amount at 20% catalyst loading in reaction) and 200 uL toluene-d_8. To this was added alkylborane **4.9** (18.0 mg, 0.075 mmol, 7.5 equiv) using 3x100 uL toluene-d_8. The solution was then transferred to a J-Young tube and an NMR spectrum at 25 °C was acquired. The J-Young tube was then removed while the NMR spectrometer was heated to 60 °C at which point the J-Young tube was re-inserted and allowed to reach temperature for 5 minutes. A spectrum was then acquired.

4.5.3.10 Alkylborane Crossover Experiment

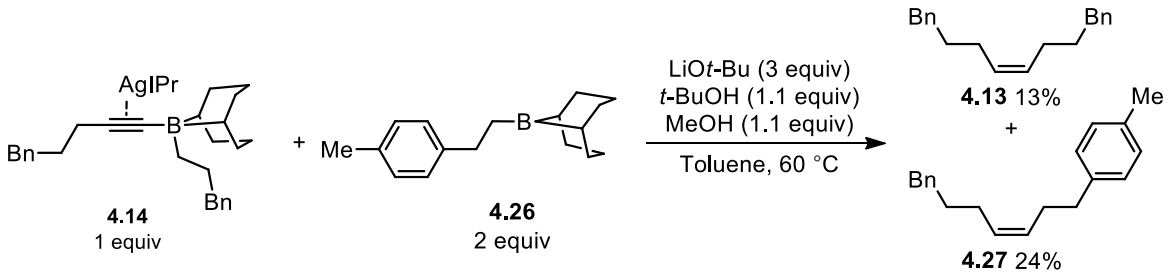

In a nitrogen filled glovebox, a 1-dram vial was charged with a stir bar and IPrAg boronate complex **4.14** (21.4 mg, 0.025 mmol, 1 equiv.). To this was added LiO*t*-Bu (6.0 mg, 0.075 mmol, 3 equiv), 50 uL of a 42.0 mg/mL solution of TMB (2.1 mg, 0.013 mmol, 0.5 equiv.) in toluene. This was followed by 100 uL of a 120.0 mg/mL solution of alkylborane **4.26** (12.0 mg 0.050 mmol, 2.0 equiv.) in toluene. Finally, 100 uL of a solution containing 8.8 mg/mL MeOH (0.9 mg, 0.028 mmol, 1.1 equiv) and 20.4 mg/mL *t*-BuOH (2.0 mg, 0.028 mmol, 1.1 equiv) in toluene was added.

The reaction mixture was heated to 60 °C. A 25 uL aliquot of the crude reaction mixture was pushed through a short plug of silica with ethyl acetate and analyzed by GC.

4.5.4 *Characterization of Organic Reagents and Products*

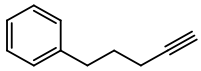

Pent-4-yn-1-ylbenzene (4.6) was purchased from GFS Chemical and distilled over calcium hydride under reduced pressure before use.

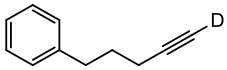

Pent-4-yn-1-ylbenzene (4.6-D) was prepared according to a known procedure and has been previously characterized[55]. Deuterium incorporation was 95% (NMR).

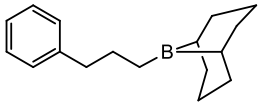

9-(3-phenylpropyl)-9-borabicyclo[3.3.1]nonane (4.9) was prepared according to a known procedure.[10]

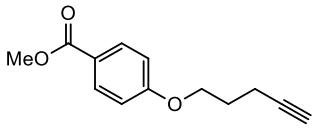

Methyl 4-(pent-4-yn-1-yloxy)benzoate (4.10) was prepared according to a known procedure and has been previously characterized.[10]

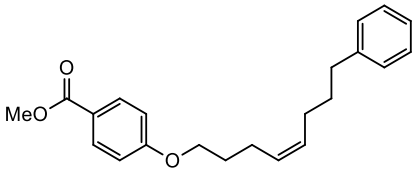

(*Z*)-methyl 4-((8-phenyloct-4-en-1-yl)oxy)benzoate (4.34) was prepared according to a known procedure and has been previously characterized.[10]

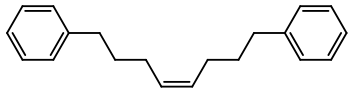

(*Z*)-1,8-diphenyloct-4-ene (4.13) was prepared according to a known procedure and has been previously characterized. [10]

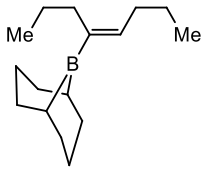

9-((Z)-Oct-4-en-4-yl)-9-borabicyclo[3.3.1]nonane (4.21) was prepared according to a known procedure and has been previously characterized.[40]

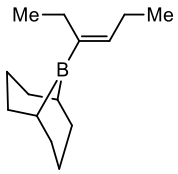

9-((Z)-hex-3-en-3-yl)-9-borabicyclo[3.3.1]nonane (4.23) was prepared according to a known procedure and has been previously characterized.[56]

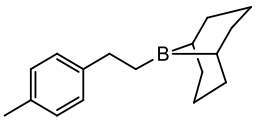

9-(4-methylphenethyl)-9-borabicyclo[3.3.1]nonane (4.26) was prepared according to a known procedure. [10]

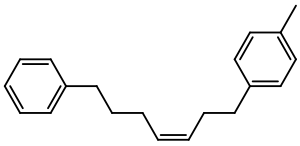

((Z)-1-methyl-4-(7-phenylhept-3-en-1-yl)benzene (4.27) was prepared according to a known procedure and has been previously characterized.[55]

4.5.5 *Synthesis and Characterization of TriAg and IPrAg Complexes*

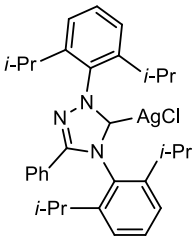

TriAgCl was prepared according to a known procedure and has been previously characterized.[10]

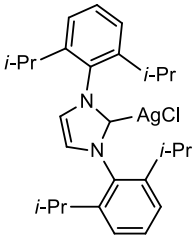

IPrAgCl was prepared according to a known procedure and has been previously characterized.[57]

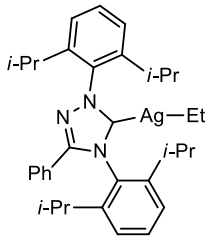

TriAgEt Complex (4.5) was synthesized following the same procedure used by Sadighi et al. for the synthesis of SIPrAgEt by using TriAgO*t*-Bu instead of SIPrAgO*t*-Bu.[31] ^{1}H NMR (500 MHz, C_6D_6) δ 7.52 (d, *J* = 7.9 Hz, 2H), 7.26 (t, *J* = 7.8 Hz, 1H), 7.20 (t, *J* = 7.8 Hz, 1H), 7.14 (d, *J* = 7.8 Hz, 2H), 7.05 (d, *J* = 7.8 Hz, 2H), 6.84 (t, *J* = 7.4 Hz, 1H), 6.76 (t, *J* = 7.7 Hz, 2H), 2.95 (hept, *J* = 6.8 Hz, 2H), 2.74 (hept, *J* = 6.6 Hz, 2H), 1.82 (dt, *J* = 11.7, 8.0 Hz, 3H), 1.52 – 1.41 (m, 12H), 1.20 (d, *J* = 6.9 Hz, 6H), 0.97 (dq, *J* = 12.5, 8.0 Hz, 2H), 0.88 (d, *J* = 6.9 Hz, 6H).

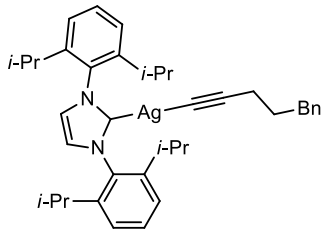

IPrAg Acetylide Complex (4.12) In a nitrogen filled glovebox, a scintillation vial was charged with a stir bar and IPrAgCl (550 mg, 1.04 mmol, 1.0 equiv). To this was added NaOt-Bu (109.9 mg 0.144 mmol, 1.1 equiv), alkyne **6** (225.0 mg 1.560 mmol, 1.5 equiv) and toluene (10 mL). The reaction mixture was stirred at 25 °C for 2 hours. After, 2 hours, the reaction mixture was filtered through a plug of celite and concentrated. The silver acetylide was then precipitated out with pentane, collected by vacuum filtration and washed several times with pentane. The product was isolated as a white powder (626.5 mg, 94% yield). ^{1}H NMR (300 MHz, C_6D_6) δ 7.21 – 7.17 (m, 2H), 7.14 – 6.94 (m, 9H), 6.28 (s, 2H), 2.67 (t, *J* = 7.6 Hz, 2H), 2.60 – 2.39 (m, 4H), 2.30 (t, *J* = 6.6 Hz, 2H), 1.83 – 1.62 (m, 2H), 1.32 (d, *J* = 6.8 Hz, 12H), 1.03 (d, *J* = 6.8 Hz, 12H). ^{13}C NMR

(126 MHz, $CDCl_3$) δ 188.0 (d, *J* = 192.1 Hz), 188.0 (d, *J* = 165.4 Hz), 145.6, 142.7, 134.9, 130.4, 128.6, 128.0, 125.3, 124.2, 123.4, 123.4, 107.2 (d, *J* = 224.1 Hz), 107.2 (d, *J* = 194.1 Hz), 106.9 (d, *J* = 57.0 Hz), 35.1, 32.0, 28.7, 24.7, 24.0, 20.3, 20.2.

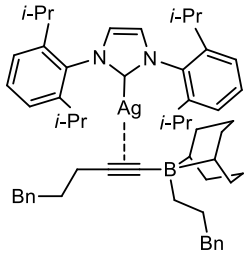

IPrAg Boronate Complex (4.14) In a nitrogen filled glovebox, a scintillation vial was charged with a stir bar and silver acetylide **4.12** (223.9 mg, 0.350 mmol, 1.0 equiv). To this was added alkylborane **9** (92.5 mg 0.385 mmol, 1.1 equiv) and toluene (3.5 mL). The reaction mixture was stirred at 25 °C for 1 hour. After 1 hour, the solvent was removed under vacuum and the boronate complex was precipitated out with pentane. It was then collected by vacuum filtration and washed several times with pentane. The complex was isolated as an off-white powder (282.8 mg, 92% yield). ^{1}H NMR (300 MHz, C_6D_6) δ 7.37 (d, J = 7.4 Hz, 2H), 7.28 – 7.17 (m, 5H), 7.14 – 7.05 (m, 5H), 7.02 (d, J = 7.7 Hz, 4H), 6.31 (s, 2H), 2.96 – 2.81 (m, 2H), 2.57 – 2.24 (m, 12H), 2.13 – 1.91 (m, 8H), 1.85 – 1.72 (m, 2H), 1.36 – 1.21 (m, 14H), 1.01 (d, J = 6.8 Hz, 12H), 0.70 (s, 4H).

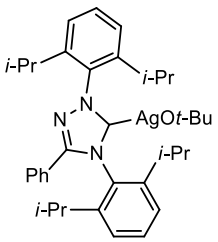

TriAgO*t*-Bu was synthesized following the same procedure used by Sadighi et al. for the synthesis of SIPrAgO*t*-Bu by using TriAgCl instead of SIPrAgCl.[58] ^{1}H NMR (500 MHz, C_6D_6) δ 7.49 (d, *J*

= 7.8 Hz, 2H), 7.28 (t, *J* = 7.8 Hz, 1H), 7.21 (t, *J* = 7.8 Hz, 1H), 7.12 (d, *J* = 7.7 Hz, 2H), 7.02 (d, *J* = 7.8 Hz, 2H), 6.83 (t, *J* = 7.4 Hz, 1H), 6.74 (t, *J* = 7.7 Hz, 2H), 2.90 – 2.79 (m, 2H), 2.71 – 2.56 (m, 2H), 1.47 (s, 9H), 1.37 (d, *J* = 6.9 Hz, 6H), 1.33 (d, *J* = 6.9 Hz, 6H), 1.16 (d, *J* = 6.9 Hz, 6H), 0.82 (d, *J* = 6.9 Hz, 6H). ^{13}C NMR (126 MHz, C_6D_6) δ 190.0 (d, *J* = 193.1 Hz), 190.0 (d, *J* = 221.2 Hz), 153.5, 153.4, 146.1, 145.5, 135.9, 132.7, 131.7, 131.4, 131.3, 129.1, 128.1, 125.3, 125.3, 124.5, 69.3, 37.9, 29.4, 24.9, 24.4, 24.0, 22.9.

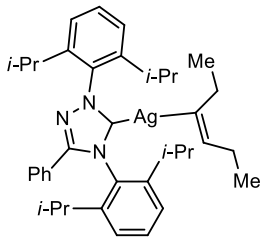

TriAg Hexenyl C**omplex (4.24)** In a nitrogen filled glovebox, a 1-dram vial was charged with a stir bar and TriAgO*t*-Bu (100 mg, 0.154 mmol, 1.1 equiv.). To this was added 1.1 ml toluene and hexenyl borane **4.23** (28.6 mg 0.14 mmol, 1.0 equiv.) using 3x300 uL toluene. Reaction was stirred for 30 min at 25 °C and then most (~1 mL) of the toluene was removed without heating under reduced pressure. Pentane was then added and the solution was put in the freezer to encourage precipitation of the product. The precipitate was collected by vacuum filtration and washed with cold pentane. ^{1}H NMR (300 MHz, C_6D_6) δ 7.52 (d, *J* = 7.3 Hz, 2H), 7.31 – 7.19 (m, 2H), 7.13 – 7.00 (m, 4H), 6.84 – 6.69 (m, 3H), 5.71 – 5.56 (m, 1H), 3.02 – 2.85 (m, 2H), 2.80 – 2.65 (m, 2H), 2.60 – 2.44 (m, 2H), 2.44 – 2.28 (m, 2H), 1.53 – 1.33 (m, 12H), 1.19 (d, *J* = 6.9 Hz, 6H), 1.10 (t, *J* = 6.6 Hz, 3H), 1.06 (t, *J* = 6.6 Hz, 3H), 0.87 (d, *J* = 6.9 Hz, 6H).

4.5.6 *DFT Calculations*

The Gaussian-16 software package was used for all calculations[59] All calculations were performed at the ωB97xD level of theory using a mixed basis set, consisting of SDD for Ag and 6-311+G(d,p) for all other atoms, and solvation by toluene using the CPCM model. Frequency calculations were performed on optimized structures. Enthalpies and free energies were calculated using the harmonic approximation and adjusted to standard state (1 M concentration).

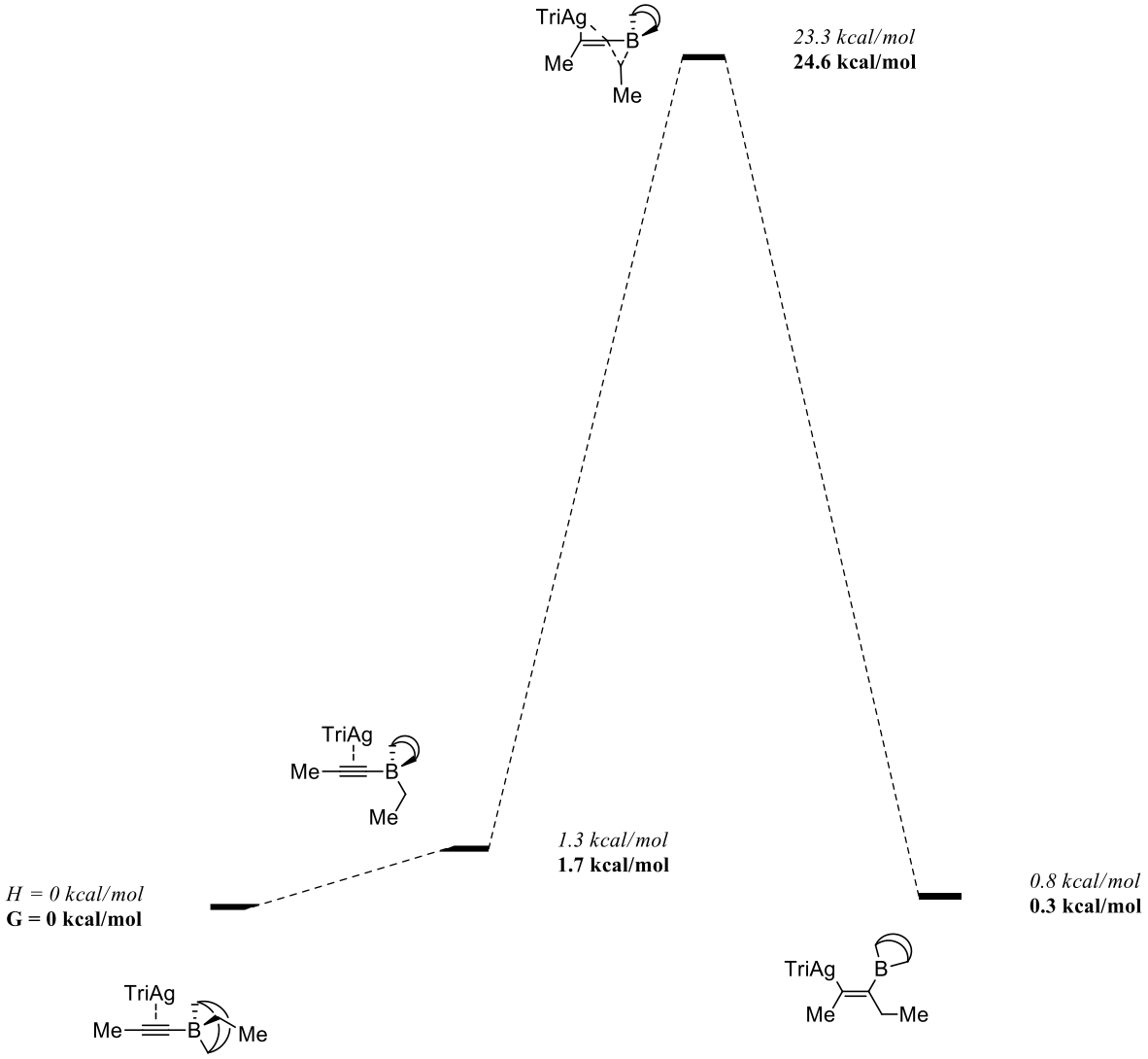

Figure 4.23. Calculated free energy diagram for the 1,2-metallate shift of a simplified boronate complex. Enthalpies are in *italics*, free energies are in **bold**.

4.5.6.1 TriAg Boronate Complex **4.19**

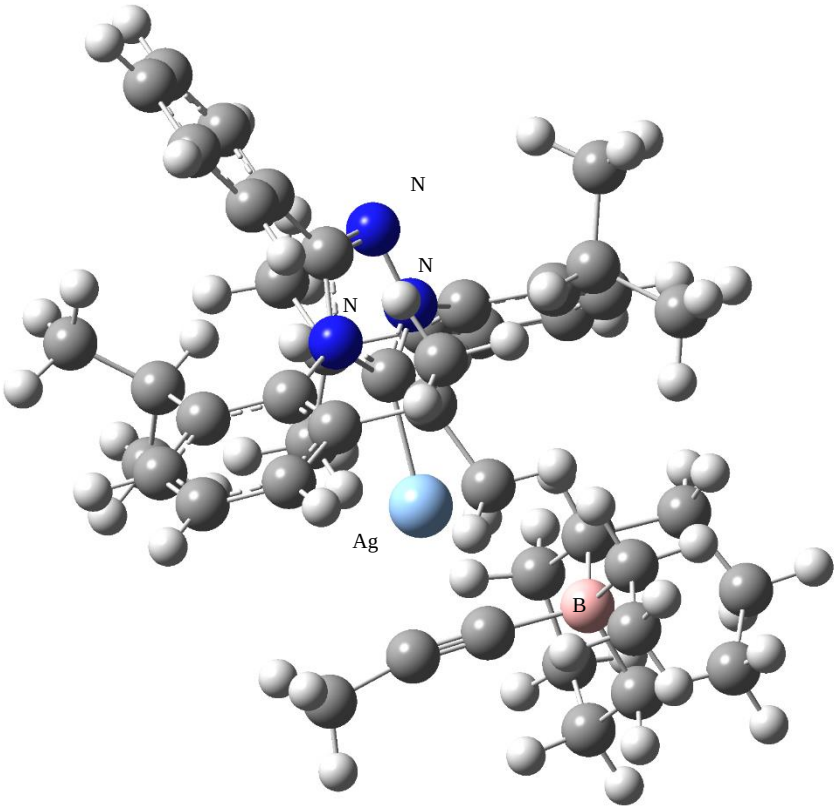

Figure 4.24 Gaussian 16 rendereing of the calculated structure of TriAg boronate complex **4.19**

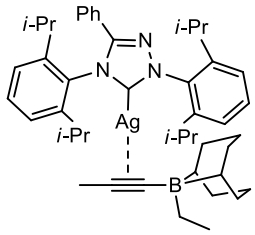

$C_{45}H_{61}$ BN_3Ag

Dihedral angle between Ag, C-B carbon of alkyne, B and B-C carbon of ethyl group = 62.893292°

Table 4.11: Calculated XYZ Coordinates: TriAg Boronate Complex **4.19**

C	5.51113100	-0.03999500	-1.97652700	C	3.13419300	-2.91632700	2.22001300
C	1.82482000	3.62529900	-1.19986400	C	-4.73592500	-0.47940400	-2.85748100
C	2.54147300	3.97330000	-0.06618800	C	-2.89558200	1.08520200	0.51845800
C	-0.67017400	3.70594000	-3.05027700	C	-4.99809900	2.27408100	0.06151000
C	4.20136500	0.64776900	-1.55366100	C	-3.22973600	-1.66439500	-1.20657600
C	6.17660000	0.54888200	1.01815700	C	-4.35812000	1.16449300	0.61826500
C	0.75710300	1.63011300	-3.31338300	C	-6.38147500	2.37136300	0.10249100
C	5.68909700	-1.47262500	-1.43855800	C	-2.66095800	-1.39032300	0.04042200
C	4.76822700	1.16271000	0.89741000	C	-3.67704700	-2.96410000	-1.42981800
C	-0.10085300	2.46384000	-2.35580000	C	-5.11536800	0.15750200	1.21757000
C	0.67465600	2.84447500	-1.10613700	C	-2.50720300	-2.34760600	1.04782000
C	2.13401600	3.54079600	1.18764200	C	-7.13446400	1.36316800	0.69559300
C	6.22223600	-0.99070300	1.03582800	C	-0.52860500	-2.78823500	2.53778400
C	3.81273500	0.45071200	-0.07838300	C	-1.85543800	-2.03462000	2.38454000
C	5.28315700	-1.68600200	0.03282200	C	-3.54909400	-3.93818200	-0.44981200
C	0.29119900	2.43321700	0.17215400	C	-6.49946300	0.25998300	1.25486200
C	1.00084600	2.74717500	1.33502000	C	-2.96730600	-3.63394200	0.77217900
C	2.76343200	-1.92337300	-0.73915400	C	-2.79436400	-2.33444300	3.55899700
C	-2.28638200	-0.90986600	-3.40082200	H	6.35803500	0.57362000	-1.65954200
C	2.04144200	-2.54730100	-1.51759000	H	2.16877200	3.95669700	-2.17330400
C	0.54531600	2.25905200	2.69816800	H	3.43926100	4.57349600	-0.16080900
C	-0.29156500	3.34012400	3.39521600	H	5.56572200	-0.06275500	-3.07233400
C	1.70659800	1.79553900	3.58039900	H	0.12983400	4.36184400	-3.40586700
C	3.18097400	-1.44217000	1.81074700	H	6.79852500	0.91345300	0.19692300
C	1.42341100	-3.43264800	-2.51436100	H	1.61961700	2.19809600	-3.67338600
C	-0.86634500	0.27510500	0.10197800	H	4.26951500	1.71923700	-1.79678400
C	-3.31556500	-0.61577300	-2.30215700	H	4.87335500	2.22245200	0.62121100

H	-1.27248300	3.41306700	-3.91493100	H	0.59756800	-4.00327200	-2.08369300
H	6.65280500	0.92999700	1.93021600	H	2.16821700	-4.13974200	-2.88821100
H	6.73437100	-1.77600900	-1.60136800	H	-0.65511600	2.97724600	4.36085800
H	0.16584200	1.32572800	-4.18158400	H	1.31540000	1.34776000	4.49803800
H	-1.30219400	4.28131400	-2.36904700	H	-4.40571400	3.04872600	-0.41058600
H	3.38577500	0.25008600	-2.17133000	H	-5.06589900	-1.39405000	-3.35792100
H	7.26370500	-1.30627000	0.87258900	H	2.52621200	-3.50069600	1.51928800
H	1.13618900	0.72921800	-2.82295200	H	-5.44490200	-0.25092600	-2.05657600
H	2.72311300	3.80383100	2.05764500	H	-6.87251000	3.23221900	-0.33577300
H	5.07903600	-2.14836000	-2.05183400	H	-4.12055300	-3.22149800	-2.38505800
H	4.30004400	1.16327900	1.88861500	H	0.15906700	-2.56577000	1.71804500
H	2.82992600	0.93169600	0.05231700	H	-1.62977100	-0.96634400	2.41426000
H	-0.95021200	1.84277400	-2.06127900	H	-4.63136200	-0.70512400	1.65625000
H	5.95803500	-1.33967000	2.04182600	H	-0.03494500	-2.50344100	3.47043000
H	5.36354400	-2.76650100	0.22456600	H	-8.21551500	1.43752300	0.72203100
H	-2.31360600	-0.12894000	-4.16586500	H	-0.69007200	-3.87018900	2.55696000
H	0.31269600	4.23513700	3.57354800	H	-3.89965200	-4.94572800	-0.64306900
H	2.35202100	2.62830800	3.87375900	H	-7.08157800	-0.52471600	1.72341600
H	-1.27408100	-0.94595100	-2.98643400	H	-2.86441200	-4.40974500	1.52262900
H	3.78823400	-0.89904300	2.54662300	H	-3.73276800	-1.77951900	3.47926400
H	2.31847300	1.04943000	3.06935500	H	-2.31525000	-2.05167400	4.49983800
H	-1.15311100	3.62443800	2.78627400	H	-3.03538700	-3.39963000	3.61588400
H	-2.49008900	-1.86946900	-3.88519600	N	-0.86562600	1.59298400	0.28770900
H	-4.77449300	0.33142200	-3.58963900	N	-2.09873600	2.11641200	0.54246200
H	2.16787300	-1.01558300	1.91765900	N	-2.16850300	-0.06032000	0.26828100
H	-3.05265100	0.35480300	-1.87787400	B	3.74974700	-1.15321000	0.29076500
H	-0.10046600	1.39001700	2.54301900	Ag	0.73525900	-0.94152900	-0.46429000
H	4.13869900	-3.35359600	2.21146500	H	2.71761100	-3.06983300	3.22313900

H	1.03645100	-2.86532500	-3.36400800

Energy = -2087.5806

Enthalpy = -2086.5558

Free Energy (1M) = -2086.6959

Number of imaginary frequencies = 0

4.5.6.2 TriAg Boronate Complex **4.19** (rotamer)

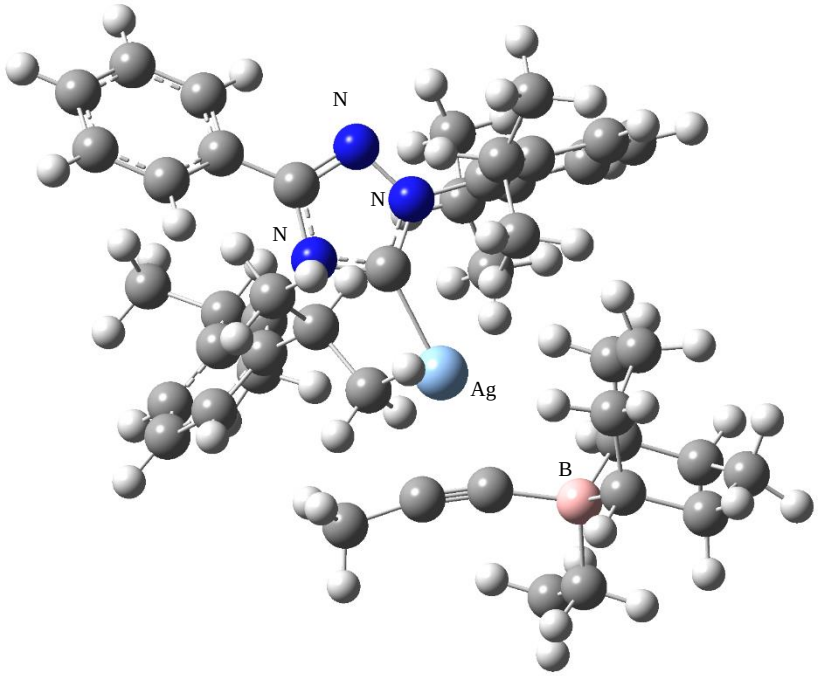

Figure 4.25 Gaussian 16 rendereing of the calculated structure of TriAg boronate complex **4.19** (rotomer)

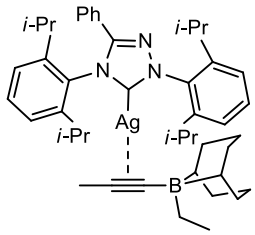

$C_{45}H_{61}BN_3Ag$

Dihedral angle between Ag, C-B carbon of alkyne, B and B-C carbon of ethyl group = 197.08347°

Table 4.12: Calculated XYZ Coordinates: TriAg Boronate Complex **4.19** (Rotamer)

C	3.73619700	1.21978800	0.99064500	C	-0.84900100	0.45778000	0.09609800
C	1.60516300	3.91968700	-1.46362800	C	-2.86901600	-1.49851300	-2.17808000
C	2.06267000	4.54470100	-0.31468900	C	4.71466200	-3.24071000	-2.27243000
C	-0.55825700	3.35713700	-3.62627100	C	-4.24346700	-1.66306200	-2.83353200
C	3.76768700	-0.04457000	1.86221000	C	-3.00320700	1.02030500	0.04269300
C	6.57743100	0.20413500	0.22464400	C	-5.12762100	1.71930900	-0.97457500
C	1.15421600	1.50995400	-3.36434600	C	-2.81683200	-2.13357600	-0.80031400
C	3.56459300	0.94855700	-0.51192700	C	-4.46303800	0.89673000	-0.06222600
C	6.14304400	-0.82489300	1.29082100	C	-6.50146300	1.61144600	-1.13583100
C	0.05576100	2.32492000	-2.67282700	C	-2.41624300	-1.42097600	0.33234200
C	0.56121700	2.99783200	-1.40857500	C	-3.12956700	-3.48011500	-0.62910400
C	1.48571300	4.26958100	0.91832500	C	-5.18780000	-0.02939600	0.68905400
C	5.88120400	0.08220600	-1.14588900	C	-2.28279100	-1.99869400	1.59972300
C	4.64202700	-1.18437700	1.31018400	C	-7.22049600	0.68280900	-0.39052900
C	4.37269200	-0.22810500	-1.08496800	C	-0.48392800	-1.81576800	3.34763200
C	0.01050700	2.74212400	-0.15248200	C	-1.79362400	-1.22409000	2.81268300
C	0.44133600	3.35679200	1.02803100	C	-3.03647600	-4.07916200	0.61820200
C	2.64816800	-2.17324700	-0.19373600	C	-6.56238400	-0.13265300	0.52317000
C	-1.73832900	-2.05050900	-3.05530200	C	-2.60925700	-3.34819900	1.71719500
C	1.64481600	-2.89076800	-0.19724600	C	-2.86080300	-1.16101800	3.91132000
C	-0.17270000	3.00042100	2.37262400	H	4.65237300	1.79159500	1.15442300
C	-0.33255300	4.21350100	3.29237300	H	2.07054100	4.14458900	-2.41682400
C	0.63568000	1.89371900	3.06426600	H	2.88253300	5.25128000	-0.37741400
C	5.01765400	-2.89047300	-0.81223100	H	2.92328900	1.87327500	1.32226400
C	0.62852300	-3.95171800	-0.22276700	H	0.19450400	4.07182100	-3.97186700

H	6.41734100	1.21309000	0.61286500	H	4.82768500	-3.77527700	-0.18569000
H	1.98872100	2.14598800	-3.67314300	H	-2.69328100	-0.42616400	-2.07422600
H	4.08353900	0.23932100	2.87740700	H	-1.17734800	2.61136600	2.18686100
H	6.46174900	-0.45201200	2.27607000	H	4.97152000	-2.40742500	-2.93656100
H	-0.97543700	2.85871800	-4.50569900	H	1.11897200	-4.92623000	-0.29228600
H	7.66169600	0.12372500	0.07926900	H	-0.04229300	-3.84291700	-1.07828400
H	3.77124900	1.87695900	-1.06375900	H	-0.89016100	3.92667000	4.18777100
H	0.75285300	1.02576400	-4.25885900	H	0.14907100	1.59680800	3.99810200
H	-1.35807300	3.91802400	-3.13597600	H	-4.55913300	2.43071900	-1.56155100
H	2.73972400	-0.42451300	1.97302100	H	-4.47429000	-2.71419800	-3.02839700
H	6.06227200	1.01241100	-1.70540300	H	3.64779800	-3.44721400	-2.41632400
H	1.55414000	0.73487100	-2.70674700	H	-5.03131300	-1.25142300	-2.19628300
H	1.86438200	4.76401000	1.80483600	H	-7.00993300	2.24831200	-1.85005200
H	2.49403800	0.76134900	-0.70211300	H	-3.44122400	-4.06970200	-1.48392700
H	6.70517400	-1.75107100	1.12956300	H	0.28170300	-1.86204800	2.56826000
H	4.53211100	-2.03424300	2.00140200	H	-1.58209700	-0.19737100	2.50769600
H	-0.73900000	1.62788800	-2.39686300	H	-4.68752900	-0.67145200	1.40187800
H	6.36768800	-0.71292400	-1.72218200	H	-0.09843900	-1.19966300	4.16405700
H	4.03519200	-0.36135900	-2.12450400	H	-8.29286200	0.59502300	-0.52162800
H	-1.74131400	-1.56101000	-4.03288200	H	-0.63426800	-2.82888700	3.73204700
H	0.63459600	4.60238500	3.62275900	H	-3.28488800	-5.12819700	0.73254100
H	1.64597900	2.24040400	3.30031100	H	-7.11905600	-0.85328700	1.11048400
H	-0.76308600	-1.87758500	-2.58983400	H	-2.52270600	-3.83553700	2.68202500
H	6.09538800	-2.70301100	-0.72395800	H	-3.77999400	-0.69089300	3.55214800
H	0.73070800	1.00753900	2.43209400	H	-2.49203800	-0.57511700	4.75741900
H	-0.87509400	5.02136100	2.79534700	H	-3.11239900	-2.15952900	4.28018300
H	-1.85296900	-3.12689800	-3.21500700	N	-1.03605300	1.76673300	-0.05348300
H	-4.26696700	-1.13547900	-3.79065200	N	-2.34893800	2.13869000	-0.09632700

N	-2.11375900	-0.02501800	0.18086400	H	5.26976300	-4.11908900	-2.62364600
B	4.17399500	-1.60514700	-0.20952700	H	0.01476800	-3.93821900	0.68100400
Ag	0.87154800	-0.74139300	-0.02075900				

Energy = -2087.5782

Enthalpy = -2086.5538

Free Energy (1M) = -2086.6932

Number of imaginary frequencies = 0

4.5.6.3 1,2-Metallate Shift Transition State

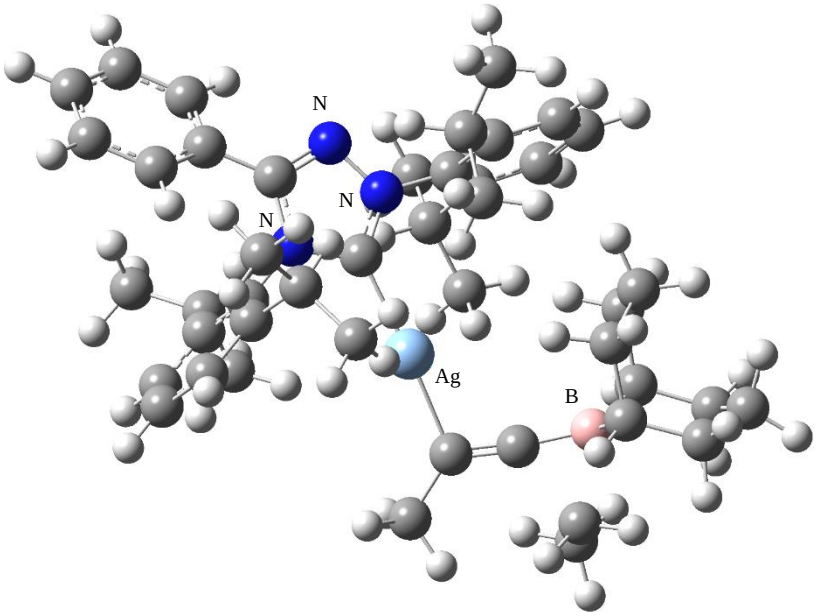

Figure 4.26 Gaussian 16 rendereing of the calculated structure of the 1,2-metallate shift transition state

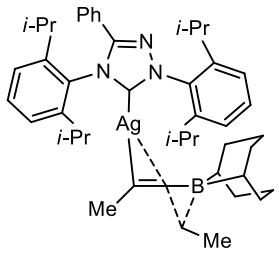

$C_{45}H_{61}BN_3Ag$

Table 4.13: Calculated XYZ Coordinates: 1,2-Metallate Shift Transition State

C	1.74425400	1.28354800	1.01483900	C	-3.59098400	1.27442000	1.13993300
C	-0.29014600	1.93794700	-2.76617000	C	-1.74644400	-0.42208700	1.42090100
C	-0.64860300	2.72315400	-1.68486500	C	5.12099200	-1.92862700	-0.10455400
C	-0.84982100	0.31443000	-5.35838000	C	3.38260800	-4.38291300	-1.38183800
C	1.99432900	0.04789600	1.89531500	C	-1.36492800	-2.31999000	-1.55625200
C	4.79368300	1.68624300	1.56080300	C	-1.60265500	-4.92888800	-4.04159600
C	1.23596500	-0.38400100	-4.09418400	C	5.78330800	-1.84928600	-1.47133100
C	2.29935900	1.16958800	-0.41591600	C	-2.54682500	-5.64670700	-5.01132900
C	4.51465600	0.41253700	2.38110700	C	-3.43937300	-2.72550300	-2.27131700
C	-0.29022500	-0.24011700	-4.04377000	C	-5.29707900	-2.95272100	-3.86335300
C	-0.71636700	0.61403700	-2.86374300	C	-1.70912000	-5.48779700	-2.63428500
C	-1.43270700	2.20228400	-0.66405900	C	-4.62461900	-3.45222700	-2.74587500
C	4.83764700	1.47683000	0.03663600	C	-6.40173500	-3.62232300	-4.36824600
C	3.42746600	-0.52160900	1.81615100	C	-2.02134200	-4.68417500	-1.53595400
C	3.72343300	0.58196700	-0.53493100	C	-1.45449000	-6.83412500	-2.38638000
C	-1.51982900	0.13041600	-1.83180000	C	-5.07561600	-4.62382900	-2.13673500
C	-1.88451700	0.88854000	-0.71251800	C	-2.06444400	-5.15791900	-0.22063400
C	3.22219500	-2.06284800	-0.37569200	C	-6.84355600	-4.79449300	-3.76423500
C	-0.14540600	-4.96280900	-4.51854500	C	-1.14825200	-4.12834100	1.88173700
C	2.70667400	-3.12024800	-0.92476600	C	-2.37022400	-4.25718200	0.96488900
C	-2.68579100	0.27140600	0.42273300	C	-1.50065700	-7.34127700	-1.09675200

C	-6.18169400	-5.28967400	-2.64722700	H	-3.01285400	2.00739200	1.70992100
C	-1.79621700	-6.51050700	-0.02601900	H	-1.09479200	0.30684900	1.91065200
C	-3.60036100	-4.73937100	1.74200500	H	0.50392800	-4.41622600	-3.82823800
H	2.15947900	2.16794000	1.50293900	H	5.65376400	-1.29284800	0.61072900
H	0.34260400	2.35298200	-3.54258600	H	-1.10424200	-1.15744700	0.93044100
H	-0.30008400	3.74792500	-1.62417600	H	-4.22951400	1.81282900	0.43536500
H	0.66624200	1.46532300	0.95168000	H	0.22434100	-5.99019000	-4.58705700
H	-0.44895500	1.30998300	-5.57066700	H	-2.49147300	-5.18543700	-6.00106000
H	4.04447700	2.44419200	1.79845600	H	5.16764600	-2.92745700	0.33245600
H	1.72087800	0.58190600	-4.26373500	H	-1.90399700	-3.87953400	-4.02103300
H	1.72726400	0.29035000	2.93374500	H	-3.33995300	-0.49072800	-0.00964800
H	4.27254700	0.70407900	3.41237900	H	5.82321600	-0.81684400	-1.82669300
H	-0.57740700	-0.33882000	-6.19226900	H	4.43250900	-4.44665400	-1.07445700
H	5.74908300	2.11342100	1.88697500	H	3.34884000	-4.46030200	-2.47416400
H	2.24738300	2.15637700	-0.89599000	H	-4.23394900	0.74878400	1.85077400
H	1.52461000	-1.05160600	-4.91102900	H	-2.32544700	-0.93511200	2.19517700
H	-1.93955200	0.39124900	-5.32094100	H	-4.94055500	-2.04340900	-4.33212300
H	1.30956200	-0.75104000	1.57917300	H	-2.28134200	-6.70209000	-5.12224300
H	4.83341000	2.46057800	-0.45283100	H	5.23886400	-2.43125400	-2.21796600
H	1.63127100	-0.79720600	-3.16216000	H	-3.58244600	-5.58990000	-4.66468100
H	-1.68569900	2.82769900	0.18321800	H	-6.91482500	-3.23139700	-5.23914400
H	1.62731700	0.51863700	-0.99092000	H	-1.20471800	-7.49137500	-3.21186600
H	5.44756500	-0.16315400	2.45289200	H	-0.27619100	-3.76351400	1.33219300
H	3.44163700	-1.44553400	2.40806800	H	-2.59758100	-3.25721900	0.58887800
H	-0.70508500	-1.24207900	-3.91018600	H	-4.56711600	-5.02268200	-1.26890500
H	5.80159700	1.01824600	-0.22447700	H	-1.35616100	-3.42660700	2.69378400
H	3.91742700	0.44484000	-1.60580100	H	-7.70320900	-5.32055800	-4.16341100
H	-0.05849900	-4.50626900	-5.50849000	H	-0.88551800	-5.09280800	2.32655300

H	-1.29399200	-8.39127400	-0.92272700	N	-3.28828300	-1.43586700	-2.36373700
H	-6.52524400	-6.19940000	-2.16891700	N	-2.28830900	-3.29344300	-1.76741500
H	-1.81222200	-6.91836000	0.97858300	B	3.66412800	-0.80958700	0.25502800
H	-4.48426200	-4.79834300	1.10099400	Ag	0.66521200	-2.68757300	-1.14868900
H	-3.82258300	-4.04700700	2.55847200	H	6.81097900	-2.22739400	-1.43403400
H	-3.43555200	-5.72741500	2.18116200	H	2.86136400	-5.26164700	-0.99209400
N	-2.01751100	-1.21314500	-1.91375200				

Energy = -2087.5428

Enthalpy = -2086.5187

Free Energy (1M) = -2086.6567

Number of imaginary frequencies = 1 at -550 cm^{-1}

Vibrational motion corresponds to the expected reaction coordinate.

4.5.6.4 Bimetallic Tetrasubstituted Alkene **4.20**

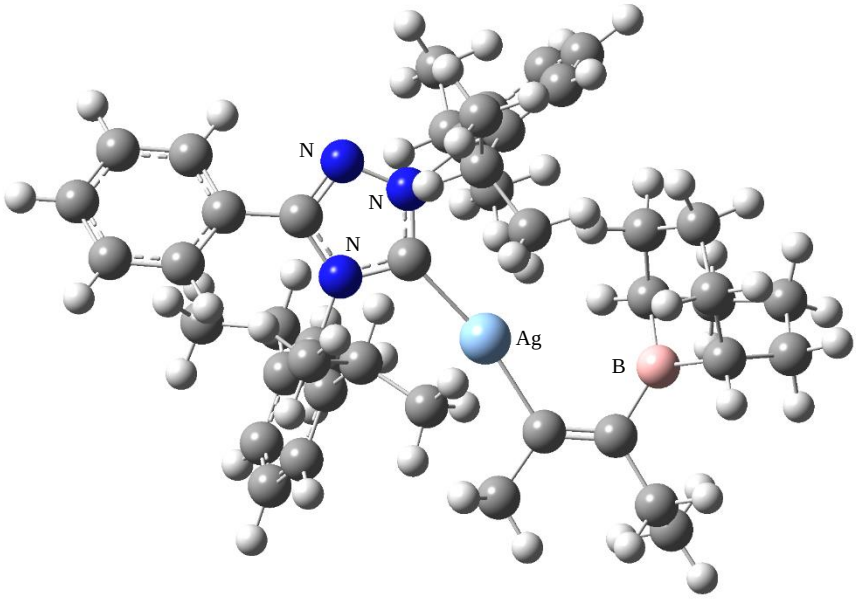

Figure 4.27 Gaussian 16 rendereing of the calculated structure of bimetallic tetrasubstituted alkene **4.20**

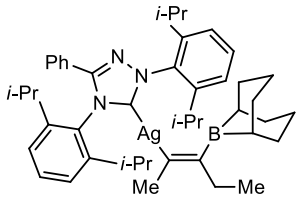

$C_{45}H_{61}BN_3Ag$

Table 4.14: Calculated XYZ Coordinates: Bimetallic Tetrasubstituted Alkene **4.20**

C	4.42615200	1.74853300	0.99939100	C	1.10308000	1.37325900	3.00322200
C	1.35776600	4.25832500	-1.11165400	C	4.33644200	-3.68639800	-0.07584500
C	1.92139200	4.65474800	0.09198400	C	1.34259500	-3.88980400	-0.25090700
C	-0.52400400	3.92802800	-3.44006800	C	-0.89063800	0.42309000	0.04811500
C	4.78038400	0.50575800	1.82729400	C	-3.03759700	-1.26930600	-2.30978500
C	6.38955600	0.40027100	-1.03224100	C	4.76754200	-4.18122700	-1.46059900
C	0.74903500	1.76858000	-3.09171700	C	-4.45148500	-1.35492900	-2.89298500
C	3.50804300	1.46355300	-0.19989100	C	-3.04166900	1.00831500	0.19397300
C	6.50907500	-0.54332700	0.17768300	C	-5.20500900	1.88501000	-0.57199000
C	-0.20802600	2.79124400	-2.46480500	C	-2.91288000	-2.04781400	-1.01288800
C	0.36072900	3.28652200	-1.14746500	C	-4.50790600	0.91692100	0.15512400
C	1.50534400	4.08605100	1.28649100	C	-6.58764400	1.82296000	-0.66836200
C	5.09255300	0.21888400	-1.83470700	C	-2.46882300	-1.45376100	0.17030600
C	5.21079100	-0.72939300	1.00492400	C	-3.19984100	-3.41026100	-0.97473400
C	3.79962400	0.16554200	-0.97494800	C	-5.21144000	-0.11033200	0.78573700
C	-0.03992200	2.74150300	0.07416300	C	-2.28023000	-2.15970500	1.36429900
C	0.50819600	3.11386800	1.30460200	C	-7.28529200	0.79492400	-0.04262100
C	3.41619700	-2.47387600	-0.17011600	C	-0.46699000	-2.16165100	3.11632800
C	-1.96916500	-1.73068100	-3.30857100	C	-1.76867800	-1.50710400	2.63921500
C	2.06202700	-2.55167700	-0.27264000	C	-3.04029200	-4.13799400	0.19494600
C	0.08526300	2.44966800	2.60345200	C	-6.59525600	-0.16720200	0.68573800
C	-0.12958100	3.45602200	3.73713400	C	-2.58143400	-3.51961500	1.34899600

C	-2.83297800	-1.52680900	3.74289600	H	-0.96771400	-1.62913700	-2.87979700
H	5.34597900	2.23159200	0.66236200	H	5.23385800	-3.41747300	0.49251900
H	1.70910400	4.70161900	-2.03605800	H	1.21202300	0.61619600	2.22170900
H	2.70260600	5.40664800	0.09813100	H	-0.83131400	4.24036700	3.44302800
H	3.93301100	2.48135700	1.64840900	H	-2.11460000	-2.77910100	-3.58548100
H	0.38328900	4.43314200	-3.78312600	H	-4.52387300	-0.73799100	-3.79270100
H	6.46954800	1.43843900	-0.70497300	H	3.87300300	-4.51298600	0.47248000
H	1.71849100	2.22831200	-3.30794500	H	-2.84210300	-0.21570000	-2.10192000
H	5.56311600	0.76765300	2.55170700	H	-0.87420100	1.95423900	2.43450600
H	7.32502000	-0.20143000	0.82832400	H	5.26746900	-3.38187800	-2.01772000
H	-1.02771400	3.52807500	-4.32409700	H	1.99304700	-4.77040900	-0.18991800
H	7.24540800	0.23422500	-1.69599800	H	0.73321400	-3.99292400	-1.15650900
H	3.52438800	2.32426900	-0.87989900	H	-0.53478500	2.94466400	4.61435400
H	0.33616700	1.38078800	-4.02734000	H	0.78656300	0.87147400	3.92217400
H	-1.17746000	4.67442800	-2.98147200	H	-4.65442300	2.67535800	-1.06782000
H	3.90205900	0.21821600	2.42127400	H	-4.71003200	-2.38063000	-3.17144400
H	5.00700600	1.02570000	-2.57415000	H	3.89768000	-4.49403300	-2.04585300
H	0.92294600	0.92558300	-2.41786900	H	-5.19332200	-0.99837200	-2.17262000
H	1.96831900	4.39807400	2.21537000	H	-7.12028500	2.57443300	-1.23929300
H	2.47697300	1.39921800	0.16754500	H	-3.54123100	-3.91058100	-1.87408200
H	6.80826000	-1.53436200	-0.18872900	H	0.29994700	-2.12909700	2.33769500
H	5.39607600	-1.54458600	1.71476800	H	-1.54017100	-0.46106200	2.42511300
H	-1.15018600	2.27873400	-2.25538700	H	-4.68745700	-0.86928200	1.35100900
H	5.15988100	-0.71444200	-2.41048500	H	-0.08392400	-1.63484500	3.99441400
H	2.96799000	-0.01228800	-1.66583700	H	-8.36500900	0.74354400	-0.12341900
H	-2.01662000	-1.12937300	-4.22067400	H	-0.62530800	-3.20741800	3.39564200
H	0.80739200	3.93152100	4.04029100	H	-3.26507700	-5.19850500	0.20517300
H	2.08748900	1.81841000	3.17777500	H	-7.13373000	-0.96789000	1.17886600

H	-2.44973000	-4.10548900	2.25185300	N	-2.16145100	-0.05074200	0.14934100
H	-3.74307700	-1.00529800	3.43541000	B	4.05636300	-1.07138400	-0.02592800
H	-2.45080600	-1.03364000	4.64078900	Ag	0.73631500	-0.92034200	-0.18443900
H	-3.10408400	-2.55173800	4.01266900	H	5.45721800	-5.02883200	-1.39181300
N	-1.07028000	1.74416700	0.07227700	H	0.63379700	-3.93541000	0.58532500
N	-2.37951700	2.12952700	0.15883900				

Energy = -2087.5809

Enthalpy = -2086.5545

Free Energy (1M) = -2086.6954

4.5.7 *Number of imaginary frequencies = 0 X-Ray Crystallography*

All silver complexes were crystalized using the same method. The specified compound was dissolved in a minimal amount of benzene. Pentane was slowly added until the solution became cloudy. A few more drops of benzene were added, and the solution was placed in a -35 °C freezer until crystals formed

4.5.7.1 TriAgEt (**4.5**)

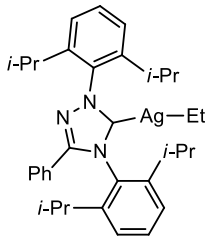

A colorless prism, measuring 0.35 x 0.25 x 0.22 mm^3 was mounted on a loop with oil. Data was collected at -173^{o}C on a Bruker APEX II single crystal X-ray diffractometer, Mo-radiation.

.

Crystal-to-detector distance was 40 mm and exposure time was 10 seconds per frame for all sets. The scan width was 0.5º. Data collection was 99.4% complete to 25º in ϑ. A total of 10929 reflections were collected covering the indices, -17<=h<=16, -15<=k<=15, 0<=l<=20. 5597 reflections were symmetry independent and the R_{int} = 0.008 indicated that the data was brilliant. Indexing and unit cell refinement indicated a monoclinic lattice. The space group was found to be P 21/c (No. 2).

The data was integrated and scaled using SAINT,[60] SADABS[61] within the APEX2[62] software package by Bruker.

Solution by direct methods (SHELXT[63] or SIR97[64,65]) produced a complete heavy atom phasing model consistent with the proposed structure. The structure was completed by difference Fourier synthesis with SHELXL.[66-68] Scattering factors are from Waasmair and Kirfel.[69] Hydrogen atoms were placed in geometrically idealized positions and constrained to ride on their parent atoms with C---H distances in the range 0.95-1.00 Angstrom. Isotropic thermal parameters U_{eq} were fixed such that they were 1.2U_{eq} of their parent atom Ueq for CH's and 1.5U_{eq} of their parent atom U_{eq} in case of methyl groups. All non-hydrogen atoms were refined anisotropically by full-matrix least-squares.

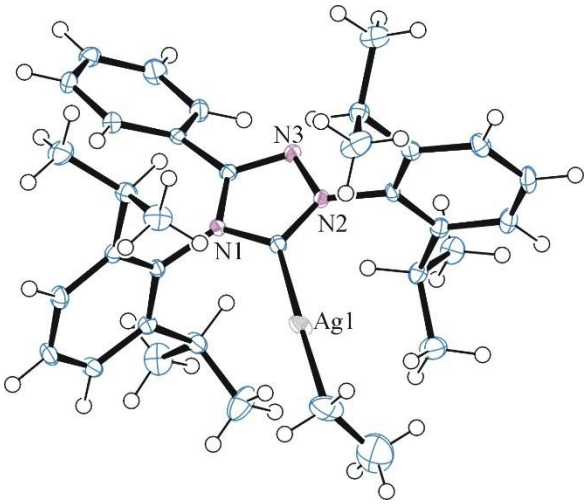

Figure 4.28. ORTEP[70] of the structure of TriAgEt. Depicted with thermal ellipsoids at the 50% probability level.

Table 4.15: Crystallographic Data: TriAgEt.

Empirical formula	C34 H44 Ag N3	
Formula weight	602.59	
Temperature	100(2) K	
Wavelength	0.71073 Å	
Crystal system	Monoclinic	
Space group	P 2_1/c	
Unit cell dimensions	a = 14.5615(6) Å	α= 90°.
	b = 13.0416(6) Å	β= 110.420(2)°.
	c = 17.2865(7) Å	γ = 90°.
Volume	3076.5(2) $Å^3$	
Z	4	
Density (calculated)	1.301 Mg/m^3	
Absorption coefficient	0.681 mm^{-1}	

F(000)	1264
Crystal size	0.350 x 0.250 x 0.220 mm^3
Theta range for data collection	1.492 to 25.350°.
Index ranges	-17<=h<=16, -15<=k<=15, 0<=l<=20
Reflections collected	10929
Independent reflections	5597 [R(int) = 0.0080]
Completeness to theta = 25.000°	99.4 %
Refinement method	Full-matrix least-squares on F^2
Data / restraints / parameters	5597 / 0 / 352
Goodness-of-fit on F^2	1.055
Final R indices [I>2sigma(I)]	R1 = 0.0319, wR2 = 0.0727
R indices (all data)	R1 = 0.0340, wR2 = 0.0745
Largest diff. peak and hole	2.075 and -1.851 $e.Å^{-3}$

4.5.7.2 IPrAg Boronate Complex **4.14**

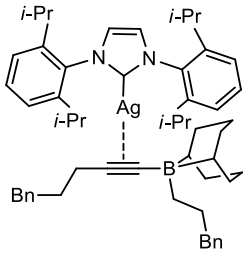

A colorless prism, measuring 0.316 x 0.179 x 0.145 mm^3 was mounted on a loop with oil. Data was collected at -173ºC on a Bruker APEX II single crystal X-ray diffractometer, Mo-radiation.

Crystal-to-detector distance was 40 mm and exposure time was 10 seconds per frame for all sets. The scan width was 0.5°. Data collection was 100% complete to 25° in ϑ. A total of 23746 reflections were collected covering the indices, -15<=h<=15, -27<=k<=27, -27<=l<=27. 8761 reflections were symmetry independent and the R_{int} = 0.0221 indicated that the data was brilliant. Indexing and unit cell refinement indicated a triclinic lattice. The space group was found to be P 2_1/n (No. 14).

The data was integrated and scaled using SAINT,[60] SADABS[61] within the APEX2[62] software package by Bruker.

Solution by direct methods (SHELXT[63] or SIR97[64,65]) produced a complete heavy atom phasing model consistent with the proposed structure. The structure was completed by difference Fourier synthesis with SHELXL.[66-68] Scattering factors are from Waasmair and Kirfel.[69] Hydrogen atoms were placed in geometrically idealized positions and constrained to ride on their parent atoms with C---H distances in the range 0.95-1.00 Angstrom. Isotropic thermal parameters U_{eq} were fixed such that they were 1.2U_{eq} of their parent atom Ueq for CH's and 1.5U_{eq} of their parent atom U_{eq} in case of methyl groups. All non-hydrogen atoms were refined anisotropically by full-matrix least-squares.

The isopropyl moieties show some elevated thermal motion.

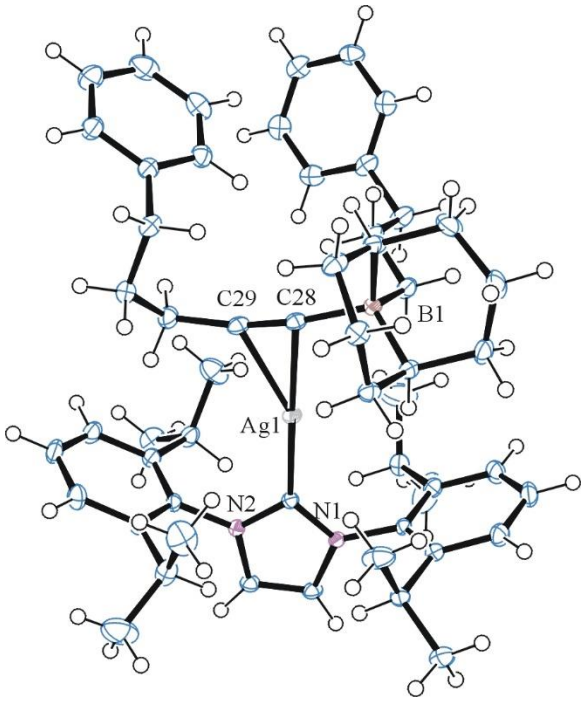

Figure 4.29. ORTEP[70] of the structure of IPrAg boronate complex **4.14**. Depicted with thermal ellipsoids at the 50% probability level.

Table 4.16: Crystallographic Data: IPrAg Boronate Complex **4.14**.

Empirical formula	C55 H72 Ag B N2	
Formula weight	879.82	
Temperature	100(2) K	
Wavelength	0.71073 Å	
Crystal system	Monoclinic	
Space group	P 2_1/n	
Unit cell dimensions	a = 11.6935(15) Å	α= 90°.
	b = 20.883(3) Å	β= 103.951(5)°.
	c = 20.370(3) Å	γ = 90°.
Volume	4827.5(12) Å^3	

Z	4
Density (calculated)	1.211 Mg/m^3
Absorption coefficient	0.454 mm^{-1}
F(000)	1872
Crystal size	0.316 x 0.179 x 0.145 mm^3
Theta range for data collection	1.418 to 28.368°.
Index ranges	-15<=h<=15, -27<=k<=27, -27<=l<=27
Reflections collected	23746
Independent reflections	12052 [R(int) = 0.0221]
Completeness to theta = 25.000°	100.0 %
Refinement method	Full-matrix least-squares on F^2
Data / restraints / parameters	12052 / 0 / 540
Goodness-of-fit on F^2	1.043
Final R indices [I>2sigma(I)]	R1 = 0.0270, wR2 = 0.0625
R indices (all data)	R1 = 0.0370, wR2 = 0.0681
Largest diff. peak and hole	0.402 and -0.558 $e.Å^{-3}$

4.5.7.3 TriAg Alkenyl Complex **4.24**

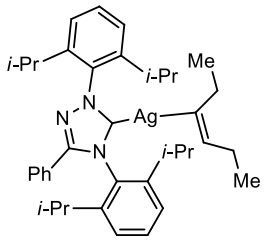

A colorless block, measuring 0.32 x 0.17 x 0.15 mm^3 was mounted on a loop with oil. Data was collected at -173°C on a Bruker APEX II single crystal X-ray diffractometer, Mo-radiation.

Crystal-to-detector distance was 40 mm and exposure time was 10 seconds per frame for all sets. The scan width was 0.5°. Data collection was 100% complete to 25° in ϑ. A total of 17432 reflections were collected covering the indices, -16<=h<=16, -17<=k<=17, -18<=l<=18. 8761 reflections were symmetry independent and the R_{int} = 0.0116 indicated that the data was brilliant. Indexing and unit cell refinement indicated a triclinic lattice. The space group was found to be P $\bar{1}$ (No. 2).

The data was integrated and scaled using SAINT,[60] SADABS[61] within the APEX2[62] software package by Bruker.

Solution by direct methods (SHELXT[63] or SIR97[64,65]) produced a complete heavy atom phasing model consistent with the proposed structure. The structure was completed by difference Fourier synthesis with SHELXL.[66-68] Scattering factors are from Waasmair and Kirfel.[69] Hydrogen atoms were placed in geometrically idealized positions and constrained to ride on their parent atoms with C---H distances in the range 0.95-1.00 Angstrom. Isotropic thermal parameters U_{eq} were fixed such that they were 1.2U_{eq} of their parent atom Ueq for CH's and 1.5U_{eq} of their parent atom U_{eq} in case of methyl groups. All non-hydrogen atoms were refined anisotropically by full-matrix least-squares.

The isopropyl moieties show some elevated thermal motion.

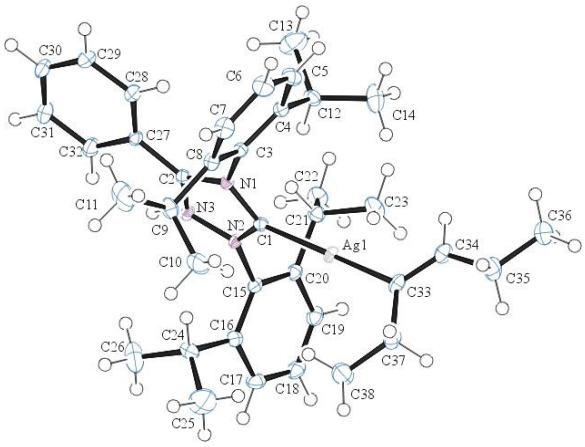

Figure 4.30. ORTEP[70] of the Structure of TriAg alkenyl complex **4.24**. Depicted with thermal ellipsoids at the 50% probability level

Table 4.17: Crystallographic Data: TriAg Alkenyl Complex **4.24**

Empirical formula	C38 H50 Ag N3	
Formula weight	656.68	
Temperature	100(2) K	
Wavelength	0.71073 Å	
Crystal system	Triclinic	
Space group	P -1	
Unit cell dimensions	a = 12.191(5) Å	α= 89.336(5)°.
	b = 12.779(5) Å	β= 71.619(5)°.
	c = 13.479(5) Å	γ = 62.415(5)°.
Volume	1743.5(12) $Å^3$	
Z	2	
Density (calculated)	1.251 Mg/m^3	
Absorption coefficient	0.606 mm^{-1}	

F(000)	692
Crystal size	0.320 x 0.170 x 0.150 mm^3
Theta range for data collection	1.613 to 28.437°.
Index ranges	-16<=h<=16, -17<=k<=17, -18<=l<=18
Reflections collected	17432
Independent reflections	8761 [R(int) = 0.0116]
Completeness to theta = 25.000°	100.0 %
Refinement method	Full-matrix least-squares on F^2
Data / restraints / parameters	8761 / 0 / 389
Goodness-of-fit on F^2	1.080
Final R indices [I>2sigma(I)]	R1 = 0.0175, wR2 = 0.0453
R indices (all data)	R1 = 0.0185, wR2 = 0.0460
Largest diff. peak and hole	0.432 and -0.231 $e.Å^{-3}$

4.6 REFERENCES FOR CHAPTER 4

(1) Hendrickson, J. B. Systematic Synthesis Design. 6. Yield Analysis and Convergency. *J. Am. Chem. Soc*. **1977**, 99, 5439.

(2) Velluz, L.; Valls, J.; Nominé, G. Recent Advances in the Total Synthesis of Steroids. *Angew. Chem., Int. Ed.* Engl. **1965**, 4, 181.

(3) Lu, X.-Y.; Liu, J.-H.; Lu, X.; Zhang, Z.-Q.; Gong, T.-J.; Xiao, B.; Fu, Y. 1,1-Disubstituted Olefin Synthesis via Ni-Catalyzed Markovnikov Hydroalkylation of Alkynes with Alkyl Halides. *Chem. Commun*. **2016**, 52, 5324.

(4) Till, N. A.; Smith, R. T.; MacMillan, D. W. C. Decarboxylative Hydroalkylation of Alkynes. *J. Am. Chem. Soc*. **2018**, 140, 5701.

(5) Cheung, C. W.; Zhurkin, F. E.; Hu, X. Z-Selective Olefin Synthesis via Iron-Catalyzed Reductive Coupling of Alkyl Halides with Terminal Arylalkynes. *J. Am. Chem. Soc*. **2015**, 137, 4932.

(6) Uehling, M. R.; Suess, A. M.; Lalic, G. Copper-Catalyzed Hydroalkylation of Terminal Alkynes. *J. Am. Chem. Soc*. **2015**, 137, 1424.

(7) Hazra, A.; Chen, J.; Lalic, G. Stereospecific Synthesis of E-Alkenes through Anti-Markovnikov Hydroalkylation of Terminal Alkynes. *J. Am. Chem. Soc*. **2019**, 141, 17086.

(8) Hazra, A.; Kephart, J. A.; Velian, A.; Lalic, G. Hydroalkylation of Alkynes: Functionalization of the Alkenyl Copper Intermediate through Single Electron Transfer Chemistry. *J. Am. Chem. Soc*. **2021**, 143, 7903.

(9) Nakamura, K.; Nishikata, T. Tandem Reactions Enable Trans- and Cis-Hydro-Tertiary-Alkylations Catalyzed by a Copper Salt. ACS Catalysis **2017**, 7, 1049.

(10) Lee, M. T.; Goodstein, M. B.; Lalic, G. Synthesis of Isomerically Pure (Z)-Alkenes from Terminal Alkynes and Terminal Alkenes: Silver-Catalyzed Hydroalkylation of Alkynes. *J. Am. Chem. Soc*. **2019**, 141, 17086.

(11) Yu, L.; Lv, L.; Qiu, Z.; Chen, Z.; Tan, Z.; Liang, Y.-F.; Li, C.-J. Palladium-Catalyzed Formal Hydroalkylation of Aryl-Substituted Alkynes with Hydrazones. *Angew. Chem., Int. Ed.* **2020**, 59, 14009.

(12) Lu, X.-Y.; Hong, M.-L.; Zhou, H.-P.; Wang, Y.; Wang, J.-Y.; Ge, X.-T. Trisubstituted Olefin Synthesis via Ni-Catalyzed Hydroalkylation of Internal Alkynes With Non-Activated Alkyl Halides. *Chem. Commun*. **2018**, 54, 4417.

(13) Zhu, Z.-F.; Tu, J.-L.; Liu, F. Ni-Catalyzed Deaminative Hydroalkylation of Internal Alkynes. *Chem. Commun*. **2019**, 55, 11478.

(14) Yue, H.; Zhu, C.; Kancherla, R.; Liu, F.; Rueping, M. Regioselective Hydroalkylation and Arylalkylation of Alkynes by Photoredox/Nickel Dual Catalysis: Application and Mechanism. *Angew. Chem., Int. Ed*. **2020**, 59, 5738.

(15) Liu, B.; Zhou, T.; Li, B.; Xu, S.; Song, H.; Wang, B. Rhodium(III)-Catalyzed Alkenylation Reactions of 8-Methylquinolines with Alkynes by C(sp3)-H Activation. *Angew. Chem., Int. Ed*. **2014**, 53, 4191.

(16) Mankad, N. P.; Laitar, D. S.; Sadighi, J. P. Synthesis, Structure, and Alkyne Reactivity of a Dimeric (Carbene)copper(I) Hydride. *Organometallics* **2004**, 23, 3369.

(17) Jordan, A. J.; Lalic, G.; Sadighi, J. P. Coinage Metal Hydrides: Synthesis, Characterization, and Reactivity. *Chem. Rev*. **2016**, 116, 8318.

(18) Jia, C.; Piao, D.; Oyamada, J.; Lu, W.; Kitamura, T.; Fujiwara, Y. Efficient Activation of Aromatic C-H Bonds for Addition to C-C Multiple Bonds. *Science* **2000**, 287, 199.

(19) Jia, C.; Lu, W.; Oyamada, J.; Kitamura, T.; Matsuda, K.; Irie, M.; Fujiwara, Y. Novel Pd(II)- and Pt(II)-Catalyzed Regio- and Stereoselective trans-Hydroarylation of Alkynes by Simple Arenes. *J. Am. Chem. Soc*. **2000**, 122, 7252.

(20) Tunge, J. A.; Foresee, L. N. Mechanistic Studies of Fujiwara Hydroarylation. C−H Activation versus Electrophilic Aromatic Substitution. *Organometallics* **2005**, 24, 6440.

(21) Gómez-Balderas, R.; Coote, M. L.; Henry, D. J.; Fischer, H.; Radom, L. What Is the Origin of the Contrathermodynamic Behavior in Methyl Radical Addition to Alkynes versus Alkenes? *J. Phys. Chem*. A. **2003**, 107, 6082.

(22) Giese, B.; Lachhein, S. Addition of Alkyl Radicals to Alkynes: Distinction between Radical and Ionic Nucleophiles. *Angew. Chem., Int. Ed*. Engl. **1982**, 21, 768.

(23) Giese, B.; González-Gómez, J. A.; Lachhein, S.; Metzger, J. O. Influence of H-Donor and Temperature on the Stereoselectivity of Radical Reactions. *Angew. Chem., Int. Ed.* Engl. **1987**, 26, 479.

(24) Wille, U. Radical Cascades Initiated by Intermolecular Radical Addition to Alkynes and Related Triple Bond Systems. *Chem. Rev*. **2013**, 113, 813.

(25) Yatham, V. R.; Harnying, W.; Kootz, D.; Neudörfl, J.-M.; Schlörer, N. E.; Berkessel, A. 1,4-Bis-Dipp/Mes-1,2,4-Triazolylidenes: Carbene Catalysts That Efficiently Overcome Steric Hindrance in the Redox Esterification of α- and β-Substituted α,β-Enals. *J. Am. Chem. Soc.* **2016**, 138, 2670.

(26) Huang, J.; Nolan, S. P. Efficient Cross-Coupling of Aryl Chlorides with Aryl Grignard Reagents (Kumada Reaction) Mediated by a Palladium/Imidazolium Chloride System. *J. Am. Chem. Soc.* **1999**, 121, 9889.

(27) Hu, L.; Gao, H.; Hu, Y.; Lv, X.; Wu, Y.-B.; Lu, G. Computational Study of Silver-Catalyzed Stereoselective Hydroalkylation of Alkynes: Pauli Repulsion Controlled Z/E Selectivity. *Chem. Commun*. **2021**, 57, 6412.

(28) Kambe, N.; Moriwaki, Y.; Fujii, Y.; Iwasaki, T.; Terao, J. Silver-Catalyzed Regioselective Carbomagnesiation of Alkynes with Alkyl Halides and Grignard Reagents. *Org. Lett.* **2011**, 13, 4656.

(29) Goumans, T. P. M.; van Alem, K.; Lodder, G. Photochemical Generation and Structure of Vinyl Radicals. *Eur. J. Org. Chem*. **2008**, 2008, 435.

(30) Jenkins, P. R.; Symons, M. C. R.; Booth, S. E.; Swain, C. J. Why is Vinyl Anion Configurationally Stable but a Vinyl Radical Configurationally Unstable? *Tetrahedron Lett*. **1992**, 33, 3543.

(31) Tate, B. K.; Jordan, A. J.; Bacsa, J.; Sadighi, J. P. Stable Mono- and Dinuclear Organosilver Complexes. *Organometallics* **2017**, 36, 964.

(32) Yamamoto, Y. Silver-Catalyzed Csp−H and Csp−Si Bond Transformations and Related Processes. *Chem. Rev*. **2008**, 108, 3199.

(33) Halbes-Letinois, U.; Weibel, J.-M.; Pale, P. The Organic Chemistry of Silver Acetylides. *Chem. Soc. Rev*. **2007**, 36, 759.

(34) Sivaguru, P.; Cao, S.; Babu, K. R.; Bi, X. Silver-Catalyzed Activation of Terminal Alkynes for Synthesizing Nitrogen-Containing Molecules. *Acc. Chem. Res*. **2020**, 53, 662.

(35) Brown, H. C.; Levy, A. B.; Midland, M. M. Reaction of Lithium Ethynyl- and Ethenyltrialkylborates With Acid. Valuable Route to the Markovnikov Alkenyl- and Alkylboranes. *J. Am. Chem. Soc*. **1975**, 97, 5017.

(36) Miyaura, N.; Yoshinari, T.; Itoh, M.; Suzuki, A. Reaction of Lithium Alkynyltrialkylborates with Propionic Acid. General and Convenient Syntheses of Internal and Terminal Olefins Using Organoboranes. *Tetrahedron Lett*. **1974**, 15, 2961.

(37) Wang, H.; Jing, C.; Noble, A.; Aggarwal, V. K. Stereospecific 1,2-Migrations of Boronate Complexes Induced by Electrophiles. *Angew. Chem., Int. Ed*. **2020**, 59, 16859.

(38) Namirembe, S.; Morken, J. P. Reactions of Organoboron Compounds Enabled by Catalyst-Promoted Metalate Shifts. *Chem. Soc. Rev*. **2019**, 48, 3464.

(39) Aggarwal Varinder, K.; Fang Guang, Y.; Ginesta, X.; Howells Dean, M.; Zaja, M. Toward an Understanding of the Factors Responsible for the 1,2-Migration of Aalkyl Groups in Borate Complexes *Pure Appl. Chem*. **2006**, 78, 215.

(40) Brown, H. C.; Molander, G. A. Vinylic Organoboranes. 2. Improved Procedures for the Protonolysis of Alkenyldialkylboranes Providing a Simplified Stereospecific Synthesis of (Z)-Alkenes. *J. Org. Chem*. **1986**, 51, 4512.

(41) Partyka, D. V. Transmetalation of Unsaturated Carbon Nucleophiles from Boron-Containing Species to the Mid to Late d-Block Metals of Relevance to Catalytic C−X Coupling Reactions (X = C, F, N, O, Pb, S, Se, Te). *Chem. Rev*. **2011**, 111, 1529.

(42) Whitesides, G. M.; Casey, C. P.; Krieger, J. K. Thermal Decomposition of Vinylic Ccopper(I) and Ssilver(I) Organometallic Compounds. *J. Am. Chem. Soc*. **1971**, 93, 1379.

(43) Köbrich, G.; Fröhlich, H.; Drischel, W. Stabile Carbenoide: XIX. 1-Chlor-2,2-Diphenylvinylsilber. *J. Organomet. Chem*. **1966**, 6, 194.

(44) Glockling, F. The Formation of Iisobut-1-Enyl Radicals from Isobut-1-Enylsilver. Part II. *J. Chem. Soc*. **1956**, 3640.

(45) Miura, K.; Saito, H.; Itoh, D.; Matsuda, T.; Fujisawa, N.; Wang, D.; Hosomi, A. Allylstannylation of Carbon−Carbon and Carbon−Oxygen Unsaturated Bonds via a Radical Chain Process1. *J. Org. Chem*. **2001**, 66, 3348.

(46) Miura, K.; Saito, H.; Fujisawa, N.; Wang, D.; Nishikori, H.; Hosomi, A. Homolytic Carbostannylation of Alkenes and Alkynes with Tributylstannyl Enolates. *Org. Lett*. **2001**, 3, 4055.

(47) Zweifel, G.; Arzoumanian, H.; Whitney, C. C. A Convenient Stereoselective Synthesis of Substituted Alkenes via Hydroboration-Iodination of Alkynes. *J. Am. Chem. Soc*. **1967**, 89, 3652.

(48) Ishida, N.; Shimamoto, Y.; Murakami, M. Stereoselective Synthesis of (E)-(Trisubstituted alkenyl)borinic Esters: Stereochemistry Reversed by Ligand in the Palladium-Catalyzed Reaction of Alkynylborates with Aryl Halides. *Org. Lett.* **2009**, 11, 5434.

(49) Zhang, L.; Lovinger, G. J.; Edelstein, E. K.; Szymaniak, A. A.; Chierchia, M. P.; Morken, J. P. Catalytic Conjunctive Cross-Coupling Enabled by Metal-Induced Metallate Rearrangement. *Science* **2016**, 351, 70.

(50) Myhill, J. A.; Wilhelmsen, C. A.; Zhang, L.; Morken, J. P. Diastereoselective and Enantioselective Conjunctive Cross-Coupling Enabled by Boron Ligand Design. *J. Am. Chem. Soc*. **2018**, 140, 15181.

(51) Slayden, S. W. Relative Migratory Aptitudes of Alkyl Groups in the Iodination of Lithium Ethynyltrialkylborates. *J. Org. Chem*. **1981**, 46, 2311.

(52) Brown, H. C.; Nambu, H.; Rogic, M. M. Reaction of Organoboranes with Bromoacetone Under the Influence of Potassium 2,6-Di-tert-Butylphenoxide. A Convenient Procedure for the Conversion of Olefins into Methyl Ketones via Hydroboration. *J. Am. Chem. Soc*. **1969**, 91, 6852.

(53) Brown, H. C.; Nambu, H.; Rogic, M. M. Reaction of Organoboranes with Chloroacetonitrile under the Influence of Potassium 2,6-Di-Tert-Butylphenoxide. A Convenient Procedure for the Conversion of Olefins into Nitriles Via Hydroboration. *J. Am. Chem. Soc.* **1969**, 91, 6854.

(54) Brown, H. C.; Nambu, H.; Rogic, M. M. Reaction of Organoboranes with Ethyl Bromoacetate and Ethyl Dibromoacetate under the Influence of Potassium 2,6-Di-Tert-Butylphenoxide, an Unusual Base with Large Steric Requirements. *J. Am. Chem. Soc.* **1969**, 91, 6855.

(55) Yu, P.; Bismuto, A.; Morandi, B. Iridium-Catalyzed Hydrochlorination and Hydrobromination of Alkynes by Shuttle Catalysis. *Angew. Chem. Int. Ed.* **2020**, *59* (7), 2904–2910.

(56) Brown, H. C.; Scouten, C. G.; Liotta, R. Hydroboration. 50. Hydroboration of Representative Alkynes with 9-Borabicyclo[3.3.1]Nonane - a Simple Synthesis of Versatile Vinyl Bora and Gem-Dibora Intermediates. *J. Am. Chem. Soc.* **1979**, *101* (1), 96–99.

(57) Yu, X.-Y.; Patrick, B. O.; James, B. R. New Rhodium(I) Carbene Complexes from Carbene Transfer Reactions. *Organometallics* **2006**, *25* (9), 2359–2363.

(58) Tate, B. K.; Wyss, C. M.; Bacsa, J.; Kluge, K.; Gelbaum, L.; Sadighi, J. P. A Dinuclear Silver Hydride and an Umpolung Reaction of CO2. *Chem. Sci.* **2013**, *4* (8), 3068–3074.

(59) Gaussian 16, Revision C.01, Frisch, M. J.; Trucks, G. W.; Schlegel, H. B.; Scuseria, G. E.; Robb, M. A.; Cheeseman, J. R.; Scalmani, G.; Barone, V.; Petersson, G. A.; Nakatsuji, H.; Li, X.; Caricato, M.; Marenich, A. V.; Bloino, J.; Janesko, B. G.; Gomperts, R.; Mennucci, B.; Hratchian, H. P.; Ortiz, J. V.; Izmaylov, A. F.; Sonnenberg, J. L.; Williams-Young, D.; Ding, F.; Lipparini, F.; Egidi, F.; Goings, J.; Peng, B.; Petrone, A.; Henderson, T.; Ranasinghe, D.; Zakrzewski, V. G.; Gao, J.; Rega, N.; Zheng, G.; Liang, W.; Hada, M.; Ehara, M.; Toyota, K.; Fukuda, R.; Hasegawa, J.; Ishida, M.; Nakajima, T.; Honda, Y.; Kitao, O.; Nakai, H.; Vreven, T.; Throssell, K.; Montgomery, J. A., Jr.; Peralta, J. E.; Ogliaro, F.; Bearpark, M. J.; Heyd, J. J.; Brothers, E. N.; Kudin, K. N.; Staroverov, V. N.;

Keith, T. A.; Kobayashi, R.; Normand, J.; Raghavachari, K.; Rendell, A. P.; Burant, J. C.; Iyengar, S. S.; Tomasi, J.; Cossi, M.; Millam, J. M.; Klene, M.; Adamo, C.; Cammi, R.; Ochterski, J. W.; Martin, R. L.; Morokuma, K.; Farkas, O.; Foresman, J. B.; Fox, D. J. Gaussian, Inc., Wallingford CT, 2016.

(60) Bruker. *SAINT*; BrukerAXS Inc: Madison, Wisconsin, USA, 2007.

(61) Bruker. *SADABS*; BrukerAXS Inc: Madison, Wisconsin, USA, 2007.

(62) Bruker. *APEX2*; BrukerAXS Inc: Madison, Wisconsin, USA, 2007.

(63) Sheldrick, G. M. SHELXT – Integrated Space-Group and Crystal-Structure Determination. *Acta Crystallogr. Sect. Found. Adv.* **2015**, *71* (1), 3–8.

(64) Altomare, A.; Burla, M. C.; Camalli, M.; Cascarano, G. L.; Giacovazzo, C.; Guagliardi, A.; Moliterni, A. G. G.; Polidori, G.; Spagna, R. SIR97: A New Tool for Crystal Structure Determination and Refinement. *J. Appl. Crystallogr.* **1999**, *32* (1), 115–119.

(65) Altomare, A.; Cascarano, G.; Giacovazzo, C.; Guagliardi, A. Completion and Refinement of Crystal Structures with SIR92. *J. Appl. Crystallogr.* **1993**, *26* (3), 343–350.

(66) G. M. Sheldrick. *SHELXL-97, Program for the Refinement of Crystal Structures*; University of Göttingen: Germany, 1997.

(67) Sheldrick, G. M. Crystal Structure Refinement with SHELXL. *Acta Crystallogr. Sect. C Struct. Chem.* **2015**, *71* (1), 3–8.

(68) S. Mackay; C. Edwards; A. Henderson; C. Gilmore; K. Shankland. *MaXus: A Computer Program for the Solution and Refinement of Crystal Structures from Diffraction Data*; University of Glasgow: Scotland, 1997.

(69) Waasmaier, D.; Kirfel, A. New Analytical Scattering-Factor Functions for Free Atoms and Ions. *Acta Crystallogr. A* **1995**, *51* (3), 416–431.

(70) Farrugia, L. J. ORTEP-3 for Windows - a Version of ORTEP-III with a Graphical User Interface (GUI). *J. Appl. Crystallogr.* **1997**, *30* (5), 565–565.

VITA

Mitchell Thomas Lee was born and raised in Seattle, Washington. In 2008, he moved to Walla Walla, Washington, where he attended Whitman College. After graduating in 2012, with a B.A. in chemistry, he worked for three years at Woods Hole Oceanographic Institution in Woods Hole, Massachusetts and at the US EPA-MED in Duluth, Minnesota. During the summer of 2015, he returned to Seattle to pursue a doctoral degree in chemistry with Professor Gojko Lalic, at the University of Washington. After earning his Ph.D. in 2021, he began work at Cepheid, in Bothell, Washington, as a synthetic organic chemist.